Influence of cellular dsRNA binding proteins in the replication process of a dsRNA virus

Dissertation

zur Erlangung des akademischen Grades

doktor rerum naturalium (Dr. rer. nat.)

vorgelegt der

Naturwissenschaftlichen Fakultät I
der Martin-Luther-Universität Halle-Wittenberg

von Frau Ruth Lydia Olga Stricker
geb. am 15.07.1981 in Düsseldorf

Gutachter:

1. Prof. Dr. S.-E. Behrens

2. PD Dr. E. Mundt

3. Prof. Dr. E. Vahlenkamp

Verteidigung: 29. Juni 2012, Halle (Saale)

Für Wolfgang

Weil Du mich losgelassen hast, als ich frei sein wollte
Weil Du wach geblieben bist, bis ich nach Hause gekommen bin
Weil Du da warst, als ich einsam war
Weil Du gesagt hast, dass ich bleiben soll, als ich zurückkommen wollte
Weil Du mich getröstet hast, als ich traurig war
Weil Du gesagt hast, dass ich durchhalten soll, als ich aufgeben wollte
Weil Du mir geholfen hast, als ich nicht weiterwusste
Weil Du gewartet hast, bis ich zurückgekommen bin
Weil Du mich liebst.
Ich liebe Dich.

Abstract

Viruses are obligatory parasites of cells and as a consequence viral components come in contact with cellular molecules. Once these interactions are detected it is interesting to reveal, if the cellular components act in concert with the host defense or if viruses use them for their own replication. It is advantageous and necessary for viruses to use cellular components, because viruses contain limited genetic information. Several cellular components are known to interact with viral proteins or RNA and can influence viral replication. Interestingly, viral components of different viruses interact with the same cellular factors, although they do not share a common primary nucleotide and amino acid sequence.

The described research was performed on infectious bursal disease virus (IBDV), a double stranded RNA (dsRNA) virus. The main target cells of IBDV are immature B lymphocytes, which are localized in the chicken bursa of Fabricius. Two cellular proteins that are known to possess dsRNA binding domains were selected for investigations, the chicken homologs of p68 and the nuclear factor 45 (NF45).

Initially, the coding regions of both genes were cloned and recombinant proteins were heterologously expressed in a baculovirus expression system. The subsequently purified proteins were used to generate protein-specific antibodies in rabbits. The specificity for anti-NF45 and anti-p68 was shown by Western blot and indirect immunofluorescence.

Both nuclear proteins, NF45 and p68, showed a change of localization, which resulted in an accumulation in the cytoplasm of IBDV infected cells. The co-localization of NF45 with the ribonucleoprotein VP3 and the RNA-dependent RNA polymerase VP1 of IBDV and the co-localization of p68 with the viral protease VP4 were initially shown by confocal laserscanning microscopy. NF45-VP3 and p68-VP4 co-localizations were confirmed by co-immunoprecipitation. The observed co-localizations were time dependent, IBDV strain independent, interferon independent and species independent. Downregulated expression of both cellular proteins by small interfering RNA resulted in increased IBDV titers, indicating an inhibitory effect of NF45 and p68 on IBDV replication. The obtained results emphasize the antiviral activity of dsRNA binding proteins NF45 and p68 in the host cell after being infected with IBDV.

Zusammenfassung

Viren sind obligate Zellparasiten und daraus ergibt sich, dass ihre Komponenten mit denen der Zelle in Kontakt treten. In solchen Fällen ist es interessant zu ergründen, ob die zellulären Moleküle mit Komponenten der zellulären Immunabwehr zusammenarbeiten, oder das Virus diese rekrutiert um sie für seine eigene Replikation zu nutzen. Dies wäre gerade für Viren hilfreich, da ihr Genom in der Größe limitiert ist. Diverse zelluläre Komponenten sind bekannt, die mit viralen Proteinen oder viraler RNA interagieren und die die Replikationseffizienz in beide Richtungen beeinflussen können. Interessanterweise interagieren die gleichen zellulären Poroteine mit den verschiedensten viralen Bestandteilen, obwohl deren primäre Nukleotid- und Aminosäuresequenz verschieden ist.

In dieser Arbeit sind die Forschungsergebnisse am Virus der infektiösen Bursitis (IBDV) beschrieben. Es ist ein doppelsträngiges RNA (dsRNA) Virus, das unreife B-Lymphoyzten infiziert, die sich in der Bursa Fabricius des Huhns ansiedeln. Als potentielle Interaktionspartner wurden zelluläre Proteine ausgesucht, die eine oder mehrere dsRNA bindende Domänen aufweisen. Dies waren die aviären Proteine p68 und NF45 (nuclear factor 45).

Zuerst wurden die kodierenden Regionen kloniert und die rekombinanten Proteine heterolog in einem Baculovirus Expressionssystem exprimiert. Aus den gereinigten Proteinen wurden Antiseren generiert. Die Spezifität von den anti-NF45 und anti-p68 Seren wurde durch Western Blot und indirekte Immunfluoreszenz gezeigt.

Beide Hühnerproteine, NF45 und p68, ändern ihre nukleäre Lokalisation nach einer Infektion mit IBDV zu einer zytoplasmatischen. Dort wurde die Kolokalisation von NF45 mit dem viralen Ribonukleoprotein VP3 und der RNA-abhängigen RNA-Polymerase VP1 und von p68 mit der viralen Protease VP4 mit konfokaler Laserscan Mikroskopie detektiert. NF45-VP3 und p68-VP4 sind beides direkte Interaktionen, was mit Hilfe der Co-Immunopräzipitation bewiesen wurde. Die Kolokalisation von beiden Paaren (NF45-VP3 & p68-VP4) war abhängig von der Zeit, aber unabhängig vom Virusstamm, von Interferonen und von der infizierten Spezies.

Bei verminderter Expression des zellulären Interaktionspartners, was durch siRNA erreicht wurde, konnten höhere Virustiter gemessen werden. Dies ist ein Hinweis, dass sowohl NF45 als auch p68 die IBDV Replikation inhibieren. Diese Ergebnisse betonen die antiviralen Eigenschaften von den dsRNA bindenden Proteinen NF45 und p68 in der Hühnherzelle nach Infektion mit IBDV.

1 Introduction

1.1 Infectious bursal disease virus

Since the fall of 1957 a new infectious and contagious disease of chickens spread in and around an area known as Gumboro in southern Delaware, which is why it was called Gumboro disease. Characteristic signs were ruffled feathers, whitish or watery diarrhea, trembling and severe prostration. This clinical picture was described the first time by Cosgrove in 1962 as a new disease in chickens (Cosgrove 1962). The bursa of Fabricius (BF) was enlarged and inflamed, which led to its second name, infectious bursal disease (IBD) (Cosgrove 1962). The BF was named after Hieronymus Fabricius (Adelmann 1942, Glick *et al* 1956) and is a sac-like extension of the hindgut that is located dorsal to the cloaca (Glick *et al* 1956). Chicken B lymphocytes develop in the BF. The agent that caused IBD was filterable so it was called infectious bursal disease virus (IBDV), infecting mainly B lymphocytes in the BF (Winterfield & Hitchner 1964).

The course of disease is closely correlated to the development of the BF, which can be divided into three stages. First, the BF rapidly grows from hatch to three or four weeks of age, in which IgM expressing B lymphocytes colonize the BF in a single wave and undergo gene conversion (Ratcliffe *et al* 1986, Mansikka *et al* 1990). Chicken in the field less than three weeks of age do not exhibit clinical signs, because they are usually still protected by maternal antibodies provided through the egg obtained either from a vaccinated or infected breeder hen. The antibodies are continuously absorbed from the yolk sac through a selective transport mechanism to the blood circulation of the developing embryo (Brierley & Hemmings 1956). Antigen-specific maternal antibodies have a half-live of 6-8 d and fall below detectable levels at day 28 post hatch (Wood *et al* 1981, Fahey *et al* 1987, Knoblich *et al* 2000). In a second phase of bursal development the BF resides in a plateau phase with little increase in size up to 10 weeks of age (Glick 1956). Due to the abundance of host cells, IBDV replicates rapidly and it is proposed that it infects only IgM bearing B cells (Hirai & Calnek 1979). This is why clinical signs of IBDV occurred in two to 15-week old chicken, but mostly between three and six weeks of age (Cosgrove 1962, Winterfield & Hitchner 1964, Ley *et al* 1979). The third phase of bursal development is a regression phase before sexual maturity (Glick 1956) and chicken older than 15 weeks do not show clinical signs after infection (Hitchner 1971). Thus, the severity of B lymphocyte depression is age-dependent (Sivanandan & Maheswaran 1980).

Clinical signs were observed 24-48 h post infection (pi) and recovery was observed 6-10 d pi (Cho & Edgar 1972). Morbidity can reach 100% on day three after infection (Ley *et al* 1983). Mortality peaked at the third day after infection and lasted up to seven days (Parkhurst 1964). IBDV infected chickens showed less weight gain than uninfected (Giambrone *et al* 1976) causing significant economic losses to the poultry industry

worldwide (Kibenge *et al* 1988). It also caused a depression of egg production and deterioration in the eggshell and the internal egg quality (Müller *et al* 2003). Until day three after infection the BF can double its size due to edema and hyperemia, but then it started to become atrophic due to necrosis (Helmboldt & Garner 1964, Cheville 1967). The BF failed to repopulate with lymphocytes (Cheville 1967) and the damage in the BF was irreversible (Ivanyi & Morris 1976). Bursectomized chickens did not show a fatal outcome of the disease (Käufer & Weiss 1980). Neither T lymphocytes (Rodenberger *et al* 1994, Hirai *et al* 1981) nor natural killer cells were infected by IBDV (Hirai *et al* 1981) and their function remained unaffected (Sharma & Lee 1983).

IBDV did not haemagglutinate erythrocytes (Wagner & Köster 1986). IBDV infection induced interferon (IFN) production *in vitro* and *in vivo* peaking at the same day as neutralizing antibodies (72 h pi) short after maximum virus titers were detected (96 h pi) (Gelb *et al* 1979a, Gelb *et al* 1979b, Gelb *et al* 1979c). Proteomic analysis revealed that proteins of the ubiquitin-proteasome pathway, the major protein degradation pathway, were downregulated after infection and also intermediate filament proteins were less expressed, which led to a collapse of the tubulin network and probably to disruption of the cytoskeleton, which subsequently promoted particle release (Zheng *et al* 2008). Molecules of innate host defense, like the dsRNA specific toll-like receptor (TLR) 3 and Mx protein, were upregulated and the human MxA inhibited IBDV replication (Mundt 2007, Wong *et al* 2007).

1.1.1 Immunosuppression

Allan *et al* (1972) described for the first time immunosuppression in IBDV infected birds detected by failure of induced protection by Newcastle disease virus vaccine after challenge and reduction of the serological response. The switch from IgM to IgY (IgY contains one more heavy chain in the constant domain than mammalian IgG) is not possible, when the BF was depleted from B lymphocytes (Faragher *et al* 1972). The earlier the infection, the more severe was the immunodeficiency, but the less was the mortality (Ivanyi & Morris 1976). Poor response to vaccines and a high degree of susceptibility to secondary infections were often seen and resulted in economic losses to the poultry industry (Saif 1998). Maternal antibodies to IBDV prevented infection with IBDV and therefore immunosuppression caused by IBDV (Sharma 1984).

Vaccination at the same time or short after IBDV infection showed less protection against Mareks disease (Sharma 1984), *Eimeria tenella* (Anderson *et al* 1977, Onaga *et al* 1989), infectious laryngotracheitis virus (Rosenberger & Gelb 1978) and infectious bronchitis virus (Winterfield & Thacker 1978, Pejkovski *et al* 1979). Humoral immune response was reduced up to seven weeks after infection (Kim *et al* 1999).

Infection of IBDV enhanced pathogenicity and reduced neutralization titers against inclusion body hepatitis virus (Fadly *et al* 1976), *E. coli* and *Salmonella typhimurium*

(Wyeth 1975), reovirus (Springer *et al* 1983, Moradian *et al* 1990), *Staphylococcus aureus* (Santivatr *et al* 1981), chicken anemia agent (Yuasa *et al* 1980), Mareks disease virus (Cho 1970) and *Aspergillus flavus* (Okoye *et al* 1991). IBDV infection also caused an increased susceptibility to hemorrhagic-aplastic-anemia-syndrome and gangrenous dermatitis (Rosenberger *et al* 1975). Co-infection of IBDV and chicken anemia virus, a virus that infects T lymphocytes, resulted in more severe clinical signs of both diseases (Toro *et al* 2009).

1.1.2 Transmission and environmental tenacity

The virus was transmitted by direct contact from bird to bird, contaminated feed, water, equipment, animal caretakers or litter, but not by air flow (Edgar & Cho 1965, Benton *et al* 1967a). IBDV does not persist in chickens for a longer period of time (Winterfield *et al* 1972). The virus is highly resistant to various chemicals like phenol, ether, chloroform and conditions such as heating to 56°C for five hours or at pH 2 (Benton *et al* 1967b, Lukert & Davis 1974). Reduction in infectivity was achieved by treatment with formalin or binary ethylenimine and treatment conditions at pH 12 (Benton *et al* 1967b, Habib *et al* 2006). In comparison to reoviruses, IBDV was more resistant to heat, ultraviolet irradiation and photodynamic inactivation (Petek *et al* 1973). The removal of the chicken litter did not reduce IBDV infection (Parkhurst 1964), but it was reported that farms with strict sanitation were negative for IBDV, while IBDV caused problems in other farms with lower sanitation regiment located in the same country (Lucio *et al* 1972).

1.1.3 Vaccination

IBDV is highly resistant to disinfectants and therefore strict hygiene is not sufficient to control spreading and the only efficient solution to protect chicken under industrial production conditions is vaccination. Maternal antibodies were beneficial during the first critical two weeks in case of infection (Hitchner 1976), but during the first three weeks of life, maternal IBDV specific antibodies interfered with vaccination using live vaccines (Thornton & Pattison 1975). Such maternal antibodies decline and consequently do not protect chicken during the whole growing period and they do not prevent bursal damage (van den Berg & Meulemans 1991).

IBDV isolated from the BF of chickens replicated more invasive in the bursal tissue than viruses propagated in cell culture or chicken embryos (Rodriguez-Chavez *et al* 2002a). Attenuated live vaccines were produced by passage of IBDV field strains either in chicken embryos or in cell culture from different origins. Adaptation to cell culture resulted in attenuation of the virus coming along with changes in the viral capsid protein VP2 (Yamaguchi *et al* 1996). Changes in VP2 were directly related to the host system used to propagate IBDV (Rodriguez-Chavez *et al* 2002b). For some field isolates it was not possible to adapt them to cell culture (Todd & McNulty 1979, McFerran *et al* 1980). Reduced mortality and better feed conversion was observed in vaccinated chickens

(Edgar & Cho 1973). Highly attenuated vaccines were classified as 'mild' and vaccines of moderate virulence as 'intermediate' (Kibenge *et al* 1988). Classical live vaccines hold the risk of reversion to virulence (Van den Berg 2000).
Mild vaccines do not induce immunity in the presence of maternal derived antibodies, because they were neutralized by them, therefore intermediate vaccines were required, but they caused bursal lesions (Winterfield & Thacker 1978, Wintefield *et al* 1980, Kibenge *et al* 1988, Tsukamoto *et al* 1995, Rautenschlein *et al* 2003). To overcome this problem, immune complex vaccines were developed, in which the vaccine virus was complexed with IBDV neutralizing antibodies (Whitfill *et al* 1995).
Based on ELISA titers of maternal antibodies the day of optimal vaccination can be determined (Lasher & Shane 1994).

1.1.4 Classification

IBDV is grouped in the genus *Avibirnavirus* of the family *Birnaviridae*, in which the suffix bi points to the doublestrandedness of the viral genome as well as the existence of two genome segments and RNA indicates the nature of the viral nucleic acid (Dobos *et al* 1979). The genus *Entomobirnavirus* with the insect virus Drosophila X virus (DXV) of the fruit fly, and the genus *Aquabirnavirus* with the three aquatic viruses infectious pancreatic necrosis virus (IPNV), oyster virus (OV) of bivalve molluscs and tellina virus (TV) were proposed to be classified in the same family (Dobos *et al* 1979. Later two other aquatic viruses, the blotched snakehead virus (BSNV) and the eel virus (EV), were discovered (Özel & Gelderblom 1985, Da Costa *et al* 2003) and TV was proposed to be classified into its own genus (Nobiron *et al* 2008). All viruses of the family *Birnaviridae* contain a bi-segmented dsRNA genome and have a diameter of 60-65 nm (Delmas *et al* 2005, Özel & Gelderblom 1985). Also the general genomic structure summarizes them into one virus family.

1.1.5 Subtypes

Typically three main IBDV subtypes were differentiated based on pathogenicity and antigenicity, but based on the virulence, six IBDV subtypes have been proposed (Jackwood & Saif 1987).

1.1.5.1 Classical IBDV

Mortality after infection with classical IBDV was 15% (Parkhurst 1964), but reached 100% in specific pathogen free (SPF) chicken (Käufer & Weiss 1980). Mortality in egg-laying hens (40-60% mortality) is higher than in broilers (1-15% mortality) although maternal derived antibodies declined faster in broilers than in layers (Edgar & Cho 1973, Winterfield & Thacker 1978, Van den Berg & Meulemans 1991). Characteristics of classical IBDV strains are lytic infection of B lymphocytes, inflammation in the BF associated with influx of heterophilic cells and edema, all leading to bursal atrophy

(Sharma *et al* 1989). IBDV spread fast through many areas of the USA (Winterfield & Hitchner 1964) and it was soon detected in Canada (Faragher 1972), in Mexico and by 1965 it was widespread (Faragher 1972, Lucio *et al* 1972). Today classical IBDV strains are distributed worldwide.

1.1.5.2 Variant IBDV

Variant strains show usually no mortality, although bursal atrophy developed within 72 h and was severe, probably because of faster replication of the virus (Kibenge *et al* 1988, van den Berg 2000, Rodriguez-Chavez *et al* 2002c). The main characteristic of variant strains is the absence of clinical signs and no inflammation in the BF, where pronounced necrosis of B lymphocytes was observed (Kibenge *et al* 1988, Sharma *et al* 1989, Nagarajan & Kibenge 1997). Vaccination against classical IBDV induced only limited protection against variant strains and vice versa (Giambrone & Closser 1990). Variant strains have been detected mainly in the USA (Saif 1984, Rosenberger *et al* 1985).

1.1.5.3 Very virulent IBDV

Very virulent (vv) IBDV is characterized by severe damage of the BF, thymus, spleen and bone marrow (Nagarajan & Kibenge 1997). Mortality can reach 70-100% (van den Berg & Meulemans 1991, Wu *et al* 2007). The antigenicity is similar to classical IBDV, but failures of vaccination with classical IBDV have been reported in relation with higher virulence of the virus (van den Berg *et al* 1996). Most neutralizing monoclonal antibodies (mAb) against classical IBDV neutralize also vvIBDV as has been shown with a panel of mAbs with a European isolate (Eterradossi *et al* 1997) and also with an IBDV isolate from China (Liu *et al* 2002).

VvIBDV was first detected in Europe in Belgium (Box 1989, van den Berg *et al* 1991) and later all over Europe (Chettle *et al* 1989, Box 1989, Öppling *et al* 1991, Eterradossi *et al* 1992), in Japan and on the Asian continent (Tsukamoto *et al* 1992, Nakamura *et al* 1992, Cao *et al* 1998), in Aftrica (Eterradossi *et al* 1999) and South America (Di Fabio *et al* 1999, Banda *et al* 2003, Banda & Villegas 2004). For a long time no vvIBDV was detected in the USA until 2008, when pullets from California were tested positive (Stoute *et al* 2009).

1.1.6 Serotypes

Two serotypes of IBDV have been identified so far by serum neutralization tests with serotype-specific antisera (McFerran *et al* 1980). Only serotype I causes bursal damage in chickens, serotype II is infectious and transmissible to chickens, but did cause neither clinical signs nor damage in any organ investigated and is therefore referred to as not pathogenic (Jackwood *et al* 1982, Jackwood *et al* 1985, Ismail *et al* 1988). Serotype II IBDV strains have been isolated from turkeys and infection of them is widespread, but no clinical signs appeared in turkeys (McNulty *et al* 1979, Jackwood *et al* 1982, Sivanandan

et al 1984). Infection of turkeys with a serotype I strain induced subclinical infection and decreased the immune response (Perelman & Heller 1983). Neutralizing antibodies to serotype II did not protect against challenge with a serotype I virus (Jackwood *et al* 1985, Zierenberg *et al* 2004).

1.1.7 Genome

The IBDV genome is based on RNA (Lukert & Davis 1974). It consists of two segments (Nick *et al* 1976) of double stranded (ds) RNA (Müller *et al* 1979). The structure of dsDNA is described as a B-form, but dsRNA contains an additional hydroxyl group at the 2' position of the ribose sugar and therefore adopts the A-form and viral dsRNA possesses also most likely an A-form (Müller & Nitschke 1987a). IBDV is a polyploid virus that can contain up to four segments of dsRNA (Luque *et al* 2009a). A cartoon of the genome is depicted in Figure 1 (sequence of IBDV strain D78, see 6.2.3 and 6.2.4). Segment A encodes the precursor (p) viral protein (VP) 2, the viral protease VP4 and the ribonucleoprotein VP3. All three proteins are encoded by open reading frame (ORF) A1 and are expressed as a single polyprotein, which is autoproteolytically cleaved *in cis* by VP4 (Dobos *et al* 1979, Hudson *et al* 1986b). The pVP2 is further processed into the mature capsid protein VP2 and four small peptides named after their length and occurrence pep46, pep7a, pep7b and pep11 (Da Costa *et al* 2002). The proteins pVP2, VP3 and VP4 are cleaved co-translationally, but pVP2 is processed during virus assembly to VP2 representing a two-step cleavage process (Müller & Becht 1982, Kibenge *et al* 1988). A second ORF on segment A (A2) overlaps with the 5'-region of ORFA1 encoding VP5 (Spies *et al* 1989). Segment B encodes the VP1 in a single ORF (B1), which represents the RNA-dependent RNA-polymerase (von Einem *et al* 2004).

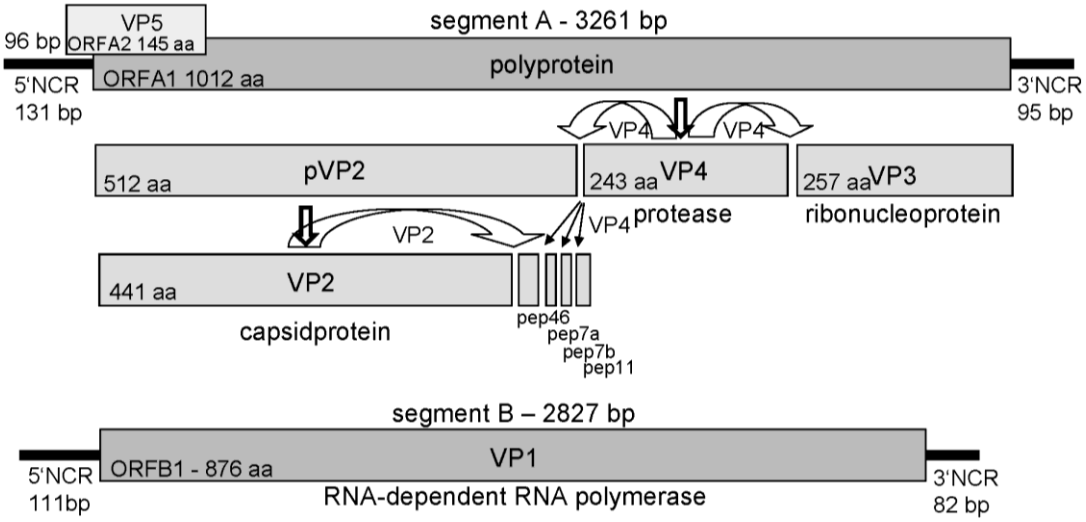

Figure 1: Genome of IBDV. Segment A encodes in the open reading frame (ORF) A1 for the polyprotein that is cleaved *in cis* by the protease VP4 into pVP2, VP4 and the ribonucleoprotein VP3. From pVP2 peptides pep11, pep7b and pep7a are cleaved off by VP4. The capsid protein VP2 itself cleaves off pep46. The second ORF on segment A (ORFA2) encodes VP5. Segment B encodes in one ORF (ORFB1) for VP1, the RNA-dependent RNA-polymerase.

Segment A is 3261 bp long in serotype I strains and 3264 bp in serotype II strains due to a 3 bp insertion in the polyprotein gene; segment B is 2827 bp long (Mundt & Müller 1995). The 5' NTR of segment A is 96 bp and the 3' NTR is 95 bp long, segment B exhibits an 111 bp long 5' NTR and a 82 bp long 3' NTR in serotype I and a 79 bp long 3' NTR in serotype II strains (Mundt & Müller 1995). Like in other multisegmented dsRNA viruses, IBDV also shares partially a common 5' NTR on both segments (28 bp out of the first 32 bp are identical), the starting point for transcription (Wickner 1993). Additionally a conserved motif (CUCCUC, nucleotide [nt] 71-76 on segment A and nt 86-91 on segment B) exists that is partially complementary to the 3' end of chicken 18 S rRNA, which might represent the binding site for ribosomes (Mundt & Müller 1995, Azad & Deacon 1980). The terminal sequences of both segments can form stem and loop structures due to terminal direct repeats that may contain signals for replication, expression and packaging (Kibenge *et al* 1996). For isolates of vvIBDV longer segments have been described (A: 3269 bp; B: 2834 bp) (Lim *et al* 1999).
Natural reassortment of both segments can occur (Wei *et al* 2006, Gao *et al* 2007). The natural reassortment rate was rather low and cannot be simply induced by co-infection of very virulent and attenuated IBDV in the same chicken, because not all reassorted viruses yielded infectious viruses (Boot *et al* 2000, Wei *et al* 2006, Wei *et al* 2008). Homologous recombination was described between live vaccines and wild-type strains (Hon *et al* 2008). The mutation rate of IBDV was determined with 3.8×10^{-3} substitutions/site/year (Owoade *et al* 2004).

1.1.8 Capsid

The capsid consists of VP2 trimers, arranged in a regular pentagonal or hexagonal array (Böttcher *et al* 1997, Hirai & Shimakura 1974, Tacken *et al* 2003). IBDV possess a T=13 dextro capsid symmetry (Böttcher *et al* 1997), although a more recent publication claimed a T=13 laevo symmetry (Pous *et al* 2005). IBDV showed a sedimentation rate of 460 S in sucrose gradient (Dobos *et al* 1979) and a buoyant density of 1.33 g/ml in a caesium chloride gradient (Nick *et al* 1976). The capsid mass was determined with 50 MDa, its thickness was 9 nm, its outer radii was 31-33 nm, its inner radii was 26-30 nm and the diameter at its widest point measured 70 nm (Böttcher *et al* 1997).

1.1.9 Attachment, penetration, uncoating

It was described that IBDV serotype I and II viruses use the same receptor (Rodríguez-Lecompte *et al* 2005) and several attempts have been made to identify it. Nieper & Müller (1996) described that the molecular weight of the IBDV receptor candidates were 40 or 46 kDa and that such proteins were present on CEC and lymphoid cells. Furthermore a N-glycosylated protein was described to be the receptor for IBDV (Ogawa *et al* 1998). Proteins with a molecular weight of 70, 82 and 110 kDa were isolated from cells of a LSCC-BK3 chicken B lymphoblastoid cell line that was able to be infected with

IBDV (Setiyono *et el* 2001). As a major component of the putative IBDV receptor was described the chicken Hsp90α (Lin *et al* 2007). Additionally proteins of 62, 68 and 72 kDa were identified to interact with IBDV (Lin *et al* 2007). A further study described α_4-integrin as the receptor. The recognition amino acid (aa) sequence for α_4-integrin was determined as the XDY motif, where X can be G, L, I or E and Y can be V or A. The motif with aa IDA is highly conserved in VP2. No replication was observed in cells lacking α_4-integrin and mutation D235A of VP2 completely omitted virus infectivity (Delgui *et al* 2009).

Receptor-mediated endocytosis was proposed as the penetration mechanism (Lin *et al* 2007). The IBDV-VP2 derived peptide pep46 was found to be associated with the viral capsid and was able to insert into membranes to form pores that disrupt the cell membrane and might allow water influx, thereby destroying the endosome to release the virus into the cytoplasm (Galloux *et al* 2010).

1.1.10 Replication

IBDV replicates in the cytoplasm and forms meanwhile crystalline aggregates of virus particles (Cheville 1967). Virus genome replication occurs very likely by the viral encoded RNA-dependent RNA polymerase VP1 (von Einem *et al* 2004). VP1 showed self-guanylylation activity resulting in VP1-pG molecules most likely bound by a phosphodiester linkage between the GMP and a serine or threonine, but lacks guanyl transferase activity (Spies & Müller 1990, Kibenge & Dhama 1997). The self-guanylylation activity of IBDV is most likely located in the N-terminal domain of VP1 (Pan *et al* 2007, Pan *et al* 2009). As shown for IPNV the VP1-pGpG serves most likely as a primer during initiation of genome replication, where it binds to the conserved pCpC at the conserved terminal end of the viral RNA template (Dobos 1993).

The genome was proposed to be replicated by asymmetric strand displacement also called semi-conservative mechanism (Spies *et al* 1987). Both genome segments were replicated simultaneous and equivalent (Wong *et al* 2007). Interestingly, viral RNA also entered the nucleus (Nieper *et al* 1999). VP1 was synthesized during early infection and later proteins of segment A (Müller & Becht 1982).

1.1.11 Morphogenesis

VP1 forms a covalent protein-DNA linkage with the 5' termini of both genome segments (Müller & Nitschke 1987b, Kibenge & Dhama 1997). The ribonucleoprotein VP3 binds also to dsRNA as well as to the genome linked form of VP1 producing the ribonucleoprotein complex (Tacken *et al* 2000, Luque *et al* 2009b). For VP3 it was proposed that it serves as a scaffolding protein for pVP2, which was subsequently processed to VP2 and can correctly bend to form the T=13 capsid (Martínez-Torrecuadrada *et al* 2000b). One virus particle can contain up to four segments, but also empty particles were observed (Luque *et al* 2009a). Package of less segments in one

particle resulted in lower buoyant density (1.33 g/ml: particles with both segments; 1.32 g/ml: one segment; 1.31 g/ml: no segment) (Müller & Becht 1982). Up to six segments were detected in IBDV propagated in chicken embryo fibroblasts by cesium chloride gradient (Müller *et al* 1986, Lange *et al* 1987).

1.1.12 Viral proteins

1.1.12.1 VP1

The smaller segment B contains one ORF encoding VP1 (Morgan *et al* 1988). Depending on the virus strain, VP1 consists of 876 aa in case of the serotype II strain OH due to deletions at position 650 and 789 (Islam *et al* 2001) or 878 aa for most of the classical isolates like P2, 2512 and Cu-1, the Australian strain 002-73 and the serotype II strain 23/82 (Mundt & Müller 1995, Yehuda *et al* 1999, Islam *et al* 2001). Due to two frameshifts in the middle of VP1, strains 002-73 and OH differ from other strains between aa 100-135 (Yehuda *et al* 1999, Yamaguchi *et al* 1997). Most of the vvIBDV strains like the British UK661 and the Japanese OKYM strain and the variant E strain encode for 879 aa (Yehuda *et al* 1999, Islam *et al* 2001). The longest VP1 with 881 aa was found for the classical strain CEF94 (Boot *et al* 2000). VP1 was described as a 90 kDa (Morgan *et al* 1988) or 97 kDa protein (Von Einem *et al* 2004). Three percent of the virion consist of VP1 (Dobos 1979). VP1 shows enzymatic activity of a RNA-dependent RNA-polymerase (Von Einem *et al* 2004), which has been suggested before (Morgan *et al* 1988, Gorbalenya & Koonin 1988, Spies *et al* 1987). VP1 has been found in a free form in the virion (Kibenge & Dhama 1997) or as a genome-linked protein called VPg that circularized segment A and B through a covalent protein-DNA linkage (Müller & Nitschke 1987b). VP3 interacts with both forms of VP1 shortly after translation, but at a late stage of infection VP3 interacts only with the genome linked form (Tacken *et al* 2000). Due to an abundance of VP3 (40% of the virion) over the amount of VP1 (3%), not all VP3 was bound to VP1 (Dobos *et al* 1979). Genome bound VP1 and free VP1 interact through their internal domain with VP3 (Tacken *et al* 2002). By this interaction, VP3 changes the conformation of VP1, removes a structural blockade of the polymerase active site that facilitates the accommodation of the template and incoming nucleotides, by that acting as a transcriptional activator (Garriga *et al* 2007). Using the yeast two-hybrid screening method an interaction of VP1 with the C-terminus of the eukaryotic initiation factor 4AII, but not with the full length protein, has been described (Tacken *et al* 2004).

1.1.12.2 VP2

The large ORF on segment A encodes the polyprotein that is processed into the N-terminal pVP2, VP4 (middle) and VP3 (C-terminal protein) by the viral protease VP4 (Hudson *et al* 1986b). The 512 aa long pVP2 is further processed during maturation into

the mature VP2 (the first 441 aa of pVP2) and four peptides named after their length pep46 (aa 442-487 of pVP2, 4875 Da), pep7a (aa 488-494 of pVP2, 633 Da), pep7b (aa 495-501 of pVP2, 660 Da) and pep11 (aa 502-512 of pVP2, 1186 Da) (Fahey *et al* 1985, Azad *et al* 1987, Sánchez & Rodriguez 1999, Martínez-Torrecuadrada *et al* 2000a, Da Costa *et al* 2002). The apparent molecular mass of pVP2 was 48 kDa (Becht 1980) and of VP2 41 kDa (Dobos 1979). VP2 was with 51% the most abundant protein of the virion (Dobos *et al* 1979). It was described that the viral capsid is composed of 780 copies of VP2 (Böttcher *et al* 1997).

Peptide cleavage between positions 487-488, 494-495 and 501-502 occurs between alanine-alanine bonds mediated by VP4 and at position 441-442 between an alanine-phenylalanine bond by VP2 autoproteolytical activity *in cis* mediated by D431 (Sánchez & Rodriguez 1999, Da Costa *et al* 2002, Irigoyen *et al* 2009). The peptides remain associated with the virion (Da Costa *et al* 2002). Pep7a, pep7b and pep11 were located at the external surface of the viral particle, whereas pep46 was at the fivefold axis underneath the surface (Chevalier *et al* 2005). Pep46 induced pores of 10 nm, which was insufficient for passage of an IBDV particle, but allowed water influx and eventually destabilization of the endosome to release the virus (Galloux *et al* 2010).

More than one self-interacting subdomain existed on VP2 so it can probably form trimers that interact with other trimers to form the capsid (Böttcher *et al* 1997, Tacken *et al* 2003). The only component of the virus icosahedral capsid is VP2 and its crystal structure has been resolved (Coulibaly *et al* 2005). VP2 is the major host-protective immunogen, because it was the only known IBDV protein to induce neutralizing antibodies (Azad *et al* 1987). Neutralizing antibodies bind in the highly hydrophobic region of VP2 called the variable domain between aa 206 and 350 with small hydrophilic regions present at each terminus between aa 212-224 (peak A) and 314-324 (peak B) (Bayliss *et al* 1990, Schnitzler *et al* 1993, Vakharia *et al* 1994). Most aa changes occurred in this variable region (Bayliss *et al* 1990). Mutations in peak B were responsible for antibody escape variants (Brown *et al* 1994, Eterradossi *et al* 1997, Eterradossi *et al* 1998). Beside the variable region, VP2 as a structural protein showed not many other mutations likely due to less structural flexibility (Lin *et al* 1993). The heptapeptide SWSASGS located in the variable region after peak B was described as another virulence marker, because it was only found in strains of high virulence (Heine *et al* 1991). It was described that VP2 can induce apoptosis in infected cells (Rodríguez-Lecompte *et al* 2005, Fernández-Arias *et al* 1997, Tham & Moon 1996).

1.1.12.3 VP3

The 257 aa long VP3 resides in the C-terminal part of the polyprotein from aa 756 to 1012 (Sánchez & Rodriguez 1999) as part of the large ORF of segment A. VP3 was described as a 32 kDa protein (Hudson *et al* 1986a) and was the second most abundant

structural protein of the virion (40%) (Dobos *et al* 1979). It was described that approximately 600 copies of VP3 are packed in a virion (Böttcher *et al* 1997). Sometimes also double bands with 33 and 32 kDa (Müller & Becht 1982, Kochan *et al* 2003) or three to four bands of 32 kDa and smaller (Tacken *et al* 2000) were observed.
VP3 has the ability to self-interact and to form trimers (Böttcher *et al* 1997, Tacken *et al* 2000, Tacken *et al* 2003), and to interact with VP1 with its C-terminus (Tacken *et al* 2002, Maraver *et al* 2003a). Co-localization of VP3 with pVP2, but not with VP2, was observed in insect cells (Oña *et al* 2004), but VP3 was not part of the capsid (Saugar *et al* 2005). A direct interaction between VP2 and VP3 was not found (Tacken *et al* 2002, Tacken *et al* 2003). VP3 is the ribonucleoprotein of IBDV that covers the dsRNA segments, which made it less accessible for RNase III (Luque *et al* 2009b). The positively charged domain of VP3 upstream of the VP1 binding domain interacted directly with the viral dsRNA genome segments (Tacken *et al* 2002). VP3 bound to ssRNA, dsRNA and ssDNA in a sequence independent manner, forming complexes of up to three VP3-ssRNA molecules (Kochan *et al* 2003). It was proposed that VP3 has a key role in virus assembly, because it probably provides a scaffold for the assembly of the capsid (Maraver *et al* 2003b). Binding of VP1 by VP3 was suggested to be the initiation step of capsid assembly (Lombardo *et al* 1999). Binding of VP1 to VP3 was crucial for pVP2 to be processed to VP2 during capsid assembly (Maraver *et al* 2003b). VP3 likely stabilizes the fivefold vertex, a crucial step for bending of the pVP2/VP2 capsomere lattice into icosahedral capsids (Martínez-Torrecuadrada *et al* 2000b). VP3 acted as a transcriptional activator for VP1 (Garriga *et al* 2007).

1.1.12.4 VP4

The large ORF on segment A encodes the polyprotein that contains in the middle VP4 from aa 513-755 (Sánchez & Rodriguez 1999). The apparent molecular mass of VP4 is 28 kDa (Hudson *et al* 1986b). Contradictory reports exist, whether VP4 is a structural protein (Dobos *et al* 1979, Hudson *et al* 1986b, Böttcher *et al* 1997) or not (Granzow *et al* 1997, Lombardo *et al* 1999, Rodríguez-Lecompte & Kibenge 2002, Wang *et al* 2009).
It was shown that VP4 was the protease that cleaved co-translational (Jagadish *et al* 1988). The exact cleavage sites were determined as ^{511}LA↓A^{513} between pVP2 and VP4 and ^{754}MA↓A^{756} between VP4 and VP3 (the numbers indicate the aa position in the polyprotein, the letter represents the aa in the one letter code) (Sánchez & Rodriguez 1999). The protease cleaved itself out of the polyprotein *in cis* (Lejal *et al* 2000). VP4 further cleaves off three peptides from pVP2 at positions ^{486}QA↓A^{488}, ^{493}RA↓A^{495} and ^{500}RA↓A^{502} *in trans* (Sánchez & Rodriguez 1999, Birghan *et al* 2000). The active center of the protease was composed of a serine at aa position 652 and a lysine at aa 692, forming together a catalytic dyad, which groups it together with Lon proteases identified in bacteria (Birghan *et al* 2000, Lejal *et al* 2000). Unlike other Lon proteases it lacked an

ATPase domain and therefore VP4 was referred to as a non-canonical Lon protease (Birghan *et al* 2000). The protease was specific for the IBDV polyprotein and was not able to cleave the polyprotein of IPNV (Lejal *et al* 2000). It was shown that VP4 interacted with itself (Tacken *et al* 2003). VP4 formed tubular structures with a diameter of 24-26 nm that localized in the cytoplasm and in the nucleus of IBDV infected cells (Harkness *et al* 1975, Özel & Gelderblom 1985, Granzow *et al* 1997).

1.1.12.5 VP5

VP5 is encoded by a second ORF on segment A overlapping with the larger ORF probably developed by gene overprinting (Spies *et al* 1989, Tan *et al* 2004). VP5 of IBDV is a non-structural protein (Mundt *et al* 1997). In classical IBDV strains the VP5 protein was usually 145 aa long (Mundt *et al* 1995), but for several vvIBDV strains, the GLS variant strain and the OH serotype II strain an earlier start codon has been described resulting in 149 aa length of VP5 (Brown & Skinner 1996, Rudd *et al* 2002, Kong *et al* 2004). The apparent molecular mass was 21 kDa in the classical European IBDV strain P2 (Mundt *et al* 1995). VP5 interacted with itself (Tacken *et al* 2000) and this domain was mapped between aa 73 and 90 and a transmembrane domain was predicted from aa 69 to 88 (Tacken *et al* 2003). VP5 accumulated in the plasma membrane and with its intracellular N-terminus, a hydrophobic helix and its extracellular C-terminus, it was classified as a class II membrane protein (Lombardo *et al* 2000). It probably forms a pore structure by the barrel stave mechanism in the plasma membrane to release IBDV progeny and thereby destroys the bursal B lymphocyte population (Lombardo *et al* 2000, Ojcius & Young 1991).

VP5 is dispensable for viral replication, but important for pathogenicity (Mundt *et al* 1997). VP5 deficient virus decreased immunosuppression *in vivo* and induced protection from vvIBDV challenge, which made it interesting to use as a vaccine, while the absence of VP5 expression serves as a marker (Qin *et al* 2010). VP5 induced apoptosis in a late stage of infection (Vasconcelos & Lam 1994, Lam 1997, Ojeda *et al* 1997, Tanimura & Sharma 1998, Yao & Vakharia 2001, Liu & Vakharia 2006).

1.2 Virus-host interaction

The interaction of cellular proteins with elements of the viral replication machinery will certainly help to understand how viruses are able to hijack cells. In turn it will be likely possible based on this knowledge to develop strategies to prevent or intervene with viral infections. It has been shown in the past that dsRNA binding proteins or proteins related to them interacted with RNA as well as protein elements of viruses.

1.2.1 Cellular dsRNA binding proteins

Proteins that are able to bind dsRNA share a common motif that is evolutionary highly conserved. This dsRNA binding domain (DRBD) is 65-68 aa long (St Johnston *et al*

1992) and binds to as little as 11-16 bp of dsRNA, whereas 11 bp are the equivalent to one single turn of the helix (Manche *et al* 1992, Ryter & Schultz 1998). The interaction was sequence independent, because binding occured with the phosphodiester backbone or the ribose 2'OH group specific for RNA (Ryter & Schultz 1998, Fierro-Monti & Mathews 2000). The DRBD attaches to two minor grooves and across one major groove of an A-form dsRNA helix (Ryter & Schultz 1998). Two hydrogen bonds are sufficient to identify uniquely one base pair (Seeman *et al* 1976).
Additional to RNA-protein interactions, the DRBD mediated also protein-protein interactions in the absence of dsRNA (Fierro-Monti & Mathews 2000).

1.2.1.1 Protein kinase RNA-activated

Environmental stress like a viral infection or cellular stress caused by nutritional deprivation results in accumulation of dsRNA in the cell and induces the innate immune response of the cell. The presence of dsRNA in the cell can be of viral origin like the dsRNA genome, a replicative intermediate, the secondary structure of a ssRNA virus or overlapping convergent transcripts of DNA viruses (Jacobs & Langland 1996). DsRNA is recognized by TLR 3, which induces activation of NFκB and the expression of type I IFN (Alexopoulou et al 2001). Production of IFN induces transcription and activation of protein kinase RNA-activated (PKR), also called p68 kinase (scheme of activation and downstream processes depicted in Figure 2) (Meurs *et al* 1990, Chu *et al* 1998).
Two DRBDs located in the N-terminus of PKR associate with dsRNA (Meurs *et al* 1990). Low concentrations of dsRNA activate PKR that undergoes RNA-dependent autophosphorylation (intra- and intermolecularly), but high concentrations of dsRNAs like poly I/C inhibit activation in a dose-dependent manner (Galabru *et al* 1989, Thomis & Samuel 1995). PKR autophosphorylation appeared on at least four different serine and threonine residues (Thomis & Samuel 1995) and was dependent on the presence of dsRNA and Mn^{2+} cations (Galabru & Hovanessian 1987). Virus associated (VA) RNA_I of adenovirus activates or inhibits PKR in a dose-dependent manner. Activation of PKR by VA RNA_I was irreversible, probably due to conformational changes (Galabru *et al* 1989).
Eucaryotic initiation factor (eIF)-2 consists of the subunits eIF-2α, eIF-2β and eIF-2γ. It mediates binding of the Met-tRNA to the ribosomal subunit, which is the initial step of translation initiation. The factor eIF-2γ is linked to the Met-tRNA and eIF-2α and eIF-2β bind GTP that increases the Met-tRNA binding rate. After hydrolysis of GTP to GDP the guanosine nucleotide exchange factor (GEF) eIF-2B exchanges GDP bound to eIF-2 with GTP and the eIF-2 complex is released (Safer 1983). PKR phosphorylates eIF-2α on serine 51 of the eIF-2 complex (Choi *et al* 1992, Farrell *et al* 1977, Galabru & Hovanessian 1985). The factor eIF-2B is unable to substitute GTP for GDP when eIF-2α is phosphorylated, which prevents eIF-2 recycling and stops initiation of translation (Panniers & Henshaw 1983, Safer 1983, Manche *et al* 1992).

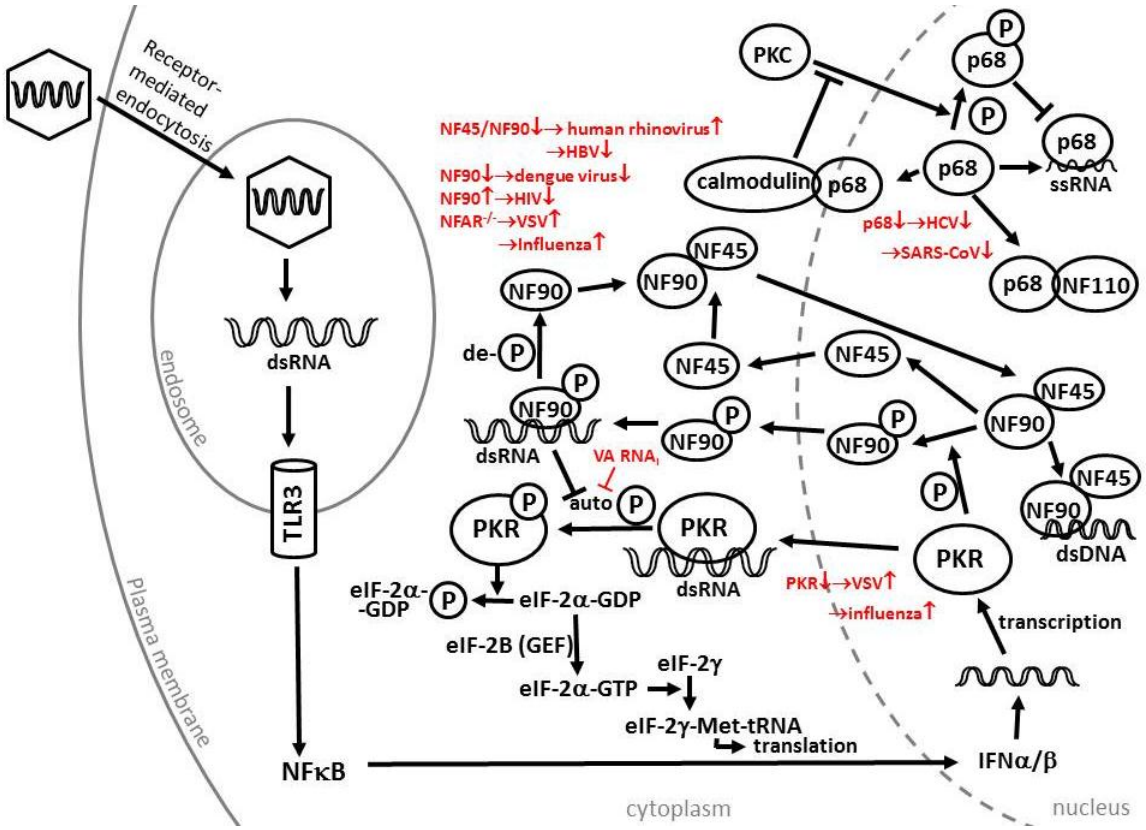

Figure 2: Simplified diagram of the recognition of dsRNA by TLR3 and downstream signaling via NFκB inducing an IFN response. PKR gets autophosphorylated and stops translation as well as phosphorylates NF90 that localizes to the cytoplasm and associates with dsRNA. Once bound to NF45, it localizes to the nucleus. Also depicted is p68 function and inhibition of its ssRNA binding activity by PKC and calmodulin.

1.2.1.2 Nuclear factor associated with dsRNA (NFAR) proteins

The NFAR group of proteins contains NF45 (=ILF2) and the DRBD containing proteins NF90 (=NFAR-1, TCP80, DRBP76 or ILF3), its splice variant NF110 (NFAR2, TCP110, CBTF and MMP4) and RNA helicase A (RHA, DHX9) (Patel *et al* 1999, Saunders *et al* 2001b, Xu *et al* 2003, Viranaicken *et al* 2006, Brzostowski *et al* 2000, Isken *et al* 2007).

The *ILF3* gene encoded on human chromosome 19p13.1-p13.2 is 38 kbp long, contains 21 exons and can be spliced at two sites alternatively, giving rise to five similar proteins (Saunders *et al* 2001a, Duchange *et al* 2000, Reichman *et al* 2003). The N-terminus of all proteins is identical and if exon 18 is translated, NF90a, b and c were translated. If exon 18 was excised, because of a different acceptor site, NF110 was observed, which is 192 aa longer than NF90. A second splicing event occurs in exon 14 inserting the peptide NVKQ between the two DRBDs (aa 401-468 and 524-591) generating NF90b (706 aa) and NF110b (898 aa); the 4 aa shorter proteins are called NF90a (702 aa) and NF110a (894 aa). NF90c carries a 2 bp insertion resulting in a shorter protein of 670 aa whose expression was not verified in comparison to NF90a, b, NF110a and b, which were detected *in vivo* (Duchange *et al* 2000, Reichman *et al* 2003). All NFAR isoforms

contain a domain of approximately 150 aa that is homologous to NF45, called NF45 Homology Domain (Reichman *et al* 2003). They also possess two DRBDs that are necessary to bind dsRNA (Saunders *et al* 2001b).

NF45 is encoded on human chromosome 1q21.3 and on murine chromosome 3F.1. Additional pseudogenes were detected on chromosome 2 and 14 in the human genome (Zhao *et al* 2005). NF45 forms heterodimers with NF90 or NF110 (Guan *et al* 2008). The NF90-NF45 complex acted as a transcriptional activator (Aoki *et al* 1998, Ranpura *et al* 2008, Kiesler *et al* 2010). The NF45 binding site is localized within the N-terminal region (aa 1-418) of NF90 (Reichman *et al* 2002). In context with NF90, NF45 was discussed to be the regulatory subunit of this complex and NF90 the mediator of transcriptional activation (Reichman *et al* 2002), because NF90 contained two DRBDs in its C-terminus (aa 334-591), by which it bound to dsRNA (Parker *et al* 2001). NF90 also possesses a nuclear localization sequence (NLS) (Reichman *et al* 2002). NF45 and NF90 were located predominantly in the cellular nucleus (Kao *et al* 1994). After stimulation of rested T cells, mRNA levels of both proteins were not altered (Kao *et al* 1994), but serine phosphorylation of NF45 increased while NF90 was unchanged (Kiesler *et al* 2010). *In vitro* translated NF45 and NF90 did not bind DNA, because phosphorylation of the complex was necessary for its binding activity (Kao *et al* 1994, Corthésy & Kao 1994).

After an unfolded protein response, cells can undergo apoptosis and translation stops. Some cellular genes like the cellular inhibitor of apoptosis protein 1 (cIAP1) possess an IRES (internal ribosome entry site) structure for cap-independent translation, for which additional *trans*-acting factors like NF45, NF90 and RHA were needed to mediate the interaction with the 40 S ribosome subunit (Graber *et al* 2010).

PKR formed heterodimers with NF90 and NF110 *in vitro* and *in vivo* (Saunders *et al* 2001b). NF45, NF90 and NF110 were phosphorylated by PKR in a dsRNA-dependent manner, whereas no direct interaction between NF45 and PKR was observed, but it was rather bridged by NF90 (Ting *et al* 1998, Parker *et al* 2001, Saunders *et al* 2001b). PKR phosphorylated NF90 and NF110 on aa T188 and T315, which led to dissociation of NF45. Phosphorylation of NF90 and NF110 resulted in shuttling to the cytoplasm where they bound viral RNAs and impeded viral replication of vesicular stomatitis virus (VSV), Sendai virus and encephalomyocarditis virus (Harashima *et al* 2010). Binding of NF45 to NF90 or NF110 induced localization to the nucleus (Harashima *et al* 2010). In the presence of dsRNA, NF90 inhibited autophosphorylation of PKR probably through competitive binding to dsRNA (Parker *et al* 2001).

1.2.1.3 DEAD box protein p68

The DEAD box was named in the one-letter amino acid code after its motif II consisting of Asp-Glu-Ala-Asp (Linder *et al* 1989). The superfamily II that contains the DEAD-box protein family represents the largest family of RNA helicases (Rocak & Linder 2004).

RNA helicases utilize energy of NTP hydrolysis to modulate RNA structures (Abdelhaleem 2005). DEAD box proteins are characterized by nine motifs (see 3.2.1) that were located in the conserved helicase core (Fuller-Pace 2006). Helicases unwind six base pairs per kinetic step and are highly specific so that a substitution for each other was not possible (Tanner & Linder 2001). They require a single strand overhang to load on the substrate (Rozen *et al* 1990). RNA helicases disrupt RNA-protein interactions (RNPase) in an energy-dependent fashion (Jankowsky *et al* 2001).

One member of the DEAD box protein family is p68, named after its molecular mass (also called DDX5) (Linder *et al* 1989). It exhibited an RNA-dependent ATPase activity and functioned as an ATP-dependent RNA helicase *in vitro* (Iggo & Lane 1989, Hirling *et al* 1989, Jost *et al* 1999). The helicase p68 possessed the ability to unwind dsRNA bidirectional, without the use of cofactors (Huang & Liu 2002). Mammalian p68 was localized in the nucleus (Iggo & Lane 1989). It was also shown that p68 was involved in modulating secondary RNA structures (Rössler *et al* 2001). Binding of p68 to dsRNA is ATP independent, but interaction with ssRNA requires ATP (Huang & Liu 2002).

In its C-terminus p68 contains an IQ motif that is able to bind either protein kinase C (PKC) or calmodulin due to an overlap of 19 aa of both binding sites (Buelt *et al* 1994). PKC phosphorylated p68 and by that inhibited binding of p68 to ssRNA (Yang *et al* 2004). The cellular protein calmodulin binds to p68 in a Ca^{2+} dependent manner, which subsequently inhibited phosphorylation by PKC (Buelt *et al* 1994). No calmodulin binding site has been detected in chicken p68 (Buelt *et al* 1994). Both, phosphorylation by PKC and binding of calmodulin, inhibited ATPase function of p68 (Buelt *et* al 1994). The p68 monomers possessed the ability to form homodimers and also interacted with p72 (Ddx17), an RNA-dependent ATPase with RNA helicase activity (Ogilvie *et al* 2003). Additionally, p68 interacted with NF110 (Ogilvie *et al* 2003).

The multifunctional p68 is involved in transcription, pre-mRNA splicing, mRNA stability and ribosome biogenesis (Liu *2*002, Linder 2006, Fuller-Pace 2006, Merz *et al* 2007). It has been identified as part of the spliceosome and in spliced mRNAs carrying an exon junction complex (Neubauer *et al* 1998, Merz *et al* 2007). In mammals p68 was involved in transcriptional activation as shown for the tumor suppressor protein p53 (Bates *et al* 2005) as well as in repression of transcription when binding to p72 (Wilson *et al* 2004).

1.2.2 Examples of virus-host interactions

Certain members of the NFAR proteins (NF90, NF45 and RHA) have been observed that they were specifically associated with both the termini of the bovine viral diarrhea virus (BVDV) and the hepatitis C virus (HCV) genome, which resulted in functional bridging of the genome displaying a loop-like configuration (Isken *et al* 2003, Isken *et al* 2007). Decrease of RHA by siRNA inhibited BVDV and HCV replication, indicating a role as a host factor supporting viral protein translation and RNA replication (Isken *et al* 2003,

Isken *et al* 2007). The cellular proteins bound to specific RNA motifs, like the domain III of the 5'NTR and the poly-U/UC and SLIII motif in the 3'NTR of HCV (Isken *et al* 2007). All NFAR proteins (NF90, NF110, NF45 and RHA) were observed in the cytoplasm during HCV infection, where they formed a viral/cellular ribonucleoprotein complex (Isken *et al* 2007). NS5A of HCV and its viral RNA specifically interacted with NF90 in cells, which resulted in functional HCV replication complexes (Isken *et al* 2007). NF90, RHA and NF45 have been identified as dengue virus 3' SL RNA binding proteins. Unlike RHA, NF90 co-localized during an infection with NS3 in the cytoplasm and was a positive regulator of dengue virus replication (Gomila *et al* 2011). In the context of HCV, binding of p68 and p72 amongst others to the 3'NTR was observed. Downregulation of p68 resulted in decreased amounts of replicon RNA of HCV (Harris *et al* 2006). The RNA-dependent RNA-polymerase of HCV NS5B interacted with p68 and recruitment of p68 enhanced viral RNA transcription. Expression of only NS5B was sufficient to localize p68 from the nucleus to the cytoplasm (Goh *et al* 2004). The dsRNA binding protein DDX3 is a helicase and normally localized in nuclear speckles, but after HCV infection it interacted with the core protein in distinct spots in the perinuclear region (Owsianka & Patel 1999). The HCV core protein also interacts with NF45 in a RNA-dependent manner and both co-localize in the cytoplasm (Lee *et al* 2011).

The helicase of severe acute respiratory syndrome-corona virus (SARS-CoV) interacted with p68 and downregulation of p68 by siRNA inhibited viral replication. Therefore, p68 seemed to be a co-activator of the SARS-CoV helicase (Chen *et al* 2009).

Overexpression and subsequent pull-down of the proteins PB1, PB2 and PA that assemble to the polymerase of human influenza virus, co-immunoprecipitated the cellular proteins p68 and DDX3 amongst others (Jorba *et al* 2008).

Without PKR, VSV and influenza A viruses were able to replicate *in vitro* and *in vivo*, which caused high mortality in infected mice (Balachandran *et al* 2000).

The NF90-NF45 heterodimer interacted with the IRES of human rhinovirus type 2 and prevented translation initiation by blocking the binding of the 40S ribosomal unit to the IRES and therefore likely inhibits effective replication of the virus. If NF45 and NF90 did not associate in a heterodimer; they were not able to inhibit viral replication (Merrill *et al* 2006, Merrill & Gromeier 2006).

VA RNA_I of adenovirus blocked activation of PKR by dsRNA and by that inhibited an IFN response (Kitajewski *et al* 1986).

NF90 and NF110 (NFAR) negatively regulated the nuclear export of mRNA through TAP-p15 export and by that modulate translation. In NFAR negative cells, VSV and influenza virus replicated to 4- and 36-fold higher viral titers, respectively, indicating a role of NFAR in cellular host defense (Pfeifer *et al* 2008). In contrast to this, RHA interacted with NS1 of influenza A virus in a RNA dependent manner and was described as a positive regulator of influenza A virus replication (Lin *et al* 2012). Similarly, the

dsRNA binding protein Staufen, which is localized in the cytoplasm, interacted and co-localized with influenza A virus protein NS1 in the nucleus during replication. A virus with mutant NS1 unable to bind to Staufen showed deficiencies in viral protein synthesis (Falcón *et al* 1999). Staufen additionally interacted with nucleoprotein (NP) of influenza virus and siRNA knock-out of Staufen resulted in a 5 to 10-fold reduced viral titer, while showing no effect on viral replication of VSV (De Lucas *et al* 2010).

The Staufen protein interacted with its DRBD3 to the transactivation responsive (TAR) region of human immunodeficiency virus (HIV) 1. Overexpression of Staufen in infected cells resulted in a threefold enhanced incorporation of RNA, but at the same time impaired infectivity 6.7-fold in a dose-dependent manner (Mouland *et al* 2000). Similarly, RHA bound to the stem of HIV-1 TAR through DRBD2 (aa 235-249) and RHA overexpression enhanced viral mRNA synthesis in a dose-dependent manner and resulted in higher HIV replication. In a TAR independent fashion, RHA interacted with the κB element in the long terminal repeat of HIV-1 (Fujii *et al* 2001).

HIV protein Rev regulates the transport of viral transcripts from the nucleus to the cytoplasm by binding to the Rev response element (RRE). For the shuttling, Rev contains a NLS and a NES, with which it was linked to CRM1 (Askjaer *et al* 1998). Rev was inhibited by interaction with the cellular protein NF90ctv that comprises the NES-, DRBD2- and RG-domain with its three SH3 motifs involved in protein-protein interaction. Competition between NF90 and Rev for CRM1 or for RRE binding was able to interfere with the function of Rev (Urcuqui-Inchima *et al* 2006). Overexpression of NF90ctv induced an antiviral state mediated by IFNs, which inhibited HIV-1 replication (Krasnoselskaya-Riz *et al* 2002). RHA released CTE-(constitutive transport element, found in simple retroviruses) and RRE-(in complex retroviruses) containing mRNA from the spliceosome, therefore, RHA regulates HIV expression at the post-transcriptional level (Li *et al* 1999). RHA facilitated the export of CTE into the cytoplasm, in which RHA interacts with the secondary structure (loop A) of the CTA RNA. Overexpression of CTE resulted in re-location of RHA to the cytoplasm (Tang *et al* 1997). DDX3 was able to bind Rev and enhances Rev-mediated, but not CTE-dependent, expression by export of HIV unspliced mRNAs. DDX3 suppression inhibited HIV-1 replication (Yedavalli *et al* 2004).

The NF90-NF45 complex bound to the highly conserved encapsidation signal ε of hepatitis B virus (HBV) pre-genomic RNA that folds into a stem-loop structure, which is important for protein priming of the HBV polymerase. Without this complex the polymerase was unable to bind RNA and viral replication was arrested (Shin *et al* 2002).

2 Material and Methods

2.1 Material

2.1.1 Virus strains

- **D78:** Nobilis Gumboro D78, classical strain of IBDV ('intermediate' vaccine strain), kindly provided by Ruud Hein, Intervet, Millsboro, DE, USA
- **8903:** variant strain of IBDV, Delaware variant E (E/Del) subtype, kindly provided by Ruud Hein, Intervet, Millsboro, DE, USA
- **GLS-05:** variant strain of IBDV, Grayson Laboratory Strain (GLS) subtype, kindly provided by Ruud Hein, Intervet, Millsboro, DE, USA
- **H5N2:** A/duck/NC/674964/07, kindly provided by David Stallknecht, University of Georgia, Athens, GA, USA

2.1.2 Bacteria strains

- ***E. coli* strain XL1-Blue** (Stratagene), endA1 gyrA96(nal^R) thi-1 recA1 relA1 lac glnV44 F'[::Tn10 proAB$^+$ lacI^q Δ(lacZ)M15] hsdR17(r_K^- m_K^+)
  This strain allows blue-white color screening for the selection of cDNA fragment containing recombinant plasmids and encodes for a tetracycline resistance protein.
- ***E. coli* strain DH10Bac™** (Invitrogen)
  F– mcrA Δ(mrr-hsdRMS-mcrBC) Φ80lacZΔM15 ΔlacX74 recA1 endA1 araD139 Δ(ara leu) 7697 galU galK λ– rpsL nupG/ pMON14272/pMON7124
  This strain was used to generate recombinant bacmids based on the Bac-to-Bac® Baculovirus Expression System (Invitrogen). The system consists of a parent bacmid that recombines with the donor plasmid, pFastBacDual™ by site-specific transposition to create a recombinant expression bacmid containing the gene of interest. Additionally it contains a helper plasmid encoding for the tetracycline resistance protein and the transposase necessary for the Tn7 transposition function *in trans*. The parent bacmid encodes the lacZα complementation factor for efficient blue-white color screening of positive recombinants and a kanamycin resistance gene.

2.1.3 Media and serum

- **Dulbecco's Modified Eagles's Medium (DMEM)**
  - with 1g/l or 4.5g/l glucose — Thermo Scientific
- **Minimal Essential Medium:**

Mixture of equal parts Minimal Essential Medium (MEM) with Earle's balanced salt solution and MEM with Hank's balanced salt solution (both with L-glutamine)

- MEM with Earle's balanced salt solution — Invitrogen
- MEM with Hank's balanced salt solution — Invitrogen

- **Recovery™ cell culture freezing medium** Invitrogen
- **HyClone SFX-Insect Cell Culture medium** Thermo Scientific
- **Fetal Bovine Serum (FBS)** Mediatech

2.1.4 Cell lines

- **BHK-21:** Baby hamster kidney cells
  Collection of Cell Lines in Veterinary Medicine, Riems, Germany; RIE 194
  Medium: MEM supplemented with 10% FBS; Condition: 37°C with 5% CO_2
- **Chicken embryo cells (CEC):** were derived from embryonated specific-pathogen-free eggs (Sunrise Farms, Catskill, NY, USA)
  Medium: DMEM containing 1g/l glucose and 10% FBS; Condition: 37°C with 5% CO_2
- **DF-1:** Chicken embryo fibroblast cell line (Himly *et al* 1998)
  American Type Culture Collection (ATCC), obtained as a gift from Dr. Sellers (PDRC, University of Georgia, Athens, GA, USA)
  Medium: DMEM with 4.5g/l glucose and 10% FBS; Condition: 37°C with 5% CO_2
- **HEK 293T:** human embryonic kidney cell line variant 293T clone 17, encodes the SV40 Large T-antigen allowing episomal replication of transfected plasmids containing the SV40 origin of replication (ATCC); received as a gift from Dr. Villegas (PDRC, University of Georgia, Athens, GA, USA)
  Medium: MEM supplemented with 10% FBS; Condition: 37°C with 5% CO_2
- **High5:** Ovarian cells of the cabbage looper *Trichoplusia ni* (Invitrogen); received as a gift from Dr. Garcia (PDRC, University of Georgia, Athens, GA, USA)
  Medium: HyClone SFX-Insect Cell Culture medium; Condition: 27°C
- **QM-7:** Quail muscle cell line
  Collection of Cell Lines in Veterinary Medicine, Riems, Germany; RIE 466
  Medium: MEM supplemented with 10% FBS; Condition: 37°C with 5% CO_2
- **Sf9:** Cell line of pupal ovarian tissue of the fall armyworm *Spodoptera frugiperda* (Invitrogen); received as a gift from Dr. Garcia (PDRC, University of Georgia, Athens, GA, USA); Medium: HyClone SFX-Insect Cell Culture medium; Condition: 27°C
- **Vero:** African green monkey kidney cell line, VERO 76
  Collection of Cell Lines in Veterinary Medicine, Riems, Germany, RIE 228
  Medium: DMEM with 4.5g/l glucose and 10% FBS; Condition: 37°C with 5% CO_2

2.1.5 Plasmids

- **pFastBac™ Dual** (Invitrogen), 5238 bp

The pFastBac™ Dual plasmid (map see 6.3.1) contains two multiple cloning sites (MCS) under two different promoters (p10 and polyhedrin promoter). Polyadenylation signals are located downstream of the MCS. Two Mini Tn7 elements permit site-specific transposition of the gene of interest to the bacmid. The MCS and a gentamicin

resistance gene are located within the Tn7 elements. This plasmid contains additionally a pUC origin of replication allowing the plasmid to replicate in bacteria cells to high copy numbers and an ampicillin resistance gene for selection.

- **pcDNA3** (Invitrogen), 5446 bp

The pcDNA3 plasmid (map see 6.3.2) can be used for expression of an inserted gene of interest. For that purpose it contains the human cytomegalovirus (CMV) immediate-early promoter upstream of the MCS and downstream a polyadenylation signal sequence. The MCS is enclosed by T7 and Sp6 promoter sequences. The plasmid also has a ColE1 origin of replication and an ampicillin resistance gene for bacteria colony selection. Additionally, it contains a neomycin resistance gene under the control of the SV40 promoter, followed by a SV40 polyadenylation signal sequence.

- **pCR®2.1-TOPO®** (Invitrogen), 3931 bp

The pCR®2.1-TOPO® plasmid (map see 6.3.3) was supplied linearized in the kit and contains single overhanging 3' deoxythymidine residues. The MCS is embedded in the gene for the lacZα complementation factor for an efficient blue/white screening of positive recombinants. It has a pUC origin of replication for high copy number replication in bacteria cells. The plasmid also contains an ampicillin resistance gene and a kanamycin resistance gene.

- **puc18** (Thermo Scientific), 2686 bp

The puc18 plasmid (map see 6.3.4) is a high copy plasmid due to the presence of the pMB1 replicon *rep*. The *bla* gene encodes the beta-lactamase allowing the bacteria cell that contains the plasmid to be resistant to ampicillin. The MCS is located within the *lacZα* complementation factor allowing blue-white screening.

2.1.6 Antibodies

- **mAb His:** Monoclonal Anti-Polyhistidine antibody produced in mouse hybridoma cells, clone His-1 (Sigma-Aldrich), recognizes synthetic poly-Histidine, as well as native or denatured, reduced forms of proteins tagged with six histidines (6x His-tag)
- **mAb His-POD:** Monoclonal Anti-poly-Histidine-Peroxidase (POD) conjugated antibody produced in mouse hybridoma cells (Sigma-Aldrich), recognizes 6xHis tagged proteins
- **R-α-FLAG:** ANTI-FLAG® antibody generated in rabbits (Sigma-Aldrich), recognizes the FLAG epitope (DYKDDDDK) located on FLAG-tagged fusion proteins
- **mAb FLAG:** Monoclonal ANTI-FLAG® M2 antibody produced in mouse hybridoma cells (5mg/ml) (Sigma-Aldrich), recognizes a FLAG epitope at any position in the fusion protein.
- **mAb Bac:** Monoclonal Anti-AcV5 antibody produced in mouse hybridoma cells (Sigma-Aldrich), recognizes a nine amino acid residue tag (SWKDASGWS) of the baculovirus *Autographa californica* GP64 envelope fusion protein

- **mAb β-Actin-POD:** Monoclonal Anti-β-Actin-POD conjugated antibody produced in mouse hybridoma cells (Sigma-Aldrich)
- **mAb MBP:** Monoclonal anti-maltose binding protein (MBP) antibody produced in mouse hybridoma cells [New England Biolabs (NEB)]
- **mAb MBP-POD:** Monoclonal anti-MBP antibody covalently linked to horseradish POD (HRP) produced in mouse hybridoma cells (NEB)
- **mAb M1:** Monoclonal anti influenzavirus A matrix (M) protein antibody, mouse hybridoma M2-1C6-4R3 (ATCC)
- **R-α-NP:** Polyclonal serum against influenzavirus A nucleoprotein from strain A/FPV/Rostock/34, generated in a rabbit (Klopfleisch *et al* 2006)
- **α-R-POD:** Anti-Rabbit IgG–POD conjugated antibody generated in goat (Sigma-Aldrich)
- **α-M-POD:** Anti-Mouse IgG−POD conjugated antibody generated in goat (Sigma-Aldrich)
- **α-Ch-POD:** Anti-Chicken IgY−POD conjugated antibody generated in rabbit (Sigma-Aldrich)
- **α-R-FITC:** Goat Anti-Rabbit IgG Fluorescein (FITC)-conjugated [(Jackson ImmunoResearch (JIR)]
- **α-R-Cy3:** Goat Anti-Rabbit IgG Cyanine (Cy) 3-conjugated (JIR)
- **α-R-Cy5:** Goat Anti-Rabbit IgG Cy5-conjugated (JIR)
- **α-M-FITC:** Goat Anti-Mouse IgG FITC-conjugated (JIR)
- **α-M-Cy3:** Goat Anti-Mouse IgG Cy3-conjugated (JIR)
- **α-M-Cy5:** Goat Anti-Mouse IgG Cy5-conjugated (JIR)
- **α-Ch-FITC:** Goat Anti-Chicken IgY FITC-conjugated (JIR)
- **α-Ch-Cy3:** Goat Anti-Chicken IgY Cy3-conjugated (JIR)
- **α-Ch-Cy5:** Goat Anti-Chicken IgY Cy5-conjugated (JIR)
- **R-α-IBDV:** Polyclonal serum raised against purified IBDV particles generated in a rabbit (Mundt *et al* 1995)
- **Ch-α-IBDV:** Polyclonal serum raised against IBDV generated in chicken, directed against the IBDV protease VP4 (kindly provided by Dr. E. Mundt)
- **mAb VP3:** Mouse monoclonal antibody raised against IBDV protein VP3 (also called IBDV2, Granzow *et al* 1987)
- **mAb VP4:** Mouse monoclonal antibody raised against IBDV protease VP4 (also called IBDV6, Granzow *et al* 1987)
- **Ch-α-VP1:**Polyclonal chicken serum raised against VP1 fused to a 6x His-tag, expressed in a baculovirus system (Letzel *et al* 2007, kindly provided by Dr. E. Mundt)

- **R-α-VP3:** Polyclonal serum raised against VP3 encoding sequence (aa 756-973 of D78) fused to a 6x His-tag, expressed in the baculovirus system and purified by its 6x His-tag, generated in a rabbit (kindly provided by Dr. E. Mundt)
- **R-α-NF45:** Polyclonal serum raised against NF45-His (NF45 fused to a 6x His-tag) expressed in the baculovirus system generated in a rabbit, described in 3.1.5
- **R-α-p68:** Polyclonal serum raised against p68-His (p68 fused to a 6x His-tag) expressed in the baculovirus system generated in a rabbit, described in 3.2.5

2.1.7 Chemicals

Acetic acid	T.J. Baker
Acrylamide/Bis-acrylamide, 30% solution, 29:1	Sigma-Aldrich
Agar Noble	Difco
Agarose	Denville Scientific Inc.
Ammonium persulfate (APS)	Fisher Scientific
Bacto™ Tryptone	BD
Bromphenol blue	BioChemika
Calcium chloride ($CaCl_2$)	Sigma-Aldrich
Chloroform	Mallinckrodt Chemicals
Complete, EDTA-free, proteinase Inhibitor Cocktail Tablet	Roche
Deoxycholic acid sodium salt	Fluka
4',6-diamidino-2-phenylindole (DAPI)	Invitrogen
1,4-Diazabicyclo[2.2.2]octane (DABCO)	Sigma-Aldrich
Dimethyl sulfoxide (DMSO)	Mediatech, Sigma-Aldrich
Dimethylformamide	Sigma-Aldrich
Dipotassium phosphate (K_2HPO_4)	T.J. Baker
Disodium phosphate (Na_2HPO_4)	Sigma-Aldrich
Dithiothreitol (DTT)	Fluka
Ethanol	Sigma-Aldrich
Ethidium bromide solution (10 mg/ml)	Sigma-Aldrich
Ethylenedinitrilotetraacetic acid (EDTA)	Sigma-Aldrich
Formaldehyde solution	Sigma-Aldrich
D-(+)-Glucose	Sigma-Aldrich
Glycerol	Sigma-Aldrich
Glycin	Sigma-Aldrich
Hydrochloric acid (HCl)	J.T. Baker
Hydrogen peroxide (H_2O_2)	Sigma-Aldrich
4-(2-hydroxyethyl)-1-piperazineethanesulfonic acid (HEPES)	Mediatech
Igepal CA-630	Sigma-Aldrich
Imidazol solution	BD
Isopropyl alcohol (2-propanol)	Sigma-Aldrich
Isopropyl β-D-1-thiogalactopyranoside (IPTG)	Thermo Scientific
Leptomycin B	Sigma-Aldrich
Magnesium chloride ($MgCl_2$) solution	Fluka
Magnesium sulfate ($MgSO_4$)	Sigma-Aldrich
2-Mercaptoethanol	Sigma-Aldrich
4-Morpholineethanesulfonic acid (MES)	Sigma-Aldrich
Methanol	Fisher Scientific
Monopotassium phosphate (KH_2PO_4)	T.J. Baker

Monosodium phosphate (NaH_2PO_4)	Fluka
Nonfat drymilk	Kroger
Phenol/Chloroform/Isoamyl	Sigma-Aldrich
Potassium acetate	Sigma-Aldrich
Potassium chloride (KCl)	T.J. Baker
Potassium hydroxide (KOH)	J.T. Baker
Propidium iodide (PI)	Invitrogen
Sodium acetate	Fluka
Sodium azide (NaN_3)	Fluka
Sodium bicabonate	Mediatech
Sodium chloride (NaCl)	Sigma-Aldrich
Sodium dodecyl sulfate (SDS)	Sigma-Aldrich
Sodium hydroxide (NaOH)	Sigma-Aldrich
Tetramethylethylenediamine (TEMED)	Sigma-Aldrich
Tris [tris(hydroxymethyl)aminomethane]	Sigma-Aldrich
Tween 20	Sigma-Aldrich
Yeast Extract	Fluka
X-gal	Denville Scientific Inc.

2.1.8 Antibiotics

Ampicillin	Fluka
Amphotericin B	Sigma-Aldrich
Chloramphenicol	Fluka
Gentamicin solution (10 mg/ml)	Sigma-Aldrich
Gentamicin solution (50 mg/ml)	Sigma-Aldrich
Kanamycin sulfate	Mediatech
Kanamycin sulfate solution (10 mg/ml)	Life Tech.
Penicillin G (1,000,000 units/vial)	Sigma-Aldrich
Penicillin/Streptomycin (P/S) solution (100x equivalent to 10,000 units/ml penicillin and 10 mg/ml streptomycin)	Sigma-Aldrich
Streptomycin	Sigma-Aldrich
Tetracycline	Fluka

2.1.9 Enzymes

Deep Vent DNA Polymerase	NEB
Dnase I	NEB
Platinum Taq DNA Polymerase	Invitrogen
Proteinase K solution	Invitrogen
Restriction enzymes	NEB
RNase A	Roche
RNase H	Fermentas
RNase OUT – Ribonuclease Inhibitor	Invitrogen
RNase T1	Fermentas
Rnase V1	Applied Biosystems
T4 DNA Ligase	Roche, NEB
T7 RNA Polymerase	Fermentas
Taq DNA Polymerase	NEB
Trypsin/EDTA	Mediatech

2.1.10 Nucleotides

ATP, CTP, GTP, UTP	Roche
dATP, dGTP, dCTP, dTTP	Invitrogen

2.1.11 Transfection reagents

Cellfectin	Invitrogen
Lipofectamine™ 2000 Reagent	Invitrogen
Lipofectin® Reagent	Invitrogen
*Trans*IT mRNA Transfection kit	Mirus Bio LLC
*Trans*IT siQuest® Transfection Reagent	Mirus Bio LLC

2.1.12 Commercially available buffers and solutions

60% USP Isopropyl Alcohol	Decon Labs Inc.
10x Elution buffer	Clontech
Bac down® Detergent Disinfectant	Decon Labs Inc.
DIG Easy Hyb buffer	Roche
DIG Wash and Block buffer set	Roche
Equilibration buffer	Clontech
Imperial™ Protein Stain	Pierce
Immobilon™ Western Chemiluminescent HRP substrate	Millipore
MOPS-EDTA-Sodium Acetate Buffer (MESA)	Sigma-Aldrich
pH 4, 7 and 10 buffer solutions	VWR
Phosphate-Buffered Saline (PBS)	Mediatech
Protein G Sepharose®, Fast Flow	Sigma-Aldrich
RNA sample loading buffer	Sigma-Aldrich
Serological Pipets (1, 5, 10, 25 and 50 ml)	Fisher Scientific
20x SSC buffer	Ambion
Talon® Metal Affinity Resin	Clontech
Trypan Blue Stain 0.4%	Gibco
Ultra Pure Distilled Water – DNase, RNase free (DEPC)	Gibco

2.1.13 Commercially available Kits

BigDye® Terminator v3.1 Cycle Sequencing kit	Applied Biosystems
DIG Northern Starter Kit	Roche
GeneJET™ Plasmid Miniprep Kit	Fermentas
High Pure RNA Isolation Kit	Roche
Micro BCA™ Protein Assay Kit	Pierce
PERFORMA® DTR Gel Filtration Cartridges	Edge BioSystems
QIAGEN® Plasmid Maxi kit	Qiagen
QIAquick Gel Extraction Kit	Qiagen
SuperScript™ III One-Step RT-PCR System with Platinum® *Taq* DNA Polymerase	Invitrogen
SigmaSpin™ Sequencing Reaction Clean-Up, Post-Reaction Purification Columns	Sigma-Aldrich
Titan One Tube RT-PCR System	Roche

2.1.14 Lab consumables

0.2 ml and 0.5 ml PCR Tubes, 2.0 ml Safe-Lock Tubes	Eppendorf
1.5 ml tubes	Denville

15 ml and 50 ml tubes	Denville
2 ml Gravity-flow column	Clontech
Aluminium foil	Kroger
Amicon Ultra-15 Centrifugal Filter Unit, 30 kDa	Millipore
Biohazard bags	Fisher Scientific
Cell culture flask T25, vented and closed	Nunc
Cell culture flask T75, vented and closed	BD
Cell culture flask T175, vented and closed	BD
Cell culture plates, 6 well	Corning
Cell culture plates, 24 well	Nunc
Cell culture plates, 48 well	Falcon
Cell culture plates, 96 well	Corning, Phenix
Cell Scraper	BD
Cryo tube™ vial, 1.8 ml	Nunc
Cryogenic vial, 1 ml	Nalgene
Disposable culture tubes	Fisher Scientific
Extra thick Blot Paper	BioRad
Filter tips	USA Scientific
Gloves	Denville
Hybridization bags	Roche
Inoculation loop	Fisher Scientific
Lab-Tek™ II Chamber Slide™ System with 4 wells	Nunc
Lab-Tek™ II Chamber Slide™ System with 8 wells	Nunc
Lysing Matrix D tubes 1.4 mm ceramic spheres	MP Biomedicals
Nylon membrane, positively charged	Roche
Parafilm	Pechiney Plastic Packaging
Protran® Nitrocellulose Transfer Membrane	Whatman
Petri Dish, Polystyrene, 100 x 15 mm	Fisher Scientific
Self sticking Tape	Fisher Scientific
Tips	Denville, USA Scientific
Tough Spots	USA Scientific
UVette	Eppendorf

2.1.15 Laboratory equipment

ABI Prism 310 Genetic Analyzer (Sequencer)	Applied Biosystems
Autoclave SG-116	AMSCO Scientific
AxioImager M1 (LSM 510 Meta confocal laser scan head)	Carl Zeiss
Axiovert 40 CFL (inverted fluorescence microscope)	Carl Zeiss
8-chanel Pipetor Ergo Comfort	Micronic
Bacteria incubator	Barnstedt
BioPhotometer	Eppendorf
Biological safety cabinet	Nuaire
Cell Counting chamber	VWR
Chemical Fume Hood	BMC
Cover glass	Fisher Scientific
Dark Reader DR-45M Non-UV Transilluminator	Clare Chemical Research
Digital Scale Explorer Pro Precision Balances	Ohaus
Electrophoresis chambers, trays and combs	Bio-Rad
Fireboy eco	INTEGRA Biosciences
Freezer (-80°C)	Revco Industries

Freezer chest (-20°C)	Thermo electron corporation
GelLogik 2200 Imaging System	Kodak
Mini-Rotator	Glas-Col
Glass Beakers and Erlenmeyer Flasks	Pyrex
Glass Bottles	Schott Duran
Glass Cylinders	Pyrex
GS Gene Linker ™ UV Chamber	BioRad
Incubator 2475	VWR
Isotemp Economy Analog-Contro Water Bath	Fisher Scientific
Isotemp Laboratory Refridgerator	Fisher Scientific
Legend RT centrifuge	Heraeus
Light microscope	BioStar
Locator JR Cryo Biological Storage System	Thermolyne
Magnetic stirrer	IKA
Magnetic stirrer with heater C-MAG HS 7	IKA
Mastercycler ep gradient S	Eppendorf
Microcentrifuge 5415D	Eppendorf
Microcentrifuge 5415R	Eppendorf
Microwave	Kenmore
Mini PROTEAN system	BioRad
pH-Meter Ultra Basic	Denver Instruments
Platform Vari-Mix	Thermolyne
Plastic Beakers	Fisher Scientific
Plastic Cylinders	Nalgene
Power Pac Basic and Universal (Power supply)	Bio-Rad
Research pipettes, adjustable volume, various sizes	Eppendorf
Shaker incubator	New Brunswick Scientific
Shake N Bake Hybridization oven, Incubator Shaker Ii	Boekel Scientific
Sonifier W-150	Branson
Stir bars	Fisher Scientific
ThermoStat plus	Eppendorf
Trans-Blot SD Semi-Dry Electrophoretic Transfer Cell	BioRad
Tube Racks	USA Scientific
Vacuboy	INTEGRA Biosciences
Vortexer	Fisher Scientific

2.1.16 Markers

1 kb DNA ladder	NEB
100 bp DNA ladder	NEB
Protein Marker, Broad Range (2-212 kDa)	NEB
Prestained Protein Marker, Broad Range (7-175 kDa)	NEB

2.1.17 Solutions and buffers

- **10% Ammonium persulfate (APS):** 1 g APS dissolved in 10 ml ddH_2O.
- **Bac-Solution I:** 15 mM Tris pH 8.0, 10 mM EDTA, RNase A (100 µg/ml)
- **Bac-Solution II:** 0.2 N NaOH, 1% (w/v) SDS
- **DABCO antifading solution:** 2.5 g 1,4-Diazabicyclo[2.2.2]octane (DABCO) were dissolved in 90 ml glycerol and 10 ml PBS at 37°C. Adjust to pH 8.6 with HCl.

- **DNA-Marker (1 kb & 100 bp):** 20 µl Marker, 100 µl 10x loading buffer, 880 µl TE buffer
- **0.5 M EDTA pH 8,0:** 186.1 g EDTA x 2 ddH_2O, 20 g NaOH. Adjust to pH 8.0 with NaOH. Adjust the volume to 1000 ml with ddH_2O.
- **1x Elution buffer:** 1 ml 10x Elution buffer, 9 ml Equilibration buffer
- **2x Gel-loading buffer (SDS-PAGE):** 1.51 g Tris, 20 ml Glycerol. Dissolve both in 35 ml distilled water and adjust to pH 6,7 with HCl. Add 4 g SDS, 10 ml 2-Mercaptoethanol, 2 g Bromphenol blue. Adjust the volume to 100 ml with ddH_2O.
- **Immunoprecipitation wash buffer 150:** 20 mM Tris-HCl pH 8.0, 150 mM KCl, 1% Igepal CA-630, 1 mM EDTA, 1 mM DTT
- **Immunoprecipitation wash buffer 300:** 20 mM Tris-HCl pH 8.0, 300 mM KCl, 1% Igepal CA-630, 1 mM EDTA, 1 mM DTT
- **Lysogeny Broth (LB) agar:** 15 g Agar, 10 g Bacto™ Tryptone, 5 g Yeast Extract, 10 g NaCl. Adjust the volume to 1000 ml with ddH_2O and autoclave.
- **LB medium:** 10 g Tryptone, 5 g Yeast Extract, 10 g NaCl. Adjust the volume to 1000 ml with ddH_2O and autoclave.
- **10x Loading buffer (agarose gel electrophoresis):** 0.25% (w/v) Bromphenol blue, 30% (v/v) Glycerol
- **Lysis buffer:** 50 mM NaH_2PO_4, 300 mM NaCl, 10 mM Imidazol. Adjust to pH 8.0 with NaOH. To be added freshly to 5 ml lysis buffer: 200 µl 25x Proteaseinhibitor-solution, 1% Igepal CA-630
- **0.1 M Potassium phosphate pH 7.2:** 71.7 ml 1 M K_2HPO_4 pH, 28.3 ml 1 M KH_2PO_4. Adjust the volume to 1000 ml with ddH_2O.
- **25x Proteaseinhibitor-solution (EDTA-free):** Solve one tablet Roche-Proteaseinhibitor in 2 ml DEPC-H_2O, aliquot á 200 µl and store at –20°C.
- **10x RIPA lysis buffer:** 0.5 M Tris/HCl pH7.4, 1.5 M NaCl, 2.5% Deoxycholic Acid, 10% Igepal CA-630, 10 mM EDTA
- **RNase A-solution:** Solve 10 mg/ml RNase A in 10 mM Tris and 15 mM NaCl. Heat 15 min at 100°C. Let equilibrate to room temperature and aliquot á 500 µl. Store at -20°C.
- **SOA:** 20 g Tryptone, 5 g Yeast Extract, 0.58 g NaCl, 0.18 g KCl. Adjust the volume to 1000 ml with H_2O and autoclave.
- **SOB (Super Optimal Broth):** 98 ml SOA, 1 ml 1 M $MgSO_4$, 1 ml 1 M $MgCl_2$
- **SOC (SOB with Catabolite repression):** 10 ml SOB, 100 µl 2 M Glucose solution
- **Solution I:** 50 mM Glucose, 25 mM Tris-HCl pH 8.0, 10 mM EDTA pH 8.0
- **Solution II:** 0.2 N NaOH, 1% (w/v) SDS
- **Solution III:** 60 ml 5 M Potassium acetate, 11.5 ml Acetic acid, 28.5 ml ddH_2O
- **50x TAE-Buffer for DNA-gel electrophoresis:** 242 g Tris, 57.1 ml Acetic acid, 100 ml 0.5 M EDTA pH 8.0. Adjust with HCl to pH 8.3. Adjust the volume to 1 l with ddH_2O.
- **Talon buffer:** 50 mM Potassium phosphate pH 7.2, 150 mM NaCl

- **TBST:** 30 ml 5 M NaCl, 10 ml 1 M Tris pH 8.0, 0.5 ml TWEEN 20. Adjust the volume to 1000 ml with ddH_2O.
- **TE-Puffer:** 10 mM Tris pH 8.0, 1 mM EDTA pH 8.0
- **TFB:** 10 mM MES (pH6.3), 45 mM $MnCl_2$, 10 mM $CaCl_2$ 100 mM KCl, 3 mM Hexamminecobalt chloride. The pH of the solution should be between 6.0 and 6.1. Aliquot á 40 ml and store at 4°C.
- **Transfer buffer:** 25 mM Tris, 150 mM Glycin, 10% (v/v) Methanol
- **1x Tris-glycine electrophoresis buffer (SDS-PAGE):** 25 mM Tris, 250 mM Glycin (pH 8.3), 0.1% (w/v) SDS. This buffer was prepared as a 5x buffer.
- **Wash buffer (BD) for protein purification:** 50 mM NaH_2PO_4, 300 mM NaCl, 20 mM Imidazol, 10% (v/v) Glycerol. Adjust to pH 8.0 with NaOH.
- **X-gal:** Solve 2% (w/v) X-Gal in Dimethylformamide.

2.1.18 Computer programs

Sequence analysis: Lasergene (DNAstar)

Microsoft Office: Microsoft Power Point 2003; Microsoft Word 2003, 2010

Image processing: Photoshop CS2 9.0.2; Zeiss LSM Image Browser Version 4.3.0.121; Image J

2.1.19 Oligonucleotides

Table 1: Oligonucleotides (FP: forward primer; RP: reverse primer)

Name[a]	**Sequence**[b]	**Orientation**[c]	**Position**[d]
Table 1a: PCR-primer for amplification of the cellular and viral genes			
NF45-FP	cc**GAATTC***ATG*AGGGGCGACCGAGGCAGAGGCC	+	1-25
NF45-His	cc**GCGGCCGC***TCA*ATGGTGATGGTGATGGTGCTCCTGGGTCTCCATGCTTTCC	-	1131-1152
NF45-FLAG	cc**GCGGCCGC***TCA*CTTATCATCATCATCCTTGTAATCCTCCTGGGTCTCCATGCTTTCC	-	1131-1152
p68-FP1	gg**GGATCC***ATG*CCCGGGTTTGGAGCCCCTCGATTTGG	+	1-29
p68-His	gg**GCGGCCGC***TTA*ATGGTGATGGTGATGGTGTTGAGAATAACTCGCTGGCATTGGG	-	1761-1785
p68-FP2	gg**GGTACC***ATG*CCCGGGTTTGGAGCCCCTCGATTTGG	+	1-29
p68-FLAG	gg**GCGGCCGC***TTA*CTTATCATCATCATCCTTGTAATCTTGAGAATAACTCGCTGGCATTGGG	-	1761-1785
MBP-FP	cc**GAATTC***ATG*AAAACTGAAGAAGGTAAACTGG	+	1-25
MBP-RP	gc**GGCCGC***CTA*CTTATCATCATCATCCTTGTAATCCCTTCCCTCGATCCCGAGGTTG	-	1160-1182
VP4-FLAG-RP	gg**GCGGCCGC***TTA*CTTATCATCATCATCCTTGTAATCAGCCATGGCAAGGTGGTACTGG	-	1889-1911

VP4-FP	gg**GAATTC***ATG*GCCGACAAGGGGTACGAGGTAGTCG	+	1-21
VP1-FP	gg**GAATTC***ATG*AGTGACATTTTCAACAGTC	+	1-22
VP1-His-RP	cc**GCGGCCGC***TTA*ATGGTGATGGTGATGGTGGCGGCTCTCCTTTTGGCGTTGC	-	2613-2634
Table 1b: Oligonucleotides for sequencing			
p68-FP3	CAGACTGGATCAGGGAAAACGC	+	379-400
B-FP-1000	GAAGCAAGGTGCAGGGACAAAGG	+	978-1000
B-RP-2200	CTTGGGGGGTACTGGCTTGTTC	-	2190-2211
T7	TAATACGACTCACTATAGGG		
Sp6	ATTTAGGTGACACTATAG		
M13R	AGCGGATAACAATTTCACACAGGA		
M13	CGCCAGGGTTTTCCCAGTCACGAC		
pFast-FP	AATAAGTATTTTACTGTTTTCG		
pFast-RP	TTCAGGGGGAGGTGTGGGAGG		

a Name of the oligonucleotide

b Sequence of the oligonucleotide in 5' to 3' direction (used **restriction enzyme cleavage sites** are bold; *start* and *stop* codons are in italics; CODING SEQUENCES are capitalized and not further changed; sequences encoding for protein tags are underlined)

c orientation of the oligonucleotide: + sense; - anti-sense

d Position on the gene whereas 1 is the A of the ATG startcodon of each gene.

Table 2: siRNA sequences

siRNA	sense sequence	Location on the gene
NF45 185	5'-UGCAGAACAGGCUUCCAUUdTdT-3'	185-103
NF45 551	5'-GCUGCACUUGGACAUCAAAdTdT-3'	551-569
p68 179	5'-GGUUGAGCAGUACAGAUCA dTdT-3'	179-197
p68 388	5'-CAGGGAAAACGCUGUCUUAdTdT-3'	388-407
NP	5'-GGAUCUUAUUUCUUCGGAGdTdT-3'	1496-1514

2.2 Methods

2.2.1 RNA Isolation

Cells were grown to confluence in a T75 tissue culture flask, trypsinized, centrifuged for 5 min at 1,000 x g and resuspended in 200 µl PBS. RNA was isolated using the High Pure RNA Isolation Kit following manufacturer's instructions.

2.2.2 Reverse Transcriptase - Polymerase Chain Reaction for ssRNA

Reverse Transcriptase – Polymerase Chain Reaction (RT-PCR) was used to amplify DNA from cellular mRNA with the SuperScript™ III One-Step RT-PCR System.
The following ingredients were pipetted in this order in a 0.2 ml tube on ice.
25 µl 2x reaction mix, 1 µl of each primer (100 µM), 2 µl SuperScript III RT/Platinum Taq Mix, 2.5 µl DMSO (5%), 13.5 µl DEPC-H_2O, 5 µl RNA
The mixture was vortexed and placed into the thermocycler with the following program:
45°C 30 min, 94°C 2 min
5x: 94°C 15 sec, 45°C 30 sec, 68°C (1 minute for 1,000 bp to amplify plus 30 sec)
35x: 94°C 30 sec, 55°C 30 sec, 68°C (1 minute for 1,000 bp to amplify plus 30 sec)
68°C 5 min, 4°C

2.2.3 RT-PCR for dsRNA (IBDV genome)

For amplification from viral dsRNA the SuperScript™ III One-Step RT-PCR kit was used. Two separate mixes were prepared on ice in a 0.2 ml tube.
RNA-mix: 0.25 µl of each primer (100 µM), 1 µl DMSO, 2.5 µl RNA
The RNA-mix was denatured at 95°C for 5 min and immediately cooled in the -80°C freezer. During this time the enzyme mix was prepared on ice: 6.25 µl 2x reaction mix, 0.25 µl SuperScript III RT/Platinum Taq Mix, 2.25 µl DEPC-H_2O
The enzyme-mix was added to the RNA-mix and the samples were placed immediately in the preheated thermocycler at 45°C, using the following program:
45°C 30 min, 94°C 2 min
5x: 94°C 15 sec, 55°C 30 sec, 68°C (1 minute for 1,000 bp to amplify plus 30 sec)
35x: 94°C 30 sec, 55°C 30 sec, 68°C (1 minute for 1,000 bp to amplify plus 30 sec)
68°C 5 min, 4°C

2.2.4 PCR with Deep Vent DNA polymerase

The Deep Vent polymerase is theromostable and has a high-fidelity during amplification.
Mix: 39.5 µl ddH_2O, 2.5 µl DMSO (5%), 0.25 µl of each primer (100 µM), 1 µl 10 mM dNTP's, 1 µl sample, 5 µl ThermoPOL Buffer 10x Conc., 0.5 µl Deep Vent (NEB)
In the thermocycler the DNA was amplified following the below described protocol.
97°C 1 min
40 x: 95°C 30 sec, 55°C 30 sec, 72°C (1 minute for 1,000 bp to amplify plus 30 sec); 4°C

2.2.5 PCR with Taq DNA Polymerase

Taq DNA Polymerase is thermostable and has lower fidelity during synthesis, but showed higher sensitivity than Deep Vent DNA Polymerase. Its reaction products were therefore not used for cloning, but to control insertion of a fragment in a plasmid.
The following solutions were added to a 0.2 ml tube kept on ice:
38.5 µl ddH_2O, 0.5 µl of each primer (100 µM), 1 µl 10 mM dNTPs, 1 µl sample, 5 µl Standard Taq Puffer, 3 µl 25 mM $MgCl_2$, 0.5 µl Taq polymerase
In the thermocycler the DNA was amplified by the following protocol: 97 °C 3 min
30x: 94°C 45 sec, 55°C 45 sec, 72°C (1 minute for 1,000 bp to amplify plus 30 sec)
72°C 7 min, 4°C

2.2.6 Agarose gel electrophoresis

Agarose gels between 0.7% and 1.5% agarose in 1 x TAE buffer were prepared to separate DNA and RNA molecules by length. Ethidium bromide was added to a final concentration of 0.5 µg/ml to visualize the nucleic acids. After boiling in a microwave, gels were poured in small (7 x 10 cm) or large (15 x 10 cm) gel trays. DNA samples were mixed with 10x sample loading buffer and pipetted into the gel slots. Depending on the expected size a 100 bp or 1 kb DNA marker was used. Large gels were run at 100 V, small gels at 80 V for 20 to 50 min. Gels were analyzed in the GelLogik 2200 Imaging System under UV light and the gel was documented.

2.2.7 Gel elution

A good visible DNA band of the appropriate size was excised under the Dark Reader light. A faint DNA band was visualized by UV-light and excised. The following DNA elution from the excised gel piece was conducted with the QIAquick Gel Extraction Kit according to the manufacturer's recommendations. Depending on the brightness of the band, which correlates directly to the amount of the DNA, it was eluted in either 30 or 50 µl. The eluate was incubated at 37°C for 5 min to evaporate residual ethanol.

2.2.8 TOPO TA Cloning

After amplification of cDNA with *Taq* polymerase it was possible to ligate it into the pCR®2.1-TOPO® plasmid using the TOPO TA Cloning® kit. *Taq* polymerase harbors a nontemplate-dependent terminal transferase activity, which adds an additional deoxyadenosine to the 3' ends of the PCR product. The pCR®2.1-TOPO® plasmid is supplied linearized in the kit and has single, overhanging 3' deoxythymidine residues. Topoisomerase I (supplied in the kit) ligates the PCR product efficiently into the plasmid.
The composition of the ligation reaction is indicated below.
6 µl PCR product (cDNA), 1 µl High Salt Buffer, 0.25 µl µl pCR®2.1-TOPO® plasmid
After incubation for 15 min at room temperature, One Shot® TOP 10 competent cells were transformed with the ligation reaction following manufacturer's recommendations.

All cells were plated on a LB agar plate which contained 20 ml agar in each petri dish of 10 cm diameter. The LB agar was supplemented with ampicillin (50 µg/ml), X-Gal (0.008%) and IPTG (0.2 mM) for selection of recombinant plasmid containing bacteria using a blue-white screening approach.
The IPTG mimics allolactose and removes the repressor from the lac promoter on the bacterial genome and therefore allows the expression of the β-galoctosidase Ω-part (LacZΩ). If there was no insert in the plasmid, the β-galactosidase α-part (LacZα) was expressed and both subunits were reassembled to a functional β-galactosidase enzyme (α-complementation). It cleaves X-gal (bromo-chloro-indolyl-galactopyranoside) and releases the blue dye 5,5'-Dibrom-4,4'-dichlor-indigo and the colonies appear blue. Colonies containing a plasmid with insert fail to express LacZα and appear white.

2.2.9 Restriction endonuclease cleavage

Restriction endonucleases (RE) cleave DNA sequence specific at a mostly palindromic DNA sequence. The DNA can have a blunt end or a sticky end with a 3' or 5' overhang after cleavage. Here, only RE were used that left different sticky ends to allow directed cloning of the fragment into the plasmid. All RE were purchased from NEB. Conditions for the reaction (buffer, temperature, addition of BSA) were chosen according to the manufacturer's recommendation. Volumes and amount of DNA used for restriction cleavage varied. The following volumes are shown as an example for a typical reaction.
4 µl DNA, 2 µl buffer, 0.5 µl RE, 0.2 µl BSA (if necessary for the enzyme), 13.3 µl ddH_2O
The reaction was incubated at least one hour at the recommended temperature. In some cases it was incubated over night (o/n) to ensure complete cleavage of the DNA.

2.2.10 Ligation

A DNA ligase links two dsDNA strands together by creating a covalent phosphodiester bond between the adjacent 3' hydroxyl and 5' phosphate end on the same strand under ATP hydrolysis. For directional cloning insert and plasmid should be cleaved with the same set of RE leaving two different sticky ends.
To ligate a fragment into a plasmid the following reaction mix was prepared:
7.5 µl fragment, 1 µl plasmid, 1 µl T4 buffer, 0.5 µl T4 ligase.
The reaction mix was incubated at 16°C o/n or at 22°C for one hour, which might result in an incomplete ligation reaction, and then used for transformation of bacteria.

2.2.11 Transformation of competent XL1-Blue cells

Bacteria cells were transformed with a plasmid in order to amplify the circular DNA. The plasmid contains an origin of replication, which allows the bacteria to amplify it independent of their own chromosome during DNA replication.
Competent XL1-Blue cells were thawed on ice and the ligation mix was added. The cells were kept 30 min on ice allowing the plasmids to attach to the cell wall. The cell

suspension was incubated 2 min at 42°C to destabilize the cell wall, which integrates the plasmid in the bacteria cell. Immediately afterwards the cells were incubated for 2 min on ice to stabilize the cell wall. Then 400 µl SOC medium were added and the cells were shaken at 37°C for 1 h. This allows the bacteria cell to duplicate at least one time and express β-lactamase, the product of the plasmid-encoded ampicillin resistance gene. Now, cells were centrifuged for 5 min with 800 x g and 350 µl of the medium were removed. The cells were resuspended in the remaining medium. The bacteria cells were plated with an inoculation loop on a LB agar plate containing the appropriate selection compounds as described above (see 2.2.8). The plates were incubated at 37°C o/n to allow the formation of bacterial colonies.

2.2.12 Plasmid DNA extraction

Depending on the purpose of the plasmid, three different methods were applied. For general screening of the plasmid containing the insert, a preparation by alkaline lysis was used. To subsequent transfect the DNA, the plasmids were column purified with the GeneJET™ Plasmid Miniprep Kit. If larger amounts of the plasmid were needed, the plasmids were purified by Maxipreparation using the QIAGEN® Plasmid Maxi kit.

2.2.12.1 Minipreparation by Alkaline Lysis

(based on Protocol 1, 1.32, Molecular Cloning 3rd edition 2001 by Sambrook & Russell)
Two milliliter LB medium containing ampicillin (100 µg/ml) were inoculated with a single bacteria colony and the culture was incubated o/n at 37°C in a bacterial shaker at 230 rpm. A 1.5 ml reaction tube was filled with the o/n culture and centrifuged for 2 min at 16,000 x g at room temperature. The supernatant was discarded, cells were resuspended in 100 µl solution I and incubated 5 min at room temperature. To lyse the cells, 200 µl freshly prepared solution II were added and the tube was mixed by inverting it. After 5 min incubation on ice 150 µl solution III were added to neutralize the lysis solution, the tube was vortexed and incubated 5 min on ice. To remove the denatured proteins and chromosomal DNA, the suspension was centrifuged for 5 min with 16,000 x g at room temperature. After centrifugation, 400 µl of the obtained supernatant were added to a new 1.5 ml reaction tube with 1 ml 95% ethanol and vortexed. The nucleic acids were precipitated for 30 min at –20°C, centrifuged for 10 min with 16,000 x g at room temperature and the supernatant was discarded. To remove residual salts from the nucleic acids, 200 µl of 70% ethanol were added and the mixture was centrifuged for 2 min at 16,000 x g at room temperature. The supernatant was discarded and the pellet was dried at 37°C. The nucleic acid was resuspended in 100 µl ddH_2O with 1 µl RNase A (10 mg/ml) and incubated for 60 min at 37°C to digest bacterial RNA. The DNA was stored at -20°C.

2.2.12.2 Minipreparation (column purified)

Bacterial cells were propagated as described in 2.2.12.1, centrifuged and purified with the GeneJET™ Plasmid Miniprep Kit following the manufacturer's protocol. The concentration of purified DNA ranged between 350 µg/ml and 400 µg/ml.

2.2.12.3 Maxipreparation

For large amounts of DNA the QIAGEN® Plasmid Maxi kit (Qiagen) was utilized according to the manufacturer's protocol except that 250 ml LB medium were inoculated with 2 ml of the bacterial starter culture. Centrifugation steps were carried out at 3,400 x g for 1 h. The final DNA pellet was resuspended in 600 µl TE buffer. The DNA concentration was at least 1 mg/ml.

2.2.13 Preparation of a glycerol stock

A glycerol stock of bacterial cells was prepared to maintain the bacteria clone containing the correct plasmid. For this purpose, 2 ml LB medium containing ampicillin (100 µg/ml) were inoculated with 0.5 ml of an over night bacterial culture. The culture was shaken for approximately 4 h at 37°C with 230 rpm until the medium became cloudy. The bacteria were in the log phase (exponential phase) of propagation. Now, 500 µl of this bacterial culture were mixed with 500 µl of sterile glycerol and stored frozen at -80°C.

2.2.14 Sequencing

Sequence reactions were conducted using the BigDye® Terminator v3.1 Cycle Sequencing kit. This is a Sanger-based method applying the chain termination sequencing method. The RR100 mix contains di-deoxynucleotides (ddNTP) labeled with four different fluorescent dyes. The sequencing reaction mix was prepared.
4 µl 5x sequencing buffer, 3 µl primer (10 µM), 1 µl DNA, 1 µl v3.1 cycle sequencing RR100 mix, 11 µl ddH_2O.
The reaction was mixed and inserted in a thermocycler using the following program:
96°C 1min; 25 x: 96°C 10 sec, 50°C 5 sec, 60°C 4min; 4°C.
Reaction products were purified using Performa® DTR Gel Filtration Cartridges. The reactions were sent for sequencing to the Sequencing & Synthesis Facility of the University of Georgia supervised by Jeffrey Wagner at the Riverbend Research Lab. For short sequences, the nucleotide sequence was sometimes determined by the ABI Prism 310 Genetic Analyzer, which is a single capillary DNA sequencer, monitored by Debborah Hilt (in Dr. Mark Jackwoods laboratory at PDRC, University of Georgia). The sequences were analyzed with Lasergene.

2.2.15 Preparation of competent cells (Hanahan-method)

XL1-Blue cells were inoculated in 2.5 ml LB medium with tetracycline (10 µl/ml) and shaken at 37°C with 230 rpm o/n. On the next day, 400 µl of the over night culture were

added to 100 ml SOB medium and shaken at 37°C with 230 rpm until they reached an OD_{600} = 0.3 with SOB medium as background optical density. The cells were cooled for 10 min on ice and then centrifuged for 10 min at 1,350 x g at 4°C. The supernatant was discarded. The cell pellet were resuspended in 32 ml TFB and incubated for 10 min on ice. After a centrifugation step of 10 min with 1,350 x g at 4°C the supernatant was discarded and the cells were resuspended in 8 ml TFB. Now 1,200 µl glycerol (15%) were added and the cells were incubated 10 min on ice. In a next step, 280 µl DMSO were added dropwise while carefully shaking the tube followed by incubation on ice for 5 min. Again 280 µl DMSO were added and incubated 5 min on ice. The cells were aliquoted á 100 µl on ice and store at -80°C.

The competent cells were now transformed with 10 pg of plasmid DNA (for example 1 µl pUC19, 10 pg/µl) to determine the competence of 100 µl bacterial cells. For this transformation the SOC medium was pre-warmed and conducted as described above (2.2.11). At the end of the protocol only 100 µl of the transformation mixture were plated on a LB agar plate with ampicillin (50 µg/ml) and incubated o/n at 37°C. The colonies grown on the plate were counted the next day to calculate the competence, which is expressed in counted colonies per microgram DNA. The counted number was multiplied by five, because only one fifth of the total reaction was plated. This number was multiplied by 100,000 to calculate the competence for 1 µg of plasmid DNA. Cells with a competence greater than 10^7 colonies per microgram DNA were used for subsequent transformation reactions.

2.2.16 Phenol/Chloroform extraction

This method was used to extract nucleic acids out of a larger volume of liquid containing a nucleic acid/protein mixture and also to inactivate and remove enzymes. For this purpose, the sample volume was mixed 1:1 with phenol/chloroform/isoamylethanol (25:24:1) and vortexed until the white emulsion became visible. After centrifugation for 5 min at 16,000 x g two phases appeared. The upper one represented the aqueous phase containing the nucleic acid, the lower phase contained mostly soluble compounds and phenol/chloroform/isoamylethanol. The interphase contained the proteins denatured by phenol. The upper phase was transferred into a new tube and mixed with an equal volume of chloroform (1:1). The chloroform removes residual phenol from the aqueous phase and this second organic solvent improves the deproteinization. After centrifugation for 2 min at 16,000 x g the upper phase containing the nucleic acids was transferred to a new tube. The nucleic acids were now recovered by ethanol precipitation. To the total volume, one-tenth of the volume 3 M sodium acetate (pH 5.3) and 2.5-fold volume ethanol was added to recover the nucleic acids from the aqueous phase and precipitated at -20°C for at least 2 h. Then the mixture was centrifuged for 10 min with 16,000 x g to sediment the nucleic acids. The supernatant was discarded,

200 µl of 70% ethanol were added and again centrifuged for 2 min with 16,000 x g. After removal of all ethanol, the pellets were dried in the air flow of a laminar flow hood and resuspended in an appropriate volume of Ultra Pure Distilled Water.

2.2.17 Linearization of plasmid DNA

For the linearization of a plasmid, 40 µl of a plasmid preparation were used in a total volume of 400 µl using 1 µl of the appropriate restriction endonuclease.
This reaction mixture was incubated for 2 h at the optimal temperature for the enzyme. Five microliter of this reaction were analyzed on a 1% agarose gel to verify complete linearization of the plasmid. When this was verified, 20 µl 10% SDS (final concentration 0.5%) and 5 µl proteinase K (20mg/ml) were added and incubated 30 min at 37°C to degrade the enzyme. The proteins were removed from this solution by phenol-chloroform extraction and the DNA was resuspended in 60 µl Ultra Pure Distilled Water. Again, 1 µl was analyzed on an agarose gel to confirm the presence of the DNA.

2.2.18 Generation of cRNA with T7 polymerase

T7 RNA polymerase transcribes *in vitro* complementary RNA (cRNA) from a DNA template (based on Mundt & Vakharia 1996). For this purpose the target sequence was located downstream of a T7 promoter. The following mixture was prepared on ice.
1.25 µl CAP-solution (NEB, one tube solved in 250 µl Ultra Pure Distilled Water), 1.25 µl ACU (10 mM each), 2.5 µl GTP (1 mM), 5 µl 5x transcription buffer, 5 µl linearized plasmid, 8 µl Ultra Pure Distilled Water, 1 µl RNase Inhibitor, 1 µl T7 RNA polymerase.
The reaction was incubated for 60 min at 37°C. After 30 min, 2 µl of the reaction were analyzed on a 1% agarose gel to verify the transcription of cRNA. After 60 min the reaction was set on ice and used for transfection of cells.

2.2.19 Transfection of cRNA

Transfections were conducted with cells reaching 80% confluence in a Lab-Tek™ II Chamber Slide™ System with 4 wells. The medium was changed on the cells to 500 µl medium with 10% FBS. In a reaction tube 50 µl serum-free medium were combined with the cRNA. Immediately 0.5 µl booster reagent and 0.5 µl transfection reagent of the *Trans*IT®-mRNA Transfection Kit were added. The mix was incubated 2-5 min at room temperature. The obtained mixture was added drop wise to the cells and the cell culture vessel was gently rocked. The cells were kept in the incubator for two hours at 37°C. Then the transfection solution was removed and medium containing 10 % FBS and 1x Penicillin/Streptomycin (P/S) was added.

2.2.20 Northern Blot

This technique was used to detect RNA transcription levels in cells. First, RNA was transcribed to serve as a positive control. In a second step the sample and the positive

control were analyzed on an agarose gel to separate RNA by size and the RNA was blotted on a membrane. This membrane was then incubated with a hybridization probe being complementary to the RNA sample that was supposed to be detected. To obtain RNA of the sense and the antisense strand, it was taken advantage of the pcDNA3 vector that has on one side of the MCS a T7 RNA polymerase promoter and on the other side a Sp6 RNA polymerase promoter.

Preparation of a positive control: To this end the transcription of cRNA with T7 polymerase was used (see 2.2.18). Single nucleotides, salts and enzymes were removed by using the SigmaSpin™ Columns.

Preparation of the agarose gel: The electrophoresis chamber with tray and comb was filled with 3% H_2O_2 o/n and then rinsed with DEPC-H_2O to remove RNases. A 1% agarose gel was prepared using 1 g agarose and 90 ml DEPC-H_2O. The mixture was boiled in a microwave and cooled down to 60°C. Then 1.5 ml formaldehyde solution and 10 ml 10x MESA buffer were added and the gel was poured.

Loading and running the agarose gel: The RNA samples (100 ng) and the positive control were mixed with 2-5 volumes of RNA loading buffer, heated to 65°C for 10 min and incubated on ice. The gel was placed in the chamber and filled with 1x MESA buffer up to the level of the gel. The samples were loaded in the wells, which were then filled with 1x MESA buffer. Electrophoresis was performed for 10 min at 100 V. Now the gel was completely covered with MESA buffer and electrophoresis was performed at 80 V for 40 min. Afterwards the gel was stained with ethidium bromide for 15-30 min in 50 ml 1x MESA buffer containing 2.5 µl ethidium bromide (10 mg/ml stock concentration) and visualized in the GelLogik 2200 Imaging System under UV light.

Blotting: The gel was washed twice with 20x SSC buffer for 15 min to remove the formaldehyde. Then the blot was assembled in an electrophoresis chamber in the following order (bottom to top): extra thick blot paper soaked in 20x SSC buffer, placed on the middle part of the chamber and reaching down to the reservoir at the ends filled with 20x SSC buffer, the gel facing down (all air bubbles removed), a dry nylon membrane, two dry extra thick blot papers and a stack of paper tissues fixed with a weight of 200-500 g. The RNA transfer from the gel to the membrane was performed o/n. Then the RNA was cross-linked by UV light. For this, the membrane was placed between two extra thick blot papers soaked in 20x SSC buffer and the program C-L in the GS Gene Linker ™ UV Chamber was used for each side. Then the membrane was washed with distilled water and dried.

Preparation of the DIG-labeled RNA: The reaction mixture was prepared with the reagents from the DIG Northern Starter Kit to prepare the DIG-labeled RNA probe:
1 µg linearized DNA, 4 µl 5x labeling mix, 4 µl 5x transcription buffer, 2 µl RNA-polymerase Sp6. DEPC-H_2O was added to reach a final volume of 20 µl.

The sample was mixed and incubated at 42°C for 2 h. Then 2 µl DNase I were added and the sample was incubated at 37°C for 15 min. To stop the reaction, 2 µl of 0.2 M EDTA (pH 8.0) were added, which was further purified using the SigmaSpin™ Column.

Hybridization: The following heat incubation steps were all performed in a hybridization oven. The membrane was placed in a hybridization bag and 10 ml DIG Easy Hyb Buffer (pre-warmed to 68°C) were added and the membrane was incubated for 30 min at 68°C. The DIG-labeled RNA was mixed with 50 µl DEPC-H_2O and boiled for 5 min, then quickly cooled on ice and added to 3.5 ml DIG Easy Hyb Buffer (pre-warmed to 68°C). The DIG Easy Hyb Buffer was removed from the membrane and replaced with the DIG-labeled RNA mix. The bag was sealed and incubated at 68°C o/n. The membrane was transferred to a tray and washed twice with 25 ml low stringency buffer (2x SSC buffer, 0.1% SDS) for 5 min at room temperature and twice with 25 ml high stringency buffer (0.1x SSC buffer, 0.1% SDS) preheated to 68°C for 15 min at 68°C.

Visualization: The membrane was washed for 2 min at room temperature in 100 ml DIG wash buffer. Then it was incubated with fresh made DIG blocking solution for 30 min on a shaker. The anti-DIG-alkaline phosphatase antibody was diluted 1:10,000 in DIG blocking solution and 20 ml were added to the membrane, which was shaken for 30 min. The membrane was washed twice with 100 ml DIG wash buffer for 15 min and then equilibrated for 3 min in 20 ml DIG detection buffer. Now the membrane was placed in the GelLogic 2200 Imaging System and a few drops of the CPD-Star solution (chemiluminescent alkaline phosphatase substrate) were placed on the membrane until it was covered and after 5 min incubation the signal was documented.

2.2.21 The Bac-to-Bac® Baculovirus expression system

The Bac-to-Bac® Baculovirus expression system was used for chicken protein expression in insect cells. It takes advantage of a eukaryotic cell system allowing correct folding, formation of disulfide bonds, oligomerization and co- or post-translational modifications such as glycosylation, phosphorylation, acetylation or myristoylation.

The gene of interest containing a 6x His-tag at its C-terminus was cloned in the MCS of the baculovirus transfer vector, the pFastBac™Dual vector (see 6.3.1). After transformation of competent DH10Bac™ *E.coli* cells (see 2.1.2) with the donor vector containing the gene of interest, the transposition mediated by the transposase at the attachment sites Tn7R and Tn7L took place and the ORF for the LacZα peptide was interrupted. The gentamicin resistance gene from the plasmid was also transferred. The screening for recombinant bacmids was carried out with kanamycin, gentamicin and tetracycline. Large white colonies were selected and plated again to assure the absence of blue staining. Then the colonies were propagated and the bacmid was purified. To confirm the insertion of the gene of interest into the bacmid, a PCR was performed on the prepared bacmid DNA with one primer located in the plasmid and the other within the

fragment. If the PCR was positive, the bacmid was transfected into High5 insect cells to obtain recombinant baculoviruses. Virus titers were increased by two more passages on *Sf*9 cells and titers were determined using the $TCID_{50}$ assay by IIFA (see 2.2.27). *Sf*9 cells infected with recombinant baculovirus were used for expression of the recombinant protein and harvested 3 d pi to purify the protein of interest by its 6x His-tag with immobilized metal affinity chromatography resin with cobalt ions in its reactive core.

2.2.22 Preparation of competent cells (Calcium chloride method)

A 2 ml culture with DH10Bac™ cells in LB medium containing kanamycin (50 µg/ml) and tetracycline (50 µg/ml) was shaken o/n with 230 rpm at 37°C. In a 200 ml Erlenmeyer flask, 20 ml of LB medium were incubated with 1/100 (200 µl) of the over night culture and shaken for 90 min at 37°C with 230 rpm. The bacteria suspension was transferred in 50 ml tubes and centrifuged with 1,560 x g for 15 min at 4°C. The supernatant was removed and the obtained pellet was carefully resuspended in 20 ml precooled 0.1 M $CaCl_2$ and incubated 30 min on ice. The bacteria were centrifuged with 450 x g for 15 min at 4°C and the obtained pellet was resuspended in 2 ml precooled 0.1 M $CaCl_2$. The cells were incubated for at least 1 h at 4°C and 100 µl were used for transformation of recombinant plasmids.

2.2.23 Transformation DH10Bac™ cells with pFastBac™ Dual

One hundred microliter of DH10Bac™ competent cells were transferred into a precooled 1.5 ml tube. One microliter of the recombinant pFastBac™ Dual-plasmid was added and the contents were mixed by carefully flipping the tube. The cells were incubated with the plasmid for 30 min on ice, then for 2 min at 42°C and cooled down 2 min on ice. Now, 400 µl of SOC medium were added and incubated at 37°C for 1 h shaking at 230 rpm. Then the cells were diluted from 10^{-1} to 10^{-3} in LB medium without antibiotics, 200 µl of each dilution were plated on LB agar plates (20 ml agar each petri dish of 10 cm diameter containing 50 µg/ml kanamycin, 10 µg/ml tetracycline, 7 µg/ml gentamicin, 0.01% X-Gal and 0.2 mM IPTG) and incubated for 48 h at 37°C.

2.2.24 Bacmid preparation

White bacteria colonies were selected and shaken with 230 rpm at 37°C o/n in 2 ml medium containing kanamycin (50 µg/ml), gentamicin (7 µg/ml) and tetracycline (10 µg/ml). The bacteria were transferred into a 1.5 ml tube and centrifuged 1 min with 15,700 x g. The supernatant was discarded and the pellet was resuspended in 300 µl Bac-Solution I. In a next step 300 µl fresh made solution II were added and incubated 5 min at room temperature. Now 300 µl 3 M potassium acetate (pH 5.5) were added and incubated for 5 min on ice. The solution was centrifuged for 10 min with 15,700 x g. The supernatant was filled in a new 2 ml tube, combined with 800 µl isopropyl alcohol and incubated 10 min on ice. The DNA was centrifuged for 15 min at 15,700 x g, the

supernatant was discarded and 500 µl of 70% ethanol were added to remove residual salts. After a centrifugation step of 5 min at 15,700 x g the supernatant was discarded and the pellet was dried in the air flow of a laminar flow hood. The bacmid DNA was resuspended in 40 µl ddH_2O, incubated 10 min at 37°C and stored at -20°C.

2.2.25 Transfection of bacmid DNA

In a 1.5 ml reaction tube 100 µl SFX-Insect medium and 5 µl of bacmid-DNA were added. In a second tube 100 µl SFX-Insect medium were combined with 6 µl of Cellfectin reagent. The Cellfectin reagent mixture was added to the first and the mixture was incubated for 30 min at room temperature. In the meantime High5 cells were counted and 9 x 10^5 cells were centrifuged 5 min at 750 x g, resuspended in 200 µl of SFX-Insect medium and added to the bacmid-Cellfectin-mixture to be incubated for 30 min. One milliliter of SFX-Insect medium was added to a well of a 6-well plate, the transfection mixture was added and incubated 5 h at 27°C. This was followed by the addition of 1.5 ml SFX-Insect medium containing 2x P/S. The plate was sealed with parafilm and incubated for 5 d at 27°C.

2.2.26 Baculovirus infection

*Sf*9 cells were grown to 60-80% confluence in a T25 tissue culture flask for the first virus passage or T75 flask for the second virus passage. The medium was discarded and 0.5 ml or 1 ml virus of the previous passage was added with 1.5 ml or 4 ml medium, respectively. The flasks were shaken at room temperature for 1 h. Then 3 ml (T25 flask) or 10 ml (T75 flask) medium were added containing 1x P/S. When a CPE was observed at 5-6 d pi in comparison to a negative control, cells were rinsed into the medium and transferred to a 15 ml tube. Cells and cell debris were centrifuged at 750 x g for 5 min at 4°C. The supernatant was transferred to another tube and either aliquoted in 1 ml samples and frozen at -80°C (first passage) or stored at 4°C (second passage).

2.2.27 Tissue culture infective dosage 50 ($TCID_{50}$) assay by IIFA

The baculovirus titer was determined applying the $TCID_{50}$ assay by IIFA. The virus was diluted 10^{-1}-10^{-10} and 100 µl of each dilution were filled into four wells of a 96-well-plate. Four wells were filled with 100 µl medium as a negative control. Then 100 µl of *Sf*9 cells with a density of 3 x 10^5 cells/ml were added to each well with virus or medium. Cells were fixed with 96% ice cold ethanol 3 d pi followed by an indirect immunofluorescence assay (see 2.2.35) with the mAb Bac in a dilution of 1:2,000 and α-M-FITC in a dilution of 1:200 as the secondary antibody. The presence of fluorescent cells was determined by fluorescence microscopy. The formula

Log_{10} $TCID_{50}$-endpoint dilution = $X_0 - \frac{d}{2} + d\sum\frac{r}{n}$ was used to calculate the $TCID_{50}$/ml.

X_0: The $\log_{10}$ of the reciprocal value of the lowest dilution, where all wells were positive in immunofluorescence/infection (for example, if all 4 wells are positive in the 10^{-4} dilution, calculate $\log_{10} \frac{1}{10^{-4}} = 4$)

d: The equivalent of the $\log_{10}$ of the dilution factor (1:10 dilution: $\log_{10}10 = 1$)

n: number of wells used for each dilution step (in this case 4)

r: number of wells positive in fluorescence; the calculation starts with the X_0 dilution.

2.2.28 Proteinexpression

For the generation of recombinant proteins, *Sf*9 cells were grown to 80-90% confluence in a T175 tissue culture flask and infected with recombinant baculovirus with a multiplicity of infection (moi) of 10. To this end, medium was reduced in the flask to 10 ml and the appropriate amount of virus was added. After 1 h shaking at room temperature, 20 ml medium with 1x P/S were added. Cells were rinsed carefully into the medium 3 d pi and centrifuged 5 min with 700 x g at 4°C. The obtained cell pellet was either processed immediately for protein purification or stored at -20°C.

2.2.29 Protein purification

Proteins were purified using a modified protocol described before (Letzel *et al* 2007 SD). The frozen cell pellet was thawed on ice, while freshly obtained cell pellets were immediately used. Pellets were lysed with 5 ml lysis buffer and incubated for 10 min on ice. Lysates were centrifuged for 30 min with 16,000 x g and the supernatant was added to 2 ml Talon resin. Before this step the talon resin was washed twice with 5 ml talon buffer and each time centrifuged for 2 min with 700 x g. The cell lysate-talon-mixture was rotated for 1 h at 4°C and then centrifuged with 700 x g for 5 min at 4°C. Three washing steps followed, two with wash buffer (BD) and the last one with equilibration buffer (Clontech). To conduct the wash steps, 10 ml buffer were added, the sample was rocked for 10 min on ice and then centrifuged for 5 min at 700 x g. Afterwards 2 ml equilibration buffer were added and the sample was vortexed and transferred to a gravity flow column. After the resin centrifuged 20 min at 4°C, it was washed with 10 ml equilibration buffer at room temperature. Three milliliter of the elution buffer (Clontech) were added and the eluate containing the recombinant protein was collected in 0.5 ml aliquots.
Samples (20 µl) were taken from the lysate, the pellet, the cleared lysate/supernatant, the flow-through, the wash steps and the eluates to analyze them by SDS-PAGE followed by Coomassie brilliant blue stain and/or Western blot with mAb His-POD.

2.2.30 Concentration of protein

Proteins were concentrated with the Amicon Ultra-15 Centrifugal Filter Unit (30 kDa). The protein samples were filled in the tube above the membrane and centrifuged for

20 min with 2,000 x g. The concentrate was the retention volume above the membrane and contained in average at least a 10-fold concentrated protein.

2.2.31 Quantification of protein

The Micro BCA™ Protein Assay Kit was used to quantify the amount of protein by colorimetric detection. First, a standard was prepared with bovine serum albumin (BSA) (2.0 mg/ml stock concentration) using serial dilutions according to Table 3.

Table 3: Directions to prepare the standard for protein quantification by serial dilutions of BSA. [1]:BSA from stock concentration; [2]: BSA from previous diulution.

	Final BSA concentration	PBS	BSA
1. dilution	200 µg/ml	450 µl	50 µl[1]
2. dilution	40 µl/ml	800 µl	200 µl[2]
3. dilution	20 µl/ml	400 µl	400 µl[2]
4. dilution	10 µl/ml	400 µl	400 µl[2]
5. dilution	5 µl/ml	400 µl	400 µl[2]
6. dilution	2 µl/ml	400 µl	266.7 µl[2]
7. dilution	1 µl/ml	300 µl	300 µl[2]
8. dilution	0.5 µl/ml	300 µl	300 µl[2]

One hundred microliter of the serial diluted BSA containing samples of 20, 10, 5, 2 and 0.5 µg/ml, 100 µl PBS used as blank and 100 µl of the sample to be analyzed were each mixed with 100 µl working reagent and incubated for 60 min at 60°C. Duplicates were made for all samples. The BSA dilutions and the sample were filled in UVette-tubes and were measured in a BioPhotometer using the BCA Micro program. The average of both sample concentrations was calculated.

2.2.32 Sodium dodecyl sulfate polyacrylamide gel electrophoresis (SDS-PAGE)

The protein sample was mixed with 2x SDS Gel-loading buffer, heated to 95°C for 2 min, sonicated with 3 W for 3-5 sec and centrifuged 2 min with 16,000 x g. The supernatant was loaded on a SDS-polyacrylamide gel. Electrophoresis was carried out using discontinuous SDS-PAGE consisting of a 5% stacking gel and a 12% resolving gel.

The following solutions were combined to prepare the resolving gel.

1.6 ml ddH_2O, 2 ml 30% acrylamide (29:1), 1.3 ml 1.5 M Tris (pH 8.8), 50 µl 10% SDS, 50 µl 10% ammonium persulfate, 2 µl TEMED.

The resolving gel was filled between the glass plates up to 2 cm below the upper rim of the glass plates. Immediately the remaining volume was filled with ddH_2O. After the gel was polymerized, the 5% stacking gel was prepared:

1.4 ml ddH_2O, 330 µl 30% acrylamide (29:1), 250 µl 1.0 M Tris (pH 6.8), 20 µl 10% SDS 20 µl 10% ammonium persulfate, 2 µl TEMED.

The water was removed and the stacking gel was filled on top of the resolving gel and the comb was placed immediately between the glass plates. Then the gel was stored at

4°C with 1x Tris-glycine electrophoresis buffer surrounding it up to one day. The gel was loaded with samples after adding the 1x Tris-glycine electrophoresis buffer into the gel chambers. The protein samples were separated in the gel for 45 min at 230 V. After electrophoresis the gel was either stained with Imperial™ Protein Stain or submitted to Western blot analysis.

2.2.33 Coomassie brilliant blue staining

Gels were protein stained with Imperial™ Protein Stain according to the manufacturer's protocol. The gels were incubated in distilled water o/n for destaining.

2.2.34 Western blot

For Western blot analysis proteins separated by SDS-PAGE were transferred to a Protran® Nitrocellulose Transfer Membrane in a Trans-Blot SD Semi-Dry Electrophoretic Transfer Cell. The following protocol refers to a 6 cm x 8.5 cm membrane size. For different sizes adequate buffer volumes were used. From bottom to top extra thick blot paper, the membrane, the gel and a second blot paper all soaked in transfer buffer were placed on the Electrophoretic Transfer Cell. The transfer of the proteins from the gel to the membrane was carried out for 1 h at 24 V. The membrane was incubated with 25 ml 5% non-fat dry milk dissolved in TBST to block free protein binding sites on the membrane for 30 min and 10 ml of the primary antibody diluted in TBST were added. After three wash steps with 10 ml TBST a HRP-conjugated anti-species secondary antibody was added, if the primary antibody was not HRP-conjugated, and incubated for 90 min. After three wash steps with 10 ml TBST the membrane was placed into the GelLogic 2200 Imaging System and the Immobilon™ Western Chemiluminescent HRP substrate was added and a picture was taken for documentation.

2.2.35 Indirect Immunofluorescence assay

Antigens were detected with an antigen-specific antibody in fixed cells and visualized with a fluorochrome-labeled secondary antibody. In multiple-labeling studies different fluorochrome dyes were used. They were detected individually, because each fluorophore absorbs and re-emits at an individual wavelength (Table 4). Excitation and emission spectra used with the Zeiss microscope are listed below.

Table 4: Excitation and emission peaks of each fluorophore used are listed and their actual excitation and emission spectrum at the LSM 150 microscope in this study is given.

Fluorophore	Excitation peak	Emission peak	Excitation	Emission spectrum
DAPI	359 nm	461 nm	405 nm	420-480 nm
FITC	490 nm	525 nm	488 nm	505-530 nm
Cy3	553 nm	575 nm	543 nm	560-615 nm
PI	536 nm	617 nm	543 nm	560-615 nm
Cy5	651 nm	674 nm	633 nm	> 650 nm

The excitation and emission spectra of the fluorophores DAPI, FITC, Cy3, propidium iodide (PI) and Cy5 used in this study are shown in Figure 3.

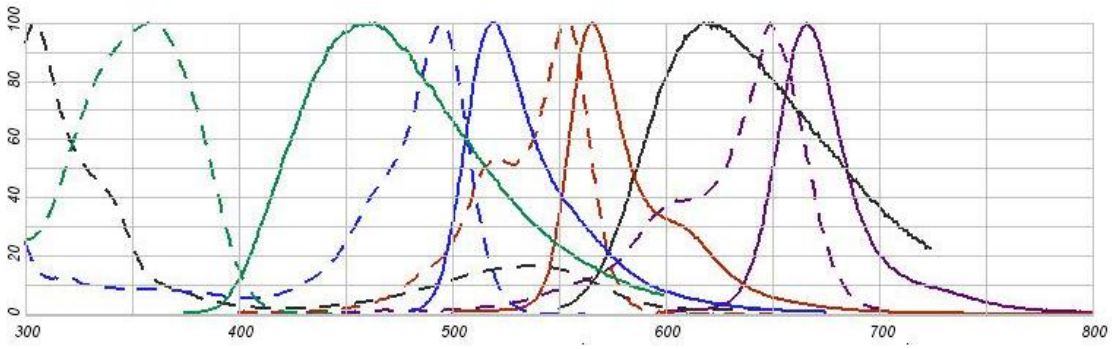

Figure 3: Excitation (dashed lines) and emission spectra (solid lines) of the fluorophores used in the study: DAPI (green lines), FITC (blue lines), Cy3 (red lines), PI (black lines) and Cy5 (purple lines). The x-axis shows the wavelength in nm and the y-axis the intensity of the excitation or emission in percent. Graph created with the Fluorescence SpectraViewer (www.invitrogen.com).

Indirect Immunofluorescence assay (IIFA) was conducted on cells fixed using 96% ice cold ethanol for 10 min at -20°C. Ethanol was removed and the cells were air dried and either stained directly or stored at 4°C for short term storage (less than a week) or at -20°C for long term storage. All steps were conducted at room temperature. Cells were rehydrated for 5 min using 1x PBS. The primary antibody diluted in PBS was incubated for 30 min. After three 5 min washing steps with PBS the secondary antibody was incubated for 30 min. Finally, cells were washed twice with PBS and once with distilled water. After cells were air dried they were overlaid with DABCO antifading solution to protect the fluorescence during exposition to the light. If cells were stained in a well of a tissue culture plate, DABCO antifading solution was mixed 1:1 with PBS and added to the wells. When cells were stained on a slide, 80 µl DABCO antifading solution were distributed dropwise and a cover slip was placed on top. Pictures were taken with the confocal laser scan microscope LSM 510 in a sequential scan at the AHRC Cell Imaging Core Facility, University of Georgia.

2.2.36 Cultivation of cells

Insect cells (S*f*9 and High5) were sub-cultivated without trypsin and rinsed into fresh medium. From all other cells old medium was removed, they were rinsed with PBS, trypsinized and incubated at 37°C until the cells detached. Cells were split in a ratio of 1:2 to 1:10 depending on the purpose of the subsequent experiment. Different amounts of PBS, trypsin/EDTA and medium were used depending on the size of the flask (Table 5). Cell line specific medium was described before (2.1.4).

Table 5: Amounts of PBS, trypsin EDTA and medium used for 3 different flask sizes.

Tissue culture flask size	T25	T75	T175
PBS	3 ml	5 ml	5 ml
Trypsin/EDTA	0.5 ml	1 ml	1ml
Medium	4 ml	9 ml	14 ml

2.2.37 Immunoprecipitation

Protein-protein interactions can be investigated by immunoprecipitation (IP) using protein G coupled to sepharose beads. Protein G binds the Fc part of IgG of several species with a very high affinity. The used target-antigen specific antibody will capture the target protein out of a cleared cellular lysate. If another protein is interacting directly or indirectly with this target protein, it will also be bound to the column. Proteins bound to protein G through the antibody can be seperated by SDS-PAGE followed by Western blot analysis. Differences between the IP of VP3/NF45 and VP4/p68 are indicated.

For both, 20 µl protein G sepharose beads were washed twice with 1 ml IP wash buffer 150 to remove ethanol from the beads. Then 5 µl of a capture antibody (mAb FLAG for NF45/VP3 and mAb His for p68/VP3) and 95 µl of the IP wash buffer 150 were added and the reaction tube was rotated o/n at 4°C. The protein G-antibody mixture was washed twice with 1 ml IP wash buffer 150 to remove not bound antibodies. Lysates were prepared from transfected/infected cells grown in a 6-well:

- NF45/VP3: DF-1 cells were transfected with NF45-FLAG pcDNA3 and infected 24 h post transfection (pt) with IBDV strain D78 (moi of 100). Lysates were prepared 24 h pi.
- p68/VP4: DF-1 cells were transfected with MBP-VP4-FLAG pcDNA3 and MBP-FLAG pcDNA3 as a control and cellular lysates were prepared 24 h pt.

For the preparation of lysates, medium was removed and cells were washed with 1 ml PBS, 100 µl trypsin/EDTA were added and incubated at room temperature until cells detached. Now, 900 µl cell culture medium containing 10% FBS were added, cells were transferred into a reaction tube and centrifuged at 1,000 x g for 5 min. The supernatant was removed, cells were washed with 1 ml PBS and centrifuged at 1,000 x g for 5 min. Then cells were resuspended in 200 µl 1x RIPA lysis buffer containing 1x proteinase inhibitor to lyse the cellular membranes. The lysate was vortexed and incubated for 10 min on ice. During incubation, the mixture was vortexed every 2 min. The cellular debris including the nucleus was then centrifuged for 5 min at 16,000 x g and the supernatant, also called cleared lysate, was transferred into a new reaction tube.

The cleared lysates were added to the protein G-antibody complex and the samples were rotated at 4°C for 2 h. The mixture was washed three times with IP wash buffer 150 and twice with IP wash buffer 300. A new reaction tube was used for the fourth washing step. Proteins were eluted by addition of 10 µl 2x gel-loading buffer.

2.2.38 DNA transfection

Cells grown in a 6-well tissue culture plate were transfected with a plasmid when they were 90% confluent. For that purpose, 100 µl OPTI-MEM were incubated with 4 µl Lipofectamine 2000 at room temperature for 5 min. In parallel 100 µl OPTI-MEM were incubated with 8 µl plasmid DNA. After 5 min both solutions were mixed together and incubated another 30 min at room temperature. During this incubation time the cell

culture medium was exchanged with 1.5 ml medium containing 10% FBS. Then the transfection mixture was added dropwise to the cells and rocked back and forth and side to side. The cells were incubated for three hours and then the cell culture medium was exchanged with 3 ml medium containing 2% FBS.

2.2.39 siRNA transfection

Small interfering (si) RNAs were ordered from Sigma-Aldrich as a duplex with a 3'TT overhang. DF-1 cells were seeded (2.75×10^6 cells/well of a 6-well plate) and 4 h later, medium was reduced to 1.25 ml each well. Cells were transfected with 150 pmol of one siRNA or 75 pmol of each siRNA, if two siRNAs were used. In a tube, 250 µl medium were mixed with 15 µl *Trans*IT-siQUEST Transfection Reagent and the siRNA. After 5 min of incubation at room temperature, the mixture was added to the cells and rocked. At 48 h pt cells were either harvested for Western blot analysis by washing the cells with PBS and scraping them off with a rubber scraper or cells were infected with D78 (moi=10) for viral replication studies. At 16 h pi the virus containing supernatant was obtained and stored at -80°C. Viral titers was determined using $TCID_{50}$ assay.

2.2.40 Tissue culture infective dosage 50 ($TCID_{50}$) assay by CPE

This method was conducted as in 2.2.27, except that DF-1 cells were used in a density of 5×10^5 cells/ml to determine the IBDV titer. At 4-5 d pi those wells showing CPE were counted as positive and the titer was calculated as described above.

2.2.41 Wilcoxon rank-sum test (Wilcoxon-Mann-Whitney test)

The Wilcoxon rank-sum test (Brüning & Trenkler 1994) is a non-parametric method that can be used for a small sample size. The paired-sample version of the Wilcoxon rank-sum test ranks the differences of both values. It is assumed that differences are independent observations from a symmetric distribution. A null hypothesis (both samples are drawn from one population, H_0:M≤0; M: median) is tested against the alternative hypothesis (two samples are drawn from two populations, H_1:M>0).The data set is paired (x_i, y_i…x_n, y_n) and the test was calculated one-sided. The difference of the values $D_i=Y_i-X_i$ is ranked based on the absolute value ($|D_i|$). If the difference is zero the value was not considered. All ranks larger than zero were summed up (W) and the test statistic Z was calculated with the formula $Z = \frac{W - n(n+1)/4}{\sqrt{n(n=1)(2n+1)/24}}$. The value of Z was compared with the table of standard normal distribution, giving 1-p. The statistical significance level was set to α=0.05 meaning if p<0.05 the null hypothesis is rejected, if α≥0.05 the null hypothesis is accepted.

3 Results

3.1 NF45

3.1.1 Comparison of NF45 homologs

To demonstrate the high conservation of the nuclear factor 45 (NF45) between species, a comparison of the amino acid (aa) sequence between different species was conducted using ClustalW (http://align.genome.jp/). The NF45 homologs were found with a protein BLAST (Basic Local Alignment Search Tool) search (blastp, to search the protein database using a protein query) on the NCBI database (http://www.ncbi.nlm.nih.gov/). The aa sequences used for the comparison were from the following species, showing the scientific name (common name), the NCBI accession number and the aa length. *Homo sapiens* (human) NP_004506, 390 aa; *Pongo abelii* (Sumatran Orangutan) CAH90963, 352 aa; *Pan troglodytes* (common chimpanzee) XP_001142410, 368 aa; *Canis familiaris* (dog) XP_537263, 390 aa; *Mus musculus* (mouse) NP_080650, 390 aa; *Rattus norvegicus* (rat) Q7TP98, 463 aa*; Gallus gallus* (chicken) XP_423437, 384 aa; *Xenopus laevis* (african clawed frog) AAH43981, 388 aa; *Danio rerio* (zebra fish) AAH66394, 387 aa; *Salmo salar* (Atlantic salmon) ACI33537, 387 aa; *Caenorhabditis elegans* (roundworm) NP_506614, 370 aa; *Tribolium castaneum* (red flour beetle) EEZ99001, 393 aa; *Apis mellifera* (European honey bee) XP_624830, 383 aa; *Aedes aegypti* (mosquito) XP_001651787, 398 aa; *Drosophila melanogaster* (fruit fly) Q9VG73, 396 aa. The results are summarized in Table 6, showing the percentage of identity. It is not surprising that all mammals except the rat showed a very high level of identity (≥93%). Only the rat sequence had a lower identity (≥82%), because it is longer (463 aa) at the N-terminus and other parts are missing. The lengths of the NF45 homologs varied between 352 aa (*P. abelii*) and 402 aa (*Strongylocentrotus purpuratus*, the California purple sea urchin, XP_001176545, not used for the ClustalW comparison). Only the sequence of *Monodelphis domestica* (Gray short tailed opossum, XP_001372472) was longer than the rat sequence (493 aa). Comparing the chicken NF45 to the mammalian proteins (except rat) revealed an identity of 94-96% due to several aa exchanges and a gap of the chicken sequence in the RGG-rich ssRNA-binding domain (see sequence below). Unfortunately, no other avian sequences were found with a blastp search using the chicken NF45 sequence and limiting the organism list to “aves” (birds). The only other protein found was the spermatid perinuclear RNA binding protein of *Taeniopygia guttata*, the zebra finch (XP_002190904), because both contain a DZF zink finger RNA binding motif. The frog sequence was the only amphibian listed. It showed still a very high aa identity to mammals (except rat) of 90%. Both fish sequences were more similar to mammals, birds and amphibian (≥72%) than to insects (≤68%), although evolutionary fish developed earlier than insects. Both fish showed an expected high identity of 96% in

NF45. Insect NF45 sequences compared with chicken NF45 showed low homology (57-63%). Only the worm had less homology with the chicken protein (33%). *C. elegans* showed in general a very low identity with other NF45 aa sequences (25-34%). The insect sequences among each other were 61-68% identical.

Table 6: Comparison of the amino acid sequences of NF45 homologs of different species. Identity is shown in percent. *G. gallus* (chicken) is emphasized (bold).

	H. sapiens	*P. abelii*	*P. troglodytes*	*C. familiaris*	*M. musculus*	*R. norvegicus*	***G. gallus***	*X. laevis*	*D. rerio*	*S. salar*	*C. elegans*	*T. castaneum*	*A. mellifera*	*A. aegypti*	*D. melanogaster*
H. sapiens	100														
P. abelii	100	100													
P. troglodytes	99	93	100												
C. familiaris	100	100	99	100											
M. musculus	100	100	99	100	100										
R. norvegicus	82	86	87	82	82	100									
G. gallus	**96**	**96**	**94**	**96**	**96**	**79**	**100**								
X. laevis	90	90	90	90	90	75	**91**	100							
D. rerio	88	88	87	88	88	72	**89**	87	100						
S. salar	89	89	89	89	89	73	**91**	88	96	100					
C. elegans	34	33	31	34	34	29	**33**	31	32	32	100				
T. castaneum	62	65	62	62	62	54	**63**	62	62	63	30	100			
A. mellifera	58	58	57	58	58	48	**57**	57	58	58	27	68	100		
A. aegypti	55	57	57	55	55	47	**56**	55	56	55	25	64	61	100	
D. melanogaster	56	57	56	56	56	47	**57**	56	56	56	28	65	61	63	100

The complete ClustalW arrangement is shown below; stars below the column indicate the same aa in all sequences. The chicken sequence is shown in bold. The RGG-rich ssRNA-binding domains were highlighted yellow. This motif was only present in mammals except the rat and partially in the frog, bird and fish, but not in insects. The green highlighted sequence represents the DZF zink-finger nucleic acid binding domain (both based on Cui *et al* 2011). In pink the glutamic acid (E)-rich region was marked that plays a role in transcriptional activation (based on Ranpura *et al* 2008).

```
S._Salar            ------------------------------------------------------------
D._rerio            ------------------------------------------------------------
X._laevis           ------------------------------------------------------------
G._gallus           ------------------------------------------------------------
C._familiaris       ------------------------------------------------------------
P._troglodytes      ------------------------------------------------------------
H._sapiens          ------------------------------------------------------------
M._musculus         ------------------------------------------------------------
P._abelii           ------------------------------------------------------------
R._norwegicus       MVSTHLTSTTLPDCYRSLIVNSELGSSALMDLNSPSFLYPLLHTPADKGTLCTYQAALGK
T._castaneum        ------------------------------------------------------------
A._mellifera        ------------------------------------------------------------
D._melanogaster     ------------------------------------------------------------
A._aegypti          ------------------------------------------------------------
C._elegans          ------------------------------------------------------------


S._Salar            ------------------------------------------------------------
D._rerio            ------------------------------------------------------------
X._laevis           ------------------------------------------------------------
G._gallus           ------------------------------------------------------------
C._familiaris       ------------------------------------------------------------
P._troglodytes      ------------------------------------------------------------
H._sapiens          ------------------------------------------------------------
M._musculus         ------------------------------------------------------------
P._abelii           ------------------------------------------------------------
R._norwegicus       VYASLEVIGVGDDKLQAVHGLNGGKPHRDILGSRITRPTGIKPLCLPRHILAYDWLAQSL
T._castaneum        ------------------------------------------------------------
A._mellifera        ------------------------------------------------------------
D._melanogaster     ------------------------------------------------------------
A._aegypti          ------------------------------------------------------------
C._elegans          ------------------------------------------------------------


S._Salar            -MRGDRGRGRGGRFGSRGGLVQGYRPFVPHIPFDFYVCEMAFPRVKPAA--DETAFSECL
D._rerio            -MRGDRGRGRGGRFGSRGGLVQGYRPFVPHIPFDFYVCEMAFPRVKPAS--DETAFSECL
X._laevis           -MRGERGRGRG-RFGSRMGPNAGFRPFVPHIPFDFHVCEMAFPRVKPAP--DDGTLSEAL
G._gallus           -MRGDRGRGRGGRFGSR------FRPFVPHIPFDFYVCEMAFPRVKPAA--DESAFSEAL
C._familiaris       -MRGDRGRGRGGRFGSRGGPGGGFRPFVPHIPFDFYLCEMAFPRVKPAP--DETSFSEAL
P._troglodytes      -MRGDRGRGRGGRFGSRGGPGGGFRPFVPHIPFDFYLCEMAFPRVKPAP--DETSFSEAL
H._sapiens          -MRGDRGRGRGGRFGSRGGPGGGFRPFVPHIPFDFYLCEMAFPRVKPAP--DETSFSEAL
M._musculus         -MRGDRGRGRGGRFGSRGGPGGGFRPFVPHIPFDFYLCEMAFPRVKPAP--DETSFSEAL
P._abelii           ------------------------------------MAFPRVKPAP--DETSFSEAL
R._norwegicus       LGIVIGSISLAYNELLMMEKLKGFRPFVPHIPFDFYLCEMAFPRVKPAP--DETSFSEAL
T._castaneum        G-----IRGRGGMNRGIGRPPYKVKMFLPRHPFDLALCESSFPRVKPAP--DETAFTQAL
A._mellifera        GRGGMIRGGRGGMGRGMG---FPRKQFLPRHPFDYTLCEAAFPRVKPAP--DESDFQMAL
D._melanogaster     ---MVRGALRGGRPMRGGIRPPFKKTFVPRHPFDLTLAEVFFPKVPSAGAVDDSALTAAL
A._aegypti          MMRGGRGGMGMGMRGMRGAPFMHKKSFLPRHPFDLTLAEPAFPRVSAP--PDDSVLTNAL
C._elegans          ------------MVPGGNFPQFGVPIPQFRTIYDYTLDKGNLEGTKNTS---DAVFEKEI
                                                     :  .  .    :  :   :


S._Salar            LKRNQDLSPTPAEQSSILSLVTKINNVIDNLIVAP-GNFEVQIEEVRQVGSYKKGTMTTG
D._rerio            LKRNQDLSPTPSEQASILSLVTKINNVIDNLIVAP-GNFEVQIEEVRQVGSYKKGTMTAG
X._laevis           LKRNQDLAPTTTEQASILSLVTKINNVIDNLIVAP-GTFEVQIEEVRQVGSYKKGTMTSG
G._gallus           LKRNQDLAPTAAEQASILSLVTKINNVIDNLIVAP-GTFEVQIEEVRQVGSYKKGTMTTG
C._familiaris       LKRNQDLAPNSAEQASILSLVTKINNVIDNLIVAP-GTFEVQIEEVRQVGSYKKGTMTTG
P._troglodytes      LKRNQDLAPNSAEQASILSLVTKINNVIDNLIVAP-GTFEVQIEEVRQVGSYKKGTMTTG
H._sapiens          LKRNQDLAPNSAEQASILSLVTKINNVIDNLIVAP-GTFEVQIEEVRQVGSYKKGTMTTG
M._musculus         LKRNQDLAPNSAEQASILSLVTKINNVIDNLIVAP-GTFEVQIEEVRQVGSYKKGTMTTG
P._abelii           LKRNQDLAPNSAEQASILSLVTKINNVIDNLIVAP-GTFEVQIEEVRQVGSYKKGTMTTG
R._norwegicus       LKRNQDLAPN--------------------------SAEQQIEEVRQVGSYKKGTMTTG
T._castaneum        LKRNVDLSPTPAEQTAILNLVTKIQTVLDNLVVAPGAFDACQLEEVRQVGSFKKGTMVTG
A._mellifera        LKKNTDMCPTPKEQTSILNLVTKLQSVLDNLIVAPGSFEACQLEEVRQVGSFKKGTMIKG
D._melanogaster     LKRNQDLSPTPSEQTAIGNLVTKVQAVLDNLVVAPGDLTTCQLEEVRQVGSFKKGTILTG
A._aegypti          LKRSQDLTPTQQEQTAISNLVTKVQAVLDNLVIAPGDFNKCQLDEVRQVGSFKKGTMMAG
C._elegans          LDRAANLTPSVEIRKRINEYAKKVIVALEKEKREK-TLVDIGIATISHVGSFVTDTTTHS
                    *.:  :: *.                              :  : :***: ..*   .
```

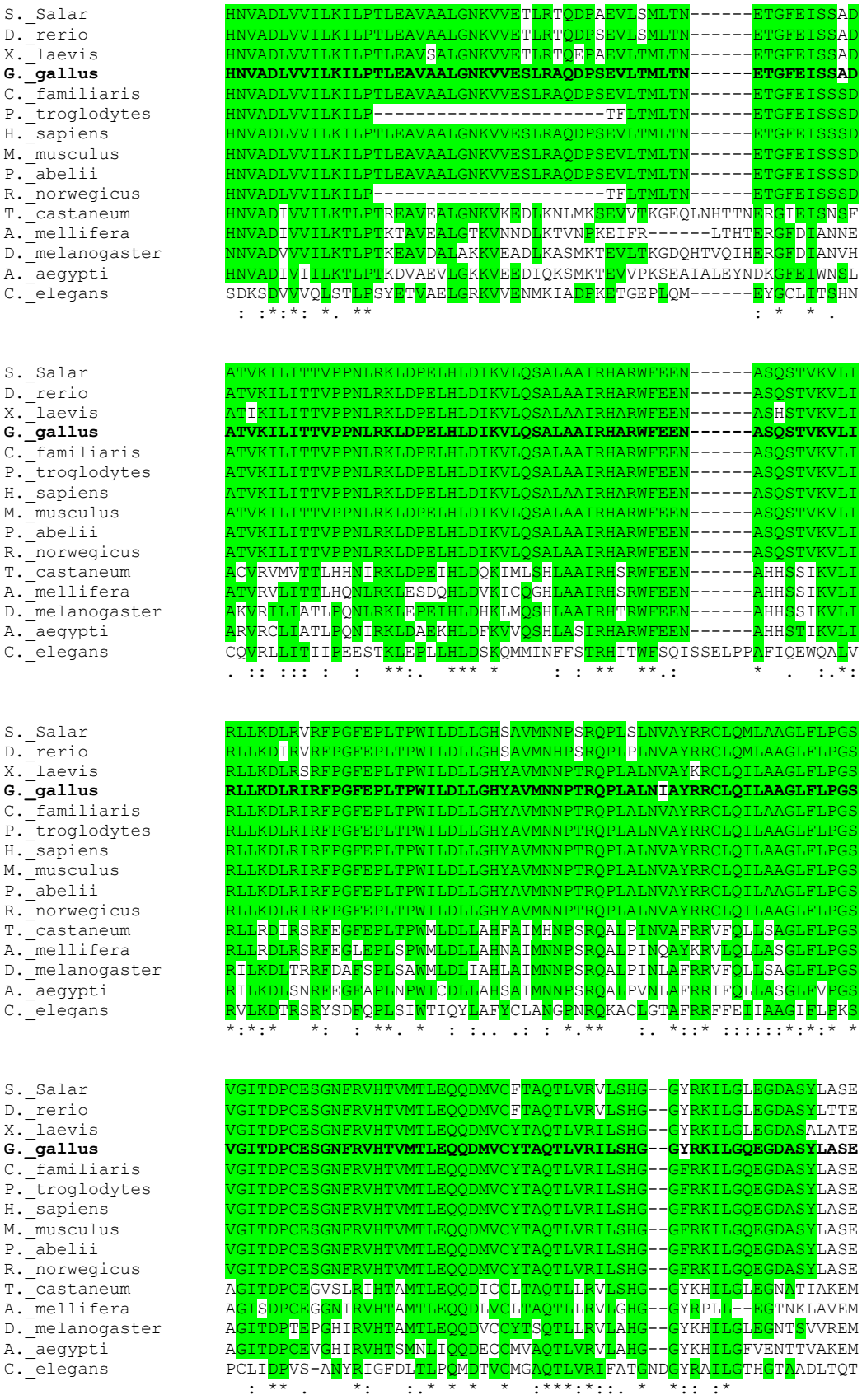
S._Salar
D._rerio
X._laevis
G._gallus
C._familiaris
P._troglodytes
H._sapiens
M._musculus
P._abelii
R._norwegicus
T._castaneum
A._mellifera
D._melanogaster
A._aegypti
C._elegans

```
S._Salar              MSTWDGVIVTPSEKAYEKPPERKE-EEDEALEEGGD--VEDESMETQE
D._rerio              MSTWDGVIVTPSEKAYEKPPERKE-EEDEALEEGVE--AEDESMETQE
X._laevis             MSTWDGVIVTPSEKAYEKPPERKE-GEEDDNQEIAEGAEEEESMETQE
G._gallus             MSTWDGVIVTPSEKAYEKPPEKKEGEEEEENQEEPAAGEEEESMETQE
C._familiaris         ISTWDGVIVTPSEKAYEKPPEKKEGEEEEENTEEPPQGEEEESMETQE
P._troglodytes        ISTWDGVIVTPSEKAYEKPPEKKEGEEEEENTEEPPQGEEEESMETQE
H._sapiens            ISTWDGVIVTPSEKAYEKPPEKKEGEEEEENTEEPPQGEEEESMETQE
M._musculus           ISTWDGVIVTPSEKAYEKPPEKKEGEEEEENTEEPPQGEEEESMETQE
P._abelii             ISTWDGVIVTPSEKAYEKPPEKKEGEEEEENTEEPPQGEEEESMETQE
R._norwegicus         ISTWDGVIVTPSEKAYEKPPEKKEGEEEEENTEEPPQGEEEESMETQE
T._castaneum          SVWDG-VVVSPLDKAYENPPEKKEGEEEDEDMEAEGDESMETIDN---
A._mellifera          SVWAGGVVASPLDKVYEPPTEQEQQEDMEESNEEMITESA--------
D._melanogaster       SVWNG-VCISPLTAVYEKPTDKKEGDLEEDIDMIENENEEEGSDDGAE
A._aegypti            SVWDG-VVVSPMEPAYEKPTEKKDDEEEDMECVEESTMEDDNGE----
C._elegans            ISTWKGIEIRPSIDAYRDGCMTRFPARAEIPTV---------------
                            :   *   .*.     .     :
```

3.1.2 Construction of recombinant plasmids encoding chicken NF45

Two recombinant plasmids encoding chicken NF45 were generated, one with a sixfold histidine-tag (6x His-tag, NF45-His-pDual), another with a FLAG tag (NF45-FLAG-pcDNA3). For NF45-His-pDual oligonucleotides were delineated based on the *Gallus gallus* sequence (XM_423437, sequence see 6.2.1) and were designed to contain at the 5' end an *Eco*RI restriction site (NF45-FP) and on the 3' end a 6x His-tag and a *Not*I restriction site (NF45-His). These two oligonucleotides were used for RT-PCR on RNA extracted from CEC to obtain the cDNA of NF45 (1173 bp), which was first cloned into pCR®2.1-TOPO® and confirmed by sequencing. The recombinant plasmid was digested with *Eco*RI and *Not*I to ligate the NF45 encoding cDNA fragment into the appropriately cleaved baculovirus transfer vector pFastBac™Dual resulting in the plasmid NF45-His-pDual. NF45-FLAG was obtained by PCR using Deep Vent DNA polymerase with the same forward primer (NF45-FP) and the reverse primer NF45-FLAG containing the FLAG sequence and also a *Not*I RE cleavage site. The resulting PCR product was first ligated with pCR®2.1-TOPO®, then digested with *Eco*RI and *Not*I to ligated the obtained cDNA fragment into the cleaved pcDNA3 vector resulting in NF45-FLAG-pcDNA3. All recombinant plasmids were transformed into *E. coli* XL1-Blue cells and plasmids were isolated and sequenced to confirm the correct nucleotide sequence with sequencing primers listed in Table 1b.

3.1.3 Detection of NF45 mRNA by Northern Blot

In next experiments it was analyzed, if NF45 mRNA levels increased during a virus infection. To this end, mRNA of control CEC and with IBDV strain D78 infected CEC at a moi of 1 was isolated 24 h pi. Both samples of RNA were separated on a gel for Northern blot analysis. As a positive control for NF45 RNA, the *Not*I linearized NF45-FLAG-pcDNA3 plasmid was used for T7 RNA polymerase transcription resulting in a 1189 bp long NF45 RNA fragment. As a control to observe RNA upregulation during IBDV infection, another gel was used for the detection of Mx RNA, which was shown to be upregulated upon IBDV infection (Mundt 2007). The positive control for Mx was the T7 RNA polymerase transcribed RNA of the *Not*I linearized Mx-pcDNA3 plasmid

(obtained from Dr. E. Mundt). Equal amounts of cellular RNA were separated on a gel and blotted on a nylon membrane, which was hybridized with a specific probe. For NF45, the DIG-labeled RNA transcribed by Sp6 RNA polymerase of an *Eco*RI linearized NF45-FLAG-pcDNA3 plasmid was used. The DIG-labeled Mx probe was RNA transcribed by Sp6 polymerase of an *Eco*RV linearized Mx-pcDNA3 plasmid. The Northern blots are shown in Figure 4. The blot with the Mx-specific probe in Figure 4A showed as expected that mRNA levels of the Mx gene were specifically upregulated upon IBDV infection. In Figure 4B the RNA levels of NF45 in infected and non-treated control CEC were shown. There was no difference in the observed intensity. Interestingly, two mRNA bands appeared on the blot. The upper one seemed to be the full length, since the positive control (full length NF45 cRNA) had the same length as the upper band. The lower band was likely also specific for NF45. This band might represent a shorter transcription product and needs to be elucidated by further experiments.

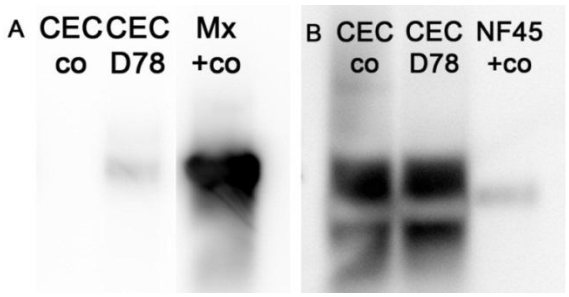

Figure 4: Northern Blot of non-infected and D78 infected CEC RNA with Mx RNA probe (A) and NF45 RNA probe (B), each with its positive control.

3.1.4 Chicken NF45 serum – Expression and purification of NF45

In order to study the phenotype of NF45 in chicken cells after virus infection, a specific serum against chicken NF45 was needed. To this end a purified recombinant NF45 of chicken origin was required to generate protein specific antiserum in a rabbit.

The Bac-to-Bac® Baculovirus expression system was used to generate such a recombinant baculovirus encoding chicken NF45. This was accomplished by applying the manufacturer's protocol to transform the recombinant plasmid NF45-His-pDual into DH10Bac™ competent *E. coli* cells to generate the recombinant NF45-bacmid. The correct insertion of the NF45 gene was confirmed by a PCR using Taq polymerase and

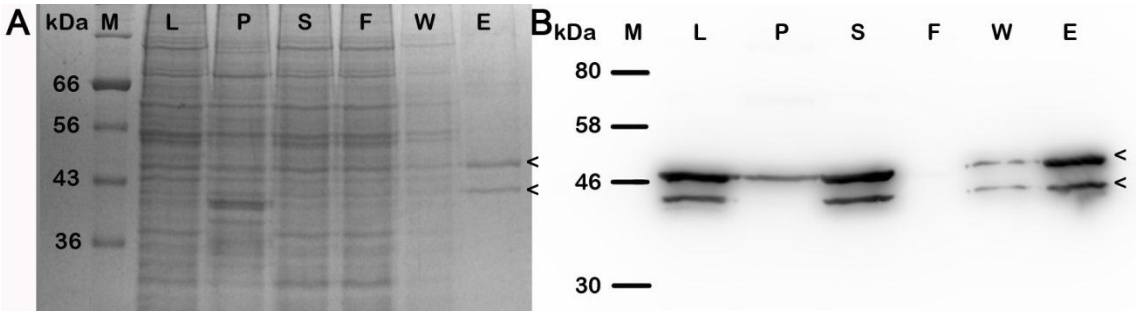

Figure 5: Analysis of the purification of NF45-His. (A) Coomassie brilliant blue stained gel and (B) Western blot using a mAb His-POD (1:5,000) of the NF45-His samples taken at different purification steps; M: marker; L: lysate; P: pellet; S: supernatant; F: flow-through; W: first wash step; E: eluate. Arrowheads indicate NF45-His and its N-terminal truncated isoform.

the primers pFast-FP and NF45-His (see Table 1a). The obtained NF45-His-bacmid was transfected into High Five™ cells and the cell culture supernatants containing the recombinant baculovirus expressing chicken NF45 (NF45-His-Bac) were passaged on *Sf*9 cells. NF45-His-Bac titers were determined by $TCID_{50}$ assay and *Sf*9 cells were infected to express recombinant chicken NF45-His, which was purified using affinity chromatography. The single purification steps were analyzed on a SDS-PAGE stained with Coomassie brilliant blue (Figure 5A) and by Western blot analysis with the mAb His-POD (Figure 5B) to track the protein during purification and the purity of the eluate. As seen on the protein stained gel in the last lane (E), two bands became visible. The upper band had the calculated molecular weight of approximately 45 kDa, while the molecular weight of the lower band was 42 kDa, both indicated by arrow heads.

It was observed that both purified predominant bands contained a 6x His-tag since they were detectable by Western blot analysis using mAb His. Both bands were excised from the gel and submitted for analysis by MALDI-TOF MS-MS at the Proteomics Resource Facility, University of Georgia. The results confirmed that the upper band was indeed the full length NF45-His and peptide analysis of the lower band revealed that a peptide at the N-terminus of NF45-His was not present, which indicated that probably a later start codon was used resulting in a shorter form of chicken NF45 encoding 6x His-tag. All NF45-His containing eluates were pooled, concentrated and the amount was determined. Seven aliquots á 400 µg/500 µl were generated and provided for the Polyclonal Antibody Production Service at the University of Georgia. A New Zealand White SPF Rabbit was immunized with the recombinant NF45-His and complete Freund's adjuvant. Approximately every three weeks the rabbit was immunized again with NF45-His mixed with incomplete Freund's adjuvant. Blood was taken before the first and two weeks after each inoculation. The final bleeding occurred after the sixth boost immunization. The obtained rabbit-anti-NF45-His serum (R-α-NF45) was used in a dilution of 1:500 in an indirect immunofluorescence assay (IIFA) and 1:1,000 for Western blot analysis as demonstrated below.

3.1.5 Specificity of the R-α-NF45 serum

The specificity of the R-α-NF45 serum was tested using Western blot and IIFA. For Western blot analysis, lysates from cells of different species were tested: DF-1 (chicken), QM-7 (quail) and Vero cells (monkey). Samples were loaded on a gel and further analyzed by Western blot incubated with the R-α-NF45 serum and a secondary α-R-POD antibody, which revealed a main band at approximately 46 kDa as indicated by an arrow (Figure 6A). Furthermore a faint band was observed at 26 kDa and 70 kDa in the lysate of DF-1 cells and three bands in the lysate of Vero cells (30 kDa, 58 kDa and 66 kDa). Based on the size of the main bands and in combination with the MALDI-TOF

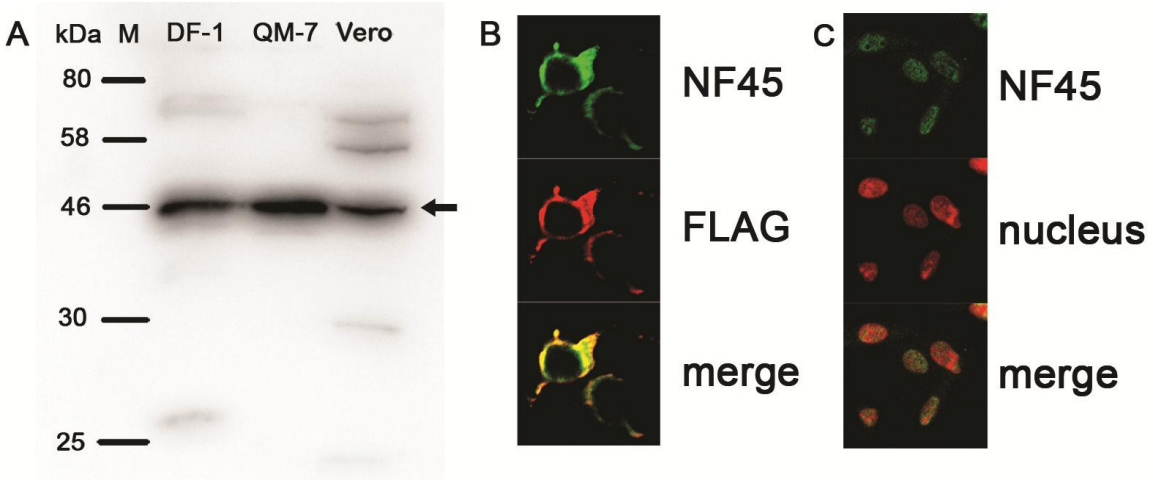

Figure 6: Specificity of the R-α-NF45 serum. (A) Western blot of DF-1, QM-7 and Vero cell lysates using the R-α-NF45 serum (1:1,000) as a primary and α-R-POD (1:20,000) as a secondary antibody; (B) IIFA of 293 T cells transfected with NF45-FLAG-pcDNA3, ethanol fixed and incubated with R-α-NF45 (1:400, green) and mAb FLAG (1:500, red) and appropriate conjugates (α-R-FITC 1:400 and α-M-Cy3 1:600). (C) IIFA of fixed DF-1 cells incubated with R-α-NF45 (1:400, green) and propidium iodide (1:5,000, nucleus, red) and the conjugate α-R-FITC (1:400). Co-localization was observed as indicated by the yellow stain. IIFA was visualized by confocal laser scanning microscopy (CLSM). Scale bar: 10 µm

MS-MS result it was concluded that the polyclonal R-α-NF45 serum detected specifically NF45 of different species.

For IIFA, 293 T cells were transfected with NF45-FLAG-pcDNA3 carrying an immediate early promoter of human cytomegalovirus for transient expression of NF45-FLAG. Twenty-four hours after transfection cells were fixed for an IIFA with R-α-NF45 serum and mAb FLAG. As secondary antibodies α-R-FITC and α-M-Cy3 were used. All IIFA pictures were taken with the confocal laser scanning microscope (CLSM) LSM 510 Meta (Zeiss). In Figure 6B endogenous NF45 was not observed in 293T cells indicating a weak cross-reactivity of R-α-NF45 serum with human NF45. Heterologous expressed NF45-FLAG of chicken origin was always observed in the cytoplasm, never in the nucleus indicating a missing transport mechanism for chicken NF45 in cells of human origin. Co-localization of the NF45 and the FLAG fluorescence is shown on the merged picture. This demonstrates that the serum specifically recognizes chicken NF45 in IIFA. In DF-1 cells, which were neither infected nor transfected, endogenous chicken NF45 was detected by IIFA using R-α-NF45 serum followed by α-R-FITC. The nucleus was visualized with propidium iodide (PI). NF45 was localized mostly in the nucleus (Figure 6C), as seen in the lowest picture merging the NF45 signal and the nuclear fluorescence. Small amounts of NF45 were observed in the cytoplasm.

3.1.6 Co-localization of cellular NF45 and VP3 of IBDV

Next, the localization of NF45 in IBDV infected cells was identified. To this end, DF-1, QM-7 and Vero cells were infected with the classical IBDV strain D78 (moi = 1). Cells were fixed 12 h pi for IIFA with R-α-NF45, mAb VP3 and PI. The binding of the primary

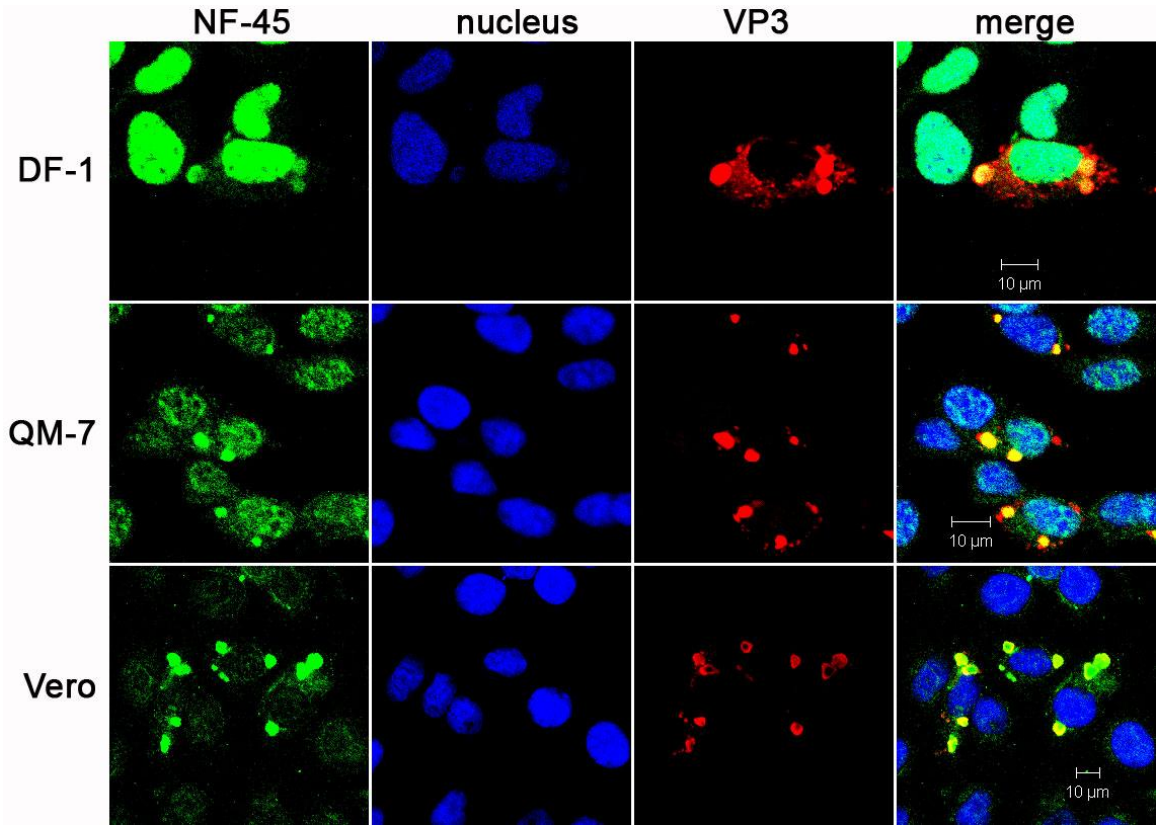

Figure 7: Indirect immunofluorescence of DF-1, QM-7 and Vero cells infected with D78 for 12 h. The R-α-NF45 serum (1:400, green), PI (1:5,000, nucleus, blue) and mAb VP3 (1:100, red) were used with α-R-FITC (1:400) and α-M-Cy5 (1:50) conjugates. IIFA was visualized by CLSM.

antibodies was detected by using species specific conjugates (α-R-FITC and α-M-Cy5). All pictures showed infected and non-infected cells to highlight the difference between the localization of NF45. To differentiate between cytoplasm and nucleus, the nuclear marker PI was used. The nuclear phenotype of NF45 was different in cells, which have been IBDV infected as indicated by the presence of VP3 (Figure 7). In infected cells NF45 accumulated in the cytoplasm and co-localized with VP3, as indicated in the merged picture by the overlapping fluorescence. This phenotype was observed in all three cell lines used, demonstrating a species independency of this phenotype (chicken, quail and monkey). Due to chromosomal deletions in their genome, Vero cells lack the ability to express IFN α and β (Mosca & Pitha 1986, Diaz *et al* 1988). Based on this knowledge it can be concluded that the VP3-NF45 co-localization was independent of the expression of IFN regulated genes, because NF45 accumulated also in the cytoplasm of infected Vero cells. Interestingly, in Vero cells less NF45 was observed in the nucleus of both, infected and uninfected cells.

3.1.7 Quantification of NF45 in the nucleus

The ratio of nuclear NF45 in comparison to the cytoplasmic fraction was determined by dividing the integrated NF45 intensity of the nuclear fraction by the integrated NF45

intensity of the whole cell. The size of the nucleus was determined by the nuclear staining with PI. This was calculated for non-infected DF-1 cells and for DF-1 cells infected with D78. In non-infected cells 88% of NF45 resided in the nucleus. As expected, more NF45 was observed in the cytoplasm after infection (36%) and only 64% were present in the nucleus (see Figure 8). The standard deviation indicated by an error bar was relatively high in the infected cell population, which might be explained by different numbers of virus entering the cell or various virus replication states.

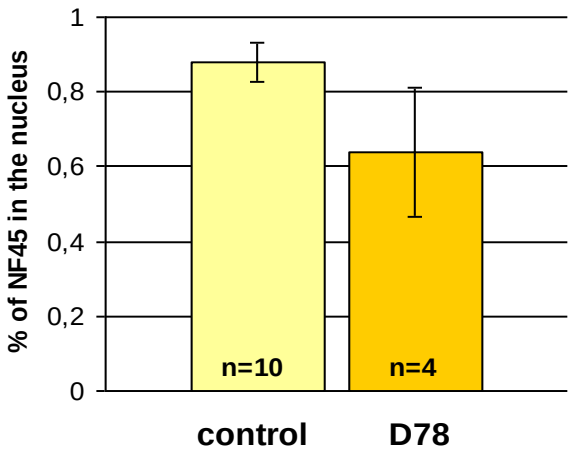

Figure 8: Quantification of NF45 fractions in the nucleus in non-infected DF-1 cells (control) and with D78 infected cells 12 h pi (D78). The diagram shows the average percentage of integrated intensity of nuclear NF45 divided by the integrated intensity of the whole cell. N is the number of cells analyzed. Error bars indicate the standard deviation.

3.1.8 Specific co-localization of cellular NF45 with viral proteins VP1 and VP3 during IBDV replication

An interaction of VP1 and VP3 has been shown before (Tacken *et al* 2002). To investigate, if VP1 was also part of a protein complex involving both proteins IBDV VP3 and NF45, IBDV infected DF-1 cells were investigated. An IIFA was conducted with R-α-NF45, mAb VP3 DAPI for nuclear stain and a VP1 specific serum obtained from a chicken immunized with recombinant VP1 (Ch-α-VP1) with appropriate conjugates α-R-FITC, α-Ch-Cy3 and α-M-Cy5. It was observed that in addition to the before observed co-localization of VP3 and NF45, VP1 was also present in the cytoplasm of infected cells and was co-localizing with VP3 and NF45 (Figure 9).

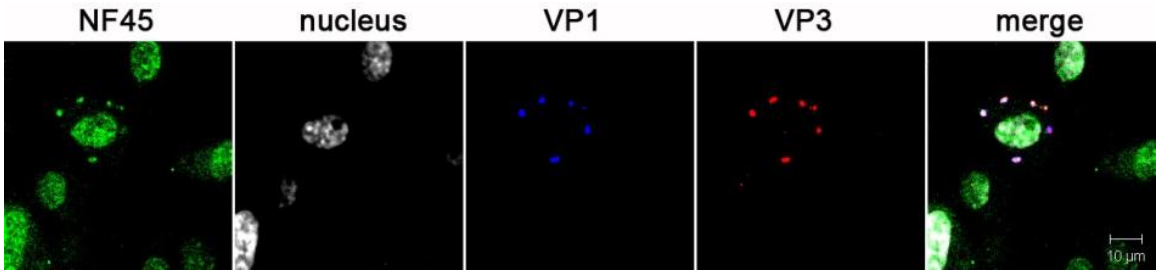

Figure 9: Indirect immunofluorescence of IBDV strain D78 infected DF-1 cells, which were ethanol fixed 12 h pi. Fixed cells were incubated with R-α-NF45 serum (1:400, green), mAb VP3 (1:100, red) ch-α-VP1 (1:400, blue) and DAPI (1:50,000, white). The binding of the primary antibodies were visualized by CLSM using α-R-FITC (1:400), α-Ch-Cy3 (1:5,000) and α-M-Cy5 (1:50) as conjugate antibodies.

3.1.9 No co-localization of cellular protein NF45 and VP4 of IBDV

With the following experiments it was examined whether the IBDV protease VP4 was also involved in a co-localization with NF45. DF-1, QM-7 and Vero cells were infected with IBDV strain D78 and 12 h pi cells were fixed and submitted for IIFA with R-α-NF45, PI and mAb VP4, a monoclonal antibody directed against the viral protease VP4, followed by incubation with α-R-FITC and α-M-Cy5 as conjugates. As expected, VP4 formed rodlike structures resembling likely tubular structures in the cytoplasm of infected cells (Figure 10) as described before (Granzow *et al* 1997). It was clearly visible that NF45 was localized in the nucleus as well as in discrete dot-like structures in the cytoplasm of infected cells, mutually exclusive from VP4. Based on these results it can be concluded that NF45 did not co-localize specifically with the IBDV protease VP4.

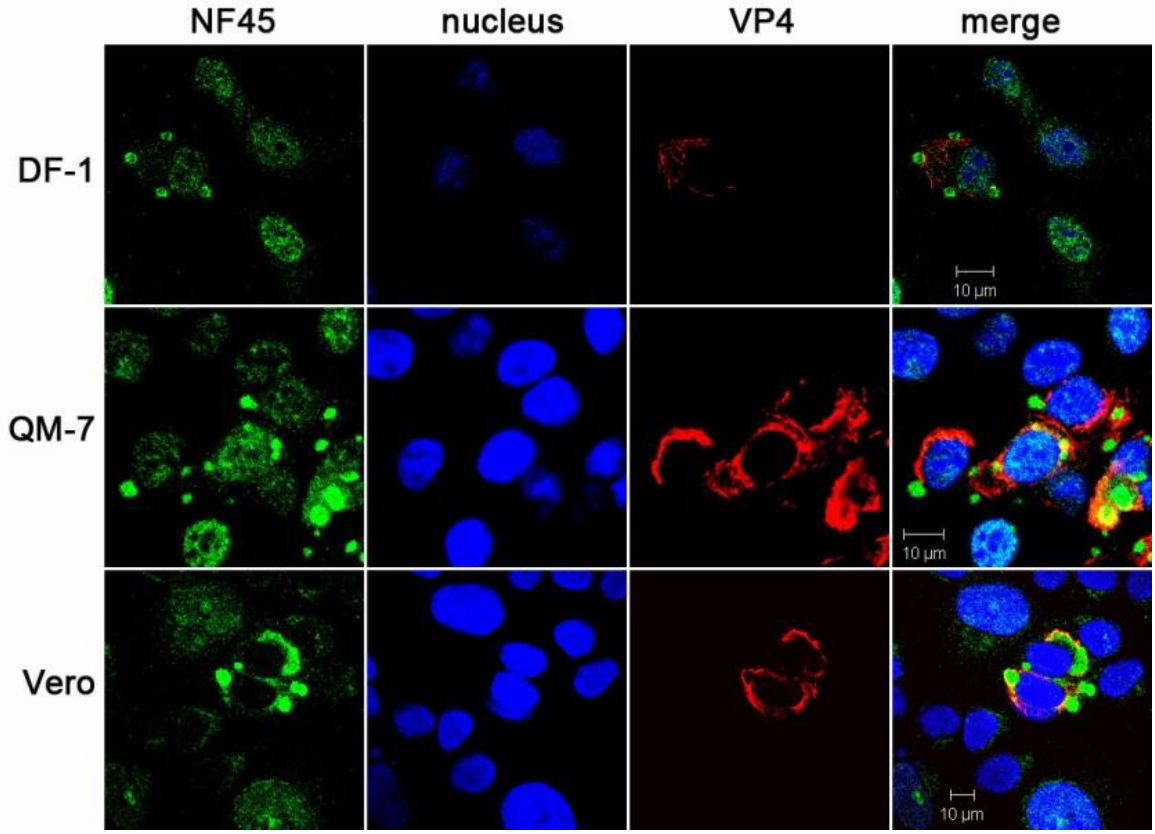

Figure 10: Indirect immunofluorescence of IBDV strain D78 infected DF-1, QM-7 and Vero cells. Twelve hours after infection cells were ethanol fixed and incubated with the R-α-NF45 serum (1:400, green), PI (1:5,000, nucleus, blue) and mAb VP4 (1:100, red). The binding of the primary antibodies was detected by use of appropriate species-specific conjugates [α-R-FITC (1:400) and α-M-Cy5 (1:50)]. The reaction of the antibodies was visualized by CLSM.

3.1.10 Co-localization of NF45 and VP3 is strain independent

To clarify, if the observed phenotype was dependent on the IBDV strain, DF-1 cells were infected with variant strains 8903 and GLS-05, belonging to the E/Del and GLS subtype, respectively. These viruses differ from the D78 strain in their pathogenic potential and

antigenic phenotype. Cells were fixed 12 h pi and incubated with R-α-NF45, mAb VP3 and PI and the respective conjugates to visualize the binding of the primary antibodies. VP3 of variant strains 8903 and GLS-05 showed the same pattern of co-localization with NF45 in the cytoplasm of infected cells (Figure 11). This shows that NF45-VP3 co-localization is independent of the investigated IBDV strains. Especially after infection with variant strains, nucleic acids accumulated in the complex as indicated by the presence of PI staining. Since PI intercalates unspecific with all nucleic acids, it is possible that the accumulated nucleic acid represents viral RNA.

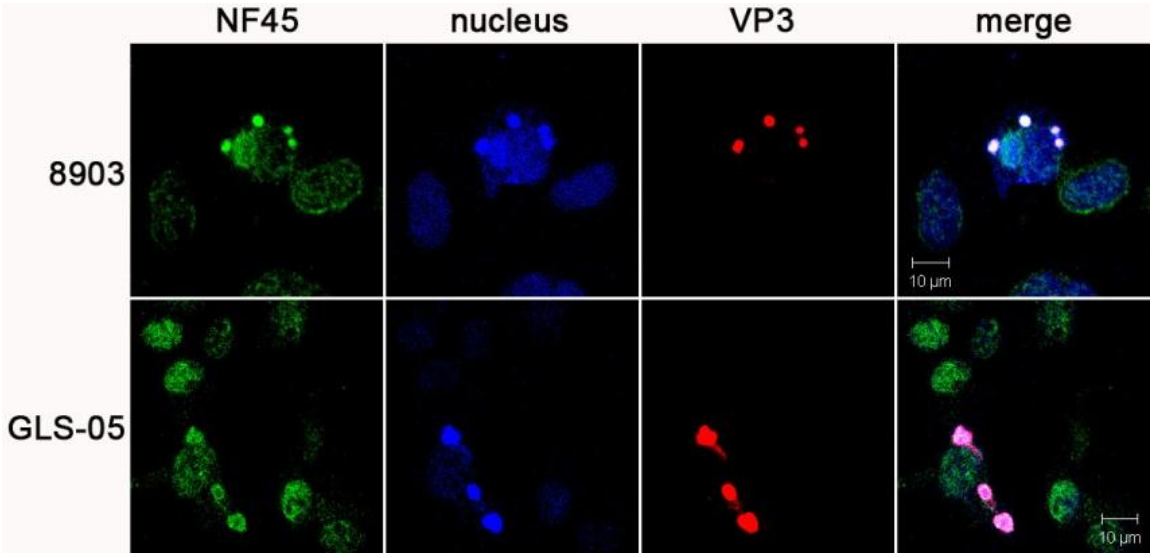

Figure 11: Indirect immunofluorescence of DF-1 cells infected with 8903 and GLS-05 were ethanol fixed 12 h pi. The cells were incubated with R-α-NF45 serum (1:400, green), PI (1:5,000, nucleus, blue) and mAb VP3 (1:100, red) and the binding of the primary antibodies was detected by CLSM using α-R-FITC (1:400) and α-M-Cy5 (1:50) conjugated antibodies.

3.1.11 Co-localization of NF45 and VP3 was correlated to the time course of viral replication

In order to investigate the dynamics of NF45 co-localizing with VP3, DF-1 cells were infected with IBDV strain D78, fixed at 4, 6, 8 and 10 h pi and incubated with R-α-NF45, PI and mAb VP3 for IIFA using appropriate conjugated antibodies (Figure 12). At 4 h pi VP3 was not observed in any cell and NF45 was detected only in the nucleus of cells. This was confirmed by the quantification of NF45 revealing 81% of NF45 being present in the cellular nucleus at 4 h pi, which is comparable to uninfected cells (see Figure 12). At 6 h pi NF45 did not change its appearance, contrary to VP3, which was detectable in the cytoplasm of infected cells in a scattered pattern. Like in control cells, 79% of NF45 resided in the nucleus, although some cells showed already 24% of NF45 in the cytoplasm as indicated by the standard deviation shown by the error bar (see Figure 12). This phenotype changed at 8 h pi dramatically and for the first time co-localization was observed in the cytoplasm of infected cells in round structures (Figure 12). Now, 45% of

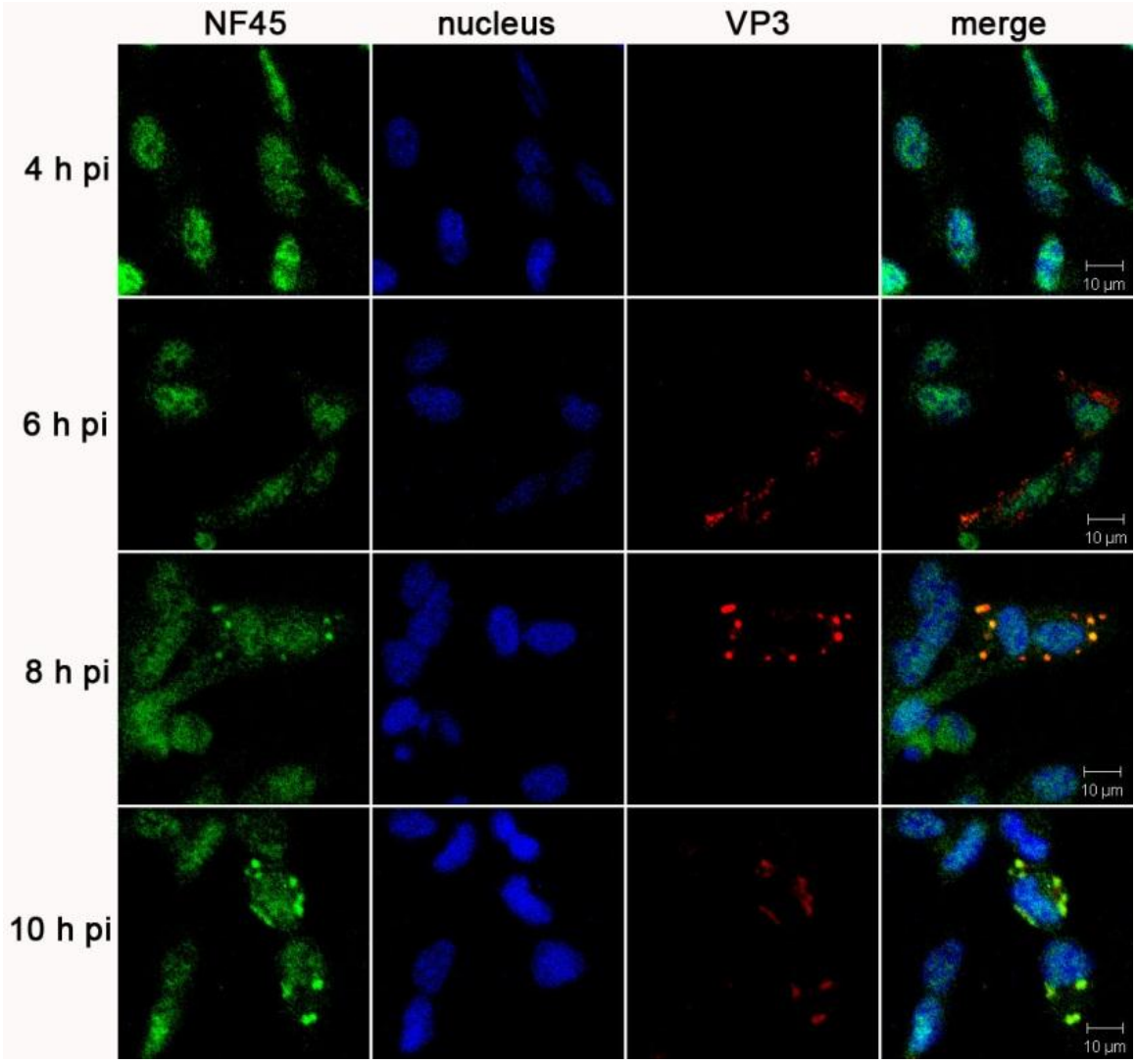

Figure 12: Localization of NF45 at different time points after IBDV infection. DF-1 cells were infected with D78 and fixed 4, 6, 8 and 10 h pi with ethanol. Fixed cells were incubated with R-α-NF45 (1:400, green) and mAb VP3 (1:100, red). The binding of the primary antibodies was visualized by the appropriate conjugates [α-R-FITC (1:400) and α-M-Cy5 (1:50)]. Nucleic acids were stained with PI (1:5,000, blue). The binding of the antibodies was documented by CLSM.

NF45 was present in the nucleus and 55% in the cytoplasm (see Figure 13). At 10 h pi the structures of co-localization were larger, but the cytoplasmic fraction of NF45 was similar to the previous time point (53% in the cytoplasm, see Figure 12 and Figure 13). From these observations it can be concluded that the co-localization of NF45 and VP3 in the cytoplasm occurs in a time dependent manner.

3.1.12 No co-localization of transiently expressed viral proteins

Several experiments were conducted to identify, which viral elements were necessary to observe NF45 in the cytoplasm of infected cells.

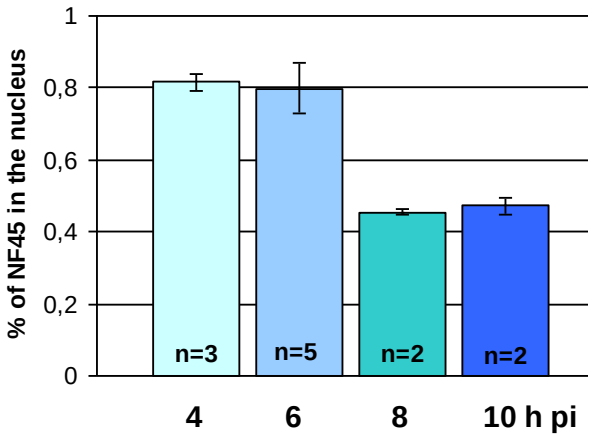

Figure 14: Quantification of the NF45 fraction in the nucleus of DF-1 cells at 4, 6, 8 and 10 h pi with D78. The column shows the average of nuclear integrated intensity divided by the integrated intensity of the whole cell. N: number of all cells analyzed. Error bars indicate the standard deviation.

3.1.12.1 Transfection of VP1-His-pcDNA3 and VP3-His-pcDNA3

It was shown that VP1 and VP3 co-localized with NF45 during an IBDV infection (see Figure 9). In the following experiment it was investigated, if expression of VP1 and VP3 alone were sufficient to induce NF45 to accumulate in the cytoplasm. For expression in DF-1 cells, VP1 was cloned in a pcDNA3 vector encoding a 6x His-tag sequence at its C-terminus. VP1 was amplified in a PCR reaction with Deep Vent DNA Polymerase and the primers VP1-FP and VP1-His-RP on puc19FLBD78 (puc19 vector with the full length segment B of the virus strain D78, provided by Dr. E. Mundt, Mundt & Vakharia 1996). The amplified product was cloned by a 5' *Eco*RI and a 3' *Not*I RE site induced with the primers into pcDNA3. A recombinant plasmid was obtained, the sequence was verified by sequencing and named VP1-His-pcDNA3. A similar construct was generated with the VP3 encoding region, which included an artificial start codon and a C-terminal located 6x His-tag encoding sequence. The sequence of the obtained recombinant plasmid VP3-His-pcDNA3 was also verified by sequencing and provided by Dr. E. Mundt. The two plasmids VP1-His-pcDNA3 and VP3-His-pcDNA3 were co-transfected into DF-1 cells and fixed 24 h pt and an IIFA with R-α-NF45, ch-α-VP1 and mAb VP3 and the appropriate conjugates was carried out (Figure 13). VP3 was sometimes observed inside the nucleus together with NF45, but mostly NF45 was solely present in the nucleus. VP1 and VP3 expressed simultaneously in one cell were not

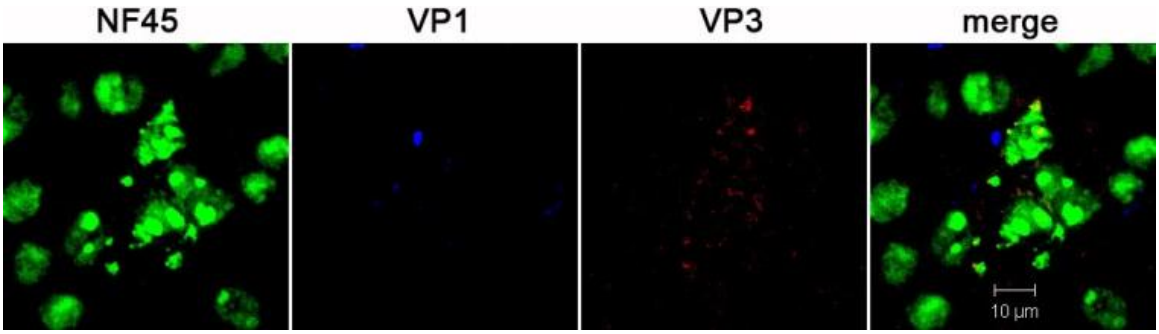

Figure 13: Transfection of VP1-His-pcDNA3 and VP3-His-pcDNA3 into DF-1 cells. Cells were fixed with ice cold ethanol 24 h pi and incubated with R-α-NF45 (1:400, green), ch-α-VP1 (1:200, blue) and mAb VP3 (1:100, red). The binding of the primary antibodies was visualized by CLSM using α-R-FITC (1:400), α-Ch-Cy3 (1:500) and α-M-Cy5 (1:50).

sufficient for endogenous NF45 to accumulate in the cytoplasm of transfected cells.

3.1.12.2 Transfection of segment A

Since NF45 was not observed in the cytoplasm when VP1 and VP3 were transiently expressed, it was further investigated whether co-localization correlated with the replication status of IBDV. QM-7 cells were transfected with cRNA of IBDV segment A containing the non-translated regions (NTR) and the two ORFs. For this, the plasmid puc19FLAD78 (puc19 vector with the full length segment A of the virus strain D78, provided by E. Mundt, Mundt & Vakharia 1996) was linearized with *Bsr*GI to transcribe viral cRNA with an exact 3' end by T7 RNA polymerase. The cRNA was transfected and 12 h pt cells were fixed for IIFA with R-α-NF45, DAPI and mAb VP3 followed by appropriate conjugates (Figure 15). It is expected that all proteins of segment A were expressed, because VP3 is encoded as the last protein of the polyprotein on segment A, although only VP3 was visualized. VP3 was localized in the cytoplasm of transfected cells, whereas NF45 was observed exclusively in the nucleus of both, transfected and non-transfected cells. In contrast to previous dot-like localization patterns, this time VP3 was visualized in a very scattered pattern, comparable to infected cells at 6 h pi. In conclusion, NF45 was not observed in the cytoplasm of cells expressing VP2, VP3 and VP4 or the NTRs of one segment of IBDV.

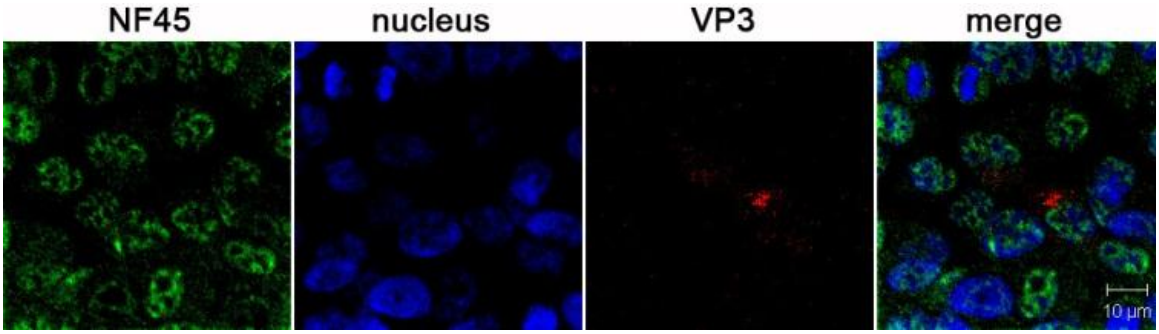

Figure 15: Viral proteins encoded by segement A were not sufficient for cytoplasmic accumulation of NF45. QM-7 cells were transfected with cRNA of segment A of IBDV strain D78 and fixed 12 h pt with ice cold ethanol. Cells were then incubated with R-α-NF45 (1:400, green) and mAb VP3 (1:100, red), followed by incubation with α-R-FITC (1:400) and α-M-Cy5 (1:50). The localization of the nucleus was visualized by binding of DAPI (1:50,000, blue) to chromosomal DNA. Pictures were taken by CLSM.

3.1.12.3 Transfection of segment B and VP3 minigenome

The aim of the next experiment was to investigate, if NF45 was accumulated in the cytoplasm, when RNA of segment B and cRNA of a minigenome of segment A encoding only VP3 were transfected into DF-1 cells, which mimics IBDV replication. The cRNA of the minigenome encoding VP3 consisted of the complete 5' NTR until the start codon of VP2 and the 3' NTRs of segment A, enclosing the coding region for VP3 (see 6.2.5). The deletion of the 5' NTR and the coding regions for VP2, VP4 and partially VP3 was achieved by cleavage of the plasmid puc19FLAD78 with *Eco*RI and *Dra*III. A cDNA

fragment consisting of the 5' NTR with an upstream located T7 promoter, a start codon and the beginning of the coding region of VP3 up to the *Dra*III cleavage site was synthesized by Genscript (pUC57-5'-NTR-VP3part). This plasmid was cleaved with *Eco*RI and *Dra*III and the obtained cDNA fragment was ligated into the *Eco*RI/*Dra*III cleaved puc19FLAD78. The obtained plasmid was named 5'A-VP3-3'A-puc19 (VP3 minigenome). The plasmid 5'A-VP3-3'A-puc19 was linearized with *Bsr*GI and puc19FLBD78 with *Pst*I and cRNA of both was transcribed with T7 RNA polymerase. Both cRNAs were co-transfected into DF-1 cells and fixed 24 h pt to be submitted for IIFA with R-α-NF45, mAb VP3, Ch-α-VP1 and DAPI and appropriate conjugates (α-R-Cy5 FITC, α-Ch-Cy3 and α-M-Cy5). As shown in Figure 16, VP3 and VP1 were expressed and localized in the cytoplasm, although they did not clearly co-localize to each other. NF45 was slightly localized in the cytoplasm, but not clearly co-localizing with the viral proteins. Possibly, the formation of a replication complex was not sufficient to clearly change the NF45 localization to the cytoplasm.

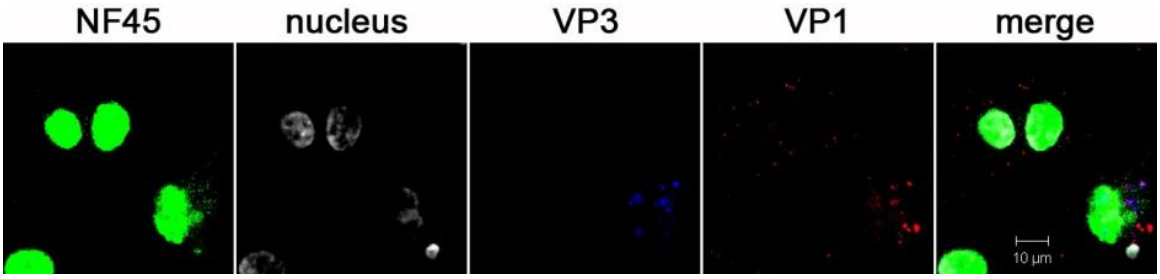

Figure 16: Co-transfection of cRNA encoding for VP1 and VP3 did not change NF45 phenotype. DF-1 cells were transfected with cRNA of segment B of strain D78 and 5'A-VP3-3'A-puc19 and fixed 24 h pt with ethanol. The cells were incubated with R-α-NF45 (1:400, green), mAb VP3 (1:100, blue), Ch-α-VP1 (1:400, red) and DAPI (1:50,000, nucleus, white). The location of the primary antibodies was detected using appropriate conjugated antibodies [α-R-FITC (1:200), α-M-Cy5 (1:50) and α-Ch-Cy3 (1:5,000)]. The presence of each component was visualized by CLSM.

3.1.12.4 Transfection of segment A and B

As positive controls for the previous experiments, both plasmids encoding full length segment A and B were linearized with the same RE as mentioned above and cRNA was generated by T7 RNA polymerase reaction. After co-transfection of both cRNAs, cells were fixed 24 h pt and used for IIFA with the same combination of primary and secondary antibodies as described before (3.1.12.3). This time the viral proteins VP1 and VP3 co-localized with each other and NF45 was present in the cytoplasm in small amounts comparable to the ones observed in an early stage of infection (Figure 17). The results of the transfection experiment indicated that probably other so far unknown factors besides VP3 and VP1 were necessary to induce the accumulation of NF45 in the cytoplasm of infected cells.

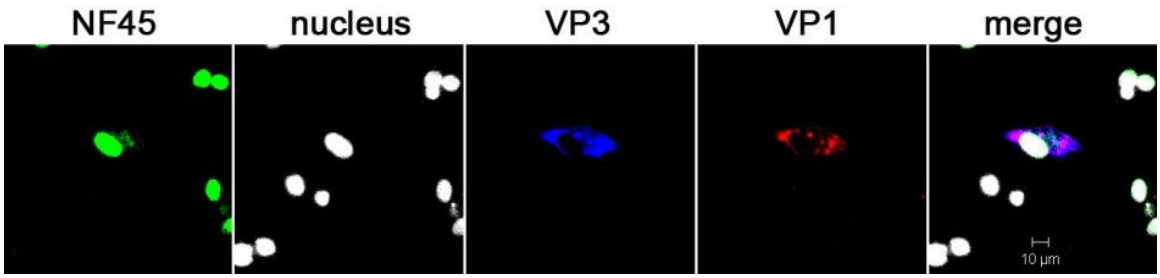

Figure 17: NF45 acuumulates in the cytoplasm after transfection of full length cRNA of both IBDV segments. DF-1 cells were transfected with *in vitro* transcribed cRNA of segment A and B of strain D78 and fixed 24 h pt with ice cold ethanol. The cells were incubated with R-α-NF45 (1:400, green), mAb VP3 (1:100, blue), Ch-α-VP1 (1:400, red) and the nuclear DAPI staining (1:50,000, white). The binding of the primary antibodies was demonstrated by the use of several species-specific conjugates [α-R-FITC (1:200), α-M-Cy5 (1:50) and α-Ch-Cy3 (1:5,000)] and visualized by CLSM.

3.1.13 Inhibition of the nuclear export of NF45 by leptomycin B

The export of proteins from the nucleus into the cytoplasm is controlled by the nuclear pore complex. Aqueous channels are 9 nm in diameter and ions, metabolites and proteins smaller than 40-60 kDa can freely diffuse through the pores without restriction (Nigg 1997). Larger proteins (26-28 nm in diameter) in the nucleoplasm need a NES (leucine-rich signal peptide) to translocate to the cytoplasm. In a first step the export receptor CRM1 (exportin 1) binds with its N-terminus to the GTPase Ran bound to GTP (RanGTP), inducing a change in the shape of CRM1 (reviewed in Nakielny & Dryfuss 1999). Then the cargo protein containing the NES can bind to the C-terminus of CRM1 (Fornerod *et al* 1997). After the export through the nuclear pore complex RanGTP is hydrolyzed to RanGDP by Ran-GAP (GTPase activating protein) that is present in the cytoplasm. This again changes the shape of CRM1 that releases the cargo into the cytoplasm. CRM1 and RanGDP are cycled back into the nucleus, where GDP is exchanged to GTP by the Ran-GEF present in the nucleus. Leptomycin B (LMB), an antifungal substance produced by a bacterial strain of *Streptomyces*, inhibits the nuclear export of proteins carrying the NES (Hamamoto *et al* 1983). NES contains hydrophobic aa, which are mostly leucins (L), but also isoleucins (I), which are separated by one to three other aa (x), L-x(2,3)-[LIVFM]-x(2,3)-L-x-[L/I] (Bogerd *et al* 1996). The aa sequence of NF45 is shown below with all leucins marked red and all isoleucins marked green to identify possible NES.

```
  1 MRGDRGRGRG GRFGSRFRPF VPHIPFDFYV CEMAFPRVKP AADESAFSEA
 51 LLKRNQDLAP TAAEQASILS LVTKINNVID NLIVAPGTFE VQIEEVRQVG
101 SYKKGTMTTG HNVADLVVIL KILPTLEAVA ALGNKVVESL RAQDPSEVLT
151 MLTNETGFEI SSADATVKIL ITTVPPNLRK LDPELHLDIK VLQSALAAIR
201 HARWFEENAS QSTVKVLIRL LKDLRIRFPG FEPLTPWILD LLGHYAVMNN
251 PTRQPLALNI AYRRCLQILA AGLFLPGSVG ITDPCESGNF RVHTVMTLEQ
301 QDMVCYTAQT LVRILSHGGY RKILGQEGDA SYLASEMSTW DGVIVTPSEK
351 AYEKPPEKKE GEEEEENQEE PAAGEEEESM ETQE
```

According to the software program NetNES (La Cour *et al* 2004, free available on http://www.cbs.dtu.dk/services/NetNES/) NF45 contains three possible NES with the hydrophobic anchor positions at aa 187-L, 221-L and 226-I, which have been highlighted yellow in the above sequence. The two sequences most similar to the consensus NES were underlined (aa 178-**L**RK**L**DPE**L**H**L**-188 and aa 217-**L**IRL**L**KD**L**R**I**-226). This shows that there are possible NES in NF45, which raised the question, if NF45 was recruited

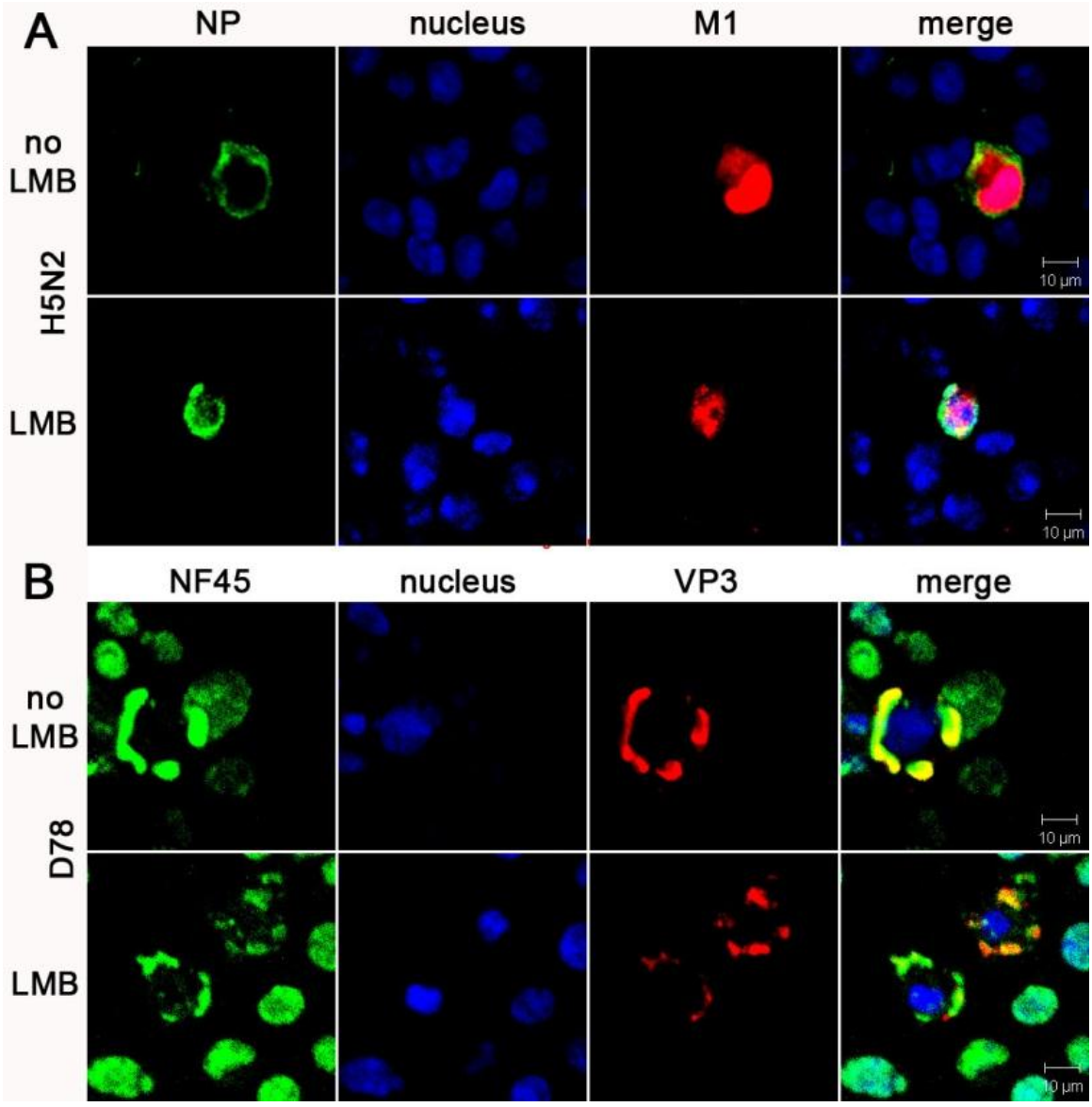

Figure 18: NF45 was not retained in the cytoplasm in the presence of leptomycin B (LMB). DF-1 cells were infected with (A) avian influenza A virus H5N2 or (B) IBDV strain D78. At 3 h pi 2 ng/ml LMB were added and 12 h pi cells were fixed with ethanol. IIFA was carried out using either (A) R-α-NP (1:100, green) and mAb M1 (1:200, red) or (B) R-α-NF45 (1:400, green) and mAb VP3 (1:100, red). For both experiments PI (1:5,000, blue) was used to visualized the nucleus. The primary antibodies were detected by the use of appropriate secondary fluorochrome conjugated antibodies [α-R-FITC (1:200) and α-M-Cy5 (1:50)]. The binding of the antibodies was visualized by CLSM.

after viral infection from the nucleus into the cytoplasm or if the viral proteins induced an accumulation of cytoplasmic translated NF45 and kept it in the cytoplasm. Therefore experiments were conducted in which the nuclear export was inhibited by LMB. The translocation of influenza A virus proteins NP and M1 from the nucleoplasm to the cytoplasm was shown to be inhibited by LMB (Ma *et al* 2001). This phenotype served as a positive control for the below described experiments. DF-1 cells were infected with either IBDV strain D78 or with avian influenza A virus of the subtype H5N2. As described before (Ma *et al* 2001), 3 h pi LMB (2ng/ml) was added to inhibit nuclear export and cells were fixed 12 h pi and later analyzed by IIFA with R-α-NF45, PI and mAb VP3 and the secondary antibodies α-R-FITC and α-M-Cy5. Influenza infected cells were incubated with R-α-NP, PI and mAb M1, followed by α-R-FITC and α-M-Cy5. The influenza proteins NP and M1 were transported into the nucleus early after influenza A virus infection, but 12 h pi both were already exported to the cytoplasm in the absence of LMB (Figure 18A). When LMB was added, NP and M1 were retained in the nucleus, which strongly indicated the inhibition of CRM1 mediated export by LMB (Figure 18A).
In contrast to the influenza A virus encoded M1 protein, NF45 was observed with and without LMB in the cytoplasm of IBDV infected cells (Figure 18B). NF45 was not retained in the nucleus after LMB treatment, indicating that accumulation of NF45 in the cytoplasm is independent of CRM1 mediated translocation. On the one hand different protein export pathways can not be excluded, but on the other hand VP3 was co-localizing with NF45, which was observed in the merged picture. Therefore a possible scenario is that the cytoplasmic translated NF45 retains in the cytoplasm and interacts with VP3.

3.1.14 NF45 interacts with VP3 in a RNA independent manner

In next experiments it was attempted to provide more evidence for the interaction of NF45 with VP3 and VP1 by IP (see 2.2.37). NF45-FLAG was expressed in DF-1 cells and 24 h pt infected with D78 for additional 24 h (transfected/infected). Appropriate control experiments (non-transfected/infected, transfected/non-infected and non-transfected/non-infected) were performed in parallel. Cells membranes were lysed in the presence of Igepal CA-630, but not the membrane of the nucleus and nucleus-free lysates obtained by centrifugation were analyzed by Western blot. Expression and infection levels of NF45-FLAG and VP3 were analyzed using R-α-NF45 and R-α-VP3 sera whose binding was detected by incubation with α-R-POD (Figure 19A). NF45 was observed always as a double band, NF45-FLAG showed 4 bands (Figure 19A, upper blot). In transfected cells, the exogenous NF45-FLAG was expressed in higher quantities in the cytoplasm than the endogenous protein, so that the endogenous protein was not visible anymore. Due to the additional FLAG tag, NF45-FLAG migrated slower than the endogenous NF45. VP3 was only observed in the infected lysates (Figure 19A, lower

blot) at similar expression levels. The IP was performed with mAb FLAG as the capture antibody and analyzed on a Western blot. Cell lysates separated on a gel showed after incubation with R-α-NF45 serum double bands of NF45-FLAG, but no endogenous NF45 (Figure 19B, upper blot). The membrane incubated with R-α-VP3 showed only a band in the transfected/infected sample (Figure 19B, lower blot, indicated by an arrow), showing co-immunoprecipitation likely due to interaction between cellular NF45 and viral ribonucleoprotein VP3.

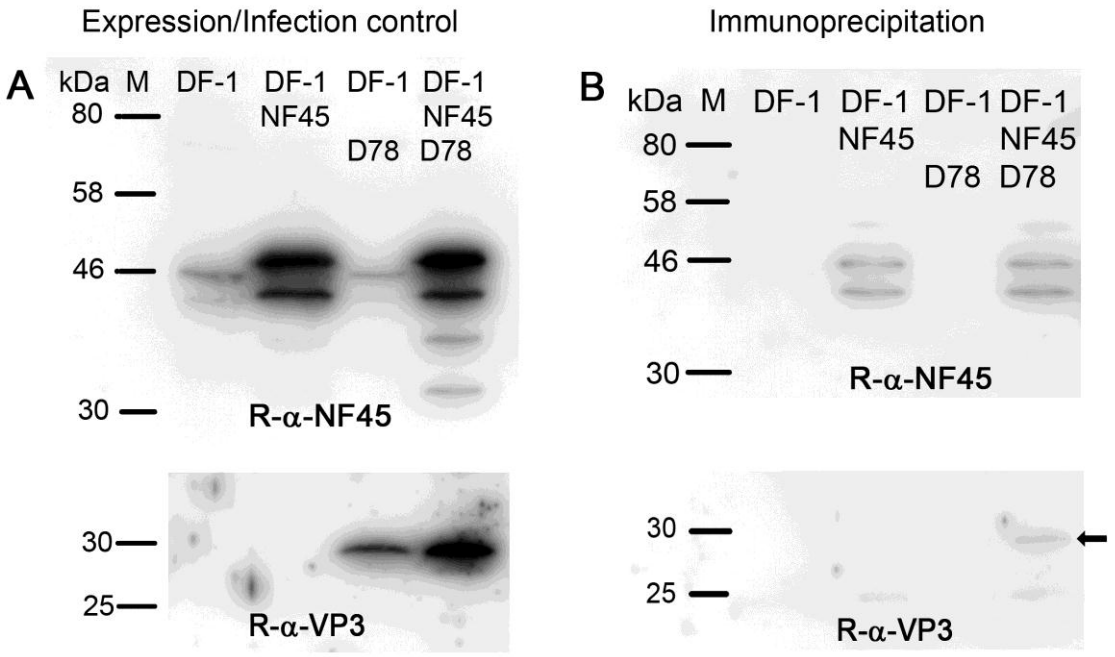

Figure 19: VP3 interacts with NF45. (A) Western blot of cellular lysates of DF-1 cells (DF-1), DF-1 cells transfected with NF45-FLAG-pcDNA3 (DF-1, NF45), DF-1 cells infected with D78 (DF-1, D78) and DF-1 cells transfected with NF45-FLAG-pcDNA3 and 24 h pt infected with D78 (DF-1, NF45, D78). Cells were harvested 24 h pi and cleared lysates were prepared. Samples were separated on a 12% SDS-PAGE gel and further analyzed by Western blot. (B) Western blot after IP using mAb FLAG of DF-1 cells (DF-1), DF-1 cells transfected with NF45-FLAG-pcDNA3 (DF-1, NF45), DF-1 cells infected with D78 (DF-1, D78) and DF-1 cells transfected with NF45-FLAG-pcDNA3 and infected with D78. For both, A and B, the upper Western blots were incubated with R-α-NF45 (1:1,000), the lower Western blots with R-α-VP3 (1:400). The binding of the primary antibodies was detected by chemoluminescence using α-R-POD (1:20,000) as secondary antibody. M: A protein marker was shown on the left of each Western blot to indicate the size of the proteins analyzed.

Protein-protein interactions are either direct between two proteins or bridged by other protein(s) or nucleic acid(s). For VP3 it was shown that it interacts with IBDV genomic dsRNA (Tacken *et al* 2002) and for the NFAR complex it was shown that it bound to viral RNA of HCV (Isken *et al* 2007). To investigate the possibility that VP3 and NF45 were co-precipitated by RNA bridging, a similar IP experiment was conducted, but this time lysates were treated with RNases. Transfection and infection was performed as

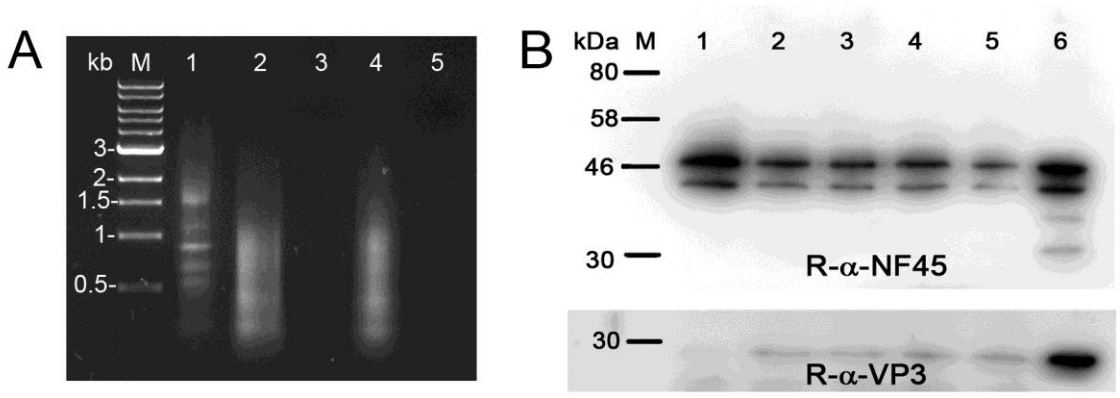

Figure 20: RNase digestion did not influence the interaction between IBDV VP3 and NF45. DF-1 cells were transfected with NF45-FLAG-pcDNA3 and 24 h pt infected with D78. The cells were harvested 24 h pi and cleared lysates were prepared. These were treated either with RNase T1 (lane 3), RNase III (lane 4) or with both RNases at 37°C (lane 5). As controls served cellular lysates incubated without RNases at 4°C (lane 1) or 37°C (lane 2). (A) Analysis of the incubated samples on a 1% agarose gel after RNA purification. (B) The RNase treated lysates and the non-treated lysate (lane 6) were submitted to IP with mAb FLAG and products were separated on a 12 % SDS-PAGE gel and subsequently used for Western blot analysis. The upper Western blot was incubated with R-α-NF45 (1:1,000), the lower Western blot with R-α-VP3 (1:400) and both blots were incubated with α-R-POD (1:20,000). A 1 kb ladder was used for the agarose gel and a protein marker for the Western blots (M). The sizes of the marker DNA fragments and the marker proteins are shown on the left of the respective gel.

described above. Obtained cleared lysates were treated either with 1 µl (1,000 units) ssRNA specific RNase T1 (Figure 20, lane 3), 1 µl (1.3 units) dsRNA specific RNase III (Figure 20, lane 4) or both RNases together (Figure 20, lane 5). Since the incubation step with RNases was conducted at 37°C and RNA was expected to be instable, two controls were carried out in parallel, one at 4°C (Figure 20, lane 1) and the other at 37°C (Figure 20, lane 2). From one half of the samples, RNA was isolated and analyzed on an agarose gel (Figure 20A). The RNA in the control at 4°C (lane 1) showed a clear laddering pattern that was lost in the control at 37°C after 1 h of incubation (lane 2). No RNA was visible after RNase T1 digestion (lane 3), indicating that the RNase degraded ssRNA and possibly also dsRNA. Another possibility is that the viral dsRNA was present in concentrations that were not visible on a standard agarose gel. After RNase III digestion (lane 4) no obvious difference was detected between the control at 37°C and the RNase III digested RNA. When both RNases were used at the same time no RNA was detected (lane 5).

The other half of cleared and subsequently RNase treated lysates was used for IP with mAb FLAG as described. The IP samples were analyzed by Western blot and were incubated either with R-α-NF45 (Figure 20B upper blot) or R-α-VP3 (lower blot). In all lanes precipitated NF45 was observed and as indicated by the lower gel NF45 co-immunoprecipitated VP3. This suggests that NF45 and VP3 interaction was not mediated by ss or ds, viral or cellular RNA. Variation between the precipitated VP3 might

be due to experimental variance, although it was noticed that in the 4°C control the least VP3 was co-immunoprecipitated, while there was most NF45.
It has been shown by IIFA that NF45 co-localized with VP3 and VP1 during IBDV infection (Figure 9) and also that NF45 interacted with VP3 (Figure 19). It was now interesting to investigate, if VP1 interacts with the NF45-VP3 complex. The same experimental design as described above was used. The products of the IP were analyzed by Western blot with a Ch-α-VP1 serum and α-Ch-POD (Figure 21). VP1 (97 kDa) was visible as a weak band in the cellular lysate prior IP. It is known that VP1 is expressed in lower levels in the cell than the proteins encoded by the larger ORF on segment A. The percentage of VP1 protein in a virion is only 3 % and not all VP3 is bound to VP1 (Dobos *et al* 1979). VP1 was not visible on the Western blot after IP, probably due to its low expression level as observed in the cellular lysates before IP (Figure 21). Additional, some bands appeared after IP and Western blot. Their molecular weight corresponds to the molecular weight of a heavy (50 kDa) and a light chain (25 kDa) of an antibody. Presumably, the α-Ch-POD serum cross-reacted with fragments of the capture mAb. Another unspecific band, little larger and more intense than the 50 kDa band, was visible in the lysate that disappeared completely after IP.

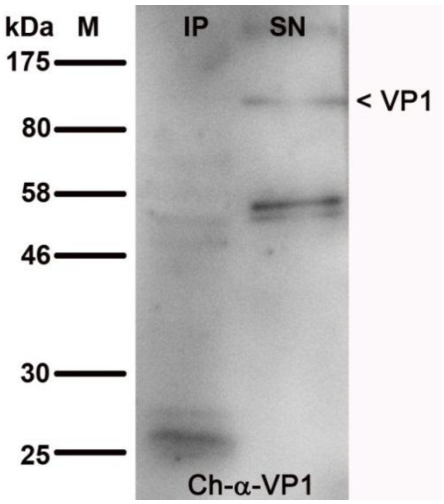

Figure 21: IBDV VP1 was not immunoprecipitated by NF45. DF-1 cells were transfected with NF45-FLAG-pcDNA3 and 24 h pt infected with D78. The cells were harvested 24 h pi and cleared lysates were prepared. The lysates were submitted for IP using NF45-FLAG. Samples of IP and supernatant (SN) were analyzed by Western blot using Ch-α-VP1 serum (1:2,500) and α-Ch-POD (1:15,000). The protein molecular weight of a marker (M) were shown on the left part of the gel.

3.1.15 Biological function of NF45 during virus replication

Interactions of cellular proteins with viral proteins can have several reasons. Among them, either the cellular proteins are needed for viral replication or the proteins are part of the cellular defense mechanism to interfere with the viral replication by binding to the viral protein and therefore inhibiting its function. To gain knowledge about the involved mechanisms there are several approaches possible. The overexpression of the target protein would be one approach, while the downregulation of protein expression would be a second and very powerful approach. The next experiments were conducted to investigate the consequence of both approaches on replication of IBDV.

3.1.15.1 Overexpression of NF45

The influence of overexpression of the investigated cellular protein NF45 was addressed by transfection of either NF45-FLAG-pcDNA3 or pcDNA3 into DF-1 cells. Twenty four

hours after transfection cells were infected with D78 with a moi of 1. Cellular supernatant was harvested 24 h and 48 h pi and viral titers were determined using the $TCID_{50}$ assay. This experiment was performed twice and transfected cells of a second plate were fixed at the time of infection to analyze transfection efficiency. Fixed cells were incubated with mAb FLAG (1:500) and α-M-FITC (1:200) and quantified by observation with the microscope. Almost all cells were transfected, so probably most infected cells were also transfected. Titers were summarized in Table 7.

Table 7: Titers of IBDV influenced by expression of NF45-FLAG. DF-1 cells were transfected with the indicated plasmids and infected 24 h pt with the IBDV strain D78 at a moi of 1. The supernatants were harvested at 16 h pi and the $TCID_{50}$/ml was determined.

Plasmids used for transfection	Time after infection	
	24 h	48 h
pcDNA3	$10^{4.25}$	10^{6}
NF45-FLAG-pcDNA3	$10^{4.5}$	$10^{4.75}$

In comparison to the pcDNA3 vector that served as a negative control, viral titers were at comparable levels at 24 h, although viral titers obtained from cells overexpressing NF45-FLAG were slightly higher. Forty eight hours after infection viral titers in NF45-FLAG-pcDNA3 transfected cells did not increase much, but viral titers from control cells were nearly 100-fold higher. This experiment was repeated with the same transfections, but cells were infected with moi of 100 and the supernatant was harvested at 0 h, 12 h and 24 h pi (see Table 8). Virus titers in the supernatant of NF45-FLAG overexpressed cells were not as high as in the supernatant of cells transfected with control plasmid pcDNA3 at 12 h pi, while 24 h pi virus titers showed the same level.

Table 8: Titers of IBDV influenced by expression of NF45-FLAG. DF-1 cells were transfected with the indicated plasmids and infected 24 h pt with a moi of 100. The supernatants were harvested at 16 h pi and the $TCID_{50}$/ml was determined.

Plasmids used for transfection	Time after infection		
	0 h	12 h	24 h
pcDNA3	10^{3}	10^{5}	$10^{6.25}$
NF45-FLAG-pcDNA3	$10^{2.5}$	$10^{4.25}$	$10^{6.25}$

Since transfection efficiency was difficult to control, a cell line constitutively expressing NF45-FLAG was generated. DF-1 cells were transfected with NF45-FLAG-pcDNA3 and 24 h pt the medium was exchanged with medium containing 400 µg/ml of the selection marker G418. Individual cell colonies were picked and grown to confluence. Some cells of each clone were seeded in separate wells of a 96-well plate, fixed and used for IIFA with mAb FLAG (1:500) and α-M-FITC (1:200) to confirm expression of NF45-FLAG (data not shown). A cell line was chosen that was positive in IIFA and did not show a delay in cell division in comparison to cells of the parent cell line DF-1. It was called DF-1-NF45-FLAG. The same number of DF-1-NF45-FLAG and wild type DF-1 cells were seeded in a 6-well cell culture plate and infected with D78 at a moi of 10 and 16 h pi cell culture supernatants were harvested and viral titers were determined. The experiment

was carried out thrice (Table 9). During all experiments virus titers of D78 replicating in DF-1-NF45-FLAG cells were lower than in the parental cells. Although cells were counted before seeding them, it was possible that the total number of cells was not exactly the same, but the confluence of the cells observed in the microscope was comparable. It is reasonable to rule out that a different number of cells was infected, which could have been a reason for different titers.

Table 9: Titers of IBDV influenced by expression of NF45-FLAG. DF-1 cells (DF-1) and DF-1 cells consecutively expressing NF45-FLAG (DF-1-NF45-FLAG) were infected with the IBDV strain D78 at a moi of 10. The supernatants were harvested at 16 h pi and the $TCID_{50}$/ml was determined.

Cells	Experiment 1	Experiment 2	Experiment 3
DF-1	$10^{8.75}$	10^{9}	$10^{8.5}$
DF-1-NF45-FLAG	$10^{8.25}$	$10^{8.75}$	$10^{8.25}$

3.1.15.2 Downregulation of NF45 using siRNA

Small interfering RNA (siRNA) silences protein expression. SiRNAs consist of 18-24 nt of dsRNAs with a 2 nt 3' overhang on each end. Longer dsRNA molecules (30 bp) are recognized by TLR 3 and the innate immune system (including PKR) is activated (Saunders & Barber 2003). Transfection of too large amounts of siRNAs result also in the activation of the innate immune system by the TLR 7 that recognizes ssRNA molecules. SiRNA can be artificially introduced into a cell by transfection. Long dsRNAs are cleaved in the cytoplasm in siRNAs by the endoribonuclease dicer. The guide strand of the siRNA is incorporated into the RNA induced silencing complex (RISC) located in the nucleus. If the mRNA molecule is complementary to the guide strand in RISC, the complex activates RNases and the mRNA is degraded and no translation occurs. The gene is silenced and the protein amount in the cell is specifically downregulated.

In order to find a target sequence for NF45, the RNAi Target Sequence Selector on the Clontech webpage (http://bioinfo.clontech.com/rnaidesigner/frontpage.jsp) was used. The first two targets, each 19 nt long, were selected starting in the NF45 RNA at basepair 185 (named si-185) and 551 (named si-551, sequences see Table 2). SiRNAs si-185 and si-551 were either transfected alone or together. Three negative controls were additionally needed. For the first control cells were treated with neither siRNA nor transfection reagent (called co) and for the second control cells were mock treated with the transfection reagent. For the third control cells were transfected with a NF45 unspecific siRNA, but specific for the coding region of the nucleoprotein (NP) of influenza A virus, called si-NP as described before (see Table 2, Tompkins *et al* 2004). Twenty four hours and 48 h pt, cell pellets were harvested and prepared for Western blot analysis. To compare expression levels of NF45, all lysates were adjusted to the same amount of β-actin by separating them on a SDS-PAGE gel and analyzing β-actin in the cell lysates with mAb β-actin-POD. Then a second Western blot was performed using exact same amounts of lysate as in the previous experiment and incubated with

R-α-NF45 followed by α-R-POD. Reduced amounts of NF45 were observed already 24 h pt (data not shown). This phenotype was even more evident 48 h pt (Figure 22A).
In a parallel experiment, cells were infected with D78 to study replication efficiency of IBDV in NF45 downregulated cells. The supernatants were harvested 16 h pi and titers were determined (see Table 10). Cell pellets were prepared for Western blot analysis, separated on a SDS-PAGE gel and submitted for Western blot analysis with mAb β-actin-POD and R-α-NF45 followed by α-R-POD (Figure 22B). Downregulation of NF45 protein was clearly observed.
To quantify the relative level of detected NF45 in artificial units, the integrated intensity of the detected signal was calculated using the free software ImageJ

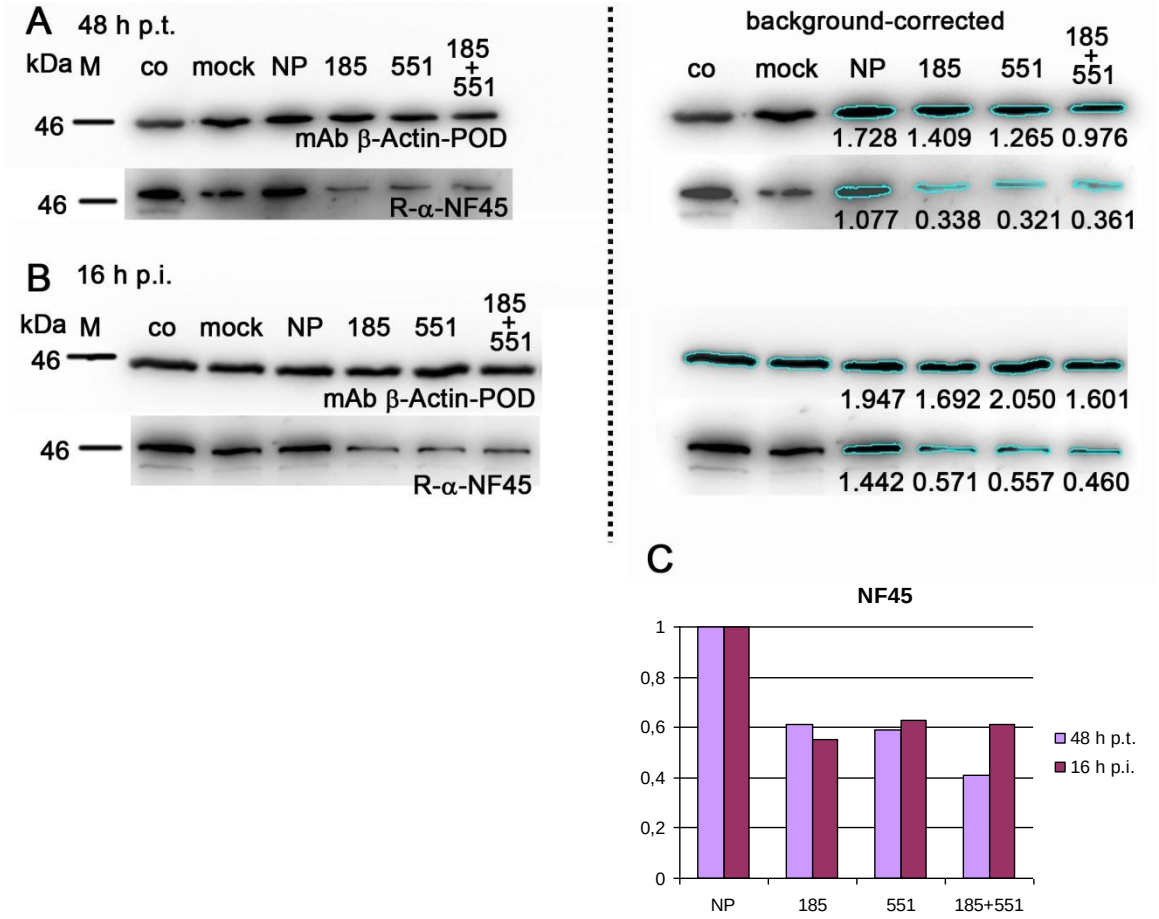

Figure 22: Downregulation of NF45 after siRNA transfection. DF-1 cells were transfected with NF45 unspecific siRNA (NP) and NF45 specific siRNA si-185 (185), si-551 (551) and both together (185+551). As controls, DF-1 cells were not treated (co) or mock-transfected for 48 h (mock). Then cells were infected with IBDV strain D78 for 16 h. Cell lysates were prepared and separated on a 12% SDS-PAGE. With subsequent Western blot analysis NF45 expression levels 48 h pt (A) and 16 h pi (B) were detected with R-α-NF45 (1:1,000) followed by α-R-POD (1:20,000) and on a parallel blot with mAb β-actin-POD (1:25,000). On the right side of the dotted line the same Western blots are shown background-corrected. The NF45 and β-actin levels were measured by integrated intensity in artificial units and written below each band. (C) Relative quantification of NF45 48 h pt of siRNA and subsequent infection with IBDV strain D78 16 h pi, normalized to the level of NF45 in si-NP transfected cells.

(http://rsbweb.nih.gov/ij/). This analysis was performed on background-corrected pictures (see Figure 22A and B, right side of the dotted line). Additionally, the integrated intensity of the β-actin was determined to normalize NF45 levels (Figure 22A and B, on the right side of the dotted line). All determined values of the integrated intensity in artificial units were written below each band. Relative NF45 amounts of cells after transfection with si-NP, si-185, si-551 and si185+si-551 were normalized by division through the β-actin value of each sample. To determine the percentage of protein expression relative to the control (si-NP), all NF45 values after transfection with specific NF45-siRNAs were divided by the NF45 amount from cells transfected with si-NP. Si-185 downregulated the amount of NF45 24 h pt by 39%, si-551 by 41% and both together by 59% (see Figure 22C). Sixteen hours post infection with IBDV strain D78, si-185 downregulated NF45 by 45%, si-551 by 37% and both together by 39% (see Figure 22C). This shows that after transfection of NF45 specific siRNA as well as after infection with D78 NF45 levels were downregulated by at least 37%.

Table 10: Titers/ml determined by $TCID_{50}$ after infection of NF45 siRNA transfected cells.

experiment	co	mock	si-NP	si-185	si-551	si-185 + si-551
1	$10^{8.5}$	$10^{6.25}$	$10^{7.25}$	10^{8}	10^{8}	$10^{8.25}$
2	10^{8}	$10^{6.75}$	$10^{7.5}$	$10^{7.25}$	$10^{8.5}$	$10^{8.25}$
3	10^{8}	$10^{5.25}$	$10^{4.75}$	$10^{5.25}$	$10^{5.5}$	10^{5}
4	$10^{7.5}$	$10^{4.75}$	$10^{4.75}$	10^{5}	$10^{5.25}$	$10^{5.5}$
5	10^{8}	10^{6}	$10^{6.5}$	$10^{6.75}$	$10^{6.5}$	10^{7}
6	10^{8}	$10^{7.75}$	$10^{7.5}$	$10^{8.25}$	$10^{7.75}$	10^{8}
7	$10^{8.75}$	$10^{6.5}$	10^{7}	10^{7}	$10^{8.5}$	$10^{7.75}$
8	$10^{8.5}$	$10^{6.75}$	$10^{6.25}$	$10^{6.5}$	$10^{6.5}$	$10^{6.25}$

The siRNA transfection/IBDV infection experiment was repeated several times (Table 10, experiment 1-8). When compared to the unspecific siRNA control (si-NP), titers of IBDV infected NF45 downregulated cells were most of the time higher than the control. Only in one case it was lower (experiment 2, si-185) and sometimes the same (experiment 5, si-551; experiment 7, si-185 and experiment 8, si-185 + si-551). Additionally, it was observed that mock-transfected cells often showed lower titers or the same as si-NP. This can be explained by the increased cell death probably caused by toxic properties of the transfection reagent. Observation of the cell morphology in the mock-transfected dish showed increased cell death. If less viable cells were present it is reasonable that less virus was able to replicate and titers were lower. When siRNA was transfected with the transfection reagent, not as many cells showed rounding and cell death as when no siRNA was in the solution. The medium containing the transfection reagent was not changed after transfection, because an exchange reduced the level of downregulation (data not shown).

3.1.16 Statistical analysis of IBDV titers after NF45 downregulation

Statistical significance was determined with the Wilcoxon rank-sum test. The titers of NP transfected siRNA (NP) were tested against si-185, si-551 and si-185+si-551 titers (Table 10). As an example how to calculate this statistic, detailed steps are shown for si-185, see Table 11. First, the differences were calculated and the ranks were given.

Table 11: Calculation of the differences between 185 and NP siRNA titers and ranks given.

experiment	si-NP	si-185	D=[si-185]-[si-NP]	|D|	rank	Ranks of D>0
1	$10^{7.25}$	10^{8}	82217206	82217206	6	6
2	$10^{7.5}$	$10^{7.25}$	-13839983	13839983	5	-
3	$10^{4.75}$	$10^{5.25}$	121594	121594	2	2
4	$10^{4.75}$	10^{5}	43766	43766	1	1
5	$10^{6.5}$	$10^{6.75}$	2461136	2461136	4	4
6	$10^{7.5}$	$10^{8.25}$	146205164	146205164	7	7
7	10^{7}	10^{7}	0	0	-	-
8	$10^{6.25}$	$10^{6.5}$	1383998	1383998	3	3

All ranks of D>0 were summed up (6+2+1+4+7+3=23) to obtain W=23. Z was calculated with n=7 resulting in Z=1.52. The Z value was compared with a table of the standard normal distribution giving p=0.064 so the null hypothesis can not be rejected and has to be accepted (for α=0.05, p> α). Viral titers of cells transfected with NF45 specific si-185 were not significant higher than titers from cells transfected with non-specific si-NP.

The same test statistic was used for titers of IBDV infected cells treated with si-551 (p=0.009) and si-185 + si-551 (p=0.009). This time the titers were significantly different from each other. Downregulation of chicken NF45 with si-551 or both siRNAs (si-185 and si-551) enhanced replication of IBDV in DF-1 cells significantly.

3.2 p68

3.2.1 Comparison of p68 homologs

Protein homologs of p68 from different species were compared to analyze similarity between species. Amino acid sequences of proteins with high homology to the human p68 were found with a Blastp search in the NCBI database and were aligned employing a ClustalW algorithm. The amino acid sequences for the comparison were derived from the following species. The scientific name is followed by the common name in parentheses, the NCBI accession number and the number of aa. *Homo sapiens* (human) NP_004387, 614 aa; *Pongo abelii* (Sumatran Orangutan) NP_001126958, 614 aa; *Pan troglodytes* (common chimpanzee) NP_001138306, 614 aa; *Canis familiaris* (dog) XP_850467, 614 aa; *Mus musculus* (mouse) CAA46581, 614 aa; *Rattus norvegicus* (rat) NP_001007614, 615 aa*; Gallus gallus* (chicken) NP_990158, 595 aa; *Xenopus laevis* (African clawed frog) AAH82849, 608 aa; *Danio rerio* (zebra fish) AAH67585, 496 aa; *Salmo salar* (Atlantic salmon) ACN11269, 614 aa; *Caenorhabditis elegans* (roundworm) NP_001041134, 561 aa; *Tribolium castaneum* (red flour beetle) XP_972501, 540 aa;

Apis mellifera (European honey bee) XP_395774, 566 aa; *Aedes aegypti* (mosquito) XP_001654592, 699 aa; *Drosophila melanogaster* (fruit fly) NP_648062, 818 aa. The results were summarized in Table 12 as indicated by the percentage of identity. Similar to the comparison of NF45 proteins (see Table 6), the mammalian aa sequences were all above 98% homology and were similar in length (614-615 aa). The chicken p68 as the only avian sequence in this table showed 88-89% identity to the mammalian p68 homologs, which might be due to the fact that the mRNA encodes for a shorter protein of 595 aa. The frog and the fish proteins showed a homology of 69-83% to the mammals/bird or among each other. Lowest homology was observed with *C. elegans*. Among the insects it was observed that the fruit fly encoded for a comparably long p68 (818 aa). The additional aa were not located at the end of the protein, but internally as it was observed with the p68 sequence of the mosquito *A. aegypti*, which had an insertion elsewhere. The p68 sequence of *A. aegypti* was longer, but not as long as the p68 sequence of *D. melanogaster*. The p68 aa homology of insects with mammals was between 51 and 60%. The highest p68 homology among the insects was 73% between the honey bee and the beetle, the remaining homologies ranged between 56-62%.

Table 12: Homology of amino acid sequences between p68 proteins of different species. Identity was shown in percent. *G. gallus* (chicken) is emphasized (bold).

	H. sapiens	*P. abelii*	*P. troglodytes*	*C. familiaris*	*M. musculus*	*R. norvegicus*	***G. gallus***	*X. laevis*	*D. rerio*	*S. salar*	*C. elegans*	*T. castaneum*	*A. mellifera*	*A. aegypti*	*D. melanogaster*
H. sapiens	100														
P. abelii	100	100													
P. troglodytes	100	99	100												
C. familiaris	100	100	100	100											
M. musculus	98	98	98	98	100										
R. norvegicus	99	98	99	99	98	100									
G. gallus	**89**	**89**	**89**	**89**	**88**	**88**	**100**								
X. laevis	78	77	78	78	77	78	**78**	100							
D. rerio	82	82	83	83	82	83	**81**	80	100						
S. salar	70	69	69	70	69	70	**71**	70	85	100					
C. elegans	48	48	48	50	48	48	**48**	48	54	50	100				
T. castaneum	60	60	60	60	59	60	**58**	58	67	63	52	100			
A. mellifera	59	59	58	59	58	58	**58**	58	67	61	51	73	100		
A. aegypti	52	51	51	52	51	52	**53**	53	62	53	52	62	59	100	
D. melanogaster	53	52	52	53	52	52	**54**	53	62	53	52	61	57	56	100

The p68 ClustalW alignment is shown below and the chicken sequence was highlighted in bold and stars below indicate identical aa. The functional aa motifs were highlighted. ATP binding and hydrolysis motifs were labeled red (motif I, II and Q), the NTP binding and hydrolysis motifs that were linked to conformational changes (RNA unwinding) were highlighted in green (motif III and VI) and the RNA binding motifs were highlighted in yellow (motif Ia, Ib, IV V) (Tanner & Linder 2001). The Q motif F-16aa-GFccPoPIQ (c is a charged group: D, E, H, K or R; o is an alcohol: S or T) responsible for ATP binding and hydrolysis was identified in yeast 16 aa before the motif I or Walker A motif A-T/SGT/SGKT that bound phosphates of NTP (Tanner & Linder 2001, Tanner *et al* 2003). Motif Ia (---PTRELA-Q) was binding to substrates through the sugar-phosphate backbone (Tanner & Linder 2001). Motif Ib (--TPGRL) was not as conserved and bound also to the substrate (Tanner & Linder 2001). The motif II or Walker B motif (VLDEAD-M) was associated to the β and γ phosphate through Mg^{2+} and coordinated the hydrolysis of NTP with water molecules (Tanner & Linder 2001). Motif III (SAT) showed binding to the γ phosphate and linked NTP hydrolysis to unwinding activity. Motif IV (LIF--T/S) and motif V (LVATDVAARGLD) bound to the substrate, motif V might interact with NTP (Tanner & Linder 2001). Motif VI (Y-HRIGRT/SGR-G) was also associated with the γ phosphate and performed NTP hydrolysis with domain 1 and 2 movements, whereas domain 1 is spanning the N-terminal region from the Q motif up to motif III and domain 2 the C-terminal region from motif III to motif VI (Tanner & Linder 2001). The core protein domain around the motifs showed increased aa identity.

```
D._rerio            ------------------------------------------------------------
S._salar            ------------------------------------------------------------
C._familiaris       ------------------------------------------------------------
H._sapiens          ------------------------------------------------------------
P._abelii           ------------------------------------------------------------
P._troglodytes      ------------------------------------------------------------
M._musculus         ------------------------------------------------------------
R._norvegicus       ------------------------------------------------------------
G._gallus           ------------------------------------------------------------
X._laevis           ------------------------------------------------------------
T._castaneum        ------------------------------------------------------------
A._mellifera        ----------------------------------------------------MGRYRSRSRD
D._melanogaster     MNMYNGQMNAFGGGGGGGAGGLAGGMVPNRMGGGAPGGGPGGAGMFQRNRSAPYPGFNGH
A._aegypti          ---------------------------------MYGNRQQSSGGFRGGNQGGGRPMNG
C._elegans          --------------------------MGDRGYGGSRSYGGSSGGGSRGGYGGGGRGGGG


D._rerio            -MPGYSDRDRGRDRGSYSSGPPRFGGSRNGPPPAKKFGNPGDRLRKKHWNLDELPKFEKN
S._salar            -MPGFSDRDRGRDRGYGSGPPRFGGGGRGG--GGGKFGNPGDRLRKKHWNLDELSKFEKN
C._familiaris       MSGYSSDRDRGRDRGFGAPR---FGGSRAGPLSGKKFGNPGEKLVKKKWNLDELPKFEKN
H._sapiens          MSGYSSDRDRGRDRGFGAPR---FGGSRAGPLSGKKFGNPGEKLVKKKWNLDELPKFEKN
P._abelii           MSGYSSDRDRGRDRGFGAPR---FGGSRAGPLSGKKFGNPGEKLVKKKWDLDEPPKFEKN
P._troglodytes      MSGYSSDRDRGRDRGFGAPR---FGGSRAGPLSGKKFGNPGEKLVKKKWNLDELPKFEKN
M._musculus         MSSYSSDRDRGRDRGFGAPR---FGGSRTGPLSGKKFGNPGEKLVKKKWNLDELPKFEKN
R._norvegicus       MSSYSSDRDRGRDRGFGAPR---FGGSRTGPLSGKKFGNPGEKLVKKKWNLDELPKFEKN
G._gallus           ------------MPGFGAPR---FGGSRAGPLSGKKFGNPGEKLTKKKWNLDELPKFEKN
X._laevis           -MPGFNDRDRGRDRGFGGGP---RFGGNRGGTSG-KYGNPGERLMKKKWNLDELPKFEKN
T._castaneum        ------MRGRSGRRSRSRDRRRSRSRDRGYGGGGGRRNTAGANLRKPRWDLSRLEPFKKD
A._mellifera        RDRRRRSRSRSRSRSPRDRRNWGSSGGRDRGGGRNSRGQPGANLRKPRWDLSRLEPFKKD
D._melanogaster     GPANGGQRRMNGGGPSMGPGGPRNQDGFGGQNGGQRSSNHGAHLPKIVWSEVNLTPFRKN
A._aegypti          GGFRGGDRPSGGSRGGMGGGMGGGGGFGGNRGTFDRQANNGATLRTLKWTSEELTPFEKD
C._elegans          GGYSGGRGGGYGGGGGGGYGGGGYGGGGRGGGRGGSNGSAGGRLRDVDWSAENLTPIEKD
                                                      *  *    *   .   :.*:
```

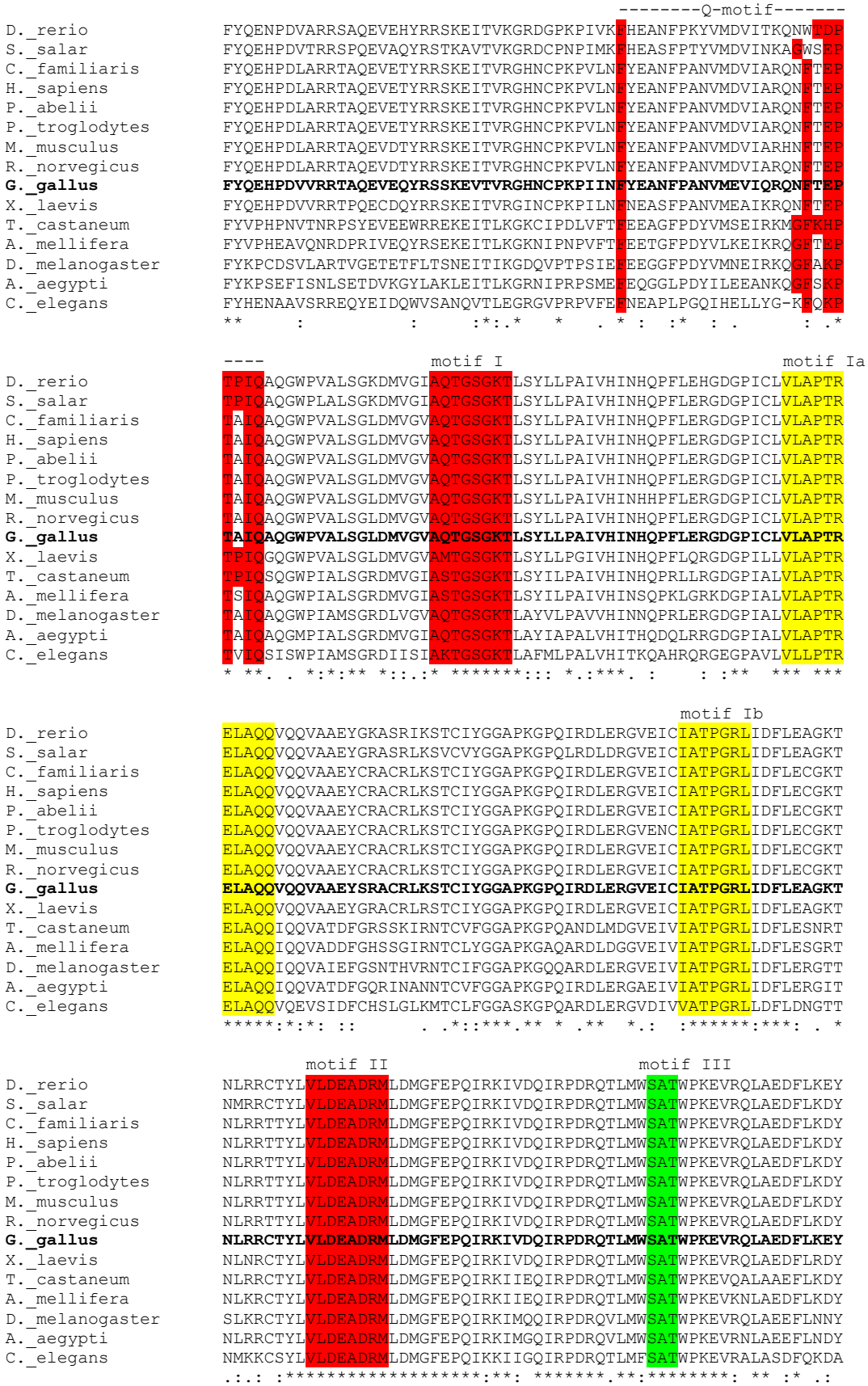
--------Q-motif-------
D._rerio FYQENPDVARRSAQEVEHYRRSKEITVKGRDGPKPIVKFHEANFPKYVMDVITKQNWTDP
S._salar FYQEHPDVTRRSPQEVAQYRSTKAVTVKGRDCPNPIMKFHEASFPTYVMDVINKAGWSEP
C._familiaris FYQEHPDLARRTAQEVETYRRSKEITVRGHNCPKPVLNFYEANFPANVMDVIARQNFTEP
H._sapiens FYQEHPDLARRTAQEVETYRRSKEITVRGHNCPKPVLNFYEANFPANVMDVIARQNFTEP
P._abelii FYQEHPDLARRTAQEVETYRRSKEITVRGHNCPKPVLNFYEANFPANVMDVIARQNFTEP
P._troglodytes FYQEHPDLARRTAQEVETYRRSKEITVRGHNCPKPVLNFYEANFPANVMDVIARQNFTEP
M._musculus FYQEHPDLARRTAQEVDTYRRSKEITVRGHNCPKPVLNFYEANFPANVMDVIARHNFTEP
R._norvegicus FYQEHPDLARRTAQEVDTYRRSKEITVRGHNCPKPVLNFYEANFPANVMDVIARQNFTEP
G._gallus FYQEHPDVVRRTAQEVEQYRSSKEVTVRGHNCPKPIINFYEANFPANVMEVIQRQNFTEP
X._laevis FYQEHPDVVRRTPQECDQYRRSKEITVRGINCPKPILNFNEASFPANVMEAIKRQNFTEP
T._castaneum FYVPHPNVTNRPSYEVEEWRREKEITLKGKCIPDLVFTFEEAGFPDYVMSEIRKMGFKHP
A._mellifera FYVPHEAVQNRDPRIVEQYRSEKEITLKGKNIPNPVFTFEETGFPDYVLKEIKRQGFTEP
D._melanogaster FYKPCDSVLARTVGETETFLTSNEITIKGDQVPTPSIEFEEGGFPDYVMNEIRKQGFAKP
A._aegypti FYKPSEFISNLSETDVKGYLAKLEITLKGRNIPRPSMEFEQGGLPDYILEEANKQGFSKP
C._elegans FYHENAAVSRREQYEIDQWVSANQVTLEGRGVPRPVFEFNEAPLPGQIHELLYG-KFQKP
motif I
motif Ia
D._rerio TPIQAQGWPVALSGKDMVGIAQTGSGKTLSYLLPAIVHINHQPFLEHGDGPICLVLAPTR
S._salar TPIQAQGWPLALSGKDMVGIAQTGSGKTLSYLLPAIVHINHQPFLERGDGPICLVLAPTR
C._familiaris TAIQAQGWPVALSGLDMVGVAQTGSGKTLSYLLPAIVHINHQPFLERGDGPICLVLAPTR
H._sapiens TAIQAQGWPVALSGLDMVGVAQTGSGKTLSYLLPAIVHINHQPFLERGDGPICLVLAPTR
P._abelii TAIQAQGWPVALSGLDMVGVAQTGSGKTLSYLLPAIVHINHQPFLERGDGPICLVLAPTR
P._troglodytes TAIQAQGWPVALSGLDMVGVAQTGSGKTLSYLLPAIVHINHQPFLERGDGPICLVLAPTR
M._musculus TAIQAQGWPVALSGLDMVGVAQTGSGKTLSYLLPAIVHINHHPFLERGDGPICLVLAPTR
R._norvegicus TAIQAQGWPVALSGLDMVGVAQTGSGKTLSYLLPAIVHINHQPFLERGDGPICLVLAPTR
G._gallus TAIQAQGWPVALSGLDMVGVAQTGSGKTLSYLLPAIVHINHQPFLERGDGPICLVLAPTR
X._laevis TPIQGQGWPVALSGLDMVGVAMTGSGKTLSYLLPGIVHINHQPFLQRGDGPILLVLAPTR
T._castaneum TPIQSQGWPIALSGRDMVGIASTGSGKTLSYILPAIVHINHQPRLLRGDGPIALVLAPTR
A._mellifera TSIQAQGWPIALSGRDMVGIASTGSGKTLSYILPAIVHINSQPKLGRKDGPIALVLAPTR
D._melanogaster TAIQAQGWPIAMSGRDLVGVAQTGSGKTLAYVLPAVVHINNQPRLERGDGPIALVLAPTR
A._aegypti TAIQAQGMPIALSGRDMVGIAQTGSGKTLAYIAPALVHITHQDQLRRGDGPIALVLAPTR
C._elegans TVIQSISWPIAMSGRDIISIAKTGSGKTLAFMLPALVHITKQAHRQRGEGPAVLVLLPTR
motif Ib
D._rerio ELAQQVQQVAAEYGKASRIKSTCIYGGAPKGPQIRDLERGVEICIATPGRLIDFLEAGKT
S._salar ELAQQVQQVAAEYGRASRLKSVCVYGGAPKGPQLRDLDRGVEICIATPGRLIDFLEAGKT
C._familiaris ELAQQVQQVAAEYCRACRLKSTCIYGGAPKGPQIRDLERGVEICIATPGRLIDFLECGKT
H._sapiens ELAQQVQQVAAEYCRACRLKSTCIYGGAPKGPQIRDLERGVEICIATPGRLIDFLECGKT
P._abelii ELAQQVQQVAAEYCRACRLKSTCIYGGAPKGPQIRDLERGVEICIATPGRLIDFLECGKT
P._troglodytes ELAQQVQQVAAEYCRACRLKSTCIYGGAPKGPQIRDLERGVENCIATPGRLIDFLECGKT
M._musculus ELAQQVQQVAAEYCRACRLKSTCIYGGAPKGPQIRDLERGVEICIATPGRLIDFLECGKT
R._norvegicus ELAQQVQQVAAEYCRACRLKSTCIYGGAPKGPQIRDLERGVEICIATPGRLIDFLECGKT
G._gallus ELAQQVQQVAAEYSRACRLKSTCIYGGAPKGPQIRDLERGVEICIATPGRLIDFLEAGKT
X._laevis ELAQQVQQVAAEYGRACRLRSTCIYGGAPKGPQIRDLERGVEICIATPGRLIDFLEAGKT
T._castaneum ELAQQIQQVATDFGRSSKIRNTCVFGGAPKGPQANDLMDGVEIVIATPGRLIDFLESNRT
A._mellifera ELAQQIQQVADDFGHSSGIRNTCLYGGAPKGAQARDLDGGVEIVIATPGRLLDFLESGRT
D._melanogaster ELAQQIQQVAIEFGSNTHVRNTCIFGGAPKGQQARDLERGVEIVIATPGRLIDFLERGTT
A._aegypti ELAQQIQQVATDFGQRINANNTCVFGGAPKGPQIRDLERGAEIVIATPGRLIDFLERGIT
C._elegans ELAQQVQEVSIDFCHSLGLKMTCLFGGASKGPQARDLERGVDIVVATPGRLLDFLDNGTT
motif II
motif III
D._rerio NLRRCTYLVLDEADRMLDMGFEPQIRKIVDQIRPDRQTLMWSATWPKEVRQLAEDFLKEY
S._salar NMRRCTYLVLDEADRMLDMGFEPQIRKIVDQIRPDRQTLMWSATWPKEVRQLAEDFLKDY
C._familiaris NLRRTTYLVLDEADRMLDMGFEPQIRKIVDQIRPDRQTLMWSATWPKEVRQLAEDFLKDY
H._sapiens NLRRTTYLVLDEADRMLDMGFEPQIRKIVDQIRPDRQTLMWSATWPKEVRQLAEDFLKDY
P._abelii NLRRTTYLVLDEADRMLDMGFEPQIRKIVDQIRPDRQTLMWSATWPKEVRQLAEDFLKDY
P._troglodytes NLRRTTYLVLDEADRMLDMGFEPQIRKIVDQIRPDRQTLMWSATWPKEVRQLAEDFLKDY
M._musculus NLRRTTYLVLDEADRMLDMGFEPQIRKIVDQIRPDRQTLMWSATWPKEVRQLAEDFLKDY
R._norvegicus NLRRTTYLVLDEADRMLDMGFEPQIRKIVDQIRPDRQTLMWSATWPKEVRQLAEDFLKDY
G._gallus NLRRCTYLVLDEADRMLDMGFEPQIRKIVDQIRPDRQTLMWSATWPKEVRQLAEDFLKEY
X._laevis NLNRCTYLVLDEADRMLDMGFEPQIRKIVDQIRPDRQTLMWSATWPKEVRQLAEDFLRDY
T._castaneum NLRRCTYLVLDEADRMLDMGFEPQIRKIIEQIRPDRQTLMWSATWPKEVQALAAEFLKDY
A._mellifera NLKRCTYLVLDEADRMLDMGFEPQIRKIIEQIRPDRQTLMWSATWPKEVKNLAEDFLKDY
D._melanogaster SLKRCTYLVLDEADRMLDMGFEPQIRKIMQQIRPDRQVLMWSATWPKEVRQLAEEFLNNY
A._aegypti NLRRCTYLVLDEADRMLDMGFEPQIRKIMGQIRPDRQVLMWSATWPKEVRNLAEEFLNDY
C._elegans NMKKCSYLVLDEADRMLDMGFEPQIKKIIGQIRPDRQTLMFSATWPKEVRALASDFQKDA

```
                                                                motif IV
D._rerio              IQINVGALQLSANHNILQIVDVCNDGEKEDKLIRLLEEIMSEKENKTIIFVETKRRCDDL
S._salar              VQINVGALQLSANHNILQIVDVCNDGEKEDKLLRLLEEIMSEKENKTIIFTETKRRCDEI
C._familiaris         IHINIGALELSANHNILQIVDVCHDVEKDEKLIRLMEEIMSEKENKTIVFVETKRRCDEL
H._sapiens            IHINIGALELSANHNILQIVDVCHDVEKDEKLIRLMEEIMSEKENKTIVFVETKRRCDEL
P._abelii             IHINIGALELSANHNILQIVDVCHDVEKDEKLIRLMEEIMSEKENKTIVFVETKRRCDEL
P._troglodytes        IHINIGALELSANHNILQIVDVCHDVEKDEKLIRLMEEIMSEKENKTIVFVETKRRCDEL
M._musculus           IHINIGALELSANHNILQIVDVCHDVEKDEKLIRLMEEIMSEKENKTIVFVETKRRCDEL
R._norvegicus         IHINIGALELSANHNILQIVDVCHDVEKDEKLIRLMEEIMSEKENKTIVFVETKRRCDEL
G._gallus             VHINIGALELSANHNILQIVDVCHDVEKDDKLIRLMEEIMSEKENKTIVFVETKRRCDDL
X._laevis             VHINIGALELSANHNILQIVDVCNDGEKDDKLVRLMEEIMSEKENKTIVFVETKRRCDDL
T._castaneum          IQINVGSLQLSANHNILQIIDVCQEYEKETKLSTLLKEIMAEKENKTIIFIETKKRVDEI
A._mellifera          AQINVGSLQLAANHNILQIIDVCQDYEKENKLSTLLKEIMAESENKTIVFIETKRRVDEI
D._melanogaster       IQVNIGSLSLSANHNILQIVDVCDENEKLMKLIKLLTDISAENETKTIIFVETKKRVDEI
A._aegypti            IQINIGSLNLSANHNILQIVDVCEDYEKDQKLMKLLTEISAENETKTIIFVETKRRVDDI
C._elegans            AFLNVGSLELAANHNITQVVDILEEHAKQAKLMELLNHIMNQKECKTIIFVETKRKADEL
                        :*:*:*.*:***** *::*: .:  *  **  *: .*  :.* ***:* ***:: *::

                                                          motif V
D._rerio              TRRMRRDGWPAMGIHGDKNQQERDWVLNEFKYGKAPILIATDVASRGLDVEDVKFVINFD
S._salar              TRRMRRDGWPAMGIHGDKSQQERDWVLNEFKFGKAPILIATDVASRGLDVEDVKFVINFD
C._familiaris         TRKMRRDGWPAMGIHGDKSQQERDWVLNEFKHGKAPILIATDVASRGLDVEDVKFVINYD
H._sapiens            TRKMRRDGWPAMGIHGDKSQQERDWVLNEFKHGKAPILIATDVASRGLDVEDVKFVINYD
P._abelii             TRKMRRDGWPAMGIHGDKSQQERDWVLNEFKHGKAPILIATDVASRGLDVEDVKFVINYD
P._troglodytes        TRKMRRDGWPAMGIHGDKSQQERDWVLNEFKHGKAPILIATDVASRGLDVEDVKFVINYD
M._musculus           TRKMRRDGWPAMGIHGDKSQQERDWVLNEFKHGKAPILIATDVASRGLDVEDVKFVINYD
R._norvegicus         TRKMRRDGWPAMGIHGDKSQQERDWVLNEFKHGKAPILIATDVASRGLDVEDVKFVINYD
G._gallus             TRKMRRDGWPAMGIHGDKSQQERDWVLNEFKHGKAPILIATDVASRGLDVEDVKFVINYD
X._laevis             TRRLRRDGWPAMGIHGDKSQQERDWVLNEFKHGKSPILIATDVASRGLDVEDVKFVINYD
T._castaneum          TRKMKRDGWPAVCIHGDKSQQERDWVLQDFRTGKAPILVATDVAARGLDVEDVKFVINFD
A._mellifera          TRKMKRDGWPAVCIHGDKTQQERDWVLQDFRSGKAPILVATDVAARGLDVEDVKFVINFD
D._melanogaster       TRNISRQGWRACAIHGDKSQQERDFVLSSFRNGRHSILVATDVAARGLDVDDVKFVINYD
A._aegypti            TRNINRNGWRAVSIHGDKSQQERDYVLNAFRNGRQGILVATDVAARGLDVEDVKFVINYD
C._elegans            TRAMRRDGWPTLCIHGDKNQGERDWVLQEFKAGKTPIMLATDVAARGLDVDDIKFVINYD
                      ** : *:** :  *****.* ***:**. *: *:  *::*****:*****:*:*****:*

                             motif VI
D._rerio              YPNNSEDYIHRIGRTARSQKTGTAYTFFTPNNMKQAHDLVSVLREANQAINPKLIQMAE-
S._salar              YPNNSEDYIHRIGRTARSQKTGTAYTFFTPNNMRQASDLVAVLREANQAINPKLLQMADR
C._familiaris         YPNSSEDYIHRIGRTARSTKTGTAYTFFTPNNIKQVSDLISVLREANQAINPKLLQLVED
H._sapiens            YPNSSEDYIHRIGRTARSTKTGTAYTFFTPNNIKQVSDLISVLREANQAINPKLLQLVED
P._abelii             YPNSSEDYIHRIGRTARSTKTGTAYTFFTPNNIKQVSDLISVLREANQAINPKLLQLVED
P._troglodytes        YPNSSEDYIHRIGRTARSTKTGTAYTFFTPNNIKQVSDLISVLREANQAINPKLLQLVED
M._musculus           YPNSSEDYIHRIGRTARSTKTGTAYTFFTPNNIKQVSDLISVLREANQAINPKLLQLVED
R._norvegicus         YPNSSEDYIHRIGRTARSTKTGTAYTFFTPNNIKQVSDLISVLREANQAINPKLLQLVED
G._gallus             YPNSSEDYIHRIGRTARSTKTGTAYTFFTPNNIKQVNDLISVLREANQAINPKLLQLIED
X._laevis             YPNSSEDYIHRIGRTARSSKTGTAYTFFTPGNIKQVNDLISVLREANQAINPKLLQLVED
T._castaneum          YPSNSEDYVHRIGRTGRSQRTGTAYTFFTPANANKAADLVSVLKEAKQVINPKLQEMADN
A._mellifera          YPSCSEDYVHRIGRTGRRQKTGTAYTFFTPNNSNKANDLIQVLKEANQVINPKLLELADS
D._melanogaster       YPSNSEDYVHRIGRTGRSNNTGTAYTLFTHSNANKANDLIQVLREANQTINPKLMNMAMN
A._aegypti            YPSNSEDYVHRIGRTGRSNNTGTAYTLFTNSNANKAGDLINVLREANQVINPKLAEMAKP
C._elegans            YPNNSEDYVHRIGRTGRSDKKGTAYTFFTHTNASKAKDLLKVLDEAKQTVPQALRDMANR
                      **. ****:******.*  ..*****:**  *  :. **: ** **:*.:   * ::


D._rerio              -----------------------------DRGGKSNWSFKGRTRWRV------------
S._salar              GGH---------------------------SRGGRGGSGFRDDRRDRYSSGGRRDFTS--
C._familiaris         RG----------------------------SGRSRGRGGMKDDRRDRYSAGKRGGFN--T
H._sapiens            RG----------------------------SGRSRGRGGMKDDRRDRYSAGKRGGFN--T
P._abelii             RG----------------------------SGRSRGRGGMKDDRRDRYSAGKRGGFN--T
P._troglodytes        RG----------------------------SGRSRGRGGMKDDRRDRYSAGKRGGFN--T
M._musculus           RG----------------------------SGRSRGRGGMKDDRRDRYSAGKRGGFN--T
R._norvegicus         RG----------------------------SGRSRGRGGMKDDRRDRYSAGKRGGFN--T
G._gallus             RG----------------------------SGRSRG------DRRDRYSAGKRGGFS--S
X._laevis             RG----------------------------RFRGRGG---MNDRRDRFSSGKRGGWDREN
T._castaneum          RNW---------------------------SS-------NGSSGRGLSPAPGRGLLA---
A._mellifera          KSG---------------------------GYGRHRGGRNRWRSRGGRNGKDRSYSR---
D._melanogaster       GGY---------------------------NKRGGGMGGGYRGGNGYQGRNPQMGGGYNG
A._aegypti            GMNRHGQRHNRYGNRYGGQQNRPPRDGGYGGQRNDGGHRFGGMNNGNKFGGPRGDAGGDK
C._elegans            SYG-----------------------------------GSNSRGRYGGGGFQKRG---
                                                             .
```

```
D._rerio            ------------------------------------------------------------
S._salar            -FRDRENDRGFDSGPKKVFGTNSQSGGYGASGFDK-------------------------
C._familiaris       FRDRENYDRGYSSLLKRDFGAKTQNGVYSAANYTN-------------------------
H._sapiens          FRDRENYDRGYSSLLKRDFGAKTQNGVYSAANYTN-------------------------
P._abelii           FRDRENYDRGYSSLLKRDFGAKTQNGAYSAANYTN-------------------------
P._troglodytes      FRDRENYDRGYSSLLKRDFGAKTQNGVYSAANYTN-------------------------
M._musculus         FRDRENYDRGYSNLLKRDFGAKTQNGVYSAANYTN-------------------------
R._norvegicus       FRDRENYDRGYSSLLKRDFGAKTQNGVYSAANYTN-------------------------
G._gallus           FRERENFERTYGALGKRDFGAKAQNGAYSTQSFSNG-----------------------
X._laevis           YDRGFGGKRDFGNKSQNGFGNKSQNGFGAQNYNGN-------------------------
T._castaneum        ------------------------------------------------------------
A._mellifera        ------------------------------------------------------------
D._melanogaster     GNNYRNNNGPGATMNRNSFNGGSAGGPPRFDQKPRTSPPNQGGQGGYRGQGGGGYQGQQQ
A._aegypti          FGSKPAQNGGYQSRDQNRIPNGSGPPSGARPSRFSAPSN---------------------
C._elegans          ------------------------------------------------------------

D._rerio            ------------------------------------------------------------
S._salar            ------------------------------------------------------------
C._familiaris       ------------------------------------------------------------
H._sapiens          ------------------------------------------------------------
P._abelii           ------------------------------------------------------------
P._troglodytes      ------------------------------------------------------------
M._musculus         ------------------------------------------------------------
R._norvegicus       ------------------------------------------------------------
G._gallus           ------------------------------------------------------------
X._laevis           ------------------------------------------------------------
T._castaneum        ------------------------------------------------------------
A._mellifera        ------------------------------------------------------------
D._melanogaster     QQQQQNGGVPFSRFNPNAACFEPNKPQNGPGSGPPQAQHQQQQQAQAAQQQHLLPDASVQ
A._aegypti          ------------------------------------------------------------
C._elegans          ------------------------------------------------------------

D._rerio            ------------------------------------------------------------
S._salar            ------------------------------SGNGFGGYGSNGQSNYGT-SQAGAFPTQNF
C._familiaris       ------------------------------GSFGSNFVSAGIQTSFRTGNPTGTYQNGYD
H._sapiens          ------------------------------GSFGSNFVSAGIQTSFRTGNPTGTYQNGYD
P._abelii           ------------------------------GSFGSNFVSAGIQTSFRTGNPTGTYQNGYD
P._troglodytes      ------------------------------GSFGSNFVSAGIQASFRTGNPTGTYQNGYD
M._musculus         ------------------------------GSFGSNFVSAGIQTSFRTGNPTGTYQNGYD
R._norvegicus       ------------------------------GSFGSNFVSAGIQTSFRTGNPTGTYQNGYD
G._gallus           ------------------------------TPFGNGFAAAGMQAGFRAGNPAGAYQNGYD
X._laevis           ----------------------------------FNSYGSNVQSGFRAGAQNGTYQNGYS
T._castaneum        ---------------------------------------EEDATEVDRETEIGERSRVAQ
A._mellifera        ---------------------------------------SRSRSHSREYNGRGNRRSYSR
D._melanogaster     AAMTAANYGVDQKRSRFSPYNMNFANMPPPAMNQQQAAAAQQQQQQQLQTPQQQQQQQQM
A._aegypti          ------------------------------APPSFPSGATGGNSYNKGAYQNGSAASGN
C._elegans          ------------------------------------------------------YGGNDNFAP

D._rerio            ------------------------------------------------------------------------
S._salar            QAPQFSANQGGAQNGMSHQQFPFTQQQAPQP-MVPYPMPPQFPQ----------------------
C._familiaris       STQQYGSNVPNMHNGMNQQAYAYP-ATAAAP-MIGYPMPTGYSQ----------------------
H._sapiens          STQQYGSNVPNMHNGMNQQAYAYP-ATAAAP-MIGYPMPTGYSQ----------------------
P._abelii           STQQYGSNVPNMHNGMNQQAYAYP-ATAAAP-MIGYPMPTGYSQ----------------------
P._troglodytes      STQQYGSNVPNMHNGMNQQAYAYP-ATAAAP-MIGYPMPTGYSQ----------------------
M._musculus         STQQYGSNVANMHNGMNQQAYAYP-VPQPAP-MIGYPMPTGYSQ----------------------
R._norvegicus       STQQYGSNVANMHNGMNQQAYAYP-ATAAAAPMIGYPMPTGYSQ----------------------
G._gallus           --QQYGSNIANMHNGMNQQQYAYP-ATGAAP-MIGYPMPASYSQ----------------------
X._laevis           -TQQTGYSAPPMQNGMTQQAYTYPTATATAPAVIGYPMPTSYPQ----------------------
T._castaneum        AGTAVLPVIANQHPLNSPLHNP----------------------------------------------
A._mellifera        SYSRSRSPVSNRAEVIGKSYWSSER------------------------------------------
D._melanogaster     QQPQAYGQYSSMSSSMATVSLNGGAAAVASSYRAPYAVPTQAAPYMMANGGDIFAYPPPPLPVQN-
A._aegypti          SAPTSNGYGSYKPYTTAPPTQSATGASFGGYQRSTPAVPSAYPSFGGALPQPGQTFAFPPPAVALN
C._elegans          KRPRYDNGGYGGGSGGGGRW------------------------------------------------
```

3.2.2 Generation of plasmids for experiments with p68

The chicken p68 encoding nucleotide sequence was obtained by RT-PCR on CEC RNA using the primers p68-FP1 and p68-His delineated from the chicken p68 sequence NM_204827 found in the NCBI database (sequence see 6.2.2). The forward primer contained a *Bam*HI RE cleavage site and the reverse primer a *Not*I site and an artificial 3'-terminal sequence encoding a 6x His-tag. The obtained cDNA (1806 bp including the 6x Histag) was first cloned into pCR®2.1-TOPO® and transformed into One Shot® TOP 10 competent cells and the purified plasmid was sequenced (primers see Table 1b). Using *Bam*HI and *Not*I RE sites, the p68-His encoding sequence was cloned from the recombinant plasmid into pFastBac™Dual resulting in p68-His-pDual. Further constructs were obtained by PCR using Deep Vent DNA polymerase with appropriate forward and reverse primer on a template described in Table 13. PCR products were incubated with specific REs and ligated into pcDNA3 vector cleaved likewise. The recombinant plasmid p68-FLAG encoded a FLAG tag instead of a 6x His-tag at the C-terminus of the p68 encoding sequence and was generated using the restriction enzymes *Kpn*I and *Not*I. All recombinant plasmids encoding for VP4 or the maltose binding protein (MBP) were generated using restriction enzymes *Eco*RI and *Xho*I. The ligation reactions were transformed into *E. coli* strain XL1-Blue and purified plasmids were sequenced with primers shown in Table 1b.

Table 13: Forward and reverse primers (FP and RP) and template DNA used for PCR

gene/tag[a]	FP[b]	RP[c]	template[d]	name of construct[e]
p68-FLAG	p68 FP2	p68-FLAG	p68-His TOPO	p68-FLAG-pcDNA3
MBP-FLAG	MBP-FP	MBP-RP	VP4 pMAL[f]	MBP-FLAG-pcDNA3
MBP-VP4-FLAG	MBP-FP	VP4-FLAG-RP	VP4 pMAL[f]	MBP-VP4-FLAG-pcDNA3
VP4	VP4-FP	VP4-RP	puc19FLAD78[f]	VP4-pcDNA3
VP4-S652R	VP4-FP	VP4-RP	puc19FLAD78-S652R[f]	VP4-S652R-pcDNA3

[a] name of the gene to be amplified with its tag or mutation
[b] FP: forward primer used for amplification
[c] RP: reverse primer used for amplification
[d] plasmid used for amplification (origin of the plasmid)
[e] name of the construct
[f] provided by Dr. E. Mundt

3.2.3 Detection of p68 mRNA by Northern Blot

The next experiment was conducted to determine, if p68 mRNA increased during an infection with IBDV strain D78.

A Northern blot was carried out as described above (3.1.3). RNA of control and IBDV infected CEC were separated on a gel for Northern blot analysis. A positive control for p68 was T7 RNA polymerase transcribed RNA of the *Not*I linearized p68-FLAG-pcDNA3 plasmid (1806 bp). Equal amounts of RNA were loaded on the gel. After blotting on a membrane, it was exposed to the specific probe, which was DIG-labeled RNA

transcribed by Sp6 RNA polymerase of a *Bam*HI linearized p68-FLAG-pcDNA3 plasmid. The Northern Blot (Figure 23) did not show increased amounts of p68 specific mRNA in IBDV strain D78 infected CEC.

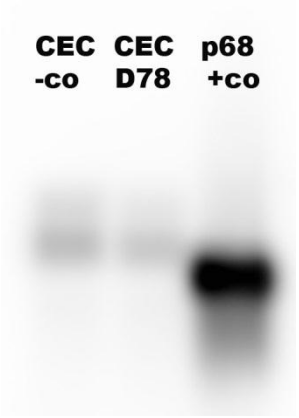

Figure 23: Northern Blot of non-infected and D78 infected CEC RNA with p68 RNA probe and its positive control.

3.2.4 Purification of p68

The plasmid p68-His-pDual was used for the Bac-to-Bac® Baculovirus expression system to obtain recombinant chicken p68-His for purification using its C-terminal located 6xHis sequence. Samples were taken at different steps of the purification process, which were separated by SDS-PAGE and then either protein stained (Figure 24A) or further analyzed by Western blot using mAb His-POD (Figure 24B). The product obtained after elution during the purification process was shown in the last lane of the protein stained gel (lane E, marked by an arrowhead). The observed single protein had an apparent molecular weight of approximately 66 kDa, which was similar to the expected 68 kDa. The excised band was send to the Proteomics Resource Facility at the University of Georgia (to Tracy Andacht) for analysis by MALDI-TOF MS-MS. Peptide analysis confirmed the identity of the chicken p68 protein. Western blot analysis revealed that a band of similar size was present as observed on the protein stained gel in the lane of the eluate. The blot showed that p68 was poorly soluble as observed by a large amount of p68-His that remained in the pellet (P) while a comparable low amount was present in the supernatant (S).

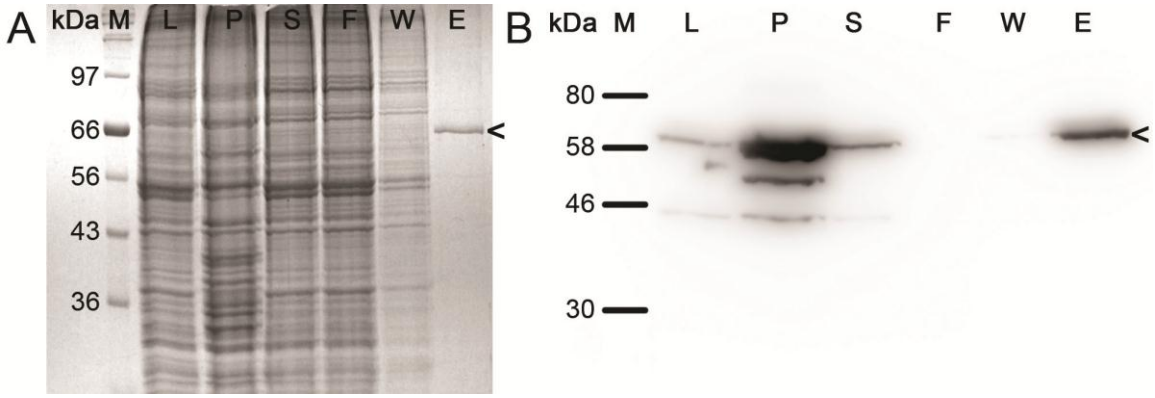

Figure 24: Expression of p68-His in a recombinant baculovirus. (A) Coomassie brilliant blue stained gel and (B) Western blot using mAb His-POD (1:5,000) of the p68-His samples taken at different purification steps; L: lysate; P: pellet; S: supernatant; F: flowthrough; W: first wash step; E: eluate. p68-His was marked by an arrowhead. The molecular weights of protein markers (M) are shown at the left side of each gel.

The p68-His containing eluates were pooled, concentrated and the amount of p68-His was determined. Seven aliquots with a volume of 500 µl containing 400 µg of p68-His were generated and provided for the Polyclonal Antibody Production Service, University of Georgia (to Amy Dryman). A SPF New Zealand White Rabbit was immunized with

p68-His and complete Freund's adjuvant. Approximately every three weeks the rabbit was immunized again with p68-His and incomplete Freund's adjuvant. Blood was taken before the initial immunization and two weeks after each boost immunization. The last blood was taken three weeks after the seventhsimmunization by exsanguination. The obtained serum against p68-His (rabbit-α-p68-His) was further called R-α-p68 and used in a dilution of 1:400 in IIFA and 1:1,000 for Western blot analysis.

3.2.5 Specificity of the R-α-p68 serum

Proteins from cell lysates of several cell lines (CEC, DF-1, QM-7, Vero and BHK-21) were separated on a SDS-PAGE gel and blotted on a membrane for Western blot analysis with the R-α-p68 serum as the primary antibody and α-R-POD as conjugated secondary antibody. A p68 specific band was observed at approximately 68 kDa in all analyzed cell lysates indicated by an arrow (Figure 25A). Additionally a band of approximately 50 kDa was also observed. Further bands were observed in the QM-7 (85 kDa) and in the Vero cell lysate (40 kDa). To verify that the band observed at 68 kDa was indeed the p68 specific band, BHK-21 cells were transfected with p68-FLAG-pcDNA3. In independent experiments it was observed that Western blot analysis using lysates of BHK-21 cells did not result in a clear p68 signal. This phenotype was used for further analysis. Cell lysates of DF-1 cells, non-transfected and p68-FLAG-pcDNA3 transfected BHK-21 cells were separated on a SDS-PAGE gel. The membrane was cut as marked by the dashed line (Figure 25B). For Western blot analysis the left part was incubated with R-α-p68 and α-R-POD and the right part with mAb FLAG and α-M-POD. On both Western blots appeared a strong band in lysates of p68-FLAG-pcDNA3 transfected BHK-21 cells (BHK p68) at the same level as the expected p68 protein in lysates of DF-1 cells when analyzed with R-α-p68 serum indicated by an arrow. A weak signal at this level was observed in non-transfected BHK-21 using R-α-p68 serum, but no signal was observed when analyzed with mAb FLAG. A band of approximately 28 kDa appeared in p68-FLAG-pcDNA3 transfected and non-transfected BHK-21 cells after incubation with mAb FLAG. The strength of the signal was similar, which indicates loading of a comparable amount of protein. This band was not related to p68, but to another protein that cross-reacted with mAb FLAG. Additional bands observed in BHK-21 cells (72, 60, 50, 46 and 40 kDa) were present independent whether BHK-21 cells were transfected or not. These results indicated that the R-α-p68 serum recognizes p68 at the expected size by Western blot analysis (Figure 25A). In Figure 25C BHK-21 cells transfected with p68-FLAG-pcDNA3 were fixed and analyzed by IIFA using R-α-p68, mAb FLAG and PI followed by incubation with appropriate conjugates α-R-FITC and α-M-Cy5. One transfected and some non-transfected cells showed weak fluorescence in the cytoplasm. Only the transfected cell showed a strong

signal in the cell nucleus. The merged picture showed the co-localization of p68 and FLAG. This experiment gave evidence that the R-α-p68 recognizes p68 also in IIFA.
In Figure 25D, DF-1 cells were used for IIFA using R-α-p68 serum and α-R-FITC as conjugate. This shows that endogenous p68 was mainly localized in the nucleus of chicken cells, which was visualized by incubation with PI. The protein p68 was also present in low amounts in the cytoplasm.

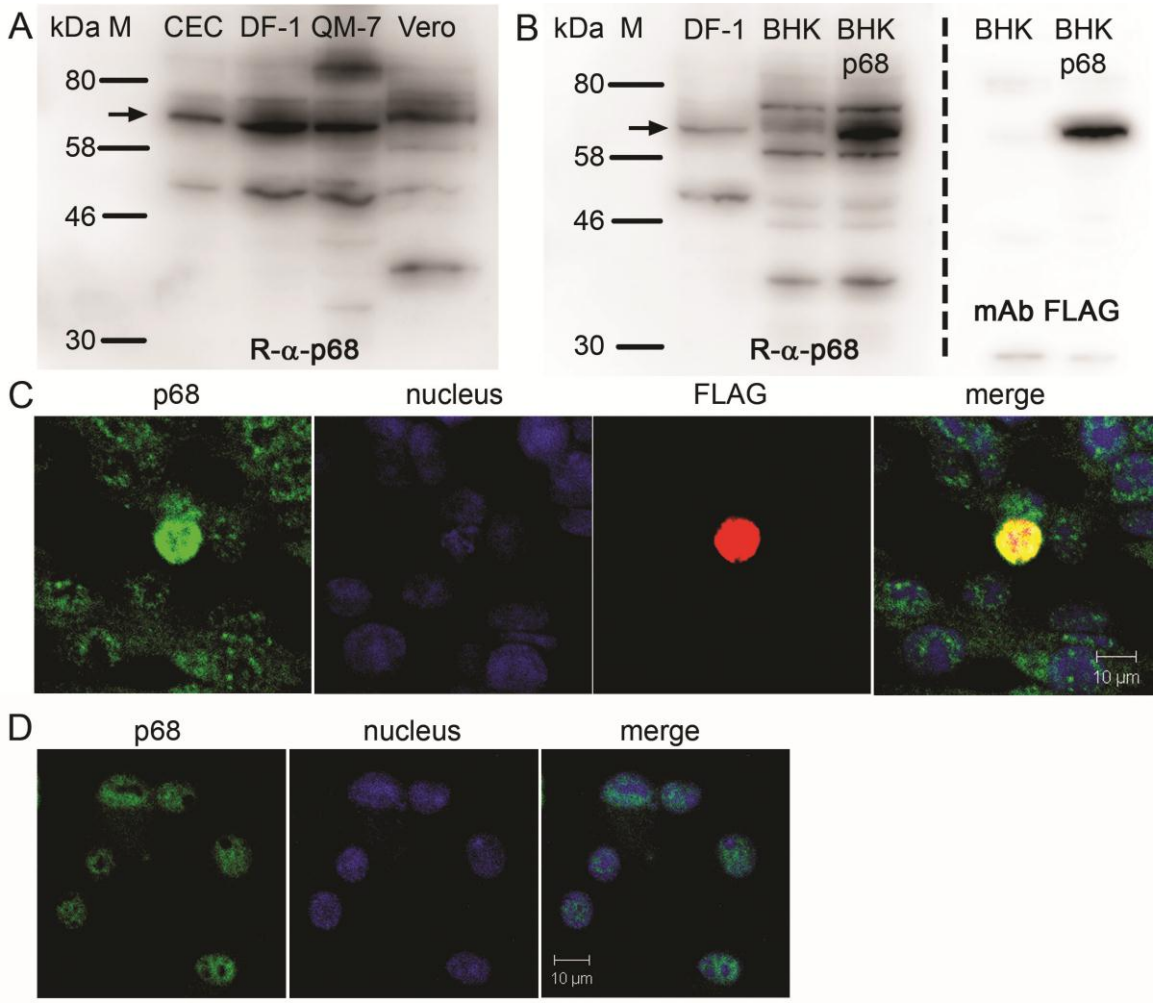

Figure 25: Specificity of the R-α-p68 serum and cellular localization of p68. (A) Western blot analysis of cellular lysates of CEC, DF-1, QM-7, Vero and BHK-21 cells, incubated with the R-α-p68 serum (1:1,000) and α-R-POD (1:20,000). An arrow marked the apparent molecular weight of endogenous p68. (B) Western blot analysis of cellular lysates of DF-1, BHK-21 (BHK) and BHK-21 cells transfected with p68-FLAG-pcDNA3 (BHK p68). The left part of the membrane was incubated with R-α-p68 serum (1:1,000) and α-R-POD conjugate (1:20,000). The right part of the membrane was incubated with mAb FLAG (1:2,500) and the conjugate α-M-POD (1:25,000). M=prestained protein marker (C) Indirect immunofluorescence of BHK-21 cells transfected with p68-FLAG-pcDNA3, which were fixed 24 h pt with ice cold ethanol and incubated with R-α-p68 (1:400, green), PI to stain the nucleus (1:5,000, blue) and mAb FLAG (1:500, red). The cells were incubated with appropriate conjugates [α-R-FITC (1:200) and α-M-Cy5 (1:50)]. (D) Fixed DF-1 cells were incubated with R-α-p68 (1:400, green) and PI to stain the nucleus (1:5,000, blue) and further with the conjugate α-R-FITC (1:200). Pictures in panel C and D were visualized by CLSM.

3.2.6 Localization of endogenous p68 and VP4 in IBDV infected cells

It was investigated, if p68 changed its localization upon IBDV infection. DF-1, QM-7 and Vero cells were infected with D78 and fixed 12 h pi and used for IIFA with R-α-p68 serum, mAb VP4 and PI followed by species-specific conjugates. In all three cell lines endogenous p68 is located in the nucleus of non-infected cells (Figure 26). In all infected cells, p68 was located additionally in the cytoplasm in needle-like structures co-localizing with VP4. For VP4 it has been described before that it localizes in infected cells in a pattern named type II tubules, which look needle-like in immunofluorescent studies (Granzow *et al* 1997). Co-localization of VP4 and p68 was species independent since it was observed in cells derived from chicken, quail and monkey. In addition it was also concluded that this phenotype was independent of the presence of interferon since it was observed in Vero cells (see 3.1.6).

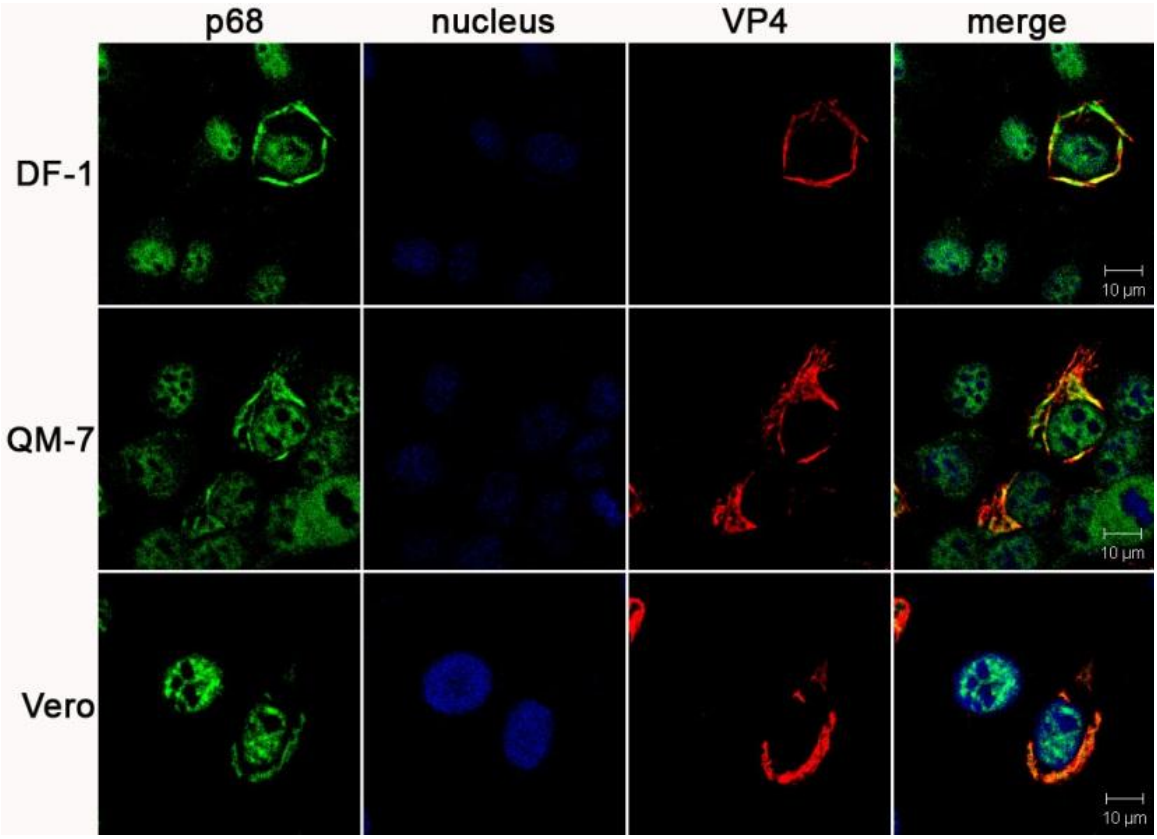

Figure 26: VP4 of IBDV and p68 co-localize. IIFA of DF-1, QM-7 and Vero cells infected with IBDV strain D78 and fixed 12 h pi with ice cold ethanol. They were incubated with R-α-p68 (1:400, green), PI to visualize the nucleus (1:5,000, blue) and mAb VP4 (1:100, red). The binding of the primary antibodies was visualized using the conjugates α-R-FITC (1:200) and α-M-Cy5 (1:50). The pictures were documented with CLSM.

3.2.7 Quantification of p68 in the nucleus

The ratio of the fraction of p68 present in the nucleus versus the cytoplasmic fraction was determined. The calculation was performed as for NF45 (see 3.1.7). Non-infected

control and with IBDV strain D78 infected DF-1 cells were analyzed and results were presented in Figure 27. In non-infected cells in average 90% of p68 was detected in the nucleus. Interestingly, at 12 h pi 62% of p68 was present in the nucleus and 38% resided in the cytoplasm. Similar to the quantification of NF45 in infected cells, the standard deviation as shown by an error bar of the population of infected cells for nuclear p68 was rather high, which might be explained with different states during viral replication.

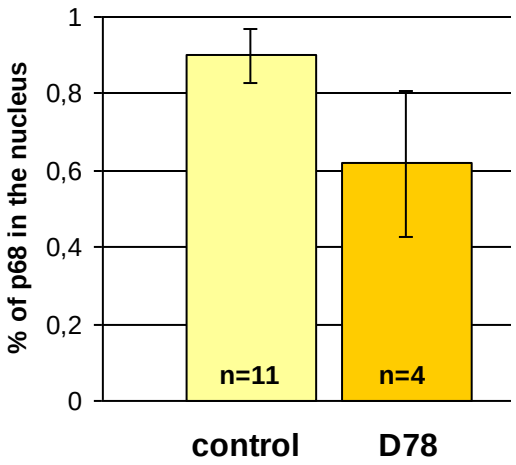

Figure 27: Quantification of p68 fractions in the nucleus in non-infected DF-1 cells (control) and cells infected with IBDV strain D78 for 12 h (D78). The columns indicate the average percentage of integrated fluorescent intensity of the nucleus divided by the integrated fluorescent intensity of the whole cell. The number (N) of all analyzed cells are indicated. Error bars depict the standard deviation.

3.2.8 No co-localization of p68 with VP3 in the cytoplasm

In next experiments it was investigated, if the p68-VP4 co-localization was VP4 specific. DF-1 cells were infected with IBDV strain D78 and fixed 12 h pi and submitted for IIFA using R-α-p68, mAb VP3 and PI and appropriate conjugates (α-R-FITC and α-M-Cy5). As already shown in above described experiments (see 3.1.6), VP3 localized in the cytoplasm of infected cells in dot-like structures. Endogenous p68 showed a needle-like structure, but localized mutually exclusive from VP3 (Figure 28). This result indicated that the observed localization of p68 in the cytoplasm was VP4 specific.

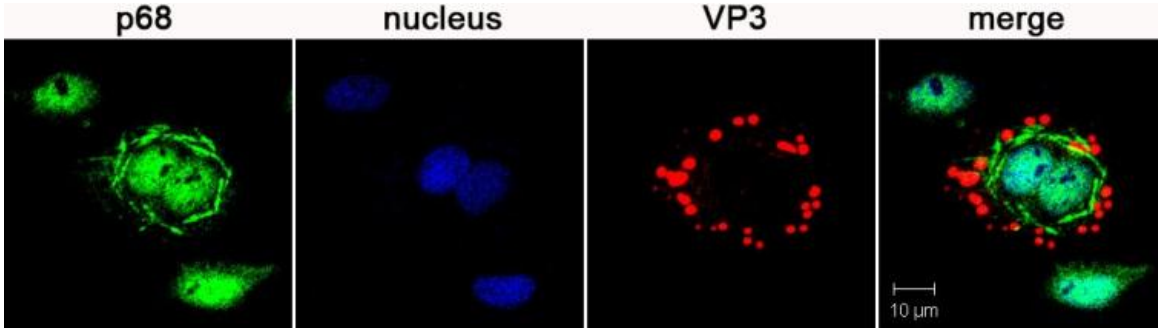

Figure 28: The cellular protein p68 does not co-localize with IBDV protein VP3. IIFA of DF-1 cells infected with IBDV strain D78. Cells were fixed with ice cold ethanol 12 h pi and incubated with R-α-p68 (1:400, green), PI to stain the nucleus (1:5,000, blue) and mAb VP3 (1:100, red). Species-specific conjugates [α-R-FITC (1:200) and α-M-Cy5 (1:50)] were used to visualize the binding of the primary antibodies by CLSM.

3.2.9 Co-localization of p68 and VP4 is strain independent

DF-1 cells were infected with IBDV variant strains 8903 (E/Del subtype) and GLS-05 (GLS subtype) and fixed 12 h pi. For IIFA cells were incubated with R-α-p68, mAb VP4

and PI, followed by conjugates α-R-FITC and α-M-Cy5. As observed before with IBDV strain D78, p68 co-localized with VP4 in the cytoplasm of cells infected with either of the variant strains, 8903 or GLS-05 (Figure 29). This indicates that the p68-VP4 co-localization was IBDV strain independent.

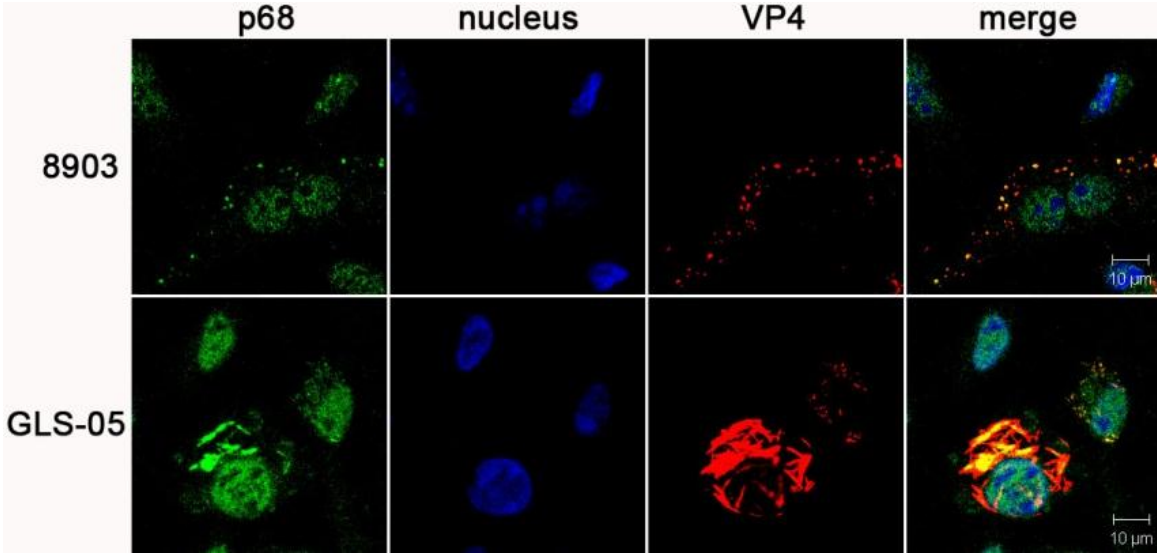

Figure 29: Co-localization of VP4 and p68 was IBDV strain independent. For IIFA DF-1 cells infected with either IBDV strain 8903 or GLS-05 and cells were fixed with ice cold ethanol 12 h pi. Cells were incubated with R-α-p68 (1:400, green), PI to visualize the nucleus (1:5,000, blue) and mAb VP4 (1:100, red). This was followed by incubation with the species-specific conjugates [α-R-FITC (1:200) and α-M-Cy5 (1:50)]. Pictures were taken by CLSM.

3.2.10 Co-localization of p68 and VP4 correlated to the time course of viral replication

Based on the findings during the experiments with cellular protein NF45, the dynamics of p68 co-localizing with VP4 were investigated. DF-1 cells were infected with IBDV strain D78, fixed at 2, 4, 6 and 8 h pi and further analyzed by IIFA using R-α-p68, PI and mAb VP4 and the appropriate species-specific conjugates (α-R-FITC and α-M-Cy5) (Figure 12). At 2 h pi VP4 was not observed and p68 showed a localization pattern as in non-infected cells, which was in agreement with the amount of p68 in the nuclear fraction (96%) (see Figure 31). At 4 h pi and at all later time points VP4 was observed in the cytoplasm of infected cells and p68 was co-localizing with VP4. The structure of VP4 at 4 h pi was rather dot-like, while at 6 h pi the structure of VP4 started to become tubular. At the last time point investigated (8 h pi) tubular structures were present as it has been already observed 12 h pi during experiments described above (Figure 26). The cytoplasmic fraction of p68 increased over time. At 4 h pi 12%, at 6 h 24% and at 8 h pi 47% of the total amount of p68 was present in the cytoplasm of infected cells (see Figure 31). Unfortunately only one cell could be analyzed at 4 h pi, which limited the significance of the result. From these observations it can be concluded that the

co-localization of p68 and VP4 in the cytoplasm and the formation of tubular structures is time dependent.

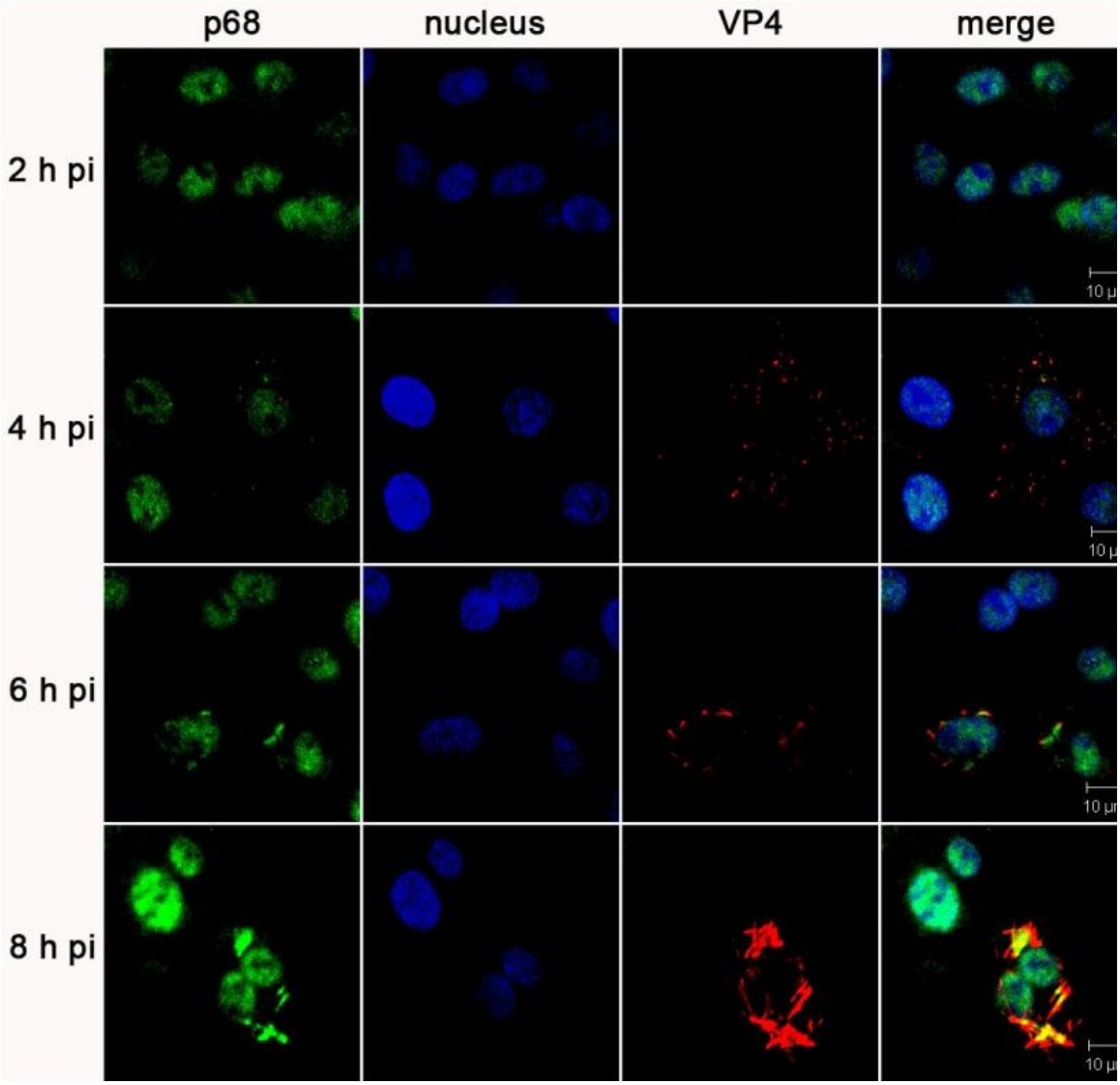

Figure 30: Presence of p68 in the cytoplasm of IBDV infected cells was time dependent. IIFA of IBDV strain D78 infected DF-1 cells, which were fixed at 2, 4, 6 and 8 h pi with ice cold ethanol. They were incubated with R-α-p68 (1:400, green), PI to stain the nucleus (1:5,000, blue) and mAb VP4 (1:100, red), followed by an incubation with species-specific conjugates [α-R-FITC (1:200) and α-M-Cy5 (1:50)] for visualization of the co-localization by CLSM.

3.2.11 Co-localization of p68 with transiently expressed VP4

The next experiments were conducted to analyze, which elements were necessary and sufficient to accumulate p68 in the cytoplasm of infected cells. DF-1 cells were transfected with different plasmids or RNAs, fixed and analyzed by IIFA using R-α-p68, PI, mAb VP4 and the appropriate conjugated secondary antibodies (α-R-FITC and α-M-Cy5). In first experiments it was evaluated, if virus replication was necessary to observe this phenotype. First, cRNA only of segment A was *in vitro* transcribed by T7

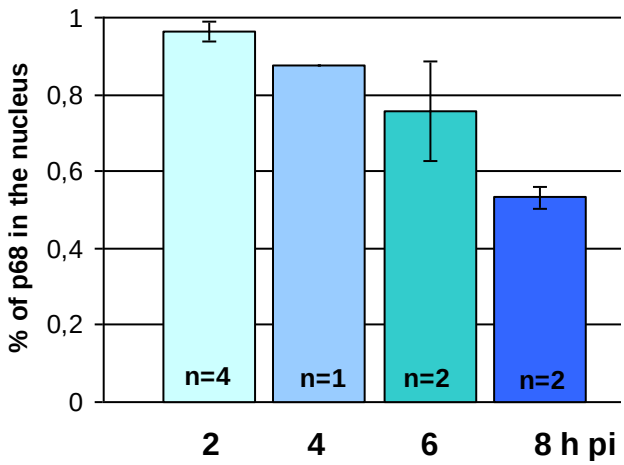

Figure 31: Quantification of the p68 fraction in the nucleus at 2, 4, 6 and 8 h pi. The columns present the average of nuclear integrated intensity divided by the integrated intensity of the whole cell. The number (N) of all cells analyzed was indicated in the column. Error bars show the standard deviation.

RNA polymerase from *Bsr*GI linearized plasmid puc19FLAD78 and transfected into DF-1 cells. As shown in Figure 32A, p68 was also observed in the cytoplasm of transfected cells co-localizing with VP4. Thus, the presence of proteins encoded by segment A or viral RNA were sufficient to accumulate p68 in the cytoplasm of transfected cells. Obviously, neither segment B encoded VP1 nor its RNA nor virus replication was necessary to observe this phenotype. In a second experiment cRNA transcribed from the VP4 minigenome (ordered from Genscript) was transfected. The cRNA of the minigenome consisted only of the segment A 5'NTR, the VP4 coding region including an artificial start and stop codon and the segment A 3'NTR (sequence see 6.2.6). Similar to the full length segment A, the plasmid was linearized with *Bsr*GI and then *in vitro* transcribed with T7 RNA polymerase. Similar to the observed phenotype after transfection with cRNA of the full length segment A, cRNA and/or VP4 induced accumulation of p68 in the cytoplasm of transfected cells (Figure 32B). Consequently, viral protein 2, 3 and 5 were not necessary for the observed phenotype of p68. In a next experiment only a recombinant plasmid encoding VP4-FLAG was transfected (VP4-FLAG-pcDNA3). Here the presence of only VP4-FLAG induced cytoplasmic p68 co-localization (Figure 32C) in the typical tubular structure. VP4 is the protease of IBDV and its function was completely inactivated by the mutation S652R. The amino acid 652 corresponds to the numbering of the amino acid sequence of the polyprotein, not to VP4 itself (Birghan *et al* 2000). A plasmid was generated (see 3.2.2) encoding the inactive form of VP4 (VP4-S652R-pcDNA3) and was used for transfection experiments. Again, p68 co-localized with VP4-S652R (Figure 32D). In a last experiment *in vitro* transcribed cRNA of segment A encoding the VP4 mutation S652R (puc19FLAD78-S652R obtained from Dr. E. Mundt) was transfected. With an inactive VP4 protease the IBDV polyprotein was not processed into the viral proteins 2, 4 and 3 and VP4 was locked between VP2 and VP3. Now, p68 was not observed in the cytoplasm of transfected cells (Figure 32E) and thus did not co-localize with VP4.

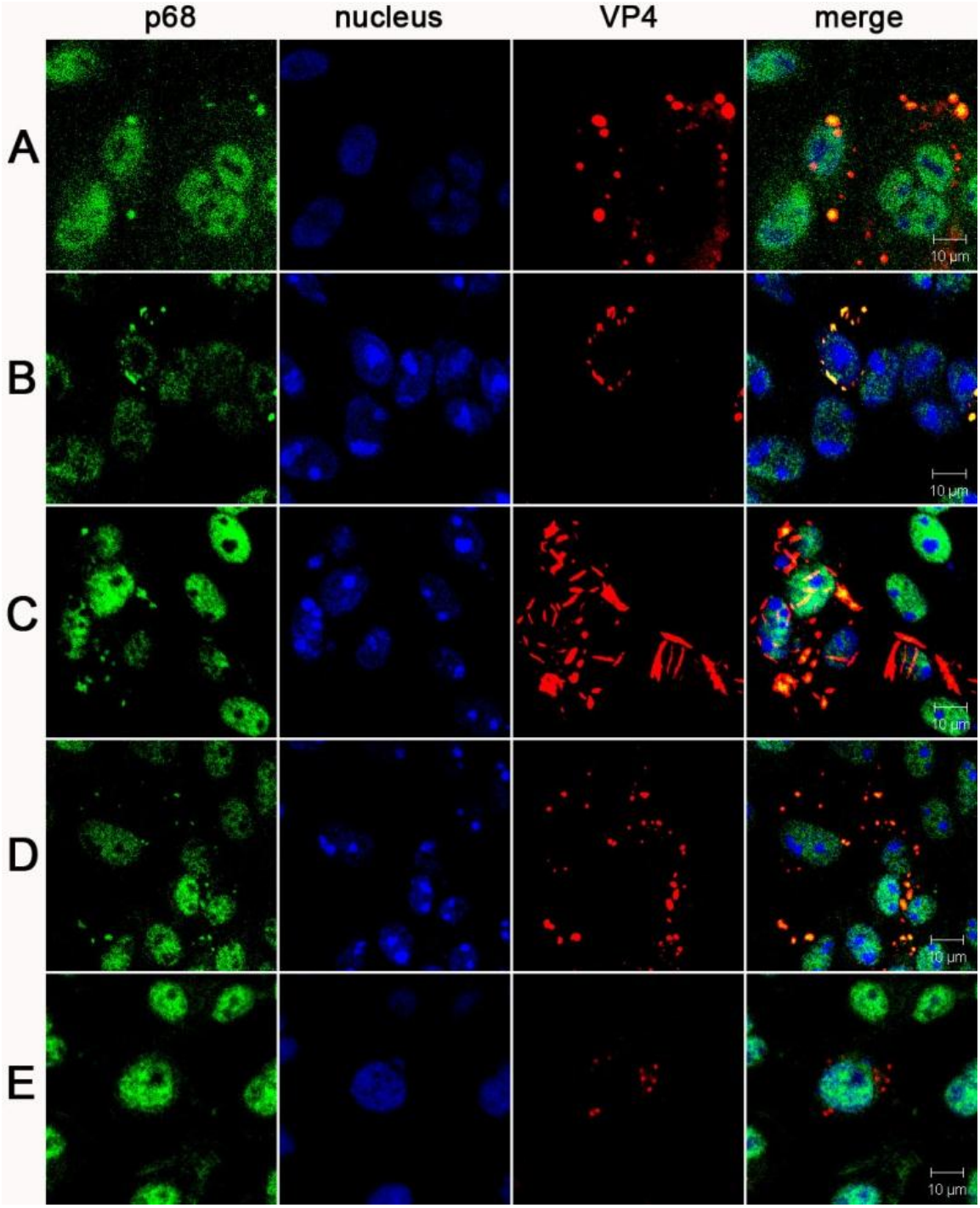

Figure 32: Accumulation of p68 was dependend on free VP4, but not on its protease fuction. DF-1 cells were transfected with the following constructs and fixed 24 h pt. (A) *In vitro* transcribed cRNA of segment A (puc19FLAD78). (B) *In vitro* transcribed cRNA of a VP4 minigenome. (C) recombinant plasmid VP4-FLAG-pcDNA3. (D) recombinant plasmid VP4-S652R-pcDNA3. (E) *In vitro* transcribed cRNA of segment A-S652R (puc19FLAD78-S652R). Fixed cells were incubated with R-α-p68 (1:400, green), PI to stain the nucleus (1:5,000, blue) and mAb VP4 (1:100, red). In a second step cells were incubated with species-specific conjugates [α-R-FITC (1:200) and α-M-Cy5 (1:50)]. The results of the IIFA was documented by CLSM.

3.2.12 Inhibition of the nuclear export of p68 by leptomycin B

The molecular weight of 68 kDa prohibits transport of the here investigated p68 through the nuclear pore without the presence of a NES. For a better understanding of the mechanism how p68 was co-localized with VP4 in the cytoplasm further experiments were performed. Two mechanisms were taken into consideration. One mechanism could be accumulation of p68 immediately after mRNA translation without entering the nucleus, where p68 resides. The second could be that p68 was transported out of the nucleus by a so far unknown signaling pathway. First, the presence of any NES that allows an active nuclear export was investigated. All leucins (L) and isoleucins (I), which have been described as part of the NES, were color coded in the p68 aa sequence:

```
  1 MPGFGAPRFG GSRAGPLSGK KFGNPGEKLT KKKWNLDELP KFEKNFYQEH
 51 PDVVRRTAQE VEQYRSSKEV TVRGHNCPKP IINFYEANFP ANVMEVIQRQ
101 NFTEPTAIQA QGWPVALSGL DMVGVAQTGS GKTLSYLLPA IVHINHQPFL
151 ERGDGPICLV LAPTRELAQQ VQQVAAEYSR ACRLKSTCIY GGAPKGPQIR
201 DLERGVEICI ATPGRLIDFL EAGKTNLRRC TYLVLDEADR MLDMGFEPQI
251 RKIVDQIRPD RQTLMWSATW PKEVRQLAED FLKEYVHINI GALELSANHN
301 ILQIVDVCHD VEKDDKLIRL MEEIMSEKEN KTIVFVETKR RCDDLTRKMR
351 RDGWPAMGIH GDKSQQERDW VLNEFKHGKA PILIATDVAS RGLDVEDVKF
401 VINYDYPNSS EDYIHRIGRT ARSTKTGTAY TFFTPNNIKQ VNDLISVLRE
451 ANQAINPKLL QLIEDRGSGR SRGDRRDRYS AGKRGGFSSF RERENFERTY
501 GALGKRDFGA KAQNGAYSTQ SFSNGTPFGN GFAAAGMQAG FRAGNPAGAY
551 QNGYDQQYGS NIANMHNGMN QQQYAYPATG AAPMIGYPMP ASYSQ
```

No typical NES was identified and the aa sequence was also scanned by using the program NetNES (La Cour *et al* 2004). No hydrophobic anchor aa sequence typical for known NES were found in p68. This result does not exclude the presence of a NES necessary for the translocation from the nucleus to the cytoplasm, but supports the hypothesis that p68 accumulates in the cytoplasm after translation in IBDV infected cells. Nevertheless, a similar experiment with LMB was conducted described for the cellular protein NF45 (see 3.1.13). IIFA was performed using R-α-p68, mAb VP4 and PI for IBDV infected cells (Figure 33B) and R-α-NP, mAb M1 and PI for H5N2 infected cells (Figure 33A), followed by α-R-FITC and α-M-Cy5. The upper row in Figure 33A and B showed the controls without addition of LMB, while the lower row showed localization of the proteins of interest in the presence of LMB.

Similar to NF45 and VP3, the IBDV protease VP4 and chicken p68 were located in the cytoplasm of IBDV infected cells, regardless whether LMB was added or not. In non-infected cells p68 showed the physiological phenotype with most of the protein residing in the nucleus. These results added more evidence to the assumption that p68 was not exported from the nucleus into the cytoplasm of infected DF-1 cells, but accumulated its cytoplasmic pool and co-localized with VP4.

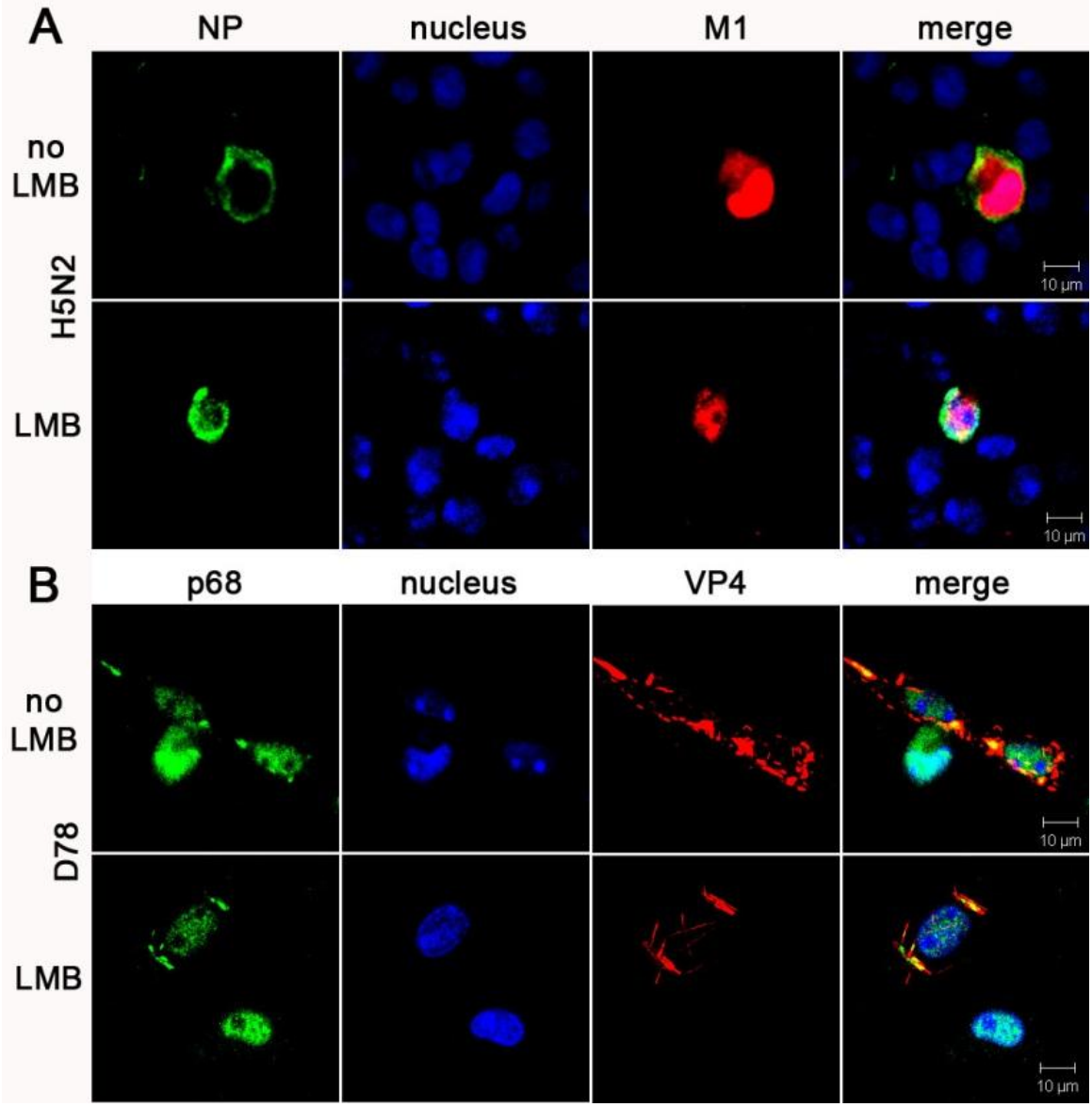

Figure 33: The cellular protein p68 co-localizes with VP4 in presence of leptomycin B. DF-1 cells were infected either with the avian influenza A virus H5N2 (A) or IBDV (B). Three hours post infection 2 ng/ml LMB were either added to one sample of each infection (LMB) or left untreated (no LMB). Twelve hours post infection cells were fixed with ice cold ethanol for IIFA using either (A) R-α-NP (1:100, green) and mAb M1 (1:200, red) or (B) R-α-p68 (1:400, green) and mAb VP4 (1:100, red). All cells were incubated with PI to stain the cellular nucleus (1:5,000, blue). In a next step cells were incubated with species-specific conjugates [α-R-FITC (1:200) and α-M-Cy5 (1:50)] and results were documented by CLSM.

3.2.13 VP4 interacts with p68

The next experiments were performed to investigate, if the interaction between VP4 and p68 during IBDV infection could also be shown by immunoprecipitation (IP). Similar to NF45/VP3, p68-FLAG was expressed in DF-1 cells, which were infected with D78. The cellular lysates were applied to mAb FLAG bound to sepharose G. Cellular lysates and products of the IP were analyzed by Western blot. The obtained results showed that only

a very small amount of p68-FLAG was bound to the column and also only very low amounts of VP4 (data not shown). As evidenced earlier during purification of baculovirus expressed p68, the recombinant protein was poorly soluble.

In a second approach, VP4 was expressed in DF-1 cells by transient expression using the recombinant plasmid VP4-pcDNA3. For IP, VP4-pcDNA3 transfected cells were lyzed and prepared lysates were used in IP experiments with mAb VP4 as the capture antibody. VP4 was mostly present in the pellet and not in the cleared lysate indicating that VP4 was also insoluble. In order to obtain a more soluble VP4, the coding sequence of MBP was fused to the VP4 5'-terminus and a FLAG tag encoding sequence was kept at the 3'-terminus resulting in the plasmid MBP-VP4-FLAG-pcDNA3. As a control, a similar plasmid without the VP4 encoding sequence, (MBP-FLAG-pcDNA3) was generated. Transfection of both plasmids in DF-1 cells resulted in expression of the fusion proteins MBP-VP4-FLAG (Figure 34B) and MBP-FLAG (Figure 34A). To document the protein localization, cells were fixed and an IIFA was performed using R-α-p68, ch-α-IBDV, mAb MBP and DAPI, followed by α-R-FITC, α-Ch-Cy3 and α-M-Cy5. In the absence of VP4, the transient expressed MBP-FLAG was localized in the cytoplasm and p68 resided in the nucleus of the same cell (Figure 34A). In cells transfected with MBP-VP4-FLAG-pcDNA3, p68 co-localized with VP4 and MBP in the cellular cytoplasm in dot-like structures additional to its cytoplasmic localization. This showed that although fused on both sides to an artificial amino acid tag, VP4 co-localized with p68 in the cytoplasm. To investigate, if this phenotype was either only a spatial co-localization or was indeed a protein-protein interaction, IP experiments were performed. It needs to be mentioned that this experimental design did not mirror the natural replication cycle, but will result in an indication, if indeed a protein-protein interaction is a possible scenario.

The IP experiments were performed by loading protein G sepharose with mAb His and either incubated with purified p68-His (see 3.2.4) (Figure 34C and D, lane 1 and 3) or left without protein (lane 2).In a next step cleared cellular lysates of DF-1 cells transfected with either MBP-FLAG-pcDNA3 or MBP-VP4-FLAG-pcDNA3 were prepared 24 h pt. The obtained cellular lysates (MBP-VP4-FLAG and MBP-FLAG) were used for incubation with the above described samples. MBP-FLAG was added to protein G/mAb His/p68 (lane1) and MBP-VP4-FLAG was added either to protein G/mAb His (lane 2) or to protein G/mAb His/p68-His (lane 3). The sepharose beads probably containing protein complexes were washed and the obtained pellet was prepared for Western blot experiments using two POD-conjugated antibodies [mAb His POD (Figure 34C) and mAb MBP POD (Figure 34D)] to detect the proteins that have been bound to p68-His. Lysates containing the target proteins MBP-FLAG, MBP-VP4-FLAG and p68-His were analyzed on lane 4, 5 and 6 as expression controls, respectively. The result showed that p68-His was able to bind to MBP-VP4-FLAG (70 kDa, lane 3), but did not precipitate MBP-FLAG (44 kDa, lane 1) indicating a specific binding of soluble VP4 to p68-His. The

absence of p68-His prevented the binding of MBP-VP4-FLAG (land 2), which showed that the presence of mAb His alone was not sufficient to bind MBP-VP4-FLAG. The obtained results strongly evidenced in conjunction with the other results that a direct interaction between p68 and VP4 of IBDV was indeed present in infected cells. Still, this is an *in vitro* binding assay that did not mimic natural conditions and binding of cellular components to VP4 that bridged the binding to p68 was also not ruled out. This approach was chosen due to the insoluble nature of both investigated proteins.

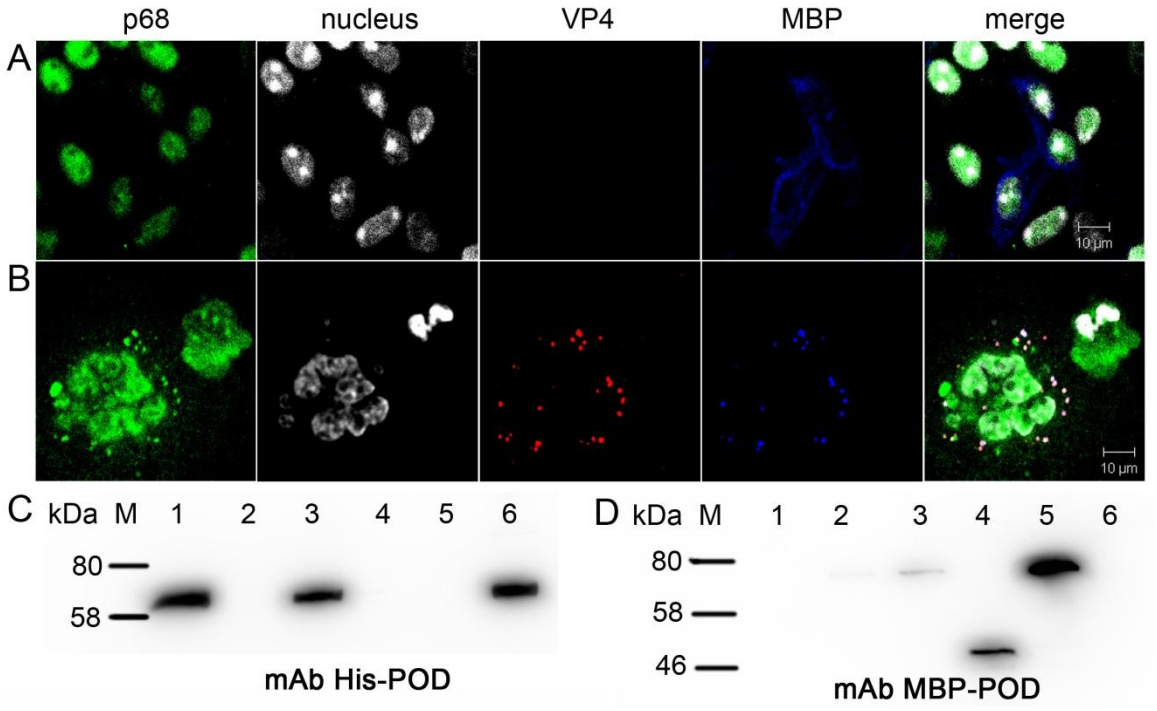

Figure 34: The cellular protein p68 interacts with VP4 employing an artificial approach. Transfection of DF-1 cells with (A) MBP-FLAG-pcDNA3 or (B) MBP-VP4-FLAG-pcDNA3. Cells were fixed with ice cold ethanol 24 h pt and analyzed by IIFA. Cells were incubated with R-α-p68 serum (1:200, green), mAb MBP (1:10,000, blue), ch-α-IBDV to stain VP4 (1:100, red) and DAPI to stain the nucleus (1:50,000, white) and with the appropriate conjugated secondary antibodies [α-R-FITC (1:200), α-M-Cy5 (1:50) and α-Ch-Cy3 (1:5,000)]. The slides were investigated using CLSM. In the lower part of the picture Western blots incubated with either mAb His POD (C) or mAb MBP-POD (D) were shown. Following samples were analyzed in the lanes 1-6: Protein G sepharose was loaded with mAb His (lanes 1-3), washed with the appropriate buffer and two samples were exposed to purified p68-His protein (lane 1 and 3). Lysates of DF-1 cells transfected with MBP-FLAG-pcDNA3 (MBP-FLAG) or MBP-VP4-FLAG-pcDNA3 (MBP-VP4-FLAG) were used to investigate p68-VP4 protein interaction. Following samples were incubated and the precipitated proteins were separated after washing steps by SDS-PAGE followed by Western blot. Lane 1: ProteinG/mAb His/p68-His/MBP-FLAG, lane 2: ProteinG/mAb His/MBP-VP4-FLAG, lane 3: ProteinG/mAb His/p68-His/MBP-VP4-FLAG, lane 4: Lysate of MBP-FLAG-pcDNA3 transfected cells. Lane 5: Lysate of MBP-VP4-FLAG-pcDNA3 transfected cells. Lane 6: Purified p68-His. The Western blot shown in panel C was incubated with mAb His-POD (1:5,000) while panel D was incubated with mAb MBP-POD (1:2,000). On the left side of each gel the molecular weights of marker proteins (M) were indicated.

3.2.14 Biological function of p68 during virus replication

In order to investigate whether the presence of more p68 or the reduction of p68 in IBDV infected cells influenced the virus replication, several experiments were performed to quantify the effect on virus titers in the cell culture supernatants.

3.2.14.1 Overexpression of p68

In first experiments, p68-FLAG was expressed after transfection of p68-FLAG-pcDNA3 in DF-1 cells. As a control, the plasmid pcDNA3 was transfected in parallel. Twenty four hours after transfection, cells were infected with D78 at a moi of 1. Cellular supernatants were harvested 24 and 48 h pi and virus titers were determined. Each experimental setup was performed twice and the second plate was used for analysis by IIFA. These cells were fixed with ethanol and then incubated with mAb FLAG (1:500) and α-M-FITC (1:200) to analyze the transfection efficiency. This assay revealed that nearly all cells were transfected, which allowed the assumption that most transfected cells were also infected. The determined viral titers were summarized in Table 14. Virus titers of the pcDNA3 transfected control cells were 24 h pi slightly higher than the supernatant of cells transfected with p68-FLAG-pcDNA3. The difference increased 48 h pi where in p68-FLAG-pcDNA3 transfected cells the virus titer was reduced in comparison to the pcDNA3 transfected cells.

Table 14: Titers of IBDV influenced by expression of p68-FLAG. DF-1 cells were transfected with the indicated plasmids and infected 24 h pt with the IBDV strain D78 at a moi of 1. The supernatants were harvested at 16 h pi and the $TCID_{50}$/ml was determined.

Plasmids used for transfection	Time after infection	
	24 h	48 h
pcDNA3	$10^{4.25}$	10^{6}
p68-FLAG-pcDNA3	10^{4}	$10^{5.25}$

In a second experiment cells were transfected as described before, but then infected with D78 at a moi of 100. The supernatants were harvested at 0, 12 and 24 h pi and the virus titer was determined (Table 15). At 12 h pi the virus titers of cells transfected with p68-FLAG-pcDNA3 were slightly lower ($10^{4.75}$/ml) than titers of control cells transfected with pcDNA3 alone (10^{5}/ml). This difference increased at 24 h pi again indicating that cells expressing p68-FLAG were inhibiting viral replication. Compared to the viral titers observed during the first experiment (10^{4}/ml), they were higher at 24 h pi ($10^{5.75}$/ml), likely due to the higher moi used for the second experiment of infection.

Table 15: Titers of IBDV influenced by expression of p68-FLAG. DF-1 cells were transfected with the indicated plasmids and infected 24 h pt with the IBDV strain D78 with a moi of 100. The supernatants were harvested at 16 h pi and the $TCID_{50}$/ml was determined.

Plasmids used for transfection	Time after infection		
	0 h	24 h	48 h
pcDNA3	10^{3}	$10^{4.25}$	10^{6}
p68-FLAG-pcDNA3	$10^{2.75}$	10^{4}	$10^{5.25}$

In next experiments it was investigated, if consecutive expression of p68-FLAG would have an influence on IBDV replication. To this end, DF-1 cells were transfected with p68-FLAG-pcDNA3 and one day after transfection the cell culture medium was changed to G418 (400 µg/ml) containing cell culture medium. Cells were kept under selection pressure for several weeks and single colonies were picked and grown in separate wells. To confirm expression of p68-FLAG, a part of the cells were fixed and used for IIFA with mAb FLAG (1:500) and α-M-FITC (1:200). It was observed that all cells expressed a FLAG-tag, which confirmed successful insertion of the p68-FLAG gene into the DF-1 cell genome and expression of p68-FLAG (data not shown) and cells were called DF-1-p68-FLAG. Now the same number of DF-1-p68-FLAG and non-treated DF-1 cells were infected with D78 at a moi of 10 and the supernatants were harvested 16 h pi and the viral titers were determined (experiment 1, Table 16). This experiment was repeated once (experiment 2, Table 16). In both experiments the $TCID_{50}$/ml of D78 replicating in DF-1-p68-FLAG cells were lower than in the control DF-1 cells. Taken together, the IBDV replication was inhibited due to the presence of p68-FLAG irrespective, if p68-FLAG was transiently or consecutively expressed in DF-1 cells.

Table 16: Titers of IBDV influenced by expression of p68-FLAG. DF-1 cells (DF-1) and DF-1 cells consecutively expressing p68-FLAG (DF-1-p68-FLAG) were infected with the IBDV strain D78 at a moi of 10. The supernatants were harvested at 16 h pi and the $TCID_{50}$/ml was determined.

Cells	Experiment 1	Experiment 2
DF-1	$10^{8.75}$	10^{9}
DF-1-p68-FLAG	$10^{8.75}$	$10^{8.25}$

3.2.14.2 Downregulation of p68 by siRNA

Now it was investigated, if downregulation of p68 expression using an siRNA approach would influence IBDV replication. Target sequences for p68 siRNA were selected using the RNAi Target Sequence Selector from Clontech. One target sequence was selected starting in the p68 mRNA at nucleotide 179 (si-179) and the second siRNA started at nucleotide 388 (si-388) (sequences see Table 2). Experiments were carried out similar to the experiments as described for NF45 (see 3.1.15.2). At 48 h pt the presence of p68 was investigated by Western blot analysis. To normalize the analyzed protein, the quantity of β-actin was equalized first (Figure 35A, upper blot). This was performed using mAb β-actin-POD. A parallel blot was prepared using the same amount of sample and analyzed by Western blot using R-α-p68 and α-R-POD (Figure 35A, lower blot). The p68 protein was reduced in cells transfected with si-179 and not as pronounced in si-388 transfected cell cultures (the band specific for p68 was indicated by an arrow). In cell cultures, which have been transfected with both p68-specific siRNAs the reduction of p68 was comparable to the cells transfected with si-179 alone. Quantification of p68 was performed as for NF45.

The results were shown below each lane of the background corrected blot that also shows the polygons used for quantification (Figure 35A, on the right side of the dotted line). Normalized values were compared with expression levels in the sample with si-NP. The expression level of p68 48 h pt was reduced to 40% when si-179 was used, 66% in case of si-388 and 30% when both siRNAs were transfected (Figure 35C).

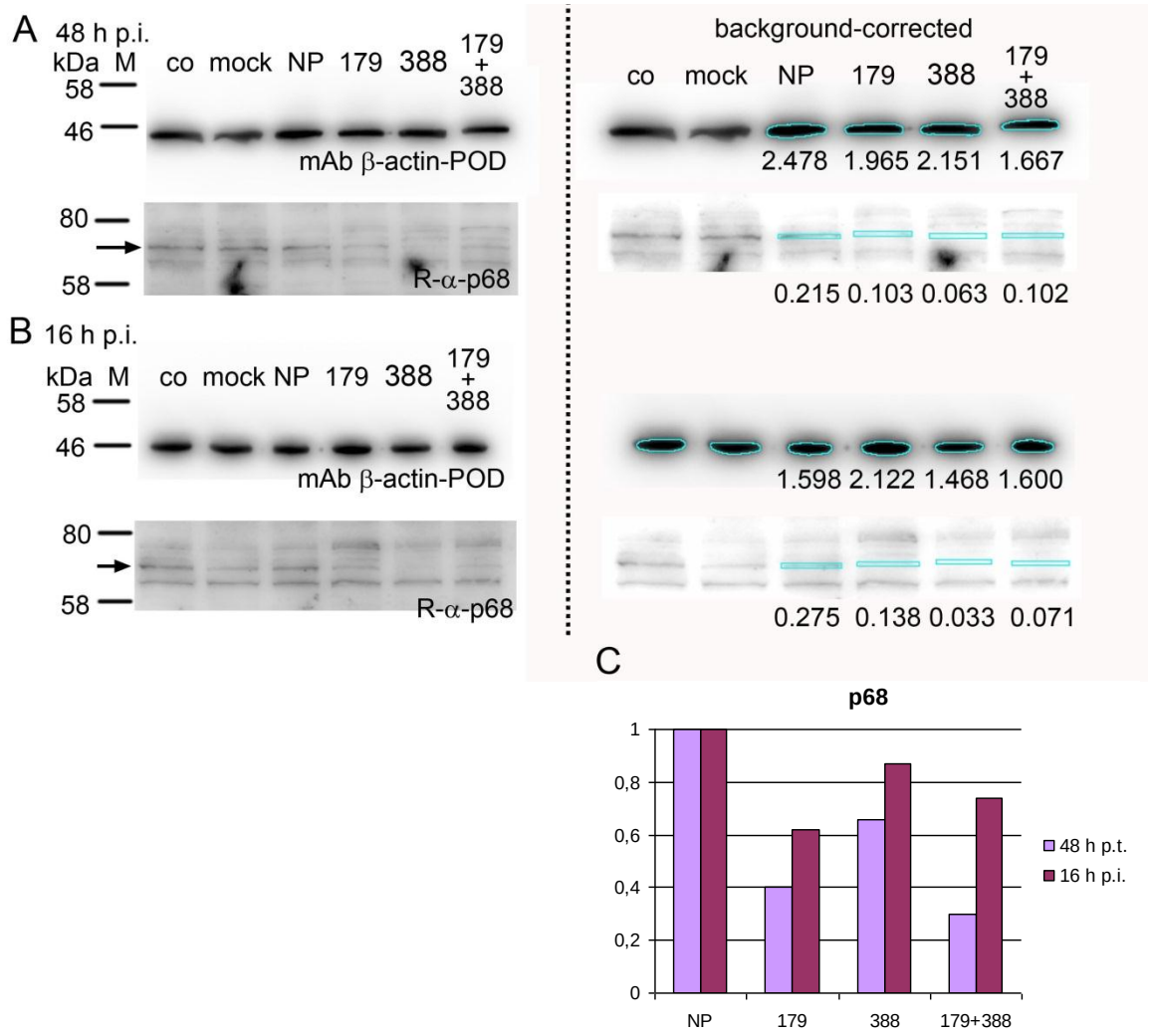

Figure 35: Transfection with p68-specific siRNA downregulated p68 expression. DF-1 cells were transfected with p68-specific siRNA: si-179 (179), si-388 (388) or both together (179+388). Non-transfected DF-1 cells (co), mock-transfected DF1 cells (mock) and DF1 cells transfected with an p68 unspecific, but influenza A virus nucleoprotein-specific siRNA (NP) were used as controls. (A) Expression levels of p68 were analyzed at 48 h pt by Western blot using R-α-p68 (1:1,000) and α-R-POD (1:20,000). The protein amount used for analysis of p68 was adjusted using mAb β-actin-POD (1:25,000). (B) After transfection with siRNAs cells were infected with IBDV strain D78. Sixteen hours after infection cell lysates were prepared and analyzed by Western blot using either mAb β-actin-POD (1:25,000) or R-α-p68 (1:1,000). The binding of the latter antibodies was detected with the conjugate α-R-POD (1:20,000). On the right side of the dashed line were the same blots shown background-corrected and polygons were drawn around the regions quantified by its signal intensity. The numbers below each lane indicated the integrated intensity of the band in arbitrary units.(C) Quantification of siRNA downregulation of p68 normalized to NP siRNA 48 h pt and 16 h pi.

Based on the obtained results, cells were transfected with siRNA, infected with D78 and supernatants were harvested to determine the viral titer and in parallel cells were used for Western blot analysis using mAb β-actin-POD and R-α-p68 and the conjugated antibody α-R-POD (Figure 35B). This revealed that p68 was downregulated 16 h pi or 64 h pt. Again, p68 was quantified on the background-corrected pictures and values of the integrated intensities are shown on the right side of the dotted line in Figure 35B. After infection, p68 is reduced to 62% when using si-179, 87% with si-388 and 74% after transfection of both siRNAs (Figure 35C).

Viral titers of IBDV strain D78 infected cells, which were transfected with either p68-specific siRNA or control siRNA (si-NP), were presented in Table 17. The experiments were conducted four times (experiment 1-4). In each case viral titers in cells transfected with p68-specific siRNA were higher or the same (experiment 4, si-179) as in si-NP transfected cells.

Table 17: Titers of D78/ml determined by $TCID_{50}$ after infection of p68 siRNA transfected cells.

experiment	co	mock	si-NP	si-179	si-388	si-179 + si-388
1	10^{8}	$10^{5.75}$	$10^{5.5}$	$10^{6.25}$	$10^{6.25}$	$10^{7.25}$
2	$10^{5.75}$	$10^{5.25}$	$10^{6.25}$	$10^{6.75}$	10^{7}	$10^{7.25}$
3	$10^{8.5}$	$10^{6.25}$	$10^{7.25}$	$10^{7.75}$	$10^{8.5}$	10^{8}
4	10^{8}	10^{7}	10^{7}	10^{7}	$10^{7.75}$	$10^{7.75}$

3.2.15 Statistical analysis of IBDV titers from p68 downregulated cells

The statistical significance of the difference between titers transfected with si-NP or p68 specific siRNAs was determined by the Wilcoxon rank-sum test. The titers of si-NP transfected cells were tested against the si-185, si-551 and si-185+si-551 (Table 10). For si-179 (p=0.055) no significant reduction was determined, but for si-388 (p=0.034) and both together (p=0.034) titers were significantly different from viral titers of cells transfected with non-specific si-NP. This means that downregulation of chicken p68 expression as observed by Western blot analysis enhances replication of IBDV strain D78 significantly in DF-1 cells.

4 Discussion

After the discovery of viruses, initially all viral components were in the center of research. But due to the nature of viruses to use cellular components for their own replication and an increased knowledge about cellular mechanisms, virus-host interactions became a major target of virus research. Discoveries in cellular biology paved the way for this research due to the development of tools for the detection of cellular components. Findings in this area of viral research will certainly help in the future and already supported the development of antiviral substances. Also, the ability of a number of viruses to escape the host antiviral immune system was and will be a very interesting and important component of virus research. Interestingly, for certain dsRNA binding proteins such as NF90, NF110, Staufen, PKR, p68, DDX3 and NF45, interactions with components of different viruses were already described. These viruses belong to different virus families and consequently have different replication mechanisms and do not share a common nucleotide sequence. Instead, a number of viruses share secondary structures like IRES (*Flaviviridae, Picornaviridae*) or their RNA forms loop structures during their replication like HIV. Others possess a DNA genome and form RNA intermediates during their replication (Hepatitis B virus, *Adenoviridae*), which have been shown to interact with cellular factors. Especially the NFAR proteins activated transcription of viral RNA by interacting with the promoter region of certain members of the *Flaviviridae* (Isken *et al* 2003, Gomila *et al* 2011). Additionally to protein-viral RNA interactions, several protein-protein interactions have been detected, for example between NS1 of influenza A virus and human Staufen protein as well as RHA, between NS5A of HCV and NF90 and between HCV core protein and NF45 (Falcón *et al* 1999, Lin *et* al 2012, Isken *et al* 2007, Lee *et al* 2011). It has been shown that such interactions were able to either increase replication levels of different viruses (HCV, SARS-CoV) or serve in the concert of the antiviral immune system to decrease replication efficiency (VSV, rhinovirus) (Isken *et al* 2003, Goh *et al* 2004, Chen *et al* 2009, Pfeifer *et al* 2008, Balachandran *et al* 2000, Merrill *et al* 2006, Merrill & Gromeier 2006). Interestingly, HIV replication was activated by RHA or DDX3, but also inhibited by NF90 (Fujii *et al* 2001, Yedavalli *et* al 2004, Urcuqui-Inchima *et al* 2006). Similarly, downregulation of PKR expression by siRNA increased the virulence of influenza A virus, but the decrease of Staufen expression by siRNA decreased viral titers of influenza A virus (Balachandran *et al* 2000, De Lucas *et al* 2010). Cellular nuclear proteins changed their localization within the cell during viral replication to the cytoplasm. This has been described for NFAR proteins and DDX3, which co-localized with viral proteins during HCV replication, Staufen co-localized with NS1 of influenza A virus, NF90 was observed in the cytoplasm of dengue virus infected cells and RHA was observed in the cytoplasm during retroviral replication (Isken *et al* 2007, Lee *et* al 2011, Owsianka & Patel 1999, Falcón *et al* 1999,

Gomila *et al* 2011, Tang *et al* 1997). If more viruses were investigated for the ability of their components to interact with cellular factors, it is most likely that more virus-host interactions will be detected. Another fact emphasized the importance of these host proteins. They are highly conserved throughout different species of mammals, bird, fish and to a lesser extend to insects, exemplarily shown on NF45 and p68 (see Table 6, Table 12, Lin *et al* 2006, Cui *et al* 2011, Seufert *et al* 2000).

Research has been described on viral components of IBDV, but only few reports have been published about virus-host interactions. Usually a good method to detect such interactions is a global screening, which has been described for the IBDV RNA-polymerase VP1 as bait employing a yeast two hybrid system (Tacken *et al* 2004). This revealed an interaction of VP1 with only the C-terminus of eukaryotic initiation factor 4AII, but not with the full length eIF4AII. A yeast two hybrid screen with the HCV core protein as a bait detected an interaction with the cellular helicase DDX3 (Owsianka & Patel 1999) showing that this method was generally useful for an initial screening. Another possibility is the expression of an ectopic protein with a fusion tag, by which it is precipitated and co-precipitates interacting proteins that can be identified by MS-MS. This method has been applied to HCV core protein and revealed an interaction with NF45 amongst others (Lee *et al* 2011). Several studies have been conducted to determine the cellular receptor for IBDV. Possible candidates to act as cellular receptors were mostly described by their molecular weight, for example 40 and 46 kDa proteins (Nieper & Müller 1996), 70, 80 and 110 kDa proteins (Ogawa *et al* 1998) and 62, 68 and 72 kDa proteins (Lin *et al* 2007). Unfortunately, the identity of these proteins has not been further characterized.

The aim of this work was to investigate, if IBDV proteins interact with cellular proteins of the large family of dsRNA binding proteins, for which it has been described that they interact with components of other viruses. Once such an interaction has been discovered, this virus-host interaction was characterized in initial studies. For this purpose, the coding regions of the chicken protein NF45 and p68 were amplified and sequenced. Both proteins were generated as recombinant proteins containing a 6x-His tag encoding sequence on their C-terminus for subsequent purification. The purified proteins were used for generation of specific sera against the chicken proteins in rabbits. In initial investigations a change of localization was detected for chicken NF45 and p68 after IBDV infection. The nuclear proteins accumulated in the cytoplasm during infection and co-localized with viral proteins. After IBDV infection of CEC the transcription levels of NF45 and p68 did not increase as observed by Northern Blots (Figure 4 and Figure 23). The level of Mx mRNA after IBDV infection was used as a control, because an increase of Mx mRNA after IBDV infection was previously described (Mundt 2007). Two bands of NF45 specific RNA were detected, which might explain the two bands of exogenous expressed NF45-FLAG and NF45-His detected by Western blot with NF45

specific serum and a monoclonal antibody directed against the 6x-His tag (Figure 5, Figure 19, Figure 20). For several cellular mRNAs an increase has been described after IBDV infection. These proteins belonged to the cytoskeleton, the lipoprotein metabolism, the ubiquitin-proteasome pathway, macromolecular biosynthesis and of course to proteins of the stress response, but no dsRNA binding proteins were described (Zheng *et al* 2008). In fish, RNA levels of NF45 were increased after infection *in vivo*, but not *in vitro* (Cui *et al* 2011). This group further postulated that the expression level of NF45 in fish correlates with the degree of pathogenicity based on viral and bacterial infection studies - the higher the pathogenicity, the more NF45 was expressed. Most infection experiments with chicken cells described here were conducted with the IBDV vaccine strain D78, which belongs to the group of vaccines with intermediate pathogenicity. It is possible that either this strain lost pathogenic properties due to cell culture attenuation that caused upregulation of NF45 transcription or, since cell culture is an *in vitro* system, no upregulation of NF45 mRNA was observed as it was described by Cui *et al* (2011) for fish NF45. One of the first studies on transcriptional activity of the NF90-NF45 complex showed no NF45 or NF90 mRNA upregulation in T cells stimulated with ionomycin and PMA (Kao *et al* 1994). Neither transcription nor translation was upregulated resulting in unchanged protein levels of NF45 and NF90 in PMA/ionomycin activated T cells. Later it was described that NF45 serine phosphorylation levels increased, indicating again a regulatory role for NF45 (Kiesler *et al* 2010) without changing the amount of NF45. The cell uses energy to constitutively express NF45. In case of an infection, NF45 can be quickly phosphorylated and likely immediately induce changes of downstream located cellular processes like initiation of transcription, which is faster than transcription and translation of NF45 itself. This additionally indicates that further messenger proteins need to be present in the cell, which phosphorylate NF45 and induce the activation of an appropriate kinase.

NF45-His and p68-His were both heterologously expressed in an insect cell system and purified by using their 6x-His tags (Figure 5, Figure 24). A double band of NF45-His was observed in both, protein stained gel and also by Western blot using mAb His (Figure 5). The upper band (higher molecular weight) was identified as the complete NF45-His protein, the lower band was truncated by an N-terminal peptide. Both forms might also be present naturally, because Northern blot results showed a double banded RNA pattern specific for NF45 (Figure 4). It is possible that a later start codon was used, for example methionine at aa position 33, which would result in a protein with a molecular weight of 39 kDa, which approximately fits to the observed molecular weight of the band. Still, this does not explain two different mRNAs detected in the Northern blot. The possibility cannot be excluded that isoforms exists due to a different exon usage resulting in various sizes as described for NF90 (Duchange *et al* 2000).

Although the eluates of NF45 and p68 did not show other bands in the protein stained gel, more bands appeared after concentration of the proteins (data not shown). It was tried to further purify the proteins with size exclusion columns, but this did not decrease the amount of proteins with higher or lower apparent molecular weight. The proteins were used in this quality for inoculation of rabbits to obtain protein specific sera against NF45 (R-α-NF45) or p68 (R-α-p68). Therefore it is not surprising that the sera detected additional proteins in Western blots of cellular lysates of different cell lines (Figure 6A, Figure 25A). Comparing both sera, R-α-NF45 serum showed less unspecific bands than R-α-p68. Regarding the intensity of the likely specific and unrelated bands, the NF45 specific band was the brightest using R-α-NF45 serum. But with the R-α-p68 serum, p68 was not in all investigated cell lines the band with the strongest signal, for example in lysates of QM-7 cells. There was one band, which was as strong as the p68 specific signal. The properties of the antisera required additional sets of experiments. Use of exogenously expressed proteins (NF45-FLAG and p68-FLAG) showed unambiguously that for the FLAG-tagged proteins the signal of mAb FLAG and the specific serum co-localized (Figure 6B, Figure 25C). When NF45 was exogenously expressed in 293T cells, it only localized in the cytoplasm unlike its endogenous counterpart (Figure 6B). Its interaction partner NF90 localized in the nucleus after overexpression of NF90 or NF90 with NF45 in 293T cells, but the localization of NF45 itself was not determined (Sakamoto *et al* 2009). Exogenous expressed p68-FLAG was observed in the nucleus of BHK-21 cells, like the endogenous protein (Figure 25C). A possible explanation for this phenotype is the species barrier that did not allow nuclear import, if the protein does not encode for the species specific import signal. The nuclear import mechanism in 293T cells of human origin obviously did not recognize a potential nuclear import signal encoded in chicken NF45. In contrast to this, the chicken p68 was imported into the nucleus of BHK-21 cells, which were derived from hamster kidney cells.

The nucleus/cytoplasm ratios of NF45 and p68 were determined in non-infected DF-1 cells, which were 88%/12% and 90%/10%, respectively (Figure 8, Figure 27). This was in agreement with previous reports showing NF45 in the nucleus of several human and fish cell lines and p68 with nuclear localization in human cells (Kao *et al* 1994, Cui *et al* 2011, Aoki *et al* 1998, Goh *et al* 2004, Jorba *et al* 2008). This was the first time that the localization of NF45 and p68 was determined in chicken cells. In IBDV infected cells the amount of protein increased in the cytoplasm, which consequently changed the appropriate ratio. In average 64% of NF45 and 62% of p68 was present in the nucleus 12 h pi when infected with IBDV strain D78, which was a decrease of approximately a quarter of the total protein in infected cells (Figure 9, Figure 28). Accumulation of these proteins in the cytoplasm was time dependent and needed eight hours until it reached a steady state (Figure 12, Figure 14, Figure 30, Figure 31). Although all pictures with infected cells were analyzed, the number of cells was too small to extrapolate

representative data, but still indicated a trend. It needs to be mentioned that the quantification was initiated after the investigations were finalized. While the proteins accumulated in the cytoplasm, they co-localized with viral proteins, NF45 with VP1, VP2 and VP3 and p68 co-localized only with VP4 (Figure 7, Figure 9, Figure 10, Figure 26, Figure 28, Stricker *et al* 2010). The first mentioned complex (NF45/VP3/VP1) localized in dot-like structures. These structures might function as a replication complex since VP1 and VP3 were present. The p68/VP4 complexes were observed as tubular structures as previously described for VP4 (Granzow *et al* 1997). It is likely that these tubular structures observed by electron microscopy might contain at least two components, VP4 and p68. Earlier attempts to purify the VP4 containing tubular structures by ultracentrifugation using cesium chloride gradients failed (Dr. E. Mundt, personal communication). Thus, other approaches might be worthwhile to try in future experiments (e.g. affinity chromatography, glycerol gradients) to investigate the true nature of these structures. Interestingly, both protein complexes (NF45/VP3/VP1 and p68/VP4) localized mutually exclusive in the cytoplasm although the natural localization of both proteins (NF45 and p68) were in the nucleus of the cell. The helicase of SARS-CoV needed p68 as a cofactor to promote viral replication (Chen *et al* 2009). It would have been possible that the RNA-dependent RNA polymerase VP1 of IBDV needed p68 as a cofactor for replication as well, but this is unlikely since p68 co-localized exclusively with VP4, but not with VP3 or VP1 (Figure 26), which are both important for viral replication.

The IBDV protein VP4 was first detected 4 h pi, but VP3 was first detected 6 h pi (Figure 12, Figure 30). This is likely due to the sensitivity of the used antibodies specific for VP3 and VP4 since both proteins are expressed in the polyprotein of IBDV at the same time. Others observed IBDV antigen in cell culture earliest 6 h pi when using serum generated against preparations of whole IBDV particles, which might not detect the viral protease VP4 as it was assumed that it is not part of the virus particle (Lukert & Davis 1974, Granzow *et al* 1997). Interestingly p68 was observed in an accumulated form earlier in the cytoplasm than NF45 (Figure 12, Figure 30). One possible explanation for this phenotype is that the formation of tubular structures (p68/VP4) occurred first since the protease in its functional form acted first to release VP3 which in turn induced together with VP1 the viral replication. The latter process itself activated the co-localization of NF45 to the replication complex. These conclusions are of hypothetical nature, but could serve as an interesting starting point for further investigations.

Co-localization of NF45 with VP3 and p68 with VP4 was cell line independent as shown in DF-1, QM-7 and Vero cells (Figure 10, Figure 26). IBDV infection leads to IFN production *in vivo*, *in vitro* and *in ovo* (Gelb *et al* 1979a, Gelb *et al* 1979c). Vero cells lack the ability to express IFN α and β due to a chromosomal deletion (Mosca & Pitha 1986, Diaz *et al* 1988). Based on this phenotype of Vero cells it can be concluded that both

co-localizations were independent of the expression of IFN regulated genes. This is an important finding, because it means that the origin of the changed location of the investigated proteins was not due to the activation of the cellular antiviral response by IFN (see 1.2.1.1), but does not exclude the possibility that PKR was solely activated by dsRNA, which activated the NF90-NF45 complex.

DF-1 cells have been infected with IBDV variant strains of the subtype E/Del (8903) and GLS (GLS-05) resulting in the same pattern of NF45 and p68 (Figure 11, Figure 29), which showed a strain independency of the co-localization of cellular proteins with viral proteins in the cytoplasm. Interestingly, nucleic acid co-localized with NF45 in cells infected with the variant strains as observed by propidium iodide staining, which is most likely viral RNA (Figure 11). This staining was most intense after infection with variant strains, but was sometimes also observed after infection with the IBDV vaccine strain D78. Some evidence has been provided that the virulence of IBDV was modulated by the replication efficiency of VP1 *in vivo* (Liu & Vakharia 2004) and VP1 of serotype I was more active than VP1 of serotype II (Zierenberg *et al* 2004). The higher accumulation of viral RNA might be the result of a higher replication rate of the IBDV variant strains compared with classical IBDV.

To determine the minimum of viral components required for localization of cellular proteins in the cytoplasm, the necessary viral elements were analyzed by transfection experiments providing only few components of the virus (proteins and/or regulatory RNA elements). Neither simultaneous expression of VP1 or VP3, nor transfection of cRNA of segment A alone induced a clear cytoplasmic localization of NF45 (Figure 13, Figure 15). Transfection of the VP3 minigenome containing the 5' as well as the 3' NTR along with the coding region of VP3 in combination with cRNA of segment B led to the presence of low amounts of NF45 in the cytoplasm, which did not co-localize with the viral components VP1 and VP3 (Figure 16). As a positive control both complete IBDV segments were transfected as cRNA, which resulted in small amounts of NF45 in the cytoplasm, which co-localized with VP1 and VP3 (Figure 17). Possibly not only replication was an important stimulus for concentrated localization of NF45 in the cytoplasm. One explanation for this phenotype is that additional processes were needed such as the viral infection process itself, for example attachment to the receptor or penetration, which possibly stimulated so far unknown components of the innate immune system. It can be concluded that for the presence of NF45 in the cytoplasm at least the replication process was necessary. Similarly, the HCV protein NS5A forms only a stable interaction with NF90, when a functional replication complex was present (Isken *et al* 2007).

Unlike NF45, p68 was present in the cytoplasm only after expression of its co-localization partner VP4, regardless, if it was expressed as an active or inactive protease (S652R), as part of the complete segment A after transfection of cRNA or in

combination with the NCRs of segment A in a VP4 minigenome construct (Figure 32). When cRNA of the complete segment A was transfected encoding for the inactive protease, the VP4 signal was observed, but it was not co-localized with p68. An explanation for this phenotype could be that for co-localization of p68 with VP4 only the free form of VP4 was needed to be present in the cytoplasm. Another explanation is that VP2 and VP3 sterically blocked the interaction site between VP4 and p68, because they were still attached to VP4.

The concentrated presence of NF45 and p68 in the cytoplasm raised the question about the mechanism of these phenotypes. Experiments were designed to investigate two possible mechanisms: i) the proteins were actively exported by the nuclear export system ii) the proteins were held back in the cytoplasm after their translation. For the nuclear export of proteins they need to contain a hydrophobic NES containing leucins and isoleucins. The NES binds to the nuclear export receptor CRM1, which transports the target protein in a GTP-dependent manner to the cytoplasm. CRM1 can be inhibited by leptomycin B (LMB), an antifungal substance produced in *Streptomyces* species. Two possible NES were predicted in the leucin-rich NF45, but none for p68 (3.1.13, 3.2.12). Both proteins were observed in the cytoplasm after infection although the CRM1 dependent nuclear export pathway was blocked with LMB (Figure 18, Figure 33). Influenza virus proteins M1 and NP were used as a positive control, because it was previously described that their export was inhibited by LMB (Ma *et al* 2001). It was also described that the influenza A virus polymerase proteins PA, PB1 and PB2 interacted with DDX3 in the cytoplasm (Jorba *et al* 2008) and for DDX3 it was shown that it interacted with CRM1, which allowed the nucleo-cytoplasmic shuttling (Yedavalli *et al* 2004). NF45 and p68 were not exported by the CRM1 pathway, although it cannot be ruled out that other nuclear export systems were used. DsRNA binding proteins containing a DRBD like NF110, a direct interaction partner of NF45, was exported by exportin-5 in a LMB-insensitive manner (Guan *et al* 2008, Brownawell & Macara 2002). NF45 has not been detected as a direct interaction partner of exportin-5 in a yeast two hybrid screening (Brownawell & Macara 2002). The presented data strongly supported the fact, but does not entirely validate, that both proteins (NF45 and p68) were retained in the cytoplasm after translation rather than being exported out of the nucleus. A possibility, why NF45 and p68 accumulated in the cytoplasm, is that VP3 for NF45 and VP4 for p68 blocked a putative NLS within the cellular proteins and prevented them from shuttling into the nucleus.

The presence of co-localized proteins detected by indirect immunofluorescence does not necessarily mean that these proteins physically interact. The next experiments employing IP showed that VP3 (Figure 19) and also VP1 (Stricker *et al* 2010) were precipitated after overexpression of NF45-FLAG and subsequent IBDV infection of transfected cells. Whether NF45 interacted with VP3 or VP1 was not resolved. But due

to the exogenous expression of the recombinant protein it is likely that a direct interaction existed.

The NF45-VP3 interaction was still observed after incubation with RNases specific for ssRNA and dsRNA, concluding that the interaction was likely not bridged by RNA (Figure 20). The protein-protein interaction seemed to be even stronger after RNase digestion, but this conclusion is rather of hypothetical nature. Still, this finding could indicate that RNA blocks the interaction site of either NF45 or the ribonucleoprotein VP3, which covers the viral genome (Luque *et al* 2009b). This would suggest that NF45 and dsRNA compete for the VP3 binding site. It is not proven that NF45 and VP3 directly interacted, because VP1 could be also a binding partner for NF45. Both viral proteins (VP1 and VP3) showed affinity to viral RNA. In cellular systems without viral infection NF45 was shown to be the regulator that does not bind RNA, whereas NF90 was the mediator of transcriptional activation that bound directly to the RNA (Reichman *et al* 2002). It is also possible that either NF45-VP3 or NF45-VP1 interaction was bridged by another protein like NF90, which would explain the small amount of co-precipitated protein. Similar to these results it was shown that NF45 interacted with HCV core protein. Unlike the observed NF45-VP3 binding, the NF45-core protein interaction was RNA-dependent (Lee *et al* 2011).

The IP experiments regarding p68 turned out to be not as straightforward as it was for NF45. The FLAG-tagged p68 was very poorly soluble and did not bind to protein G sepharose beads, which were loaded with mAb FLAG (data not shown). Similarly, VP4 was poorly soluble after overexpression and no protein was bound to protein G sepharose beads loaded with a mAb against VP4. To make these proteins more accessible to IP, both proteins needed to become more soluble. The viral protein VP4 was tagged N-terminal with a MBP tag, which has a higher molecular weight than VP4 itself, and C-terminal with the FLAG tag. The expressed recombinant protein co-localized with p68 in the cytoplasm of DF-1 cells (Figure 34B). Next, purified p68-His was added to the mAb His loaded sepharose column and a cellular lysate containing MBP-VP4-FLAG protein was added. Only with this partially *in vitro* binding assay interaction of p68 and VP4 was shown (Figure 34D). Since exogenous expressed MBP-VP4-FLAG co-localized with endogenous p68 in cells, probably several p68 binding sites in VP4 molecules were blocked by endogenous p68. This would reduce the protein amount that would be accessible to p68-His bound to the column. Although this system was partially *in vitro* it was the only approach to show an interaction between VP4 and p68. Whether other cellular factors were involved cannot be excluded since recombinant VP4 was expressed in cells and possibly could have interacted there with other cellular proteins.

Several ways were attempted to investigate the biological function of the NF45-VP3 or NF45-VP1 and p68-VP4 interaction, which was either overexpression or down-regulation

of the cellular protein expression. Further infection of these cells was conducted and viral titers were compared with control cells. To overexpress the proteins, transient transfections as well as stable cell lines were prepared and infected with variable amounts of virus (moi= 1 or 100) and titers were analyzed at 12, 24 and 48 h pi. In most cases overexpression of NF45 or p68 resulted in lower titers of the virus (Table 7, Table 8, Table 14, Table 15). Although the differences of viral titers between cells overexpressing the target protein were very low, the results were mostly consistent and indicated a trend. The problem with transfections for transient expression was that either not all cells were transfected or not all transfected cells were infected. The resulting titers were therefore a mixture of virus progeny from cells with exogenous overexpressed proteins (either NF45 or p68) and from not-transfected cells. The amount of virus used for infection did not result in highly different titers, because even at high moi only a limited number of cells was infected and supported viral replication as has been described before (Hirai *et al* 1979, Müller 1986). The problem with transient expression in transfected cells was tried to overcome by generation of recombinant cells, which constitutively expressed the protein of interest. Another problem surfaced that these recombinant cells might have a different dividing rate than the naïve control cells, which itself resulted in a different number of infected cells. Viral titers might still not be comparable between two experiments, likely because of the unequal number of cells. After successful generation of a NF45 and a p68 expressing DF-1 cell lines, viral titers of these cells were generally lower than after infection of parental DF-1 cells (Table 9, Table 16).

Based on these results and to support or reject the previous findings as described above, siRNA approaches were used for specific downregulation of NF45 and p68 expression. For each coding region two specific target sequences were chosen to generate siRNA. Only 60% of total NF45 was present in cytoplasmic extracts of siRNA treated cells in comparison to cells transfected with a non-specific siRNA. Similarly, p68 was reduced by 30 to 60% depending on the siRNA used (Figure 22, Figure 35). Cells transfected with siRNA were infected with IBDV and viral titers were quantified. The viral titers increased significantly in NF45-siRNA as well as p68-siRNA transfected cells as determined with the Wilcoxon rank-sum test (Table 10, Table 11, 3.1.16, Table 17, 3.2.15) in comparison to the non-specific siRNA control. Based on the performed experiments it can be concluded that both cellular proteins (NF45 and p68) were negative regulators of IBDV replication. Both dsRNA binding proteins likely served as antiviral response elements of the cell. In contrast, for VSV it was described that NF45 supported viral replication and siRNA specific for NF45 resulted in lower VSV titers (Harashima *et al* 2010). NF45 does not seem to have a general function during viral replication. It is likely that the mechanism depends on the virus and its replication mechanism. Either it was supporting viral replication as described for VSV, which

contained a negative-oriented ssRNA genome, or it acted as part of the antiviral defense response as shown here for IBDV. In case of IRES containing viruses HCV and BVDV of the family *Flaviviridae*, NF45, NF90 and RHA were needed as cofactors to mediate interaction with the 40S subunit of ribosomes (Isken *et al* 2007). All three proteins bound to the 3' and 5' NTR of the virus (Isken *et al* 2003). It is not surprising that expression of these proteins resulted in higher virus titers (Isken *et al* 2007). Similarly, NF90 was described as a positive regulator of dengue virus replication (Gomila *et al* 2011). In the context of IBDV replication, NF45 did not seem to bind to viral RNA, but rather to viral proteins. It should be pointed out that NF45 is part of a large complex of cellular proteins and looking only at NF45 will not explain the complete picture of viral-cellular interactions and pathways (Guan *et al* 2008). In this context it is very unfortunate that no antibodies existed that were able to detect chicken NF90, because NF90 is a well-known interaction partner of NF45. They are mostly detected as a heterodimer, but not as a monomer (Merrill & Gromeier 2006). It has also been reported that the heterodimer NF45/NF90 acted only in human as a transcriptional activator, but not in mice (Kiesler *et al* 2010). Therefore its function as an activator for transcription in chicken needs to be explored. The role of chicken NF45 and p68 during IBDV infection seemed to be in the context of the cellular antiviral response and it is very likely that they are not the only mediators, but are part of a complex cellular antiviral network. Both proteins resided under natural conditions mainly in the nucleus and were recruited by an IFN independent pathway to the cytoplasm and interacted there with viral proteins. After six hours, p68 co-localized with VP4 and two hours later NF45 with VP3. It is not possible to distinguish, if p68 was involved in NF45 recruitment to the cytoplasm, or if these were two independent antiviral pathways.

The initial hypothesis that these cellular proteins might be involved in IBDV replication was not confirmed. IBDV is a rather small virus encoding for only five different viral proteins, of which only four were necessary for viral replication (Mundt *et al* 1997). Therefore it was not unlikely that the virus needed cellular support during replication and it is likely that other cellular proteins like chaperones are utilized for its replication process. Replication mediated by VP1 seemed to be independent of cellular proteins, because the RNA-dependent RNA-polymerase function of VP1 was shown in an *in vitro* system with the sole addition of ions and nucleotides (Von Einem *et al* 2004).

In the future it will be interesting to investigate the detected protein interactions in more detail. The exact interaction domains could be mapped with mutated or truncated proteins. As soon as the exact chicken NF90 sequence is determined and an appropriate serum is generated, it will be interesting to find out, if NF90 is part of the NF45-VP3 or NF45-VP1 complex. It is also possible that even more cellular proteins are involved in viral replication. This could be approached by pull down assays using VP3 as a target and the possibly co-purified proteins could be detected by stained gels after

SDS-PAGE and identified by MALDI-TOF MS-MS. All experiments of this work have been done in cell culture, which is an artificial system. It would be interesting, if p68 and NF45 have antiviral functions *in vivo*, too. For this, transgenic chickens would be needed that overexpress one of the cellular proteins. The generation of transgenic chickens is work intense and it is very questionable, if embryos will survive, because the proteins are very likely involved in more than just antiviral response and this treatment might disorder cellular pathways. It is possible that chicken might survive IBDV infection without immunosuppression or might not show any symptoms at all due to a decreased viral replication efficiency, which would give the viral host an advantage to develop anti-viral responses. On the other hand, viruses like the avian coronaviruses might replicate even better, which might cause even more problems to the poultry industry as it does in the current situation with the different avian bronchitis virus serotypes circulating in the field. This could be a scenario since it has been shown that SARS-CoV replicated even better in cells overexpressing for example p68, because p68 is known as a co-activator for the SARS-CoV helicase (Chen *et al* 2009).

As mentioned earlier, there is a possibility that more chicken viruses interact with NF45 or p68, for example avian influenza virus, because an interaction between the polymerase PB1, PB2 and PA of human influenza virus and p68 is known (Jorba *et al* 2008). There is a probability that proteins of infectious pancreatic necrosis virus (IPNV), a member of the family *Birnaviridae*, in which also IBDV is grouped, interacts with NF45 and p68, because the amino acid sequences from *G. gallus* and *S. salar* were highly conserved (NF45: 91%; p68: 71%) (Table 6, Table 12). Also, expression of NF45 was observed in several fish tissues (Lin *et al* 2006).

In summary, the presented data demonstrated that chicken proteins NF45 and p68 interacted with VP3 and VP4 of IBDV, respectively. The appropriate protein pairs co-localized in cells in a cell line-independent, virus strain-independent, IFN-independent and time-dependent mechanism. The biological function of these cellular proteins seemed to be part of the innate antiviral response system in chicken cells.

5 References

Abdelhaleem, M. (2005) RNA helicases: regulators of differentiation. *Clin Biochem.* 38(6):499-503. Review.

Adelmann, H.B. (1942). The Embryological Treatises of Hieronymus Fabricius of Aquapendente, Vol. 1, Cornell Univ. Press, Ithaca, NY.

Alexopoulou, L., Holt, A.C., Medzhitov, R. & Flavell, R.A. (2001) Recognition of double-stranded RNA and activation of NF-kappaB by Toll-like receptor 3. Nature. 413(6857):732-738.

Anderson, W.I., Reid, W.M., Lukert, P.D. & Fletcher, O.J. Jr. (1977) Influence of infectious bursal disease on the development of immunity to Eimeria tenella. *Avian Dis.* 21(4):637-641.

Allan, W.H., Faragher, J.T. & Cullen, G.A. (1972) Immunosuppression by the infectious bursal agent in chickens immunised against Newcastle disease. *Vet Rec.* 29;90(18):511-512.

Aoki, Y., Zhao, G., Qiu, D., Shi, L. & Kao, P.N. (1998) CsA-sensitive purine-box transcriptional regulator in bronchial epithelial cells contains NF45, NF90, and Ku. *Am J Physiol.* 275(6 Pt 1):L1164-1172.

Askjaer, P., Jensen, T.H., Nilsson, J., Englmeier, L. & Kjems, J. (1998) The specificity of the CRM1-Rev nuclear export signal interaction is mediated by RanGTP. *J Biol Chem.* 273(50):33414-33422.

Azad, A.A. & Deacon, N.J. (1980) The 3'-terminal primary structure of five eukaryotic 18S rRNAs determined by the direct chemical method of sequencing. The highly conserved sequences include an invariant region complementary to eukaryotic 5S rRNA. *Nucleic Acids Res.* 8(19):4365-4376.

Azad, A.A., Jagadish, M.N., Brown, M.A. & Hudson, P.J. (1987) Deletion mapping and expression in Escherichia coli of the large genomic segment of a birnavirus. *Virology* 161(1):145-152.

Balachandran, S., Roberts, P.C., Brown, L.E., Truong, H., Pattnaik, A.K., Archer, D.R. & Barber, G.N. (2000) Essential role for the dsRNA-dependent protein kinase PKR in innate immunity to viral infection. *Immunity.* 13(1):129-141.

Banda, A., Villegas, P. & El-Attrache, J. (2003) Molecular characterization of infectious bursal disease virus from commercial poultry in the United States and Latin America. *Avian Dis.* 47(1):87-95.

Banda, A. & Villegas, P. (2004) Genetic characterization of very virulent infectious bursal disease viruses from Latin America. *Avian Dis.* 48(3):540-549.

Bates GJ, Nicol SM, Wilson BJ, Jacobs AM, Bourdon JC, Wardrop J, Gregory DJ, Lane DP, Perkins, N.D. & Fuller-Pace, F.V. (2005) The DEAD box protein p68: a novel transcriptional coactivator of the p53 tumour suppressor. *EMBO J.* 24(3):543-553.

Bayliss, C.D., Spies, U., Shaw, K., Peters, R.W., Papageorgiou, A., Müller, H. & Boursnell, M.E. (1990) A comparison of the sequences of segment A of four infectious bursal disease virus strains and identification of a variable region in VP2. *J Gen Virol.* 71 (Pt 6):1303-1312.

Becht, H. (1980) Infectious bursal disease virus. *Curr Top Microbiol Immunol.* 90:107-121. Review.

Benton, W.J., Cover, M.S. & Rosenberger, J.K. (1967a) Studies on the transmission of the infectious bursal agent (IBA) of chickens. *Avian Dis.* 11(3), 430-438.

Benton, W.J., Cover, M.S., Rosenberger, J.K. & Lake R.S. (1967b) Physicochemical properties of the infectious bursal agent (IBA). *Avian Dis.* 11(3):438-445.

Birghan, C., Mundt, E. & Gorbalenya, A.E. (2000) A non-canonical lon proteinase lacking the ATPase domain employs the ser-Lys catalytic dyad to exercise broad control over the life cycle of a double-stranded RNA virus. *EMBO J.* 19(1):114-123.

Bogerd, H.P., Fridell, R.A., Benson, R.E., Hua, J. & Cullen, B.R. (1996) Protein sequence requirements for function of the human T-cell leukemia virus type 1 Rex nuclear export signal delineated by a novel in vivo randomization-selection assay. *Mol Cell Biol.*16(8):4207-4214.

Boot, H.J., ter Huurne, A.A., Hoekman, A.J., Peeters, B.P. & Gielkens, A.L. (2000) Rescue of very virulent and mosaic infectious bursal disease virus from cloned cDNA: VP2 is not the sole determinant of the very virulent phenotype. *J Virol.* 74(15):6701-6711.

Böttcher, B., Kiselev, N.A., Stel'Mashchuk, V.Y., Perevozchikova, N.A., Borisov, A.V. & Crowther, R.A. (1997) Three-dimensional structure of infectious bursal disease virus determined by electron cryomicroscopy. *J Virol.* 71(1):325-330.

Box, P. (1989) High maternal antibodies help chicks beat virulent virus. *World Poultry* 53:17-19.

Brierley, J. & Hemmings, W.A. (1956) The Selective Transport of Antibodies from the Yolk Sac to the Circulation of the Chick. *J Embryol Exp Morphol* 4, 34-41.

Brown, M.D., Green, P. & Skinner, M.A. (1994) VP2 sequences of recent European 'very virulent' isolates of infectious bursal disease virus are closely related to each other but are distinct from those of 'classical' strains. *J Gen Virol.* 75 (Pt 3):675-680.

Brown, M.D. and Skinner, M.A. (1996) Coding sequences of both genome segments of a European 'very virulent' infectious bursal disease virus. *Virus Res.* 40(1):1-15.

Brownawell, A.M. & Macara, I.G. (2002) Exportin-5, a novel karyopherin, mediates nuclear export of double-stranded RNA binding proteins. *J Cell Biol.* 156(1):53-64.

Brüning, H., & Trenkler, G (1994) Nichtparametrische statistische Methoden, Berlin; New York: *de Gruyer*, 171-174.

Brzostowski, J., Robinson, C., Orford, R., Elgar, S., Scarlett, G., Peterkin, T., Malartre, M., Kneale, G., Wormington, M. & Guille, M. (2000) RNA-dependent cytoplasmic anchoring of a transcription factor subunit during Xenopus development. EMBO J. 19(14):3683-3693.

Buelt, M.K., **Glidden, B.J**. **& Storm, D.R**. (1994) Regulation of p68 RNA helicase by calmodulin and protein kinase C. *J Biol Chem.* 269(47):29367-29370.

Cao, Y.C., Yeung, W.S., Law, M., Bi, Y.Z., Leung, F.C. & Lim, B.L. (1998) Molecular characterization of seven Chinese isolates of infectious bursal disease virus: classical, very virulent, and variant strains. *Avian Dis.* 42(2):340-351.

Chen, J.Y., Chen, W.N., Poon, K.M., Zheng, B.J., Lin, X., Wang, Y.X. & Wen, Y.M. (2009) Interaction between SARS-CoV helicase and a multifunctional cellular protein (Ddx5) revealed by yeast and mammalian cell two-hybrid systems. *Arch Virol.* 154(3):507-512.

Chettle, N., Stuart, J.C. & Wyeth, P.J. (1989) Outbreak of virulent infectious bursal disease in East Anglia. *Vet Rec.* 125(10):271-272.

Chevalier, C., Galloux, M., Pous, J., Henry, C., Denis, J., Da Costa, B., Navaza, J., Lepault, J. & Delmas, B. (2005) Structural peptides of a nonenveloped virus are involved in assembly and membrane translocation. *J Virol.* 79(19):12253-12263.

Cheville, N.F. (1967) Studies on the pathogenesis of Gumboro disease in the bursa of Fabricius, spleen, and thymus of the chicken. *Am J Pathol.* 51(4):527-551.

Cho, B.R. (1970) Experimental dual infections of chickens with infectious bursal and Marek's disease agents. I. Preliminary observation on the effect of infectious bursal agent on Marek's disease. Avian Dis. 14(4):665-675.

Cho, Y. & Edgar, S.A. (1972) Characterization of infectious bursal disease. Poult Sci. 51(1):60-69.

Choi, S.Y., Scherer, B.J., Schnier, J., Davies, M.V., Kaufman, R.J. & Hershey, J.W. (1992) Stimulation of protein synthesis in COS cells transfected with variants of the alpha-subunit of initiation factor eIF-2. *J Biol Chem.* 267(1):286-293.

Chu, W.M., Ballard, R., Carpick, B.W., Williams, B.R. & Schmid, C.W. (1998) Potential Alu function: regulation of the activity of double-stranded RNA-activated kinase PKR. Mol Cell Biol. 1998 Jan;18(1):58-68.

Corthésy, B. & Kao, P.N. (1994) Purification by DNA affinity chromatography of two polypeptides that contact the NF-AT DNA binding site in the interleukin 2 promoter. *J Biol Chem.* 269(32):20682-20690.

Cosgrove, A.S. (1962) An apparently new disease of chickens-avian nephrosis. *Avian Dis.* 6, 385-389.

Coulibaly, F., Chevalier, C., Gutsche, I., Pous, J., Navaza, J., Bressanelli, S., Delmas, B. & Rey, F.A. (2005) The birnavirus crystal structure reveals structural relationships among icosahedral viruses. *Cell* 120(6):761-772.

Cui, H., Yan, Y., Wei, J., Hou, Z., Huang, Y., Huang, X. & Qin Q. (2011) Cloning, characterization, and expression analysis of orange-spotted grouper (Epinephelus coioides) ILF2 gene (EcILF2). *Fish Shellfish Immunol.* 30(1):378-388.

Da Costa, B., Chevalier, C., Henry, C., Huet, J.C., Petit, S., Lepault, J., Boot, H. & Delmas, B. (2002) The capsid of infectious bursal disease virus contains several small peptides arising from the maturation process of pVP2. *J Virol.* 76(5):2393-2402.

Da Costa, B., Soignier, S., Chevalier, C., Henry, C., Thory, C., Huet, J.C. & Delmas, B. (2003) Blotched snakehead virus is a new aquatic birnavirus that is slightly more related to avibirnavirus than to aquabirnavirus. *J Virol.* 77(1):719-725.

De Lucas, S., Peredo, J., Marión, R.M., Sánchez, C. & Ortín, J. (2010) Human Staufen1 protein interacts with influenza virus ribonucleoproteins and is required for efficient virus multiplication. *J Virol.* 84(15):7603-7612.

Delgui, L., Oña, A., Gutiérrez, S., Luque, D., Navarro, A., Castón, J.R. & Rodríguez, J.F. (2009a) The capsid protein of infectious bursal disease virus contains a functional alpha 4 beta 1 integrin ligand motif. *Virology.* 386(2):360-372.

Delmas, B., Kibenge, F.S.B., Leong, J.C., Mundt, E., Vakharia, V.N. & Wu, J.L. (2005) *Birnaviridae*, p. 561-569. *In* C.M. Fauquet, M.A. Mayo, J. Maniloff, U. Desselberger and A.L. Ball (ed.), Virus taxonomy, Academic Press, London, England.

Di Fabio, J., Rossini, L.I., Eterradossi, N., Toquin, M.D. & Gardin, Y. (1999) European-like pathogenic infectious bursal disease viruses in Brazil. *Vet Rec.* 145(7):203-204.

Diaz, M. O., Ziemin, S., Le Beau, M.M., Pitha, P., Smith, S.D., Chilcote, R.R. & Rowley, J.D. (1988) Homozygous deletion of the alpha- and beta 1-interferon genes in human leukemia and derived cell lines. *Proc. Natl. Acad. Sci.* USA 85:5259–5263.**Dobos, P.** (1979) Peptide map comparison of the proteins of infectious bursal disease virus. *J Virol.* 32(3):1047-1050.

Dobos, P. (1979) Peptide map comparison of the proteins of infectious bursal disease virus. *J Virol.* 32(3):1047-1050.

Dobos, P., Hill, B.J., Hallett, R., Kells, D.T., Becht, H. & Teninges, D. (1979) Biophysical and biochemical characterization of five animal viruses with bisegmented double-stranded RNA genomes. *J Virol*. 32(2):593-605.

Dobos, P. (1993) *In vitro* guanylylation of infectious pancreatic necrosis virus polypeptide VP1. *Virology* 193(1):403-413.

Duchange, N., Pidoux, J., Camus, E. & Sauvaget, D. (2000) Alternative splicing in the human interleukin enhancer binding factor 3 (ILF3) gene. *Gene.* 261(2):345-353.

Edgar, S.A. & Cho, Y. (1965) Avian Nephrosis (Gumboro Disease) and its control by immunization. *Poult. Sci.* 44(5)1366

Edgar, S.A. & Cho, Y. (1973) Immunization of chickens for the control of infectious bursal disease. *Poult Sci.* 52(2):492-497.

Eterradossi, N., Picault, J.P., Drouin, P., Guittet, M., L'Hospitalier, R. & Bennejean, G. (1992) Pathogenicity and preliminary antigenic characterization of six infectious bursal disease virus strains isolated in France from acute outbreaks. *Zentralbl Veterinarmed B.* 39(9):683-691.

Eterradossi, N., Toquin, D., Rivallan, G. & Guittet, M. (1997) Modified activity of a VP2-located neutralizing epitope on various vaccine, pathogenic and hypervirulent strains of infectious bursal disease virus. *Arch Virol.* 142(2):255-270.

Eterradossi, N., Arnauld, C., Toquin, D. & Rivallan, G. (1998) Critical amino acid changes in VP2 variable domain are associated with typical and atypical antigenicity in very virulent infectious bursal disease viruses. *Arch Virol.* 143(8):1627-1636.

Eterradossi, N., Arnaud, C., Tekaia, F., Toquin, D., Le Coq, H., Rivallan, G., Guittet, M., Domenech, J., van den Berg, T.P. & Skinner, M.A. (1999) Antigenic and genetic relationships between European very virulent infectious bursal disease viruses and an early West African isolate. *Avian Pathol.* 28, 36–46.

Fadly, A.M., Winterfield, R.W. & Olander, H.J. (1976) Role of the bursa of Fabricius in the pathogenicity of inclusion body hepatitis and infectious bursal disease viruses. *Avian Dis.* 20(3):467-477.

Fahey, K.J., O'Donnell, I.J. & Bagust, T.J. (1985) Antibody to the 32K structural protein of infectious bursal disease virus neutralizes viral infectivity in vitro and confers protection on young chickens. *J Gen Virol.* 66 (Pt 12):2693-2702.

Fahey, K.J., Crooks, J.K. & Fraser, R.A. (1987) Assessment by ELISA of passively acquired protection against infectious bursal disease virus in chickens. *Aust Vet J.* 64(7), 203-207.

Falcón, A.M., Fortes, P., Marión, R.M., Beloso, A. & Ortín, J. (1999) Interaction of influenza virus NS1 protein and the human homologue of Staufen in vivo and in vitro. *Nucleic Acids Res.* 27(11):2241-2247.

Faragher, J.T. (1972) Infectious bursal disease of chickens. *The Veterinary Bulletin* 42(6):361-369.

Faragher, J.T., Allan, W.H. & Cullen, G.A. (1972) Immunosuppressive effect of the infectious bursal agent in the chicken. Nat *New Biol.* 237(73):118-119.

Farrell, P.J., Balkow, K., Hunt, T., Jackson, R.J. & Trachsel, H. (1977) Phosphorylation of initiation factor elF-2 and the control of reticulocyte protein synthesis. *Cell.* 11(1):187-200.

Fernández-Arias, A., Martínez, S. & Rodríguez, J.F. (1997) The major antigenic protein of infectious bursal disease virus, VP2, is an apoptotic inducer. *J Virol.* 71(10):8014-8018.

Fierro-Monti, I. & Mathews, M.B. (2000) Proteins binding to duplexed RNA: one motif, multiple functions. *Trends Biochem Sci.* 25(5):241-246.

Fornerod, M., Ohno, M., Yoshida, M. & Mattaj, I.W. (1997) CRM1 is an export receptor for leucine-rich nuclear export signals. *Cell* 90(6):1051-60.

Fujii, R., Okamoto, M., Aratani, S., Oishi, T., Ohshima, T., Taira, K., Baba, M., Fukamizu, A. & Nakajima, T. (2001) A Role of RNA Helicase A in cis-Acting Transactivation Response Element-mediated Transcriptional Regulation of Human Immunodeficiency Virus Type 1. *J Biol Chem.* 276(8):5445-5451.

Fuller-Pace, F.V. (2006) DExD/H box RNA helicases: multifunctional proteins with important roles in transcriptional regulation. *Nucleic Acids Res.* 34(15):4206-4215.

Galabru, J. & Hovanessian, A.G. (1985) Two interferon-induced proteins are involved in the protein kinase complex dependent on double-stranded RNA. *Cell.* 43(3 Pt 2):685-694.

Galabru, J. & Hovanessian, A. (1987) Autophosphorylation of the protein kinase dependent on double-stranded RNA. *J Biol Chem.* 262(32):15538-15544.

Galabru, J., Katze, M.G., Robert, N. & Hovanessian, A.G. (1989) The binding of double-stranded RNA and adenovirus VAI RNA to the interferon-induced protein kinase. *Eur J Biochem.* 178(3):581-589.

Galloux, M., Libersou, S., Morellet, N., Bouaziz, S., Da Costa, B., Ouldali, M., Lepault, J. & Delmas, B. (2007) Infectious bursal disease virus, a non-enveloped virus, possesses a capsid-associated peptide that deforms and perforates biological membranes. *J Biol Chem.* 282(28):20774-20784.

Galloux, M., Libersou, S., Alves, I.D., Marquant, R., Salgado, G.F., Rezaei, H., Lepault, J., Delmas, B., Bouaziz, S. & Morellet, N. (2010) NMR structure of a viral peptide inserted in artificial membranes: a view on the early steps of the birnavirus entry process. *J Biol Chem.* 285(25):19409-19421.

Gao, H.L., Wang, X.M., Gao, Y.L. & Fu, C.Y. (2007) Direct evidence of reassortment and mutant spectrum analysis of a very virulent infectious bursal disease virus. *Avian Dis.* 51(4):893-899.

Garriga, D., Navarro, A., Querol-Audí, J., Abaitua, F., Rodríguez, J.F. & Verdaguer, N. (2007) Activation mechanism of a noncanonical RNA-dependent RNA polymerase. *Proc Natl Acad Sci U S A* 104(51):20540-20545.

Gelb, J., Eidson, C.S. & Kleven, S.H. (1979a) Studies on Interferon Induction by Infectious Bursal Disease Virus (IBDV). I. Interferon Production in Chicken Embryo Cell Cultures Infected with IBDV. *Avian Dis.* 23(2):485-492.

Gelb, J., Eidson, C.S. & Kleven, S.H. (1979b) Interferon Production in Embryonating Chicken Eggs Following Inoculation with Infectious Bursal Disease Virus. *Avian Dis.* 23(2): 534-538.

Gelb, J., Eidson, C.S., Fletcher, O.J. & Kleven, S.H. (1979c) Studies on interferon induction by infectious bursal disease virus (IBDV). II. Interferon production in White Leghorn chickens infected with an attenuated or pathogenic isolant of IBDV. *Avian Dis.* 23(3):634-645.

Giambrone, J.J., Eidson, C.S., Page, R.K., Fletcher, O.J., Barger, B.O. & Kleven, S.H. (1976) Effect of infectious bursal agent on the response of chickens to Newcastle disease and Marek's disease vaccination. *Avian Dis.* 20(3):534-544.

Giambrone, J.J. & Closser, J. (1990) Efficacy of live vaccines against serologic subtypes of infectious bursal disease virus. *Avian Dis.* 34(1):7-11.

Glick, B., Chang, T.S., Jaap, G. (1956). The bursa of Fabricius and antibody production. *Poult. Sci.* 35(1), 224-225.

Glick, B. (1956). Normal growth of the bursa of Fabricius in chickens. *Poult. Sci.* 35(4), 843-851.

Goh, P.Y., Tan, Y.J., Lim, S.P., Tan, Y.H., Lim, S.G., Fuller-Pace, F. & Hong, W. (2004) Cellular RNA helicase p68 relocalization and interaction with the hepatitis C virus (HCV) NS5B protein and the potential role of p68 in HCV RNA replication. *J Virol.* 78(10):5288-5298.

Gomila, R.C., Martin, G.W. & Gehrke, L. (2011) NF90 binds the dengue virus RNA 3' terminus and is a positive regulator of dengue virus replication. *PLoS One*. 6(2):e16687.

Graber, T.E., Baird, S.D., Kao, P.N., Mathews, M.B. & Holcik, M. (2010) NF45 functions as an IRES trans-acting factor that is required for translation of cIAP1 during the unfolded protein response. *Cell Death Differ.* 17(4):719-29.

Granzow H, Birghan C, Mettenleiter TC, Beyer J, Köllner B & Mundt E. (1997) A second form of infectious bursal disease virus-associated tubule contains VP4. *J Virol.* 71(11):8879-8885.

Guan, D., Altan-Bonnet, N., Parrott, A.M., Arrigo, C.J., Li, Q., Khaleduzzaman, M., Li, H., Lee, C.G., Pe'ery, T. & Mathews, M.B. (2008) Nuclear factor 45 (NF45) is a regulatory subunit of complexes with NF90/110 involved in mitotic control. *Mol Cell Biol.* 28(14):4629-4641.

Habib, M., Hussain, I., Fang, W.H., Rajput, Z.I., Yang, Z.Z. & Irshad, H. (2006) Inactivation of infectious bursal disease virus by binary ethylenimine and formalin. *J Zhejiang Univ Sci B.* 7(4), 320-3.

Hamamoto, T., Gunji, S., Tsuji, H. & Beppu, T. (1983) Leptomycins A and B, new antifungal antibiotics. I. Taxonomy of the producing strain and their fermentation, purification and characterization. *J Antibiot (Tokyo)* 36(6):639-645.

Harashima, A., Guettouche, T. & Barber, G.N. (2010) Phosphorylation of the NFAR proteins by the dsRNA-dependent protein kinase PKR constitutes a novel mechanism of translational regulation and cellular defense. *Genes Dev.* 24(23):2640-2653.

Harkness, J.W., Alexander, D.J., Pattison, M. & Scott, A.C. (1975) Infectious bursal disease agent: morphology by negative stain electron microscopy. *Arch Virol.* 48(1):63-73.

Harris, D., Zhang, Z., Chaubey, B. & Pandey, V.N. (2006) Identification of cellular factors associated with the 3'-nontranslated region of the hepatitis C virus genome. *Mol Cell Proteomics.* 5(6):1006-1018.

Heine, H.G., Haritou, M., Failla, P., Fahey, K. & Azad, A. (1991) Sequence analysis and expression of the host-protective immunogen VP2 of a variant strain of infectious bursal disease virus which can circumvent vaccination with standard type I strains. *J Gen Virol.* 72 (Pt 8):1835-1843.

Helmboldt, C.F. & Garner, E. (1964) Experimentally induced Gumboro Disease (IBA). *Avian Dis.* 8(4):561-575.

Hirai, K. & Calnek, B.W. (1979) In vitro replication of infectious bursal disease virus in established lymphoid cell lines and chicken B lymphocytes. *Infect Immun.* 25(3):964-970.

Hirai, K., Kunihiro, K. & Shimakura, S. (1979) Characterization of Immunosuppression in chickens by infectious bursal disease virus. *Avian Dis.* 23(4):950-965.

Hirai, K., Funakoshi, T., Nakai, T. & Shimakura, S. (1981) Sequential changes in the number of surface immunoglobulin-bearing B lymphocytes in infectious bursal disease virus-infected chickens. *Avian Dis.* 25(2):484-496.

Hirling, H., Scheffner, M., Restle, T. & Stahl, H. (1989) RNA helicase activity associated with the human p68 protein. *Nature.* 339(6225):562-564.

Hitchner, S.B. (1971) Persistence of parental infectious bursal disease antibody and its effect on susceptibility of young chickens. *Avian Dis.* 15(4):894-900.

Hitchner, S.B. (1976) Immunization of adult hens against infectious bursal disease virus. *Avian Dis.* 20(3):611-613.

Hon, C.C., Lam, T.T., Yip, C.W., Wong, R.T., Shi, M., Jiang, J., Zeng, F. & Leung, F.C. (2008) Phylogenetic evidence for homologous recombination within the family Birnaviridae. *J Gen Virol.* 89(Pt 12):3156-3164.

Huang, Y. & Liu, Z.R. (2002) The ATPase, RNA unwinding, and RNA binding activities of recombinant p68 RNA helicase. *J Biol Chem.* 277(15):12810-12815.

Hudson, P.J., McKern, N.M., Fahey, K.J. & Azad, A.A. (1986a) Predicted sequence of the host-protective immunogen of infectious bursal disease virus. *FEBS Lett.* 26;201(1):143-146.

Hudson, P.J., McKern, N.M., Power, B.E. & Azad, A.A. (1986b) Genomic structure of the large RNA segment of infectious bursal disease virus. *Nucleic Acids Res.* 14(12):5001-5012.

Iggo, R.D. & Lane, D.P. (1989) Nuclear protein p68 is an RNA-dependent ATPase. *EMBO J.* 8(6):1827-1831.

Irigoyen, N., Garriga, D., Navarro, A., Verdaguer, N., Rodríguez, J.F. & Castón, J.R. (2009) Autoproteolytic activity derived from the infectious bursal disease virus capsid protein. *J Biol Chem.* 284(12):8064-8072.

Isken, O., Grassmann, C.W., Sarisky, R.T., Kann, M., Zhang, S., Grosse, F., Kao, P.N. & Behrens, S.E. (2003) Members of the NF90/NFAR protein group are involved in the life cycle of a positive-strand RNA virus. EMBO J. 22(21):5655-5665.

Isken, O., Baroth, M., Grassmann, C.W., Weinlich, S., Ostareck, D.H., Ostareck-Lederer, A. & Behrens, S.E. (2007) Nuclear factors are involved in hepatitis C virus RNA replication. RNA. 13(10):1675-1692.

Islam, M.R., Zierenberg, K. & Müller, H. (2001) The genome segment B encoding the RNA-dependent RNA polymerase protein VP1 of very virulent infectious bursal disease virus (IBDV) is phylogenetically distinct from that of all other IBDV strains. *Arch Virol.* 146(12):2481-92.

Ivanyi, J. & Morris, R. (1976) Immunodeficiency in the chicken. IV. An immunological study of infectious bursal disease. *Clin Exp Immunol.* 23(1):154-165.

Jackwood, D.J., Saif, Y.M. & Hughes, J.H. (1982) Characteristics and serologic studies of two serotypes of infectious bursal disease virus in turkeys. *Avian Dis.* 26(4):871-882.

Jackwood, D.J., Saif, Y.M. & Moorhead, P.D. (1985) Immunogenicity and antigenicity of infectious bursal disease virus serotypes I and II in chickens. *Avian Dis.* 29(4):1184-1194.

Jackwood, D.H. & Saif, Y.M. (1987) Antigenic diversity of infectious bursal disease viruses. *Avian Dis.* 31(4):766-770.

Jacobs, B.L. & Langland, J.O. (1996) When two strands are better than one: the mediators and modulators of the cellular responses to double-stranded RNA. Virology. 219(2):339-349. Review.

Jagadish, M.N., Staton, V.J., Hudson, P.J. & Azad, A.A. (1988) Birnavirus precursor polyprotein is processed in Escherichia coli by its own virus-encoded polypeptide. *J Virol.* 62(3):1084-1087.

Jankowsky, E., **Gross, C.H**., **Shuman, S. & Pyle, A.M**. (2001) Active disruption of an RNA-protein interaction by a DExH/D RNA helicase. *Science.* 291(5501):121-125.

Jorba, N., Juarez, S., Torreira, E., Gastaminza, P., Zamarreño, N., Albar, J.P. & Ortín, J. (2008) Analysis of the interaction of influenza virus polymerase complex with human cell factors. *Proteomics.* 8(10):2077-2088.

Jost, J.P., Schwarz, S., Hess, D., Angliker, H., Fuller-Pace, F.V., Stahl, H., Thiry, S. & Siegmann, M. (1999) A chicken embryo protein related to the mammalian DEAD box protein p68 is tightly associated with the highly purified protein-RNA complex of 5-MeC-DNA glycosylase. *Nucleic Acids Res.* 27(16):3245-3252.

Kao, P.N., Chen, L., Brock, G., Ng, J., Kenny, J., Smith, A.J. & Corthésy, B. (1994) Cloning and expression of cyclosporin A- and FK506-sensitive nuclear factor of activated T-cells: NF45 and NF90. *J Biol Chem.* 269(32):20691-20699.

Käufer, I. & Weiss, E. (1980) Significance of bursa of Fabricius as target organ in infectious bursal disease of chickens. *Infect Immun.* 27(2):364-367.

Kibenge, F.S.B., Dhillon, A.S. & Russell, R.G. (1988) Biochemistry and immunology of infectious bursal disease virus. *J Gen Virol.* 69 (Pt 8):1757-1775.

Kibenge, F.S.B., Nagarajan, M.M. & Qian, B. (1996) Determination of the 5' and 3' terminal noncoding sequences of the bi-segmented genome of the avibirnavirus infectious bursal disease virus. *Arch Virol.* 141(6):1133-1141.

Kibenge, F.S.B. & Dhama, V. (1997) Evidence that virion-associated VP1 of avibirnaviruses contains viral RNA sequences. *Arch Virol.* 142(6):1227-1236.

Kiesler, P., Haynes, P.A., Shi, L., Kao, P.N., Wysocki, V.H. & Vercelli, D. (2010) NF45 and NF90 regulate HS4-dependent interleukin-13 transcription in T cells. *J Biol Chem.* 285(11):8256-8267.

Kim, I.J., Gagic, M. & Sharma, J.M. (1999) Recovery of antibody-producing ability and lymphocyte repopulation of bursal follicles in chickens exposed to infectious bursal disease virus. *Avian Dis.* 43(3):401-413.

Kitajewski, J., Schneider, R.J., Safer, B., Munemitsu, S.M., Samuel, C.E., Thimmappaya, B. & Shenk, T. (1986) Adenovirus VAI RNA antagonizes the antiviral action of interferon by preventing activation of the interferon-induced eIF-2 alpha kinase. *Cell.* 45(2):195-200.

Knoblich, H.V., Sommer, S.E. & Jackwood, D.J. (2000) Antibody titers to infectious bursal disease virus in broiler chicks after vaccination at one day of age with infectious bursal disease virus and Marek's disease virus. *Avian Dis.* 44(4), 874-884.

Kochan, G., Gonzalez, D. & Rodriguez, J.F. (2003) Characterization of the RNA-binding activity of VP3, a major structural protein of Infectious bursal disease virus. *Arch Virol.* 148(4):723-744.

Kong, L.L., Omar, A.R., Hair-Bejo, M., Aini, I. & Seow, H.F. (2004) Sequence analysis of both genome segments of two very virulent infectious bursal disease virus field isolates with distinct pathogenicity. *Arch Virol.* 149(2):425-434.

Krasnoselskaya-Riz, I., Spruill, A., Chen, Y.W., Schuster, D., Teslovich, T., Baker, C., Kumar, A. & Stephan, D.A. (2002) Nuclear factor 90 mediates activation of the cellular antiviral expression cascade. AIDS Res Hum Retroviruses. 2002 May 20;18(8):591-604.

Lam, K.M. (1997) Morphological evidence of apoptosis in chickens infected with infectious bursal disease virus. *J Comp Pathol.* 116(4):367-377.

Lange, H., Müller, H., Käufer, I. & Becht, H. (1987) Pathogenic and structural properties of wild type infectious bursal disease virus (IBDV) and virus grown in vitro. *Arch Virol.* 92(3-4):187-196.

Lasher, H. N. & Shane, M. (1994) Infectious bursal disease. *World's Poult. Sci. J.* 50, 133–166.

Lee, J.W., Liao, P.C., Young, K.C., Chang, C.L., Chen, S.S., Chang, T.T., Lai, M.D. & Wang, S.W. (2011) Identification of hnRNPH1, NF45, and C14orf166 as novel host interacting partners of the mature hepatitis C virus core protein. *J Proteome Res.* 10(10):4522-4534.

Lejal, N., Da Costa, B., Huet, J.C. & Delmas, B. (2000) Role of Ser-652 and Lys-692 in the protease activity of infectious bursal disease virus VP4 and identification of its substrate cleavage sites. *J Gen Virol.* 81(Pt 4):983-92.

Letzel, T., Mundt, E. & Gorbalenya, A.E. (2007) Evidence for functional significance of the permuted C motif in Co2+-stimulated RNA-dependent RNA polymerase of infectious bursal disease virus. *J Gen Virol.* 88(Pt 10):2824-2833.

Ley, D.H., Storm, N., Bickford, A.A. & Yamamoto, R. (1979) An infectious bursal disease virus outbreak in 14- and 15-week-old chickens. *Avian Dis.* 23(1):235-240.

Ley, D.H., Yamamoto, R. & Bickford, A.A. (1983) The pathogenesis of infectious bursal disease: serologic, histopathologic, and clinical chemical observations. *Avian Dis.* 27(4):1060-1085.

Li, J., Tang, H., Mullen, T.M., Westberg, C., Reddy, T.R., Rose, D.W. & Wong-Staal, F. (1999) A role for RNA helicase A in post-transcriptional regulation of HIV type 1. *Proc Natl Acad Sci U S A.* 96(2):709-714.

Lim, B.L., Cao, Y., Yu, T. & Mo, C.W. (1999) Adaptation of very virulent infectious bursal disease virus to chicken embryonic fibroblasts by site-directed mutagenesis of residues 279 and 284 of viral coat protein VP2. *J Virol.* 73(4):2854-2862.

Lin, Z., Kato, A., Otaki, Y., Nakamura, T., Sasmaz, E. & Ueda, S. (1993) Sequence comparisons of a highly virulent infectious bursal disease virus prevalent in Japan. *Avian Dis.* 37(2):315-323.

Lin, H.F., Shao, J.Z., Xiang, L.X. & Wang, H.J. (2006) Molecular cloning, characterization and expression analysis of grass carp (Ctenopharyngodon idellus) NF45 (ILF2) cDNA, a subunit of the nuclear factor of activated T-cells (NF-AT). *Fish Shellfish Immunol.*;21(4):385-392.

Lin, T.W., Lo, C.W., Lai, S.Y., Fan, R.J., Lo, C.J., Chou, Y.M., Thiruvengadam, R., Wang, A.H. & Wang, M.Y. (2007) Chicken heat shock protein 90 is a component of the putative cellular receptor complex of infectious bursal disease virus. *J Virol.* 81(16):8730-8741.

Lin, L., Li, Y., Pyo, H.M., Lu, X., Raman, S.N., Liu, Q., Brown, E.G. & Zhou, Y. (2012) Identification of RNA helicase A as a cellular factor that interacts with influenza A virus NS1 protein and its role in the virus life cycle. *J Virol.* 86(4):1942-1954.

Linder, P., Lasko, P.F., Ashburner, M., Leroy, P., Nielsen, P.J., Nishi, K., Schnier, J. & Slonimski, P.P. (1989) Birth of the D-E-A-D box. *Nature.* 337(6203):121-122.

Linder, P. (2006) Dead-box proteins: a family affair--active and passive players in RNP-remodeling. *Nucleic Acids Res.* 34(15):4168-4180.

Liu, Z.R. (2002) p68 RNA helicase is an essential human splicing factor that acts at the U1 snRNA-5' splice site duplex. *Mol Cell Biol.* 22(15):5443-5450.

Liu, J., Zhou, J. & Kwang, J. (2002) Antigenic and molecular characterization of recent infectious bursal disease virus isolates in China. *Virus Genes.* 24(2):135-147.

Liu, M. & Vakharia, V.N. (2006) Nonstructural protein of infectious bursal disease virus inhibits apoptosis at the early stage of virus infection. *J Virol.* 80(7):3369-3377.

Lombardo, E., Maraver, A., Castón, J.R., Rivera, J., Fernández-Arias, A., Serrano, A., Carrascosa, J.L. & Rodriguez, J.F. (1999) VP1, the putative RNA-dependent RNA polymerase of infectious bursal disease virus, forms complexes with the capsid protein VP3, leading to efficient encapsidation into virus-like particles. *J Virol.* 73(8):6973-6983.

Lombardo, E., Maraver, A., Espinosa, I., Fernández-Arias, A. & Rodriguez, J.F. (2000) VP5, the nonstructural polypeptide of infectious bursal disease virus, accumulates within the host plasma membrane and induces cell lysis. *Virology* 277(2):345-357.

Lucio, B., Antillón, A. & Fernández, P. (1972) Identification of the infectious bursal disease virus in Mexico. *Avian Dis.* 16(2):241-248.

Lukert, P.D. & Davis, R.B. (1974) Infectious bursal disease virus: growth and characterization in cell cultures. *Avian Dis.* 18(2):243-250.

Luque, D., Rivas, G., Alfonso, C., Carrascosa, J.L., Rodríguez, J.F. & Castón, J.R. (2009a) Infectious bursal disease virus is an icosahedral polyploid dsRNA virus. *Proc Natl Acad Sci U S A.* 106(7):2148-2152.

Luque, D., Saugar, I., Rejas, M.T., Carrascosa, J.L., Rodríguez, J.F. & Castón, J.R. (2009b) Infectious Bursal disease virus: ribonucleoprotein complexes of a double-stranded RNA virus. *J Mol Biol.* 386(3):891-901.

Ma, K., Roy, A.M. & Whittaker, G.R. (2001) Nuclear export of influenza virus ribonucleoproteins: identification of an export intermediate at the nuclear periphery. *Virology* 282(2):215-220.

Manche, L., Green, S.R., Schmedt, C. & Mathews, M.B. (1992) Interactions between double-stranded RNA regulators and the protein kinase DAI. *Mol Cell Biol.* 12(11):5238-5248.

Mansikka, A., Sandberg, M., Lassila, O. & Toivanen, P. (1990) Rearrangement of immunoglobulin light chain genes in the chicken occurs prior to colonization of the embryonic bursa of Fabricius. *Proc Natl Acad Sci* 87(23), 9416-9420.

Maraver, A., Clemente, R., Rodríguez, J.F. & Lombardo, E. (2003a) Identification and molecular characterization of the RNA polymerase-binding motif of infectious bursal disease virus inner capsid protein VP3. *J Virol.* 77(4):2459-2468.

Maraver, A., Oña, A., Abaitua, F., González, D., Clemente, R., Ruiz-Díaz, J.A., Castón, J.R., Pazos, F. & Rodriguez, J.F. (2003b) The oligomerization domain of VP3, the scaffolding protein of infectious bursal disease virus, plays a critical role in capsid assembly. *J Virol.* 77(11):6438-6449.

Martínez-Torrecuadrada, J.L., Lázaro, B., Rodriguez, J.F. & Casal, J.I. (2000a) Antigenic properties and diagnostic potential of baculovirus-expressed infectious bursal disease virus proteins VPX and VP3. *Clin Diagn Lab Immunol.* 7(4):645-651.

Martínez-Torrecuadrada, J.L., Castón, J.R., Castro, M., Carrascosa, J.L., Rodriguez, J.F. & Casal, J.I. (2000b) Different architectures in the assembly of infectious bursal disease virus capsid proteins expressed in insect cells. *Virology* 20;278(2):322-331.

McFerran, J.B., McNulty, M.S., McKillop, E.R., Connor, T.J., McCracken, R.M., Collins, D.S. & Allan, G.M. (1980) Isolation and serological studies with infectious bursal disease viruses from fowl, turkeys and ducks: demonstration of a second serotype. *Avian Pathol.* 9(3):395-404.

Merrill, M.K., Dobrikova, E.Y. & Gromeier, M. (2006) Cell-type-specific repression of internal ribosome entry site activity by double-stranded RNA-binding protein 76. *J Virol.* 80(7):3147-3156.

Merrill, M.K. & Gromeier, M. (2006) The double-stranded RNA binding protein 76:NF45 heterodimer inhibits translation initiation at the rhinovirus type 2 internal ribosome entry site. *J Virol.* 80(14):6936-6942.

Merz, C., Urlaub, H., Will, C.L. & Lührmann, R. (2007) Protein composition of human mRNPs spliced in vitro and differential requirements for mRNP protein recruitment. *RNA.* 13(1):116-128.

Meurs, E., Chong, K., Galabru, J., Thomas, N.S., Kerr, I.M., Williams, B.R. & Hovanessian, A.G. (1990) Molecular cloning and characterization of the human double-stranded RNA-activated protein kinase induced by interferon. *Cell.* 62(2):379-390.

Moradian, A., Thorsen, J. & Julian, R.J. (1990) Single and combined infections of specific-pathogen-free chickens with infectious bursal disease virus and an intestinal isolate of reovirus. *Avian Dis.* 34(1):63-72.

Morgan, M.M., Macreadie, I.G., Harley, V.R., Hudson, P.J. & Azad, A.A. (1988) Sequence of the small double-stranded RNA genomic segment of infectious bursal disease virus and its deduced 90-kDa product. *Virology* 163(1):240-242.

Mosca, J.D. & Pitha, P.M. (1986) Transcriptional and posttranscriptional regulation of exogenous human beta interferon gene in simian cells defective in interferon synthesis. *Mol Cell Biol.* 6(6):2279-2283.

Mouland, A.J., Mercier, J., Luo, M., Bernier, L., DesGroseillers, L. & Cohen, E.A. (2000) The double-stranded RNA-binding protein Staufen is incorporated in human immunodeficiency virus type 1: evidence for a role in genomic RNA encapsidation. *J Virol.* 74(12):5441-5451.

Müller, H., Scholtissek, C. & Becht, H. (1979) The genome of infectious bursal disease virus consists of two segments of double-stranded RNA. *J Virol.* 31(3):584-589.

Müller, H. & Becht, H. (1982) Biosynthesis of virus-specific proteins in cells infected with infectious bursal disease virus and their significance as structural elements for infectious virus and incomplete particles. *J Virol.* 44(1):384-392.

Müller, H. (1986) Replication of infectious bursal disease virus in lymphoid cells. *Arch Virol.* 87(3-4):191-203.

Müller, H., Lange, H. & Becht, H. (1986) Formation, characterization and interfering capacity of a small plaque mutant and of incomplete virus particles of infectious bursal disease virus. *Virus Res.* 4(3):297-309.

Müller, H. & Nitschke, R. (1987a) Molecular weight determination of the two segments of double-stranded RNA of infectious bursal disease virus, a member of the birnavirus group. *Med Microbiol Immunol.* 176(2):113-121.

Müller, H. & Nitschke, R. (1987b) The two segments of the infectious bursal disease virus genome are circularized by a 90,000-Da protein. *Virology* 159(1):174-177.

Müller, H., Islam, M.R. & Raue, R. (2003) Research on infectious bursal disease--the past, the present and the future. *Vet Microbiol.* 97(1-2):153-165. Review.

Mundt, E. & Müller, H. (1995) Complete nucleotide sequences of 5'- and 3'-noncoding regions of both genome segments of different strains of infectious bursal disease virus. *Virology* 209(1):10-18.

Mundt, E., Beyer, J. & Müller, H. (1995) Identification of a novel viral protein in infectious bursal disease virus-infected cells. *J Gen Virol.* 76 (Pt 2):437-443.

Mundt, E. & Vakharia, V.N. (1996) Synthetic transcripts of double-stranded Birnavirus genome are infectious. *Proc Natl Acad Sci U S A.* 93(20):11131-11136.

Mundt, E., Köllner, B. & Kretzschmar, D. (1997) VP5 of infectious bursal disease virus is not essential for viral replication in cell culture *J Virol.* 71(7):5647-5651.

Mundt, E. (2007) Human MxA protein confers resistance to double-stranded RNA viruses of two virus families. *J Gen Virol.* 88(Pt 4):1319-1323.

Nagarajan, M.M. & Kibenge, F.S. (1997) Infectious bursal disease virus: a review of molecular basis for variations in antigenicity and virulence. *Can J Vet Res.* 61(2):81-88. Review.

Nakamura, T., Otaki, Y. & Nunoya, T. (1992) Immunosuppressive effect of a highly virulent infectious bursal disease virus isolated in Japan. *Avian Dis.* 36(4):891-896.

Nakielny, S. & Dreyfuss, G. (1999) Transport of proteins and RNAs in and out of the nucleus. *Cell* 99(7):677-690. Review

Neubauer, G., King, A., Rappsilber, J., Calvio, C., Watson, M., Ajuh, P., Sleeman, J., Lamond, A. & Mann, M. (1998) Mass spectrometry and EST-database searching allows characterization of the multi-protein spliceosome complex. *Nat Genet.* 20(1):46-50.

Nick, H., Cursiefen, D. & Becht, H. (1976) Structural and growth characteristics of infectious bursal disease virus. *J Virol.* 18(1):227-234.

Nieper, H. & Müller, H. (1996) Susceptibility of chicken lymphoid cells to infectious bursal disease virus does not correlate with the presence of specific binding sites. *J Gen Virol.* 77 (Pt 6):1229-1237.

Nieper, H., Teifke, J. P., Jungmann, A., Löhr, C. & Müller, H. (1999) Infected and apoptotic cells in the IBDV-infected bursa of Fabricius by double-labelling techniques. *Avian Pathology.* 28:279-285

Nigg, E.A. (1997) Nucleocytoplasmic transport: Signals, mechanisms and regulation. *Nature* 386(6627): 779-787. Review

Nobiron, I., Galloux, M., Henry, C., Torhy, C., Boudinot, P., Lejal, N., Da Costa, B. & Delmas, B. (2008) Genome and polypeptides characterization of Tellina virus 1 reveals a fifth genetic cluster in the Birnaviridae family. *Virology* 371(2):350-361.

Ogawa, M., Yamaguchi, T., Setiyono, A., Ho, T., Matsuda, H., Furusawa, S., Fukushi, H. & Hirai, K. (1998) Some characteristics of a cellular receptor for virulent infectious bursal disease virus by using flow cytometry. *Arch Virol.* 143(12):2327-2341.

Ogilvie, V.C., **Wilson, B.J**., **Nicol, S.M**., **Morrice, N.A**., **Saunders, L.R**., **Barber, G.N. & Fuller-Pace, F.V**. (2003) The highly related DEAD box RNA helicases p68 and p72 exist as heterodimers in cells. *Nucleic Acids Res.* 31(5):1470-480.

Ojcius, D.M. & Young, J.D. (1991) Cytolytic pore-forming proteins and peptides: is there a common structural motif? *Trends Biochem Sci.* 16(6):225-229. Review.

Ojeda, F., Skardova, I., Guarda, M.I., Ulloa, J. & Folch, H. (1997) Proliferation and apoptosis in infection with infectious bursal disease virus: a flow cytometric study. *Avian Dis.* 41(2):312-316.

Okoye, J.O., Okeke, C.N. & Ezeobele, F.K. (1991) Effect of infectious bursal disease virus infection on the severity of Aspergillus flavus aspergillosis of chickens. *Avian Pathol.* 20(1):167-171.

Oña, A., Luque, D., Abaitua, F., Maraver, A., Castón, J.R. & Rodríguez, J.F. (2004) The C-terminal domain of the pVP2 precursor is essential for the interaction between VP2 and VP3, the capsid polypeptides of infectious bursal disease virus. *Virology* 322(1):135-142.

Onaga, H., Togo, M., Otaki, Y. & Tajima, M. (1989) Influence of live virus vaccination against infectious bursal disease on coccidial infection in chickens. *Nippon Juigaku Zasshi.* 51(2):463-465.

Öppling, V., Müller, H. & Becht, H. (1991) Heterogeneity of the antigenic site responsible for the induction of neutralizing antibodies in infectious bursal disease virus. *Arch Virol.* 119(3-4):211-223.

Owoade, A.A., Mulders, M.N., Kohnen, J., Ammerlaan, W. & Muller, C.P. (2004) High sequence diversity in infectious bursal disease virus serotype 1 in poultry and turkey suggests West-African origin of very virulent strains. *Arch Virol.* 149(4):653-672.

Owsianka, A.M. & Patel, A.H. (1999) Hepatitis C virus core protein interacts with a human DEAD box protein DDX3. Virology. 1999 May 10;257(2):330-40.

Özel, M. & Gelderblom, H. (1985) Capsid symmetry of viruses of the proposed Birnavirus group. *Arch Virol.* 84(3-4):149-161.

Pan, J., Vakharia, V.N. & Tao, Y.J. (2007) The structure of a birnavirus polymerase reveals a distinct active site topology. *Proc Natl Acad Sci U S A.* 104(18):7385-7390.

Pan, J., Lin, L. & Tao, Y.J. (2009) Self-guanylylation of birnavirus VP1 does not require an intact polymerase activity site. *Virology* 395(1):87-96.

Panniers, R. & Henshaw, E.C. (1983) A GDP/GTP exchange factor essential for eukaryotic initiation factor 2 cycling in Ehrlich ascites tumor cells and its regulation by eukaryotic initiation factor 2 phosphorylation. *J Biol Chem.* 258(13):7928-7934.

Parker, L.M., Fierro-Monti, I. & Mathews, M.B. (2001) Nuclear factor 90 is a substrate and regulator of the eukaryotic initiation factor 2 kinase double-stranded RNA-activated protein kinase. *J Biol Chem.* 276(35):32522-32530.

Parkhurst, R.T. (1964) On-the-Farm Studies of Gumboro Disease in Broilers. *Avian Dis.* 8(4):584-596.

Patel, R.C., Vestal, D.J., Xu, Z., Bandyopadhyay, S., Guo, W., Erme, S.M., Williams, B.R. & Sen, G.C. (1999) DRBP76, a double-stranded RNA-binding nuclear protein, is phosphorylated by the interferon-induced protein kinase, PKR. J Biol Chem. 274(29):20432-20437.

Pejkovski, C., Davelaar, F.G. & Kouwenhoven, B. (1979) Immunosuppressive effect of infectious bursal disease virus on vaccination against infectious bronchitis. *Avian Pathol.* 8(1):95-106.

Perelman, B. & Heller, E.D. (1983) The effect of infectious bursal disease virus on the immune system of turkeys. *Avian Dis.* 27(1):66-76.

Petek, M., D'Aprile, P.N. & Cancellotti, F. (1973) Biological and physico-chemical properties of the infectious bursal disease virus (IBDV). *Avian Pathol.* 2(2):135-152.

Pfeifer, I., Elsby, R., Fernandez, M., Faria, P.A., Nussenzveig, D.R., Lossos, I.S., Fontoura, B.M., Martin, W.D. & Barber, G.N. (2008) NFAR-1 and -2 modulate translation and are required for efficient host defense. *Proc Natl Acad Sci U S A.* 105(11):4173-4178.

Pous, J., Chevalier, C., Ouldali, M., Navaza, J., Delmas, B. & Lepault, J. (2005) Structure of birnavirus-like particles determined by combined electron cryomicroscopy and X-ray crystallography. *J Gen Virol.* 86(Pt 8):2339-2346.

Qin, L., Qi, X., Gao, Y., Gao, H., Lu, X., Wang, Y., Bu, Z. & Wang, X. (2010) VP5-deficient mutant virus induced protection against challenge with very virulent infectious bursal disease virus of chickens. *Vaccine.* 28(21):3735-3740.

Ranpura, S.A., Deshmukh, U. & Reddi, P.P. (2008) NF45 and NF90 in murine seminiferous epithelium: potential role in SP-10 gene transcription. *J Androl.* 29(2):186-197.

Ratcliffe, M.J.H., Lassila, O., Pink, J.R. & Vainio, O. (1986) Avian B cell precursors: surface immunoglobulin expression is an early, possibly bursa-independent event. *Eur J Immunol.* 16(2), 129-133.

Rautenschlein, S., Yeh, H.Y. & Sharma, J.M. (2003) Comparative immunopathogenesis of mild, intermediate, and virulent strains of classic infectious bursal disease virus. *Avian Dis.* 47(1):66-78.

Reichman, T.W., Muñiz, L.C. & Mathews, M.B. (2002) The RNA binding protein nuclear factor 90 functions as both a positive and negative regulator of gene expression in mammalian cells. *Mol Cell Biol.* 22(1):343-356.

Reichman, T.W. & Mathews, M.B. (2003) RNA binding and intramolecular interactions modulate the regulation of gene expression by nuclear factor 110. *RNA.* 9(5):543-554.

Rodenberg, J., Sharma, J.M., Belzer, S.W., Nordgren, R.M. & Naqi, S. (1994) Flow cytometric analysis of B cell and T cell subpopulations in specific-pathogen-free chickens infected with infectious bursal disease virus. *Avian Dis.* 38(1):16-21.

Rodriguez-Chavez, I.R., Rosenberger, J.K. & Cloud, S.S. (2002a) Characterization of the antigenic, immunogenic, and pathogenic variation of infectious bursal disease virus due to propagation in different host systems (bursa, embryo, and cell culture). I. Antigenicity and immunogenicity. *Avian Pathol.* 31(5):463-471.

Rodriguez-Chavez, I.R., Rosenberger, J.K. & Cloud, S.S. (2002b) Characterization of the antigenic, immunogenic, and pathogenic variation of infectious bursal disease virus due to propagation in different host systems (bursa, embryo, and cell culture). II. Antigenicity at the epitope level. *Avian Pathol.* 31(5):473-483.

Rodriguez-Chavez, I.R., Rosenberger, J.K., Cloud, S.S. & Pope, C.R. (2002c) Characterization of the antigenic, immunogenic, and pathogenic variation of infectious bursal disease virus due to propagation in different host systems (bursa, embryo, and cell culture). III. Pathogenicity. *Avian Pathol.* 31(5):485-492.

Rodríguez-Lecompte, J.C. & Kibenge, F.S.B. (2002) Site-directed mutagenesis of Avibirnavirus VP4 gene. *Virology.* 292(2):241-246.

Rodríguez-Lecompte, J.C., Niño-Fong, R., Lopez, A., Frederick Markham, R.J. & Kibenge, F.S.B. (2005) Infectious bursal disease virus (IBDV) induces apoptosis in chicken B cells. *Comp Immunol Microbiol Infect Dis.* 28(4):321-337.

Rocak, S. & Linder, P. (2004) DEAD-box proteins: the driving forces behind RNA metabolism. *Nat Rev Mol Cell Biol.* 5(3):232-241.

Rosenberger, J.K., Klopp, S., Eckroade, R.J. & Krauss, W.C. (1975) The roles of the infectious bursal agent and several avian adenoviruses in the hemorrhagic-aplastic-anemia syndrome and gangrenous dermatitis. *Avian Dis.* 19(4):717-729.

Rosenberger, J.K. & Gelb, J. Jr. (1978) Response to several avian respiratory viruses as affected by infectious bursal disease virus. *Avian Dis.* 22(1):95-105.

Rosenberger, J.K., Cloud, S.S., Gelb, J., Odor, E. and Dohms, S.E. (1985) Sentinel birds survey of Delmarva broiler flocks. In: Proceedings of the 20th national meeting on poultry health and condemnation, Ocean City, MD, pp 94–101.

Rössler, O.G., Straka, A. & Stahl, H. (2001) Rearrangement of structured RNA via branch migration structures catalysed by the highly related DEAD-box proteins p68 and p72. *Nucleic Acids Res.* 29(10):2088-2096.

Rozen, F., Edery, I., Meerovitch, K., Dever, T.E., Merrick, W.C. & Sonenberg, N. (1990) Bidirectional RNA helicase activity of eucaryotic translation initiation factors 4A and 4F. *Mol Cell Biol.* 10(3):1134-1144.

Rudd, M.F., Heine, H.G., Sapats, S.I., Parede, L. & Ignjatovic, J. (2002) Characterisation of an Indonesian very virulent strain of infectious bursal disease virus. *Arch Virol.* 147(7):1303-22.

Ryter, J.M. & Schultz, S.C. (1998) Molecular basis of double-stranded RNA-protein interactions: structure of a dsRNA-binding domain complexed with dsRNA. *EMBO J.* 17(24):7505-7513.

Safer, B. (1983) 2B or not 2B: regulation of the catalytic utilization of eIF-2. *Cell.* 33(1):7-8. Minireview.

Saif, Y.M. (1984) Infectious bursal disease virus type. In: Proceedings of the 19th national meeting on poultry health and condemnations, Ocean City, MD, pp 105–107.

Saif, Y.M. (1998) Infectious bursal disease and hemorrhagic enteritis. *Poult Sci.* 77(8):1186-1189.

Sakamoto, S., Aoki, K., Higuchi, T., Todaka, H., Morisawa, K., Tamaki, N., Hatano, E., Fukushima, A., Taniguchi, T. & Agata, Y. (2009) The NF90-NF45 complex functions as a negative regulator in the microRNA processing pathway. Mol Cell Biol. 29(13):3754-3769.

Sánchez, A.B. & Rodriguez, J.F. (1999) Proteolytic processing in infectious bursal disease virus: identification of the polyprotein cleavage sites by site-directed mutagenesis. *Virology* 262(1):190-199.

Santivatr, D., Maheswaran, S.K., Newman, J.A. & Pomeroy, B.S. (1981) Effect of infectious bursal disease virus infection on the phagocytosis of Staphylococcus aureus by mononuclear phagocytic cells of susceptible and resistant strains of chickens. *Avian Dis.*25(2):303-311.

Saugar, I., Luque, D., Oña, A., Rodríguez, J.F., Carrascosa, J.L., Trus, B.L. & Castón, J.R. (2005) Structural polymorphism of the major capsid protein of a double-stranded RNA virus: an amphipathic alpha helix as a molecular switch. *Structure* 13(7):1007-1017.

Saunders, L.R., Jurecic, V. & Barber, G.N. (2001a) The 90- and 110-kDa human NFAR proteins are translated from two differentially spliced mRNAs encoded on chromosome 19p13. Genomics. 71(2):256-259.

Saunders, L.R., Perkins, D.J., Balachandran, S., Michaels, R., Ford, R., Mayeda, A. & Barber, G.N. (2001b) Characterization of two evolutionarily conserved, alternatively spliced nuclear phosphoproteins, NFAR-1 and -2, that function in mRNA processing and interact with the double-stranded RNA-dependent protein kinase, PKR. J Biol Chem. 276(34):32300-32312.

Saunders, L.R. & Barber, G.N. (2003) The dsRNA binding protein family: critical roles, diverse cellular functions. *FASEB J.* 17(9):961-983. Review.

Schnitzler, D., Bernstein, F., Müller, H. & Becht, H. (1993) The genetic basis for the antigenicity of the VP2 protein of the infectious bursal disease virus. *J Gen Virol.* 74 (Pt 8):1563-1571.

Seeman, N.C., Rosenberg, J.M. & Rich, A. (1976) Sequence-specific recognition of double helical nucleic acids by proteins. *Proc Natl Acad Sci U S A.* 73(3):804-808.

Setiyono, A., Hayashi, T., Yamaguchi, T., Fukushi, H. & Hirai, K. (2001) Detection of cell membrane proteins that interact with virulent infectious bursal disease virus. *J Vet Med Sci.* 63(2):219-221.

Seufert, D.W., Kos, R., Erickson, C.A. & Swalla, B.J. (2000) p68, a DEAD-box RNA helicase, is expressed in chordate embryo neural and mesodermal tissues. *J Exp Zool.* 288(3):193-204.

Sharma, J.M. & Lee, L.F. (1983) Effect of infectious bursal disease on natural killer cell activity and mitogenic response of chicken lymphoid cells: role of adherent cells in cellular immune suppression. *Infect Immun.* 42(2):747-754.

Sharma, J.M. (1984) Effect of infectious bursal disease virus on protection against Marek's disease by turkey herpesvirus vaccine. *Avian Dis.* 28(3):629-640.

Sharma, J.M., Dohms, J.E. & Metz, A.L. (1989) Comparative pathogenesis of serotype 1 and variant serotype 1 isolates of infectious bursal disease virus and their effect on humoral and cellular immune competence of specific-pathogen-free chickens. *Avian Dis.* 33(1):112-124.

Shin, H.J., Kim, S.S., Cho, Y.H., Lee, S.G. & Rho, H.M. (2002) Host cell proteins binding to the encapsidation signal epsilon in hepatitis B virus RNA. *Arch Virol.* 147(3):471-491.

Sivanandan, V. & Maheswaran, S.K. (1980) Immune profile of infectious bursal disease: I. Effect of infectious bursal disease virus on peripheral blood T and B lymphocytes of chickens. *Avian Dis.* 24(3):715-725.

Sivanandan, V., Limcumpao, J.A., Benson, H.J. & Newman, J.A. (1984) Serologic evidence of infectious bursal disease virus serotype II infection in Minnesota turkeys. *Avian Dis.* 28(3):765-769.

Spies, U., Müller, H. & Becht, H. (1987) Properties of RNA polymerase activity associated with infectious bursal disease virus and characterization of its reaction products. *Virus Res.* 8(2):127-140.

Spies, U., Müller, H. & Becht, H. (1989) Nucleotide sequence of infectious bursal disease virus genome segment A delineates two major open reading frames. *Nucleic Acids Res.* 17(19):7982.

Spies, U. & Müller, H. (1990) Demonstration of enzyme activities required for cap structure formation in infectious bursal disease virus, a member of the birnavirus group. *J Gen Virol.* 71 (Pt 4):977-981.

Springer, W.T., Olson, N.O., Kerr, K.M. & Fabacher, C.J. (1983) Responses of specific-pathogen-free chicks to concomitant infections of reovirus (WVU-2937) and infectious bursal disease virus. *Avian Dis.* 27(4):911-917.

St Johnston, D., Brown, N.H., Gall, J.G. & Jantsch, M. (1992) A conserved double-stranded RNA-binding domain. *Proc Natl Acad Sci U S A.* 89(22):10979-10983.

Stoute, S.T., Jackwood, D.J., Sommer-Wagner, S.E., Cooper, G.L., Anderson, M.L., Woolcock, P.R., Bickford, A.A., Sentíes-Cué, C.G. & Charlton, B.R. (2009) The diagnosis of very virulent infectious bursal disease in California pullets. *Avian Dis.* 53(2):321-326.

Stricker, R.L.O., Behrens, S.E. & Mundt, E. (2010) Nuclear factor NF45 interacts with viral proteins of infectious bursal disease virus and inhibits viral replication. *J Virol.* 84(20):10592-10605.

Tacken, M.G., Rottier, P.J., Gielkens, A.L. & Peeters, B.P. (2000) Interactions in vivo between the proteins of infectious bursal disease virus: capsid protein VP3 interacts with the RNA-dependent RNA polymerase, VP1. *J Gen Virol.* 81(Pt 1):209-218.

Tacken, M.G., Peeters, B.P., Thomas, A.A., Rottier, P.J. & Boot, H.J. (2002) Infectious bursal disease virus capsid protein VP3 interacts both with VP1, the RNA-dependent RNA polymerase, and with viral double-stranded RNA. *J Virol.* 76(22):11301-11311.

Tacken, M.G., Van Den Beuken, P.A., Peeters, B.P., Thomas, A.A., Rottier, P.J. & Boot, H.J. (2003) Homotypic interactions of the infectious bursal disease virus proteins VP3, pVP2, VP4, and VP5: mapping of the interacting domains. *Virology* 312(2):306-319.

Tacken, M.G., Thomas, A.A., Peeters, B.P., Rottier, P.J. & Boot, H.J. (2004) VP1, the RNA-dependent RNA polymerase and genome-linked protein of infectious bursal disease virus, interacts with the carboxy-terminal domain of translational eukaryotic initiation factor 4AII. *Arch Virol.* 149(11):2245-2260.

Tan, D.Y., Hair Bejo, M., Aini, I., Omar, A.R. & Goh, Y.M. (2004) Base usage and dinucleotide frequency of infectious bursal disease virus. *Virus Genes* 28(1):41-53.

Tang, H., Gaietta, G.M., Fischer, W.H., Ellisman, M.H. & Wong-Staal, F. (1997) A cellular cofactor for the constitutive transport element of type D retrovirus. *Science.* 276(5317):1412-1415.

Tanimura, N. & Sharma, .J.M. (1998) In-situ apoptosis in chickens infected with infectious bursal disease virus. *J Comp Pathol.* 118(1):15-27.

Tanner, N.K. & Linder, P. (2001) DExD/H box RNA helicases: from generic motors to specific dissociation functions. *Mol Cell.* 8(2):251-262.

Tham, K.M. & Moon, C.D. (1996) Apoptosis in cell cultures induced by infectious bursal disease virus following in vitro infection. *Avian Dis.* 40(1):109-113.

Thomis, D.C. & Samuel, C.E. (1995) Mechanism of interferon action: characterization of the intermolecular autophosphorylation of PKR, the interferon-inducible, RNA-dependent protein kinase. *J Virol.* 69(8):5195-5198.

Thornton, D.H. & Pattison, M. (1975) Comparison of vaccines against infectious bursal disease. *J Comp Pathol.* 85(4):597-610.

Ting, N.S., Kao, P.N., Chan, D.W., Lintott, L.G. & Lees-Miller, S.P. (1998) DNA-dependent protein kinase interacts with antigen receptor response element binding proteins NF90 and NF45. *J Biol Chem.* 273(4):2136-2145.

Todd, D. & McNulty, M.S. (1979) Biochemical studies with infectious bursal disease virus: comparison of some of its properties with infectious pancreatic necrosis virus. *Arch Virol.* 60(3-4):265-277.

Toro, H., van Santen, V.L., Hoerr, F.J. & Breedlove, C. (2009) Effects of chicken anemia virus and infectious bursal disease virus in commercial chickens. *Avian Dis.* 53(1):94-102.

Tsukamoto, K., Tanimura, N., Hihara, H., Shirai, J., Imai, K., Nakamura, K. & Maeda, M. (1992) Isolation of virulent infectious bursal disease virus from field outbreaks with high mortality in Japan. *J Vet Med Sci.* 54(1):153-155.

Tsukamoto, K., Tanimura, N., Kakita, S., Ota, K., Mase, M., Imai, K. & Hihara, H. (1995) Efficacy of Three Live Vaccines against Highly Virulent Infectious Bursal Disease Virus in Chickens with or without Maternal Antibodies. *Avian Dis.* 39(2):218-229.

Urcuqui-Inchima, S., Castaño, M.E., Hernandez-Verdun, D., St-Laurent, G. 3rd & Kumar, A. (2006) Nuclear Factor 90, a cellular dsRNA binding protein inhibits the HIV Rev-export function. *Retrovirology.* 3:83.

Vakharia, V.N., He, J., Ahamed, B. & Snyder, D.B. (1994) Molecular basis of antigenic variation in infectious bursal disease virus. *Virus Res.* 31(2):265-273.

Van den Berg, T.P. & Meulemans, G. (1991) Acute infectious bursal disease in poultry: protection afforded by maternally derived antibodies and interference with live vaccination. *Avian Pathol.* 20(3):409-421.

Van den Berg, T.P., Gonze, M. & Meulemans, G (1991) Acute infectious bursal disese in poultry: Isolation and characterisation of a highly virulent strain. *Avian Pathol.* 20(1):133-143.

Van den Berg, T.P., Gonze, M., Morales, D. & Meulemans, G. (1996) Acute infectious bursal disease in poultry: Immunological and molecular basis of antigenicity of a highly virulent strain. *Avian Pathol.* 25(4):751-768.

Van den Berg, T.P. (2000) Acute infectious bursal disease in poultry: a review. *Avian Pathol.* 29(3):175-194.

Vasconcelos, A.C. & Lam, K.M. (1994) Apoptosis induced by infectious bursal disease virus. *J Gen Virol.* 75 (Pt 7):1803-1806.

Viranaicken, W., Gasmi, L., Chauvin, C., Denoulet, P. & Larcher, J.C. (2006) Identification of a newly spliced exon in the mouse Ilf3 gene generating two long and short isoforms of Ilf3 and NF90. Genomics. 88(5):622-632.

Von Einem, U.I., Gorbalenya, A.E., Schirrmeier, H., Behrens, S.E., Letzel, T. & Mundt E. (2004) VP1 of infectious bursal disease virus is an RNA-dependent RNA polymerase. *J Gen Virol.* 85(Pt 8):2221-2229.

Wagner, K. & Kösters, J. (1968) Serologische Untersuchungen über die infektiöse Bursitis der Junghennen (Gumboro disease) [Serological examinations into infectious bursitis in young pullets (Gumboro disease)]. *Berl Munch Tierarztl Wochenschr.* 81(23):464-466.

Wang, Y., Wu, X., Li, H., Wu, Y., Shi, L., Zheng, X., Luo, M., Yan, Y. & Zhou, J. (2009) Antibody to VP4 protein is an indicator discriminating pathogenic and nonpathogenic IBDV infection. *Mol Immunol.* 46(10):1964-1969.

Wei, Y., Li, J., Zheng, J., Xu, H., Li, L. & Yu, L. (2006) Genetic reassortment of infectious bursal disease virus in nature. *Biochem Biophys Res Commun.* 350(2):277-287.

Wei, Y., Yu, X., Zheng, J., Chu, W., Xu, H., Yu, X. and Yu, L. (2008) Reassortant infectious bursal disease virus isolated in China. *Virus Res.* 131(2):279-282.

Whitfill, C.E., Haddad, E.E., Ricks, C.A., Skeeles, J.K., Newberry, L.A., Beasley, J.N., Andrews, P.D., Thoma, J.A. and Wakenell, P.S. (1995) Determination of optimum formulation of a novel infectious bursal disease virus (IBDV) vaccine constructed by mixing bursal disease antibody with IBDV. *Avian Dis.* 39(4):687-699.

Wickner, R.B. (1993) Double-stranded RNA virus replication and packaging. *J Biol Chem.* 25;268(6):3797-3800. Review.

Wilson, B.J., Bates, G.J., Nicol, S.M., Gregory, D.J., Perkins, N.D. & Fuller-Pace, F.V. (2004) The p68 and p72 DEAD box RNA helicases interact with HDAC1 and repress transcription in a promoter-specific manner. *BMC Mol Biol.* 5:11.

Winterfield, R.W. & Hitchner, S.B. (1964) Gumboro disease - new threat to the poultry industry. *Poultry Digest* May, 206-207.

Winterfield, R.W. & Thacker, H.L. (1978) Immune response and pathogenicity of different strains of infectious bursal disease virus applied as vaccines. *Avian Dis.* 22(4):721-731.

Winterfield, R.W., Dhillon, A.S., Thacker, H.L. & Alby, L.J. (1980) Immune Response of White Leghorn Chicks from Vaccination with Different Strains of Infectious Bursal Disease Virus and in the Presence of Maternal Antibodies Avian Dis. 24(1):179-188.

Wong, R.T., Hon, C.C., Zeng, F. & Leung, F.C. (2007) Screening of differentially expressed transcripts in infectious bursal disease virus-induced apoptotic chicken embryonic fibroblasts by using cDNA microarrays. *J Gen Virol.* 88(Pt 6):1785-1796.

Wood, G.W., Muskett, J.C. & Thornton, D.H. (1981) The interaction of live vaccine and maternal antibody in protection against infectious bursal disease. *Avian Pathol.* 10(3):365-373.

Wu, C.C., Rubinelli, P. & Lin, T.L. (2007) Molecular detection and differentiation of infectious bursal disease virus. *Avian Dis.* 51(2):515-526. Review.

Wyeth, P.J. (1975) Effect of infectious bursal disease on the response of chickens to S typhimurium and E coli infections. *Vet Rec.* 96(11):238-243.

Xu, Y.H., Leonova, T. & Grabowski, G.A. (2003) Cell cycle dependent intracellular distribution of two spliced isoforms of TCP/ILF3 proteins. Mol Genet Metab. 80(4):426-436.

Yamaguchi, T., Ogawa, M., Inoshima, Y., Miyoshi, M., Fukushi, H. & Hirai, K. (1996) Identification of sequence changes responsible for the attenuation of highly virulent infectious bursal disease virus. *Virology* 223(1):219-223.

Yamaguchi, T., Ogawa, M., Miyoshi, M., Inoshima, Y., Fukushi, H. & Hirai, K. (1997) Sequence and phylogenetic analyses of highly virulent infectious bursal disease virus. *Arch Virol.* 142(7):1441-1458.

Yang, L., Yang, J., Huang, Y. & Liu, Z.R. (2004) Phosphorylation of p68 RNA helicase regulates RNA binding by the C-terminal domain of the protein. *Biochem Biophys Res Commun.* 314(2):622-630.

Yao, K. & Vakharia, V.N. (2001) Induction of apoptosis in vitro by the 17-kDa nonstructural protein of infectious bursal disease virus: possible role in viral pathogenesis. *Virology* 285(1):50-58.

Yedavalli, V.S., Neuveut, C., Chi, Y.H., Kleiman, L. & Jeang, K.T. (2004) Requirement of DDX3 DEAD box RNA helicase for HIV-1 Rev-RRE export function. *Cell.* 119(3):381-392.

Yehuda, H., Pitcovski, J., Michael, A., Gutter, B. & Goldway, M. (1999) Viral protein 1 sequence analysis of three infectious bursal disease virus strains: a very virulent virus, its attenuated form, and an attenuated vaccine. Avian Dis. 43(1):55-64.

Yuasa, N., Taniguchi, T., Noguchi, T. & Yoshida, I. (1980) Effect of Infectious Bursal Disease Virus Infection on Incidence of Anemia by Chicken Anemia Agent. Avian Dis. 24(1):202-209.

Zhao, G., Shi, L., Qiu, D., Hu, H. & Kao, P.N. (2005) NF45/ILF2 tissue expression, promoter analysis, and interleukin-2 transactivating function. *Exp Cell Res.* 305(2):312-323.

Zheng, X., Hong, L., Shi, L., Guo, J., Sun, Z. & Zhou, J. (2008) Proteomics analysis of host cells infected with infectious bursal disease virus. *Mol Cell Proteomics.* 7(3):612-625.

Zierenberg, K., Raue, R., Nieper, H., Islam, M.R., Eterradossi, N., Toquin, D. & Müller, H. (2004) Generation of serotype 1/serotype 2 reassortant viruses of the infectious bursal disease virus and their investigation in vitro and in vivo. Virus Res. 15;105(1):23-34.

6 Appendix

6.1 Abbreviations

°	degree
%	percent
A	alpha, anti
A	alanine, adenosine
aa	amino acid(s)
APS	Ammonium persulfate
ATCC	American Type Culture Collection
b	base
bp	basepair(s)
β	beta
BHK	baby hamster kidney
BLAST	Basic Local Alignment Search Tool
BSA	bovine serum albumin
BSV	Blotched Snakehead virus
BF	bursa of Fabricius
BVDV	bovine viral diarrhea virus
c	centi, complementary
C	Celsius, cytidine, cysteine, carboxy
CEC	Chicken embryo cells
CEF	Chicken embyo fibroblasts
Ch	chicken
CLSM	confocal laser scanning microscopy
CMV	cytomegalovirus
co	control
CO_2	carbon dioxide
CPE	cytopathic effect
CTE	constitutive transport element
Ctv	C-terminal variant
Cy	Cyanine
d	day(s), deoxy
D	aspartic acid
Da	Dalton
DABCO	1,4-Diazabicyclo[2.2.2]octane
DAPI	4',6-diamidino-2-phenylindole
dd	di-deoxy
ddH_2O	double-distilled water
DEPC	Diethylpyrocarbonate
DMEM	Dulbecco's Modified Eagles's Medium
DMSO	Dimethyl sulfoxide
DNA	Deoxiribonucleic Acid
DNase	Deoxyribonuclease
DRBD	double stranded RNA-binding domain
ds	double stranded
DTT	Dithiothreitol
DXV	Drosophila X virus
E	glutamic acid
EDTA	Ethylenedinitrilotetraacetic acid
EGTA	ethylene glycol tetraacetic acid
eIF	eukaryotic initiation factor
ELISA	enzyme-linked immunosorbent assay
EM	electron microscope
EV	Eel virus
F	phenylalanine
FBS	Fetal Bovine Serum
FITC	fluorescein
FL	full length
FP	forward primer
g	gram
G	glycine, guanosine
GAP	GTPase activating protein
GEF	guanosine nucleotide exchange factor
h	hour(s)
H	histidine
HBV	hepatitis B virus
HCl	Hydrochloric acid
HCV	hepatitis C virus
HEPES	4-(2-hydroxyethyl)-1-piperazineethanesulfonic acid
His	histidine
HIV	Human immunodeficiency virus
HRP	horseradish peroxidase
I	isoleucine
IBD/IBDV	Infectious bursal disease/ Infectious bursal disease virus
Ig	Immunoglobulin
IIFA	indirect immunofluorescence assay
Il	Interleukin
IFN	interferon
IP	Immunoprecipitation
IPNV	Infectious Pancreatic Necrosis virus
IPTG	Isopropyl β-D-1-thiogalactopyranoside

IRES	internal ribosome entry site
JIR	Jackson Immuno Research
k	kilo
K	lysine
l	liter
L	leucine
LB	Lysogeny Broth
LMB	Leptomycin B
m	milli, meter, messenger
M	mouse, Molar, Mega, methionine
µ	micro
mAb	monoclonal Antibody(s)
MALDI-TOF	matrix-assisted laser desorption/Ionization – time of flight
MBP	maltose binding protein
MCS	multiple cloning site
MEM	Minimal Essential Medium
MES	4-Morpholineethanesulfonic acid
MESA	MOPS-EDTA-Sodium Acetate Buffer
mi	micro
min	Minute(s)
moi	multiplicity of infection
MS	mass spectrometry
n	nano
N	normal, asparagine, nucleoside, amino
NEB	New England Biolabs
NES	nuclear export signal(s)
NF	nuclear factor
NFAR	nuclear factor associated with dsRNA
NLS	nuclear localization sequence
NP	nucleoprotein
nt	nucleotide
NTR	non-translated region
o/n	over night
ORF	open reading frame
OV	Oyster virus
p	precursor, pico
P	proline
P/S	Penicillin/Streptomycin
PBS	Phosphate-Buffered Saline
PCR	Polymerase Chain Reaction
pi	post infection
PI	Propidium iodide
PKC	protein kinase C
PKR	protein kinase RNA-activated
PMA	phorbol myristate acetate
POD	Peroxidase
pt	post transfection
Q	glutamine
R	rabbit, arginine
RE	Restriction endonuclease
RIPA	Radio Immuno Precipitation Assay
RHA	RNA helicase A
RISC	RNA-induced silencing complex
RNA	Ribonucleic Acid
RNase	Ribonuclease
RP	reverse primer
rpm	revolutions per minute
RRE	Rev response element
RT	Reverse Transcriptase
S	serine
SARS-CoV	severe acute respiratory syndrome-corona virus
SDS-PAGE	Sodium dodecyl sulfate polyacrylamide gel electrophoresis
sec	Second(s)
si	small interfering
SN	supernatant(s)
SOB	Super Optimal Broth
SOC	Super Optimal Broth with Catabolite repression
SPF	specific pathogen free
ss	single stranded
SSC	saline-sodium citrate
T	threonine, thymidine
TAE	Tris-acetate-EDTA
TAR	transactivation responsive region
TBST	Tris-buffered Saline & Tween 20
TE	Tris-EDTA
TEMED	Tetramethylethylenediamine
TLR	toll-like receptor
TP	triphosphate
TV	Tellina virus
U	uridine
USA	United States of America
UV	ultraviolet
V	Volt(s), variable, valine
VP	viral protein
VSV	vesicular stomatitis virus
vv	very virulent
W	tryptophan, watt
X-gal	bromo-chloro-indolyl-galactopyranoside
Y	tyrosine

6.2 Nucleotide and amino acid sequences

Nucleotide sequences of the regulatory elements and genes with their deduced amino acid sequence used.

6.2.1 NF45

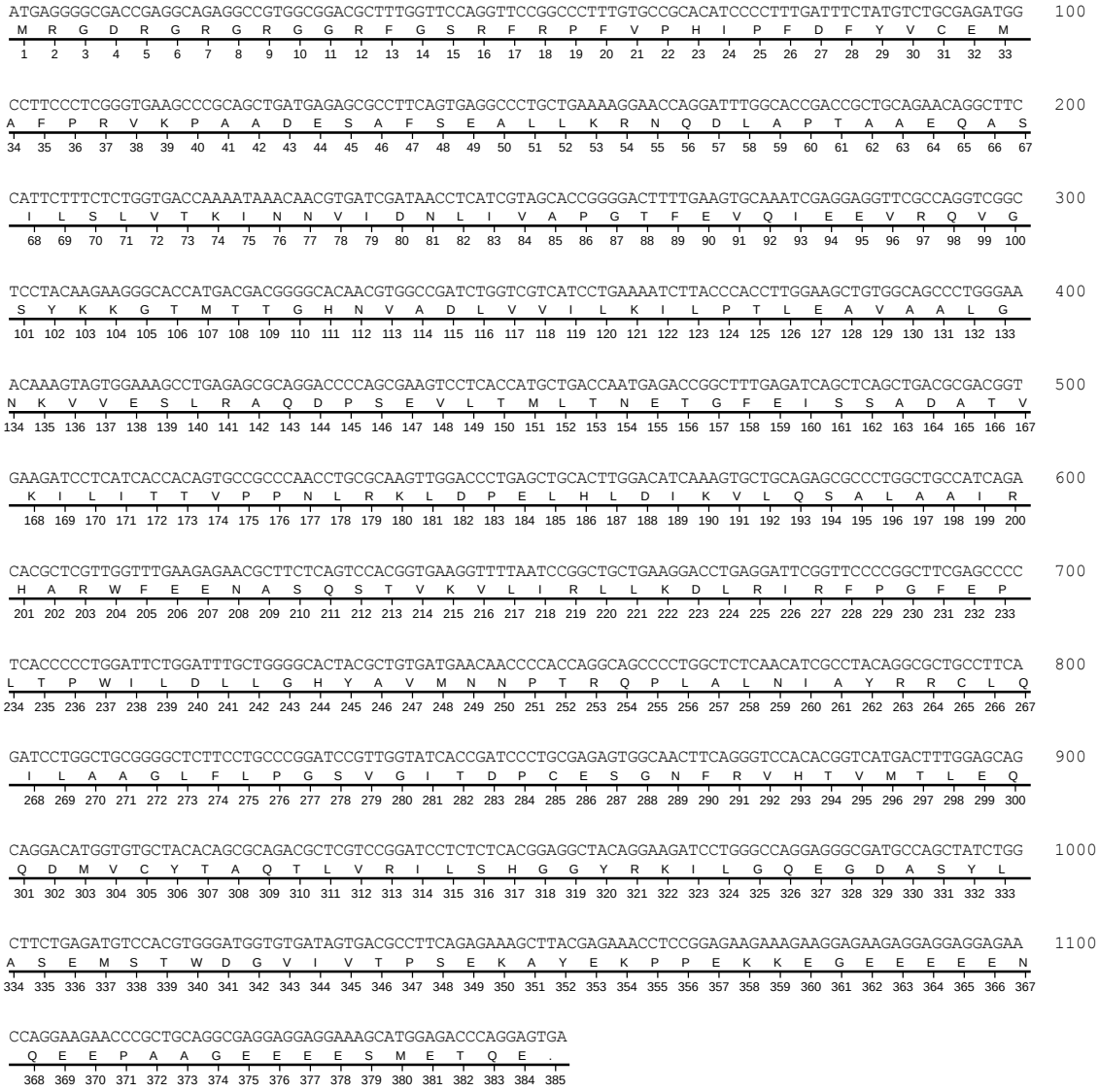

6.2.2 p68

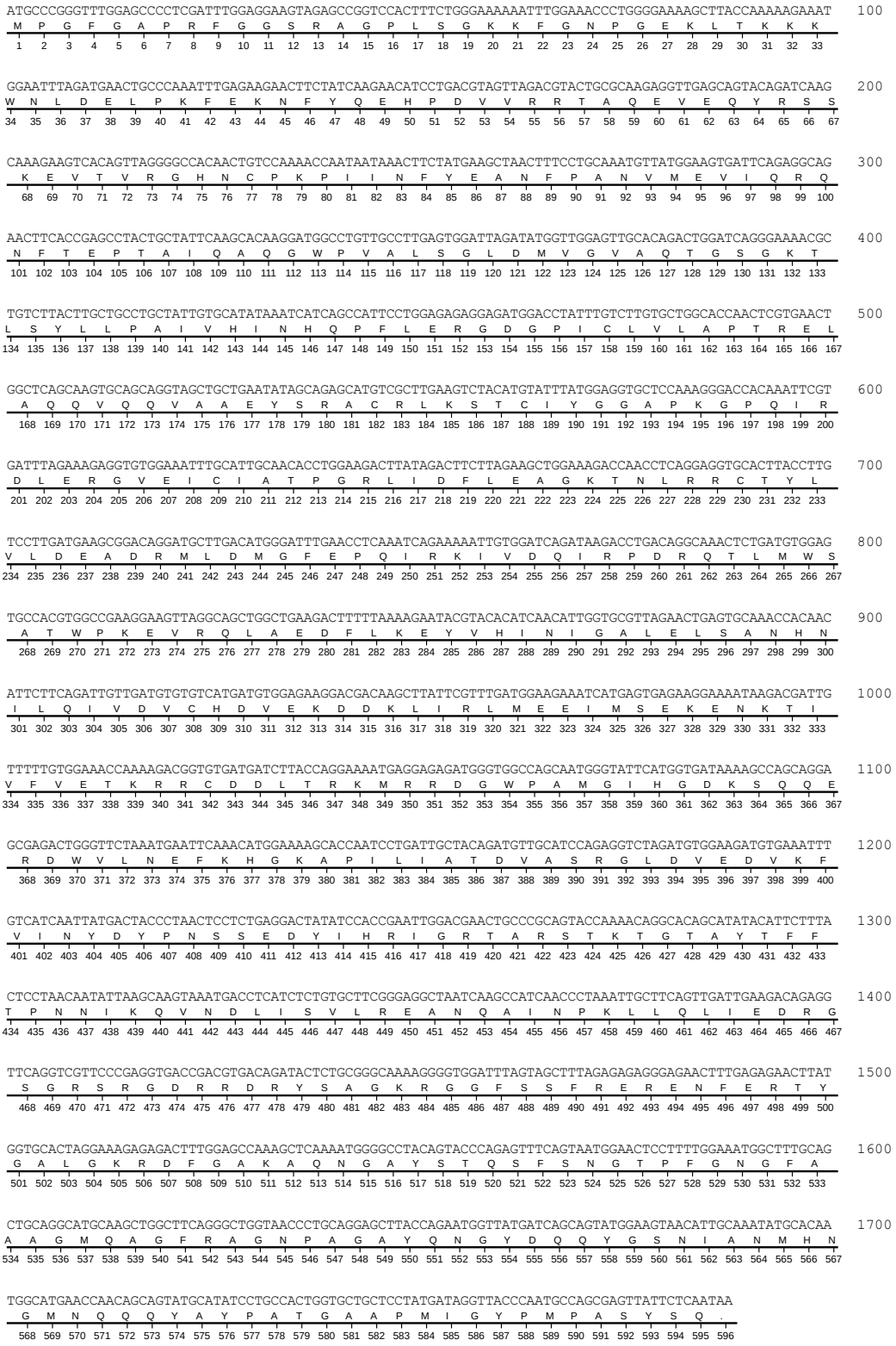
ATGCCCGGGTTTGGAGCCCCTCGATTTGGAGGAAGTAGAGCCGGTCCACTTTCTGGGAAAAAATTTGGAAACCCTGGGGAAAAGCTTACCAAAAAGAAAT 100
M P G F G A P R F G G S R A G P L S G K K F G N P G E K L T K K K
1 2 3 4 5 6 7 8 9 10 11 12 13 14 15 16 17 18 19 20 21 22 23 24 25 26 27 28 29 30 31 32 33
GGAATTTAGATGAACTGCCCAAATTTGAGAAGAACTTCTATCAAGAACATCCTGACGTAGTTAGACGTACTGCGCAAGAGGTTGAGCAGTACAGATCAAG 200
W N L D E L P K F E K N F Y Q E H P D V V R R T A Q E V E Q Y R S S
34 35 36 37 38 39 40 41 42 43 44 45 46 47 48 49 50 51 52 53 54 55 56 57 58 59 60 61 62 63 64 65 66 67
CAAAGAAGTCACAGTTAGGGGCCACAACTGTCCAAAACCAATAATAAACTTCTATGAAGCTAACTTTCCTGCAAATGTTATGGAAGTGATTCAGAGGCAG 300
K E V T V R G H N C P K P I I N F Y E A N F P A N V M E V I Q R Q
68 69 70 71 72 73 74 75 76 77 78 79 80 81 82 83 84 85 86 87 88 89 90 91 92 93 94 95 96 97 98 99 100
AACTTCACCGAGCCTACTGCTATTCAAGCACAAGGATGGCCTGTTGCCTTGAGTGGATTAGATATGGTTGGAGTTGCACAGACTGGATCAGGGAAAACGC 400
N F T E P T A I Q A Q G W P V A L S G L D M V G V A Q T G S G K T
101 102 103 104 105 106 107 108 109 110 111 112 113 114 115 116 117 118 119 120 121 122 123 124 125 126 127 128 129 130 131 132 133
TGTCTTACTTGCTGCCTGCTATTGTGCATATAAATCATCAGCCATTCCTGGAGAGAGGAGATGGACCTATTTGTCTTGTGCTGGCACCAACTCGTGAACT 500
L S Y L L P A I V H I N H Q P F L E R G D G P I C L V L A P T R E L
134 135 136 137 138 139 140 141 142 143 144 145 146 147 148 149 150 151 152 153 154 155 156 157 158 159 160 161 162 163 164 165 166 167
GGCTCAGCAAGTGCAGCAGGTAGCTGCTGAATATAGCAGAGCATGTCGCTTGAAGTCTACATGTATTTATGGAGGTGCTCCAAAGGGACCACAAATTCGT 600
A Q Q V Q Q V A A E Y S R A C R L K S T C I Y G G A P K G P Q I R
168 169 170 171 172 173 174 175 176 177 178 179 180 181 182 183 184 185 186 187 188 189 190 191 192 193 194 195 196 197 198 199 200
GATTTAGAAAGAGGTGTGGAAATTTGCATTGCAACACCTGGAAGACTTATAGACTTCTTAGAAGCTGGAAAGACCAACCTCAGGAGGTGCACTTACCTTG 700
D L E R G V E I C I A T P G R L I D F L E A G K T N L R R C T Y L
201 202 203 204 205 206 207 208 209 210 211 212 213 214 215 216 217 218 219 220 221 222 223 224 225 226 227 228 229 230 231 232 233
TCCTTGATGAAGCGGACAGGATGCTTGACATGGGATTTGAACCTCAAATCAGAAAAATTGTGGATCAGATAAGACCTGACAGGCAAACTCTGATGTGGAG 800
V L D E A D R M L D M G F E P Q I R K I V D Q I R P D R Q T L M W S
234 235 236 237 238 239 240 241 242 243 244 245 246 247 248 249 250 251 252 253 254 255 256 257 258 259 260 261 262 263 264 265 266 267
TGCCACGTGGCCGAAGGAAGTTAGGCAGCTGGCTGAAGACTTTTTAAAAGAATACGTACACATCAACATTGGTGCGTTAGAACTGAGTGCAAACCACAAC 900
A T W P K E V R Q L A E D F L K E Y V H I N I G A L E L S A N H N
268 269 270 271 272 273 274 275 276 277 278 279 280 281 282 283 284 285 286 287 288 289 290 291 292 293 294 295 296 297 298 299 300
ATTCTTCAGATTGTTGATGTGTGTCATGATGTGGAGAAGGACGACAAGCTTATTCGTTTGATGGAAGAAATCATGAGTGAGAAGGAAAATAAGACGATTG 1000
I L Q I V D V C H D V E K D D K L I R L M E E I M S E K E N K T I
301 302 303 304 305 306 307 308 309 310 311 312 313 314 315 316 317 318 319 320 321 322 323 324 325 326 327 328 329 330 331 332 333
TTTTTGTGGAAACCAAAAGACGGTGTGATGATCTTACCAGGAAAATGAGGAGAGATGGGTGGCCAGCAATGGGTATTCATGGTGATAAAAGCCAGCAGGA 1100
V F V E T K R R C D D L T R K M R R D G W P A M G I H G D K S Q Q E
334 335 336 337 338 339 340 341 342 343 344 345 346 347 348 349 350 351 352 353 354 355 356 357 358 359 360 361 362 363 364 365 366 367
GCGAGACTGGGTTCTAAATGAATTCAAACATGGAAAAGCACCAATCCTGATTGCTACAGATGTTGCATCCAGAGGTCTAGATGTGGAAGATGTGAAATTT 1200
R D W V L N E F K H G K A P I L I A T D V A S R G L D V E D V K F
368 369 370 371 372 373 374 375 376 377 378 379 380 381 382 383 384 385 386 387 388 389 390 391 392 393 394 395 396 397 398 399 400
GTCATCAATTATGACTACCCTAACTCCTCTGAGGACTATATCCACCGAATTGGACGAACTGCCCGCAGTACCAAAACAGGCACAGCATATACATTCTTTA 1300
V I N Y D Y P N S S E D Y I H R I G R T A R S T K T G T A Y T F F
401 402 403 404 405 406 407 408 409 410 411 412 413 414 415 416 417 418 419 420 421 422 423 424 425 426 427 428 429 430 431 432 433
CTCCTAACAATATTAAGCAAGTAAATGACCTCATCTCTGTGCTTCGGGAGGCTAATCAAGCCATCAACCCTAAATTGCTTCAGTTGATTGAAGACAGAGG 1400
T P N N I K Q V N D L I S V L R E A N Q A I N P K L L Q L I E D R G
434 435 436 437 438 439 440 441 442 443 444 445 446 447 448 449 450 451 452 453 454 455 456 457 458 459 460 461 462 463 464 465 466 467
TTCAGGTCGTTCCCGAGGTGACCGACGTGACAGATACTCTGCGGGCAAAAGGGGTGGATTTAGTAGCTTTAGAGAGAGGGAGAACTTTGAGAGAACTTAT 1500
S G R S R G D R R D R Y S A G K R G G F S S F R E R E N F E R T Y
468 469 470 471 472 473 474 475 476 477 478 479 480 481 482 483 484 485 486 487 488 489 490 491 492 493 494 495 496 497 498 499 500
GGTGCACTAGGAAAGAGAGACTTTGGAGCCAAAGCTCAAAATGGGGCCTACAGTACCCAGAGTTTCAGTAATGGAACTCCTTTTGGAAATGGCTTTGCAG 1600
G A L G K R D F G A K A Q N G A Y S T Q S F S N G T P F G N G F A
501 502 503 504 505 506 507 508 509 510 511 512 513 514 515 516 517 518 519 520 521 522 523 524 525 526 527 528 529 530 531 532 533
CTGCAGGCATGCAAGCTGGCTTCAGGGCTGGTAACCCTGCAGGAGCTTACCAGAATGGTTATGATCAGCAGTATGGAAGTAACATTGCAAATATGCACAA 1700
A A G M Q A G F R A G N P A G A Y Q N G Y D Q Q Y G S N I A N M H N
534 535 536 537 538 539 540 541 542 543 544 545 546 547 548 549 550 551 552 553 554 555 556 557 558 559 560 561 562 563 564 565 566 567
TGGCATGAACCAACAGCAGTATGCATATCCTGCCACTGGTGCTGCTCCTATGATAGGTTACCCAATGCCAGCGAGTTATTCTCAATAA
G M N Q Q Q Y A Y P A T G A A P M I G Y P M P A S Y S Q .
568 569 570 571 572 573 574 575 576 577 578 579 580 581 582 583 584 585 586 587 588 589 590 591 592 593 594 595 596

6.2.3 Segment A of the IBDV strain D78

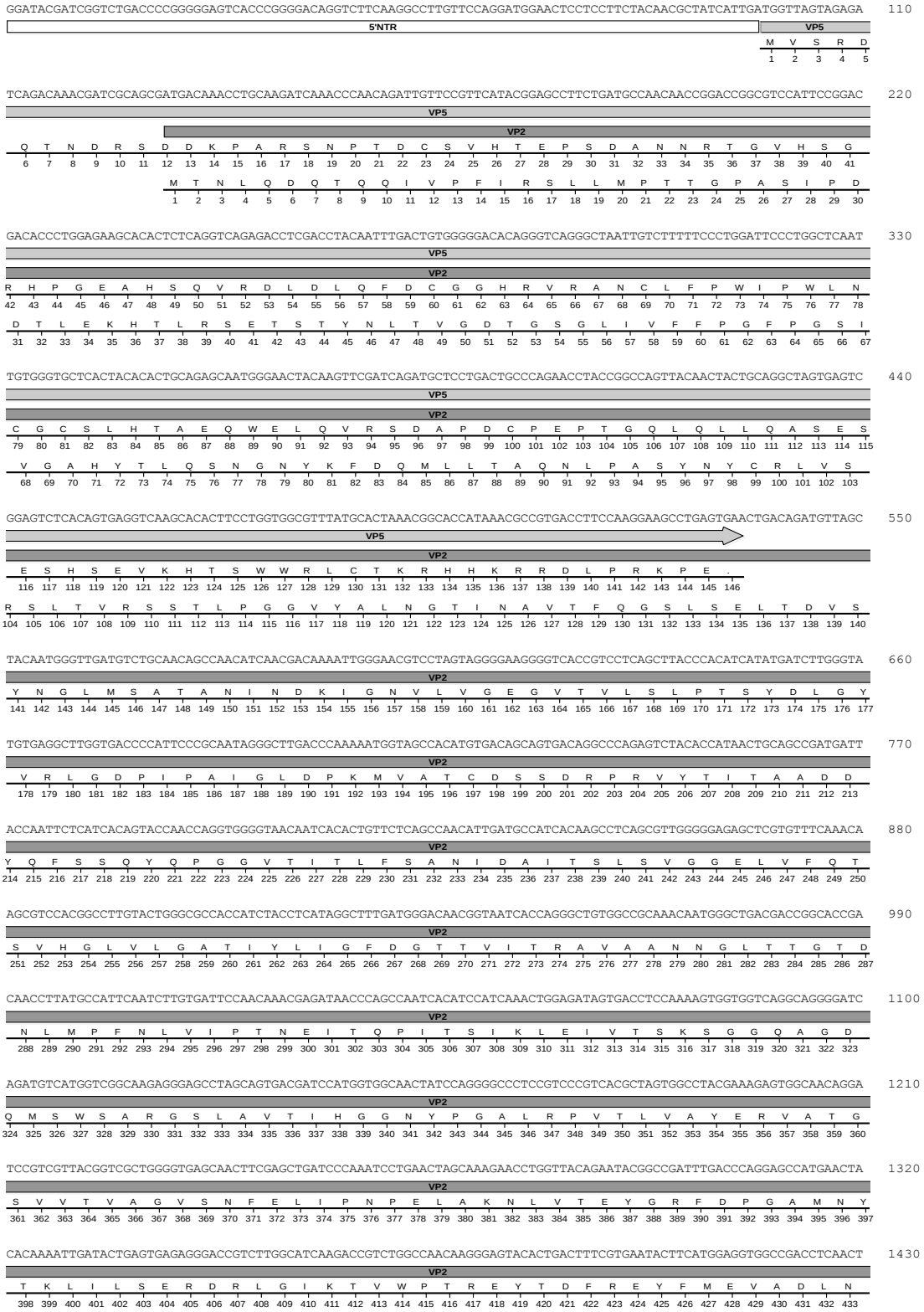

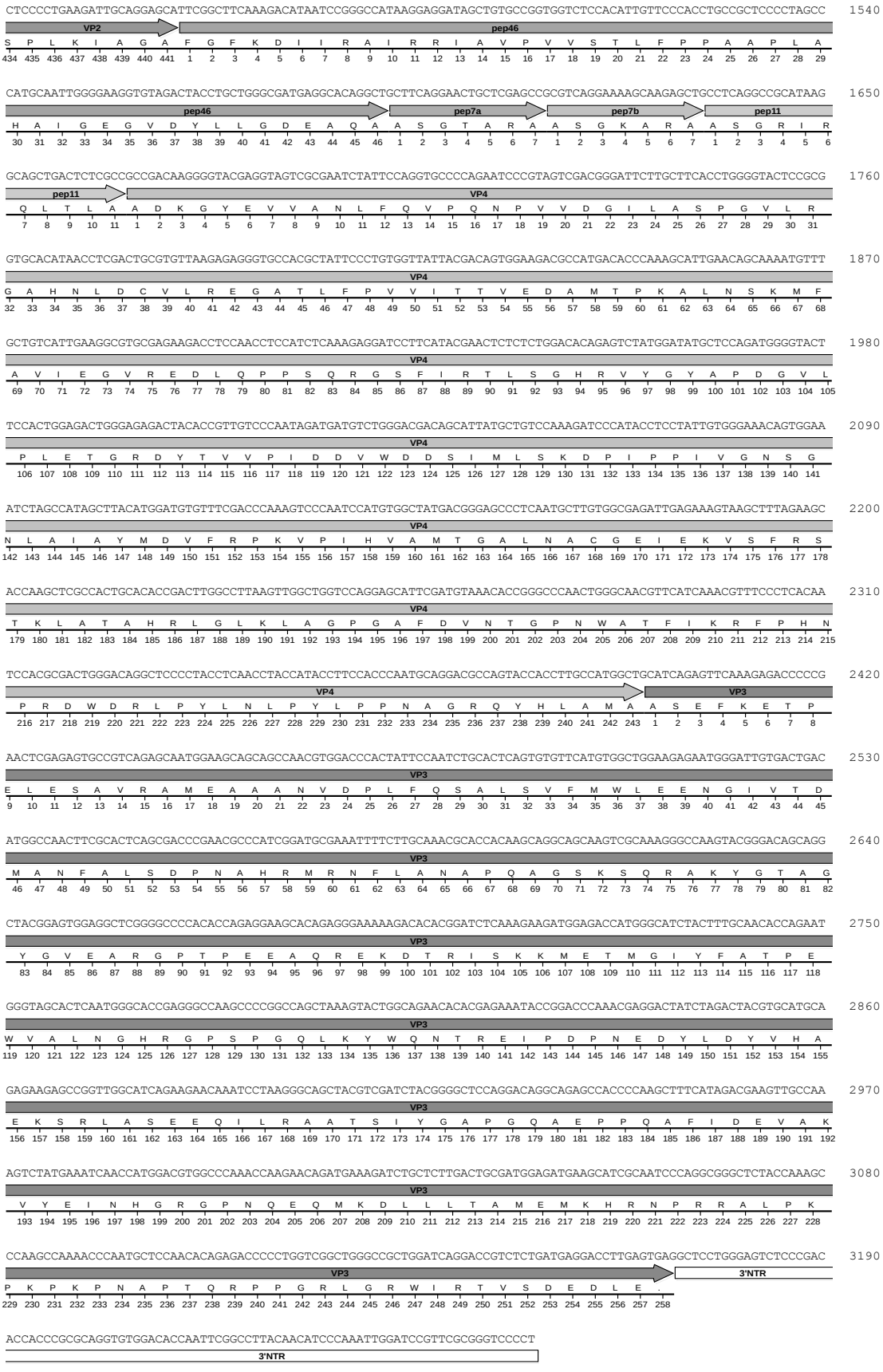
CTCCCCTGAAGATTGCAGGAGCATTCGGCTTCAAAGACATAATCCGGGCCATAAGGAGGATAGCTGTGCCGGTGGTCTCCACATTGTTCCCACCTGCCGCTCCCCTAGCC 1540
VP2
pep46
S P L K I A G A F G F K D I I R A I R R I A V P V V S T L F P P A A P L A
434 435 436 437 438 439 440 441 1 2 3 4 5 6 7 8 9 10 11 12 13 14 15 16 17 18 19 20 21 22 23 24 25 26 27 28 29
CATGCAATTGGGGAAGGTGTAGACTACCTGCTGGGCGATGAGGCACAGGCTGCTTCAGGAACTGCTCGAGCCGCGTCAGGAAAAGCAAGAGCTGCCTCAGGCCGCATAAG 1650
pep46
pep7a
pep7b
pep11
H A I G E G V D Y L L G D E A Q A A S G T A R A A S G K A R A A S G R I R
30 31 32 33 34 35 36 37 38 39 40 41 42 43 44 45 46 1 2 3 4 5 6 7 1 2 3 4 5 6 7 1 2 3 4 5 6
GCAGCTGACTCTCGCCGCCGACAAGGGGTACGAGGTAGTCGCGAATCTATTCCAGGTGCCCCAGAATCCCGTAGTCGACGGGATTCTTGCTTCACCTGGGGTACTCCGCG 1760
pep11
VP4
Q L T L A A D K G Y E V V A N L F Q V P Q N P V V D G I L A S P G V L R
7 8 9 10 11 1 2 3 4 5 6 7 8 9 10 11 12 13 14 15 16 17 18 19 20 21 22 23 24 25 26 27 28 29 30 31
GTGCACATAACCTCGACTGCGTGTTAAGAGAGGGTGCCACGCTATTCCCTGTGGTTATTACGACAGTGGAAGACGCCATGACACCCAAAGCATTGAACAGCAAAATGTTT 1870
VP4
G A H N L D C V L R E G A T L F P V V I T T V E D A M T P K A L N S K M F
32 33 34 35 36 37 38 39 40 41 42 43 44 45 46 47 48 49 50 51 52 53 54 55 56 57 58 59 60 61 62 63 64 65 66 67 68
GCTGTCATTGAAGGCGTGCGAGAAGACCTCCAACCTCCATCTCAAAGAGGATCCTTCATACGAACTCTCTCTGGACACAGAGTCTATGGATATGCTCCAGATGGGGTACT 1980
VP4
A V I E G V R E D L Q P P S Q R G S F I R T L S G H R V Y G Y A P D G V L
69 70 71 72 73 74 75 76 77 78 79 80 81 82 83 84 85 86 87 88 89 90 91 92 93 94 95 96 97 98 99 100 101 102 103 104 105
TCCACTGGAGACTGGGAGAGACTACACCGTTGTCCCAATAGATGATGTCTGGGACGACAGCATTATGCTGTCCAAAGATCCCATACCTCCTATTGTGGGAAACAGTGGAA 2090
VP4
P L E T G R D Y T V V P I D D V W D D S I M L S K D P I P P I V G N S G
106 107 108 109 110 111 112 113 114 115 116 117 118 119 120 121 122 123 124 125 126 127 128 129 130 131 132 133 134 135 136 137 138 139 140 141
ATCTAGCCATAGCTTACATGGATGTGTTTCGACCCAAAGTCCCAATCCATGTGGCTATGACGGGAGCCCTCAATGCTTGTGGCGAGATTGAGAAAGTAAGCTTTAGAAGC 2200
VP4
N L A I A Y M D V F R P K V P I H V A M T G A L N A C G E I E K V S F R S
142 143 144 145 146 147 148 149 150 151 152 153 154 155 156 157 158 159 160 161 162 163 164 165 166 167 168 169 170 171 172 173 174 175 176 177 178
ACCAAGCTCGCCACTGCACACCGACTTGGCCTTAAGTTGGCTGGTCCAGGAGCATTCGATGTAAACACCGGGCCCAACTGGGCAACGTTCATCAAACGTTTCCCTCACAA 2310
VP4
T K L A T A H R L G L K L A G P G A F D V N T G P N W A T F I K R F P H N
179 180 181 182 183 184 185 186 187 188 189 190 191 192 193 194 195 196 197 198 199 200 201 202 203 204 205 206 207 208 209 210 211 212 213 214 215
TCCACGCGACTGGGACAGGCTCCCCTACCTCAACCTACCATACCTTCCACCCAATGCAGGACGCCAGTACCACCTTGCCATGGCTGCATCAGAGTTCAAAGAGACCCCCG 2420
VP4
VP3
P R D W D R L P Y L N L P Y L P P N A G R Q Y H L A M A A S E F K E T P
216 217 218 219 220 221 222 223 224 225 226 227 228 229 230 231 232 233 234 235 236 237 238 239 240 241 242 243 1 2 3 4 5 6 7 8
AACTCGAGAGTGCCGTCAGAGCAATGGAAGCAGCAGCCAACGTGGACCCACTATTCCAATCTGCACTCAGTGTGTTCATGTGGCTGGAAGAGAATGGGATTGTGACTGAC 2530
VP3
E L E S A V R A M E A A A A N V D P L F Q S A L S V F M W L E E N G I V T D
9 10 11 12 13 14 15 16 17 18 19 20 21 22 23 24 25 26 27 28 29 30 31 32 33 34 35 36 37 38 39 40 41 42 43 44 45
ATGGCCAACTTCGCACTCAGCGACCCGAACGCCCATCGGATGCGAAATTTTCTTGCAAACGCACCACAAGCAGGCAGCAAGTCGCAAAGGGCCAAGTACGGGACAGCAGG 2640
VP3
M A N F A L S D P N A H R M R N F L A N A P Q A G S K S Q R A K Y G T A G
46 47 48 49 50 51 52 53 54 55 56 57 58 59 60 61 62 63 64 65 66 67 68 69 70 71 72 73 74 75 76 77 78 79 80 81 82
CTACGGAGTGGAGGCTCGGGGCCCCACACCAGAGGAAGCACAGAGGGAAAAAGACACACGGATCTCAAAGAAGATGGAGACCATGGGCATCTACTTTGCAACACCAGAAT 2750
VP3
Y G V E A R G P T P E E A Q R E K D T R I S K K M E T M G I Y F A T P E
83 84 85 86 87 88 89 90 91 92 93 94 95 96 97 98 99 100 101 102 103 104 105 106 107 108 109 110 111 112 113 114 115 116 117 118
GGGTAGCACTCAATGGGCACCGAGGGCCAAGCCCCGGCCAGCTAAAGTACTGGCAGAACACACGAGAAATACCGGACCCAAACGAGGACTATCTAGACTACGTGCATGCA 2860
VP3
W V A L N G H R G P S P G Q L K Y W Q N T R E I P D P N E D Y L D Y V H A
119 120 121 122 123 124 125 126 127 128 129 130 131 132 133 134 135 136 137 138 139 140 141 142 143 144 145 146 147 148 149 150 151 152 153 154 155
GAGAAGAGCCGGTTGGCATCAGAAGAACAAATCCTAAGGGCAGCTACGTCGATCTACGGGGCTCCAGGACAGGCAGAGCCACCCCAAGCTTTCATAGACGAAGTTGCCAA 2970
VP3
E K S R L A S E E Q I L R A A T S I Y G A P G Q A E P P Q A F I D E V A K
156 157 158 159 160 161 162 163 164 165 166 167 168 169 170 171 172 173 174 175 176 177 178 179 180 181 182 183 184 185 186 187 188 189 190 191 192
AGTCTATGAAATCAACCATGGACGTGGCCCAAACCAAGAACAGATGAAAGATCTGCTCTTGACTGCGATGGAGATGAAGCATCGCAATCCCAGGCGGGCTCTACCAAAGC 3080
VP3
V Y E I N H G R G P N Q E Q M K D L L L T A M E M K H R N P R R A L P K
193 194 195 196 197 198 199 200 201 202 203 204 205 206 207 208 209 210 211 212 213 214 215 216 217 218 219 220 221 222 223 224 225 226 227 228
CCAAGCCAAAACCCAATGCTCCAACACAGAGACCCCCTGGTCGGCTGGGCCGCTGGATCAGGACCGTCTCTGATGAGGACCTTGAGTGAGGCTCCTGGGAGTCTCCCGAC 3190
VP3
3'NTR
P K P K P N A P T Q R P P G R L G R W I R T V S D E D L E .
229 230 231 232 233 234 235 236 237 238 239 240 241 242 243 244 245 246 247 248 249 250 251 252 253 254 255 256 257 258
ACCACCCGCGCAGGTGTGGACACCAATTCGGCCTTACAACATCCCAAATTGGATCCGTTCGCGGGTCCCCT
3'NTR

6.2.4 Segment B of the IBDV strain D78

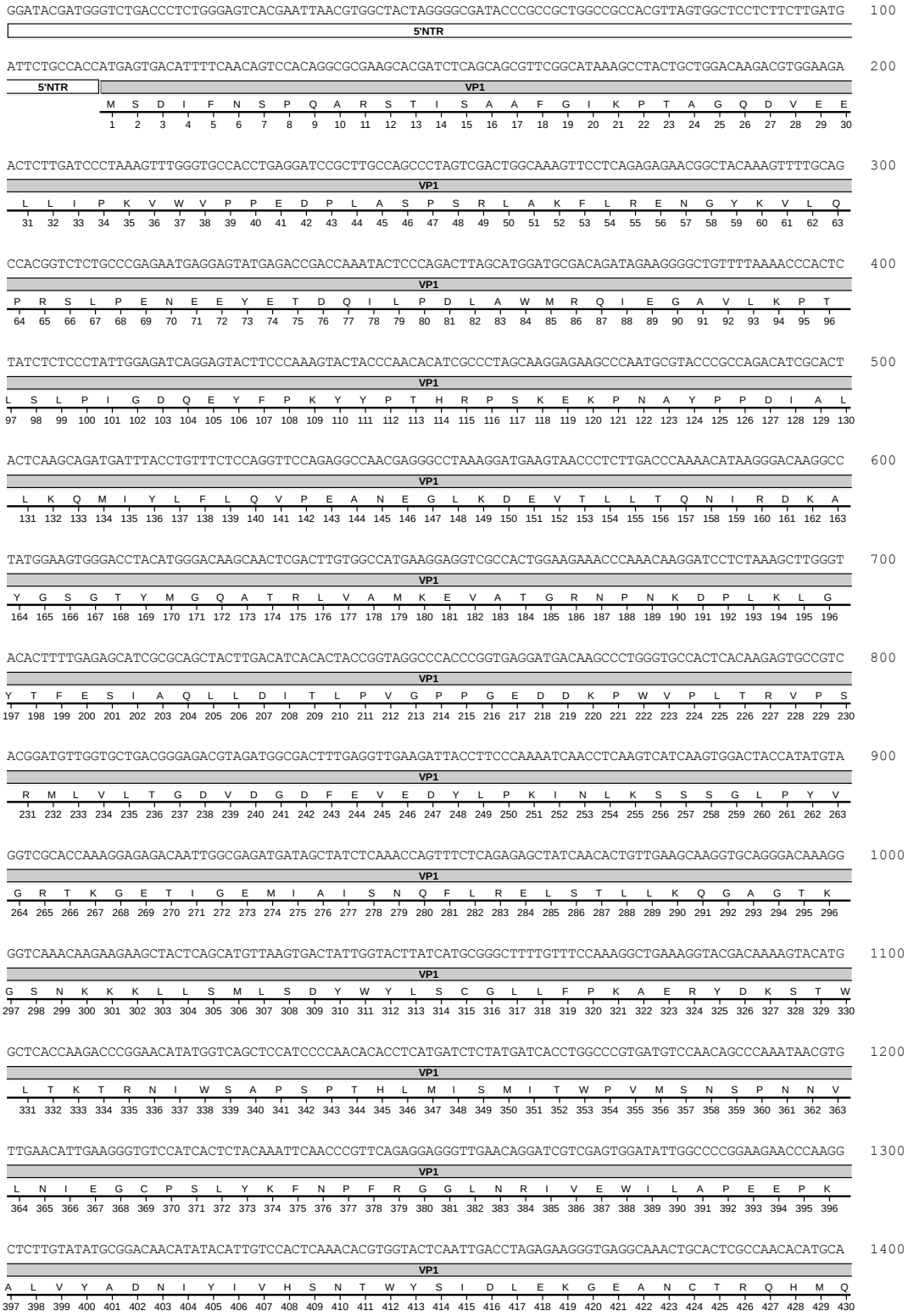

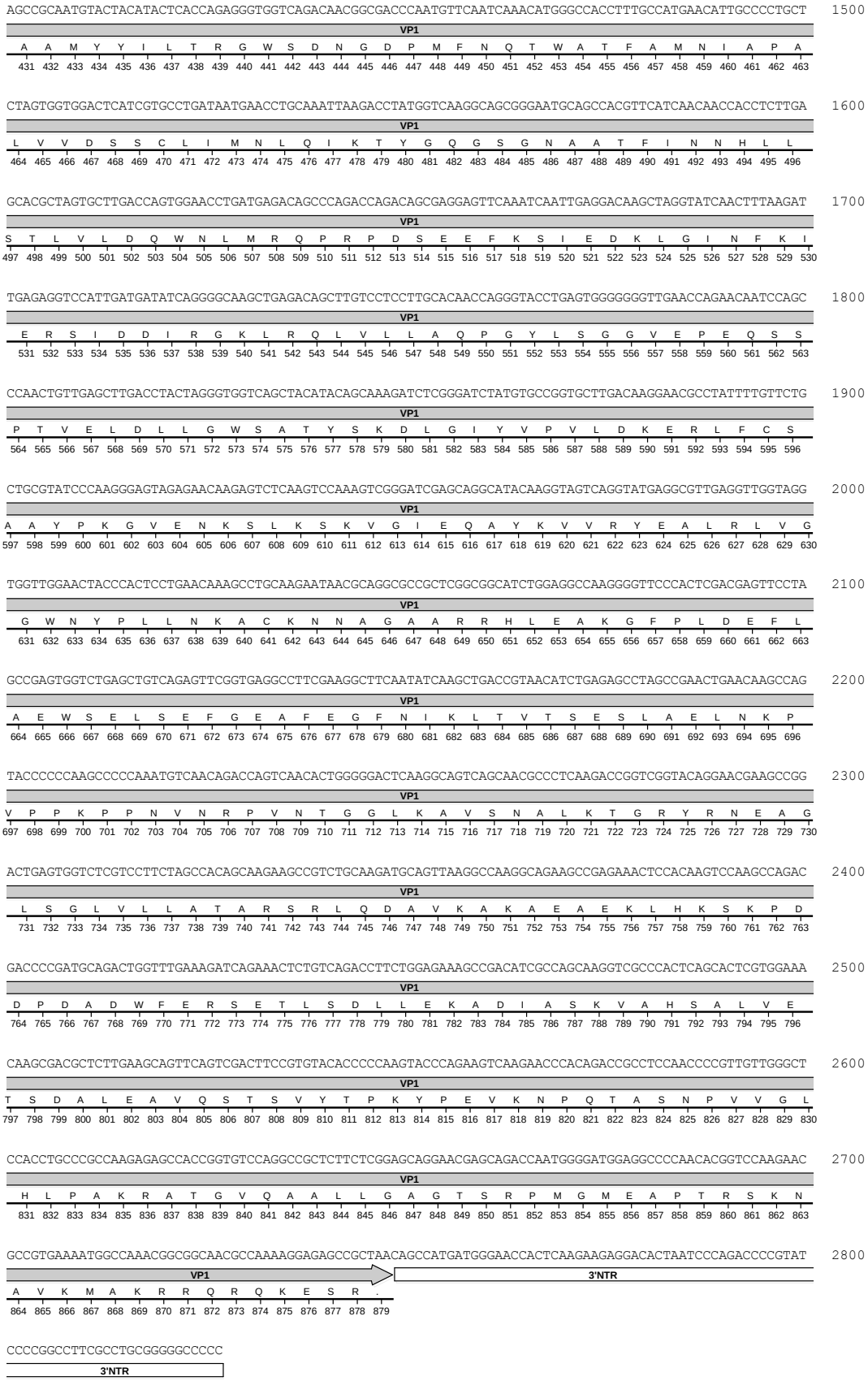
AGCCGCAATGTACTACATACTCACCAGAGGGTGGTCAGACAACGGCGACCCAATGTTCAATCAAACATGGGCCACCTTTGCCATGAACATTGCCCCTGCT 1500
VP1
A A M Y Y I L T R G W S D N G D P M F N Q T W A T F A M N I A P A
431 432 433 434 435 436 437 438 439 440 441 442 443 444 445 446 447 448 449 450 451 452 453 454 455 456 457 458 459 460 461 462 463
CTAGTGGTGGACTCATCGTGCCTGATAATGAACCTGCAAATTAAGACCTATGGTCAAGGCAGCGGGAATGCAGCCACGTTCATCAACAACCACCTCTTGA 1600
VP1
L V V D S S C L I M N L Q I K T Y G Q G S G N A A T F I N N H L L
464 465 466 467 468 469 470 471 472 473 474 475 476 477 478 479 480 481 482 483 484 485 486 487 488 489 490 491 492 493 494 495 496
GCACGCTAGTGCTTGACCAGTGGAACCTGATGAGACAGCCCAGACCAGACAGCGAGGAGTTCAAATCAATTGAGGACAAGCTAGGTATCAACTTTAAGAT 1700
VP1
S T L V L D Q W N L M R Q P R P D S E E F K S I E D K L G I N F K I
497 498 499 500 501 502 503 504 505 506 507 508 509 510 511 512 513 514 515 516 517 518 519 520 521 522 523 524 525 526 527 528 529 530
TGAGAGGTCCATTGATGATATCAGGGGCAAGCTGAGACAGCTTGTCCTCCTTGCACAACCAGGGTACCTGAGTGGGGGGGTTGAACCAGAACAATCCAGC 1800
VP1
E R S I D D I R G K L R Q L V L L A Q P G Y L S G G V E P E Q S S
531 532 533 534 535 536 537 538 539 540 541 542 543 544 545 546 547 548 549 550 551 552 553 554 555 556 557 558 559 560 561 562 563
CCAACTGTTGAGCTTGACCTACTAGGGTGGTCAGCTACATACAGCAAAGATCTCGGGATCTATGTGCCGGTGCTTGACAAGGAACGCCTATTTTGTTCTG 1900
VP1
P T V E L D L L G W S A T Y S K D L G I Y V P V L D K E R L F C S
564 565 566 567 568 569 570 571 572 573 574 575 576 577 578 579 580 581 582 583 584 585 586 587 588 589 590 591 592 593 594 595 596
CTGCGTATCCCAAGGGAGTAGAGAACAAGAGTCTCAAGTCCAAAGTCGGGATCGAGCAGGCATACAAGGTAGTCAGGTATGAGGCGTTGAGGTTGGTAGG 2000
VP1
A A Y P K G V E N K S L K S K V G I E Q A Y K V V R Y E A L R L V G
597 598 599 600 601 602 603 604 605 606 607 608 609 610 611 612 613 614 615 616 617 618 619 620 621 622 623 624 625 626 627 628 629 630
TGGTTGGAACTACCCACTCCTGAACAAAGCCTGCAAGAATAACGCAGGCGCCGCTCGGCGGCATCTGGAGGCCAAGGGGTTCCCACTCGACGAGTTCCTA 2100
VP1
G W N Y P L L N K A C K N N A G A A R R H L E A K G F P L D E F L
631 632 633 634 635 636 637 638 639 640 641 642 643 644 645 646 647 648 649 650 651 652 653 654 655 656 657 658 659 660 661 662 663
GCCGAGTGGTCTGAGCTGTCAGAGTTCGGTGAGGCCTTCGAAGGCTTCAATATCAAGCTGACCGTAACATCTGAGAGCCTAGCCGAACTGAACAAGCCAG 2200
VP1
A E W S E L S E F G E A F E G F N I K L T V T S E S L A E L N K P
664 665 666 667 668 669 670 671 672 673 674 675 676 677 678 679 680 681 682 683 684 685 686 687 688 689 690 691 692 693 694 695 696
TACCCCCCAAGCCCCCAAATGTCAACAGACCAGTCAACACTGGGGGACTCAAGGCAGTCAGCAACGCCCTCAAGACCGGTCGGTACAGGAACGAAGCCGG 2300
VP1
V P P K P P N V N R P V N T G G L K A V S N A L K T G R Y R N E A G
697 698 699 700 701 702 703 704 705 706 707 708 709 710 711 712 713 714 715 716 717 718 719 720 721 722 723 724 725 726 727 728 729 730
ACTGAGTGGTCTCGTCCTTCTAGCCACAGCAAGAAGCCGTCTGCAAGATGCAGTTAAGGCCAAGGCAGAAGCCGAGAAACTCCACAAGTCCAAGCCAGAC 2400
VP1
L S G L V L L A T A R S R L Q D A V K A K A E A E K L H K S K P D
731 732 733 734 735 736 737 738 739 740 741 742 743 744 745 746 747 748 749 750 751 752 753 754 755 756 757 758 759 760 761 762 763
GACCCCGATGCAGACTGGTTTGAAAGATCAGAAACTCTGTCAGACCTTCTGGAGAAAGCCGACATCGCCAGCAAGGTCGCCCACTCAGCACTCGTGGAAA 2500
VP1
D P D A D W F E R S E T L S D L L E K A D I A S K V A H S A L V E
764 765 766 767 768 769 770 771 772 773 774 775 776 777 778 779 780 781 782 783 784 785 786 787 788 789 790 791 792 793 794 795 796
CAAGCGACGCTCTTGAAGCAGTTCAGTCGACTTCCGTGTACACCCCCAAGTACCCAGAAGTCAAGAACCCACAGACCGCCTCCAACCCCGTTGTTGGGCT 2600
VP1
T S D A L E A V Q S T S V Y T P K Y P E V K N P Q T A S N P V V G L
797 798 799 800 801 802 803 804 805 806 807 808 809 810 811 812 813 814 815 816 817 818 819 820 821 822 823 824 825 826 827 828 829 830
CCACCTGCCCGCCAAGAGAGCCACCGGTGTCCAGGCCGCTCTTCTCGGAGCAGGAACGAGCAGACCAATGGGGATGGAGGCCCCAACACGGTCCAAGAAC 2700
VP1
H L P A K R A T G V Q A A L L G A G T S R P M G M E A P T R S K N
831 832 833 834 835 836 837 838 839 840 841 842 843 844 845 846 847 848 849 850 851 852 853 854 855 856 857 858 859 860 861 862 863
GCCGTGAAAATGGCCAAACGGCGGCAACGCCAAAAGGAGAGCCGCTAACAGCCATGATGGGAACCACTCAAGAAGAGGACACTAATCCCAGACCCCGTAT 2800
VP1
3'NTR
A V K M A K R R Q R Q K E S R .
864 865 866 867 868 869 870 871 872 873 874 875 876 877 878 879
CCCCGGCCTTCGCCTGCGGGGGCCCCC
3'NTR

6.2.5 VP3 minigenome

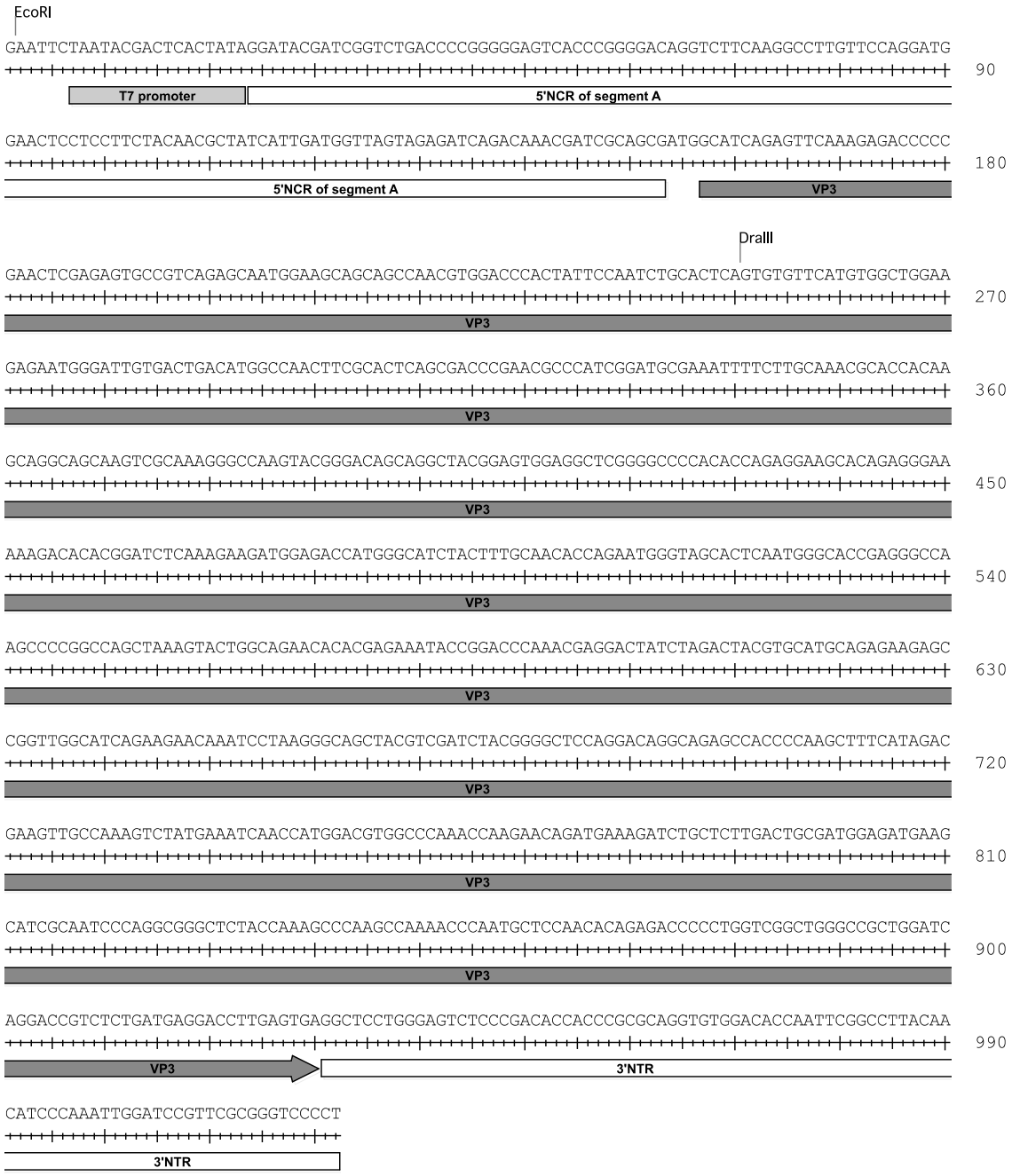

6.2.6 VP4 minigenome

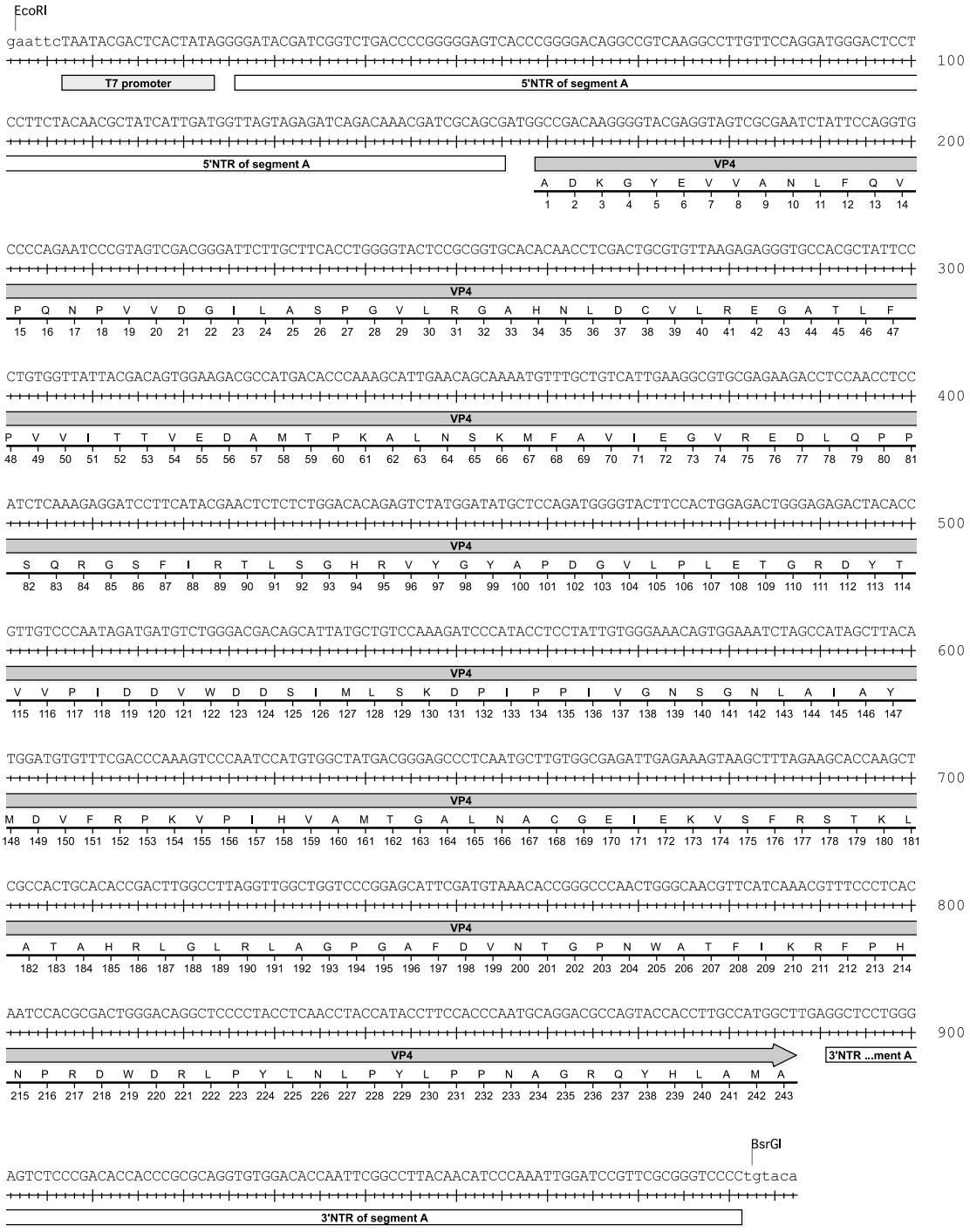

6.3 Plasmid maps of used vectors

6.3.1 pFastBac™ Dual

Map of the plasmid pFastBac™Dual, from the "Bac-to-Bac® Baculovirus Expression System" (downloaded from www.invitrogen.com)

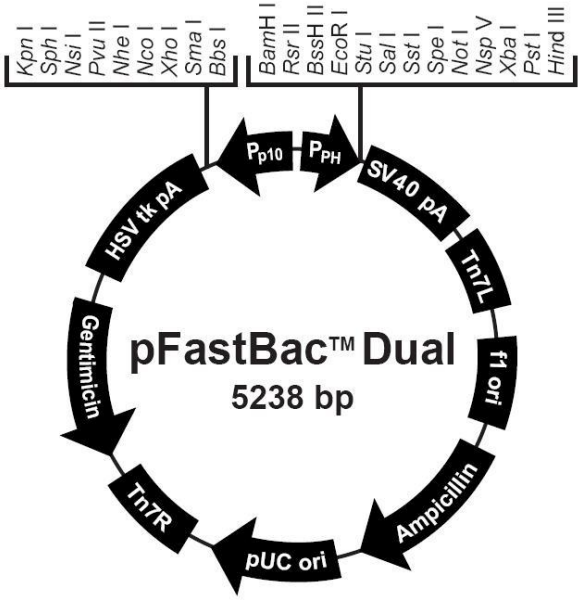

6.3.2 pcDNA3

Map of the pcDNA3 plasmid (downloaded from www.invitrogen.com)

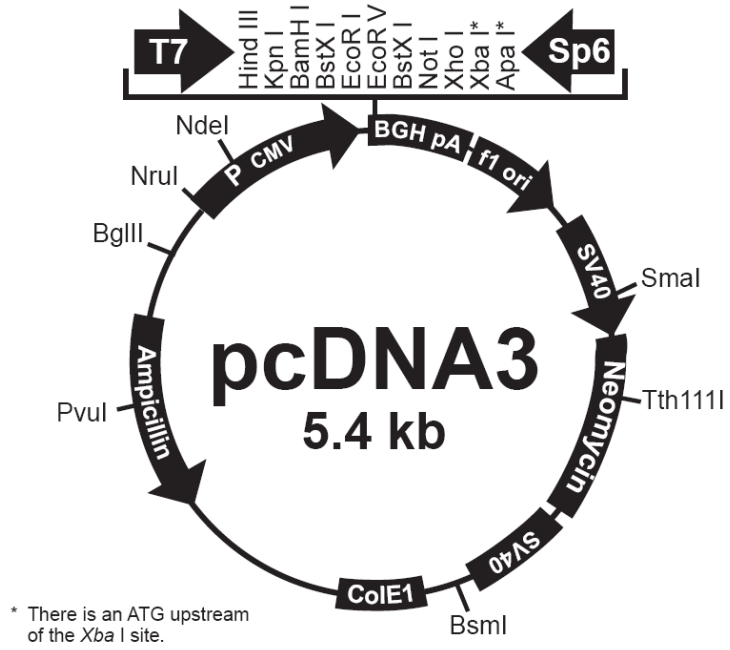

6.3.3 pCR2.1-TOPO

Map of the plasmid pCR®2.1-TOPO®; modified from the “TOPO TA Cloning Kit” (downloaded from www.invitrogen.com)

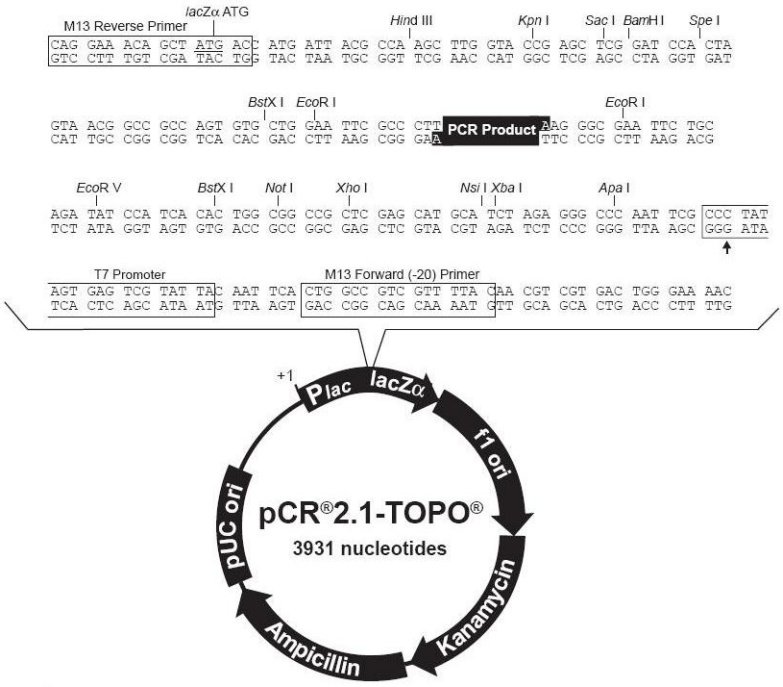

6.3.4 pUC18

Map of the puc18 plasmid with its MCS (downloaded and modified from www.fermentas.com)

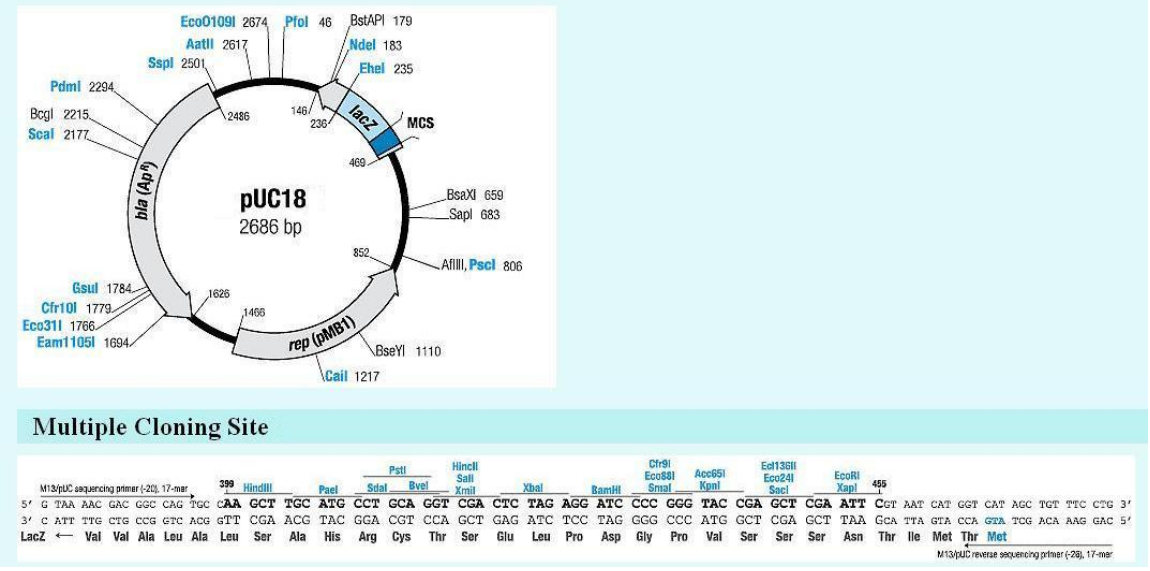

7 Acknowledgements

First and foremost, I would like to thank my advisor PD Dr. Egbert Mundt for his continual guidance, encouragement and academic, but also personal, support throughout my three years of research. I highly appreciate that I was allowed to visit several conferences to present my data and that it was possible to discuss my results with him any time.

Additionally, I appreciate all advice given by my co-advisor Prof. Dr. Sven-Erik Behrens and for allowing me to hand in my work at his university.

I would like to thank Dr. John Glisson for his offer to perform my research at the Poultry Diagnostic and Research Institute of the University of Georgia.

I am deeply grateful to Dr. Ashwini Warke for her help and advice, but more importantly for her friendship, which made me enjoy the good times even more and helped me meet every challenge.

I am indebted to Deborah Hilt, who supported me in every situation and is a true friend.

I am also thankful to Dr. Tracy Andacht (Proteomics Resource Facility) for analyzing my proteins by MALDI-TOF MS-MS in such a short time; Amy Dryman (Polyclonal Antibody Production Service) for reliable production of the sera; Jefferey Wagner for sequencing; Jamie Barber for his help with the Zeiss microscope; Ruud Hein (Intervet) for providing the IBDV strains; Dr. David Stallknecht for supplying me with H5N2 serum; Dr. Sven Müller for analysis of my microscopy data; Dr. Hernan Grecco for advice on how to quantify Western blots and edit images and Jakob Wieczorek for his help with the statistical analysis.

A special thanks to Virginia Booth, Sylva Riblet, Veronica Walker, Dr. Susan Williams, Dr. Mark Jackwood, Dr. Holly Sellers, Erich Linnemann, Dr. Maricarmen Garcia, Fred Smith, Bettyann Lyle, Joan King, Diane Baird, Teresa Byrd, Lauren Appleby, Daniel Dlugolenski and Alan Icard for your support over the years.

My deepest gratitude goes to my family, especially my parents Dorothea Stricker and Friedrich Stricker and my partner Wolfgang Lambertz, who constantly pushed me through this and never gave up believing in me.

It would have been impossible to do this without you.

8 Lebenslauf

Ruth Lydia Olga Stricker,
geboren am 15.07.1981 in Düsseldorf, Deutschland
weiblich, deutsch

2001	Abitur am Heinrich-Heine Gymnasium Mettmann-Metzkausen
2001-2006	Studium der Humanbiologie an der Ernst-Moritz-Arndt Universität Greifswald, Deutschland; Abschluss als Diplom-Humanbiologin Hauptfach: Mikrobiologie/Virologie Nebenfächer: Biochemie und Immunologie Diplomarbeitsthema: „Expression, Reinigung und Charakterisierung der zentralen Domäne der RNA-abhängigen RNA-Polymerase des Virus der infektiösen Bursitis“; Durchführung am Friedrich-Loeffler-Institut, Bundesforschungsinstitut für Tiergesundheit, Insel Riems, Deutschland.
2006-2009	Praktische Durchführung der Promotionsarbeiten am Poultry Diagnostic and Research Center, University of Georgia, Athens, GA, USA Thema: „Influence of cellular dsRNA binding proteins in the replication process of a dsRNA virus“
Seit 2009	Wissenschaftliche Mitarbeiterin am Max-Planck Institut für Molekulare Physiologie, Dortmund, Deutschland

9 Eidesstattliche Erklärung

Hiermit versichere ich, dass ich meine Dissertation mit dem Thema „Influence of cellular dsRNA binding proteins in the replication process of a dsRNA virus“ selbständig und ohne fremde Hilfe verfasst habe und keine anderen als die von mir angegebenen Quellen und Hilfsmittel benutzt und die den benutzten Werken wörtlich oder inhaltlich entnommenen Stellen als solche kenntlich gemacht habe.

Ruth Stricker
Essen, 09. April 2012